TECHNICAL UNIVERSITY OF CRETE
SCHOOL OF CHEMICAL & ENVIRONMENTAL ENGINEERING

Fate of plastics and microplastics in the marine environment

Τύχη των πλαστικών και μικροπλαστικών στο θαλάσσιο περιβάλλον

Karkanorachaki Aikaterini

June 2023

This research is co-financed by Greece and the European Union (European Social Fund- ESF) through the Operational Programme «Human Resources Development, Education and Lifelong Learning» in the context of the project "Strengthening Human Resources Research Potential via Doctorate Research – 2nd Cycle" (MIS-5000432), implemented by the State Scholarships Foundation (IKY).

THESIS COMMITTEE

Nicolas Kalogerakis, supervisor

Professor Emeritus
School of Chemical & Environmental Engineering
Technical University of Crete

Danae Venieri, advisory committee

Associate Professor
School of Chemical & Environmental Engineering
Technical University of Crete

Alexandros D. Gotsis, advisory committee

Professor
School of Mineral Resources Engineering
Technical University of Crete

Nikolaos A. Diangelakis, examination committee

Assistant Professor
School of Chemical & Environmental Engineering
Technical University of Crete

Anestis Vlysidis, examination committee

Assistant Professor
School of Chemical Engineering
National Technical University of Athens

Pagona-Noni Maravelaki, examination committee

Professor
School of Architecture
Technical University of Crete

Silvia Fiore, examination committee

Associate Professor
Department of Environment, Land and Infrastructure Engineering
Politecnico di Torino

ACKNOWLEDGEMENTS

First of all, I would like to express my gratitude for my advisor, Professor Emeritus Nicolas Kalogerakis. It has been an honor to work with such a brilliant scientist since my undergraduate years, testing my limits and, occasionally, his patience. His trust, guidance and resources of all kinds allowed me to reach this moment.

I would also really like to thank Associate Professor Danae Venieri and Professor Alexandros D. Gotsis, the members of my advisory committee, for their guidance and feedback. Also, the rest of the members of the examination committee for the time and effort they put into the evaluation of my efforts, and especially Professor Pagona Noni Maravelaki for granting me access to the ATR-FTIR instrument available in the laboratory of Materials for Cultural Heritage and Modern Building.

This work would never have been completed without the help, patience, and insights of Dr. Evdokia Syranidou. Brainstorming, thinking outside of the box, and working beside me tirelessly in offices, labs, and boats, she made sure that I did not overlook things, I did not settle, and I kept actual and sometimes made-up, or self-inflicted deadlines. Thank you for your time and energy and constantly balancing my eternal pessimism.

It is equally important that I thank the personnel of the laboratory of Biochemical Engineering and Environmental Biotechnology for helping and sharing their knowledge and time with me; Ariadni Pantidou, who doesn't think that 18 years is too much time of seeing my face; Dr. Eleftheria Antoniou, my co-sailor, for the help and guidance; Georgia Charalambous and Voula Fragkou, for the time spent working, and not working; Dr. Evina Gontikaki for showing me the kind of scientist I want to be from now on. Also, I would like to thank all the students I have worked with for the chance to teach them and learn from them. Especially Naya, whom I proudly also call my friend.

Additionally, I would like to stress the importance of the contribution of the Hellenic Center for Marine Research (ΕΛΚΕΘΕ) for hosting my field experiment, and especially Mr. Michalis Asderis for the time and effort put into setting up my field experiment and samplings.

I would be amiss if I did not express my gratitude for Plastika Kritis S.A., Chantzopoulos S.A. for the polymers used in the experiments, and the State Scholarship foundation for the financial support.

My friends, colleagues, and fellow PhD candidates at the Technical University of Crete, Petroula Seridou and Giasemi Morianou; We have been travelling, metaphorically and literally, together for the past 6 years. Thank you for sharing food, drinks, successes, and disappointments. I would not have done this without you.

I would also like to thank my family, and especially my mother Giota, for supporting me in any way they could; emotionally, financially, and practically. Most importantly, I would like to thank them for instilling in me a love for the environment and the habit of looking at the world with wide eyes, which contributed to my pursuing this PhD, and environmental engineering, in general. My other, chosen, family, Eleftheria and Nikolas were there for me when I needed their love, their time or even their veterinary and electrical services and equally accepted my absences. Their son, Orfeas, will pay for their choice of godmother, by being lectured about plastics in the sea as a bedtime story. To all my friends, for the support and love throughout the years, thank you.

Finally, I would like to thank my partner (in crime), Giannis, for putting up with having a PhD candidate in his life and his home. No one could have been more supportive and tolerant of absentmindedness, mood swings or late-night food and music cravings than him. No one would have dealt with them more efficiently, too. Miltos, you were, unknowingly, my emotional support dog, and you will be getting extra treats for that forever.

Table of Contents

Contents

List of Figures

List of Tables

List of Abbreviations

AI	After the Storm- Initial Maturation
AM	After the Storm - Final Maturation
ANOVA	Analysis Of Variance
ARISA	Automated Method of Ribosomal Intergenic Spacer Analysis
ASV	Amplicon Sequence Variant
ATR-FTIR	Attenuation Total Reflectance - Fourier Transform Infrared Spectroscopy
BET analysis	Brunauer Emmet Teller analysis
BI	Before the Storm- Initial Maturation
BM	Before the Storm - Final Maturation
bp	Base pairs
BSA	Bovine Serum Albumine
C_d	Drag Coefficient
CFU	Colony Forming Units
CI	Carbonyl Index
CLSM	Confocal Laser Scanning Microscopy
COD	Chemical Oxygen Demand
d	Diameter of sphere
D	Diameter of tube
DLS	Dynamic Light Scattering
DLVO Theory	Derjaguin-Landau-Verwey-Overbeek Theory
DNA	Deoxyribonucleic acid
DSC	Differential Scanning Calorimetry
dsDNA	Double Stranded Deoxyribonucleic Acid
EC	Electrical Conductivity
ECBI	Ester Carbonyl Bond Index
EDS	Energy-Dispersive X-ray Spectroscopy
EPS	Extracellular Polymeric Substances
EPS	Extended Polystyrene
EtOH	Ethanol
EU	European Union
f	Wall factor
FITC	Fluorescein Isothiocyanate
FSC	Forward Scattering
FTIR	Fourier Transform Infrared Spectroscopy
GC-MS	Gas Chromatography-Mass Spectroscopy
GESAMP	Group of Experts on the Scientific Aspects of Marine Environmental Protection
GPC	Gel Permeation Chromatography
HDPE	High Density Polyethylene
HPLC	High Pressure Liquid Chromatography
IDBI	Internal Double Bond Index

ITS2	Internal Transcribed Spacer 2
KCBI	Keto Carbonyl Bond Index
LDPE	Low Density Polyethylene
LEfSe	Linear discriminant analysis Effect Size
LLDPE	Linear Low Density Polyethylene
MMD	Molecular Mass Distribution
MPs	MicroPlastics
NGS	Next Generation Sequencing
NMDS	Non-Metric Multidiensional Scaling
NMR	Nuclear Magnetic Resonance
NPs	NanoPlastics
OD	Optical Density
OECD	Organisation for Economic Co-operation and Development
PA	Polyamide
PAHs	Polycyclic Aromatic Hydrocarbons
PBDEs	Polybrominated Diphenyl Ethers
PBS	Phosphate Buffer Solution
PC	Principal Component
PCA	Principal Component Analysis
PCBs	Polychlorinated Biphenyls
PCL	Polycaprolactone
PCR	Polymer Chain Reaction
PE	Polyethylene
PERMANOVA	Permutational Analysis of Variance
PET	Polyethylene Terephthalata
PMD	Plastic Marine Debris
PMMA	Polymethyl Methylacrylate
POM	Polyoxymethylene
PP	Polypropylene
PPA	polyphthalamide
PS	Polystyrene
PU	Polyurethane
PVC	PolyVinyl Chloride
Py-GC-MS	Pyrolysis - Gas Chromatography - Mass Spectrometry
R^2	Coefficient of Determination
RDA	Redundancy Analysis
Re	Reynolds Number
RI	Refractive Index
RMSE	Root Mean Square Error
RNA	Ribonucleic Acid
ROS	Reactive Oxygen Species
rpm	Rounds per minute
rRNA	Ribosomic Ribonucleic Acid

SDS	Sodium Dedocyl Sulfate
SEM	Scanning Electron Microscopy
sp.	Spieces
SSC	Side Scatterinf
TEM	Transmission Electron Microscopy
TGA	Thermal Gravimetric Analysis
TG-DTG-DTA	Thermogravimetry/Derivative ThermoGravimetry/Differential Thermal Analysis
TLC	Thin Layer Chromatography
TSS	Total Suspended Solids
u	Sinking Velocity
u_∞	Terminal boundless sinking velocity
UV	Ultraviolet
v	Kinematic viscosity
VBI	Vinyl Bond Index
WEEE	Electrical and Electronic Equipment Waste
XPS	X-ray Photoelectron Spectroscopy
ζ	Sinking velocity between liquids correlation factor
λ	Sphere-to-tube diameter ratio

Abstract

The ease of use and versatile properties of plastics have turned them from the novelty product they were 80 years ago to one of the most non-replaceable families of materials of our time, with predictions for increased demand in the following years despite recent bans. In 2019 alone, 640 Mt of plastics were used. Various types of plastics have been developed, from simple polyolefin, such as polyethylene (PE) and polypropylene (PP) to more complex, such as polystyrene (PS) and polyethylene terephthalate (PET). Traditional fossil-based plastics account for 8% of the global petroleum production. The demand for single use plastic materials, mostly used for packaging, understandably contributes to the production of vast amounts of plastic waste. In 2020, 29.5 Mt of plastic waste was generated in the EU alone. Worldwide, 22% of the plastic waste is mismanaged, ending up in landfills or being discarded, and eventually ending up in the environment, especially the seas. Mismanaged plastic land originating waste corresponds to 80% of the plastic waste entering the marine environment.

There exist disagreements between the estimated amounts of plastic in the seas. Model outputs are significantly lower than calculations based on waste production and management statistics. That could be attributed either to a combination of model underestimations and plastic waste input overestimations, or to the fact that during their residence in the marine environments interact with it in ways that result in "obscuring" it. For instance, owing to their inherent density, or due to the attachment of biological factors (biofouling), plastics can move vertically within the water column and float or settle to the benthos. The effect of the UV fraction of solar radiation, heat and microorganisms can lead to photodegradation, thermodegradation or biodegradation, while mechanical stress can result in the breakdown of plastics to smaller pieces (fragmentation). While plastic particles of smaller sizes enter the ocean directly (primary partilces), fragmentation results in the formation of secondary microplastics (<5mm) and nanoplastics (<1 μm). All plastics have negative impacts on the environment and the health of marine life, but microplastics and nanoplastics can enter more organisms and in more than one way and have more pronounced impacts on the health of the receiving biota.

For that reason, it is important to understand the fate of plastics and microplastics in the marine environment, what are the processes that affect them and their interactions. The aim of this dissertation is to attempt to study these processes as they occur in the marine environment, so that their role and contribution to the fate of plastics can be better understood. That was achieved in a series of microcosm, mesocosm and field experiments. These allowed the study of the plastic polymers themselves, as well as their interactions with radiation and marine organisms, the

establishment of the baseline of the south-eastern Mediterranean plastic colonizing community and the examination of their effect on the polymers. The multiple scale of the experiments revealed whether it is possible to simulate the marine environment in the sea and extrapolate the results of smaller scale experiments in the actual environment.

In the microcosm experiment, secondary low-density polyethylene (LDPE) and high-density polyethylene (HDPE) microplastics were incubated with two marine communities. One of the communities (Souda) was wild and the other (Agios) had previously been acclimatized to utilize plastics as a carbon source. Over the 120 days of the experiment, biofilm was formed on the surface of the microplastics of both treatments, revealing that both communities had the potential to survive with weathered plastics as the sole carbon source. Examination of the plastic particles with FTIR (Fourier-transform infrared spectroscopy) revealed chemical changes concurrent with biodegradation. Dynamic light scattering (DLS) allowed the observation of plastic particles with sizes between 56 nm and 4.5 μm and confirmed that biodeterioration and biofragmentation, prerequisite processes for biodegradation, occurred in the microcosms.

Having established that prior acclimatization is not required for the utilization of plastics by microorganisms, polypropylene (PP) pellets with and without prior artificial weathering were incubated in mesocosms non-acclimated marine communities under semi-realistic environmental conditions for 180 days. Bacterial attachment and biofilm formation were observed in this experiment, as well. Surface changes, observed with ATR-FTIR (attenuation total reflectance Fourier-transform infrared spectroscopy) revealed that also in that setup the polymer was altered as a result of solar radiation and the activity of microorganisms. No microscopic particles could be detected during dynamic light scattering (DLS) examination. Measurements of zeta-potential and colloid particle hydrodynamic diameter contained in the seawater implied that any microplastic or nanoplastic particles produced were trapped in marine aggregates. Intriguingly, a phase shift could be observed between the mesocosm containing the virgin and artificially weathered pellets, in terms of number of viable cells, in accordance with the chemical alterations of the surface of the pellets. It was thus shown that while weathered polymer substrates are readily available for biodegradation, leading to the removal of the affected layer to reveal fresh virgin polymer, virgin polymers must first undergo weathering through abiotic processes to be able to act as carbon source for marine communities.

The vertical movement of plastic particles in the water column was examined over a 300-day incubation period in the bay of Souda. 5 types of plastic films (PS, PET – denser / LDPE, HDPE, PP lighter than seawater), and 3 types of plastic pellets (LDPE, HDPE, PP), before and after weathering,

were examined. The accumulation of biofouling on the surface of the samples was studied. Simultaneously, their sinking velocity was determined, using a novel semi-theoretical methodology. The sinking velocity of the same plastics, after the biofouling had been removed allowed the establishment of the determining effect of biofouling on the sinking characteristics of the plastic samples. The removal of biofouling by two severe storm events allowed the examination of removal and reattachment of the biofouling agents and the better understanding of its effect on sinking and allowed the correlation of sinking velocity with the biofouling quantity. Density and sample form were found to play a role in the sinking behavior of the plastics, while weathering did not significantly affect the sinking fate of the pellets. Thus, semi-empirical mathematical expressions of sigmoid nature were proposed for the description of both the fouling development rate, as well as the changes in sinking velocity as it progressed.

The same plastics used for the examination of their sinking characteristics were examined at four timepoints (35, 152, 202 and 242 days) for the fungal and bacterial community composition and succession via next generation sequencing, along with the chemical changes of their surface to investigate biodegradation. Bacterial communities were found to be more diverse and variable, dominated by *Proteobacteria* and *Bacteroidetes*. Fungal *Ascomycota,* which have been found to dominate epiplastic communities in the literature and potentially biodegrade plastics, dominated communities were more stable. Biodegradation was not actively confirmed in this work. The effect of one of the storm events which affected the samples for sinking behavior examination also affected the samples used for this chapter, allowing the determination of the effect of stochasticity on the plastisphere communities. Plastic type did not play a significant role towards the determination of the plastisphere community, in contrast with the stage of biofilm development along with the stochastic effect of the storm-induced biofouling removal.

In conclusion, it was determined that microcosms and mesocosms are effective tools of studying plastic biodegradation, since their small volume and high concentrations allow the examination of parameters which the infinite dilution of the sea would deem impossible. The cyclical pattern of weathering and de-weathering by microorganisms was confirmed in all three scales employed here. The unreliable nature of weight measurements as a biodegradation metric was demonstrated, unless thorough sample pre-treatment has preceded. The determining effect of biofouling on the sinking behavior of samples of various sizes and densities was shown, which until now, had only been speculated. The south-easter Mediterranean plastisphere, and much more so the fungal side of it, was studied for the first time, implying that further and deeper study is needed, since plastic biodegrading taxa were observed. However, since biodegradation could not be proven in the field scale experiment,

it is natural to assume that plastic biodegradation in the marine environment is minimal. Finally, while the results from scale to scale are transferrable, the process of translating lab or mesocosm derived results must be realized with extreme caution.

Περίληψη

Η πληθώρα χρήσεων και η ευκολία στη χρήση που προσφέρουν τα πλαστικά τα ανέδειξαν από τα καινοτόμα προϊόντα που ήταν πριν 80 χρόνια σε μια από τις αναντικατάστατες ομάδες υλικών της εποχής μας, με προβλέψεις για αύξηση της ζήτησής τους, παρά τις πρόσφατες απαγορεύσεις. Το 2019 μόνο, χρησιμοποιήθηκαν 640 Mt πλαστικών. Διάφοροι τύποι πλαστικών έχουν εμφανιστεί, από τις απλές πολυολεφίνες, όπως το πολυαιθυλένιο (PE) και το πολυπροπυλένιο (PP) ως πιο πολύπλοκοι, όπως το πολυστυρένιο (PS) και το τερεφθαλικό πολυαιθυλένιο (PET). Τα παραδοσιακά πλαστικά που αποτελούν παράγωγα του πετρελαίου αποτελούν το 8% της παγκόσμιας παραγωγής πετρελαίου. Η απαίτηση για πλαστικά μιας χρήσης, που χρησιμοποιούνται κυρίως ως υλικά συσκευασίας, συντελούν στην παραγωγή τεράστιων ποσοτήτων πλαστικών αποβλήτων. Το 2020 παράχθηκαν 29,5 Mt πλαστικών αποβλήτων στην ΕΕ μόνο. Παγκοσμίως, το 22% των πλαστικών αποβλήτων δεν χαίρει ορθής διαχείρισης και καταλήξει σε χωματερές ή απλώς απορρίπτεται και καταλήγει στο περιβάλλον, ειδικά στη θάλασσα. Κακώς διαχειρισμένα πλαστικά απορρίμματα με προέλευση από τη στεριά αντιστοιχεί στο 80% των πλαστικών αποβλήτων που καταλήγουν στο θαλάσσιο περιβάλλον.

Διαφωνίες υπάρχουν για τις αναμενόμενες ποσότητες πλαστικών στις θάλασσες. Τα μοντέλα δίνουν σημαντικά χαμηλότερες τιμές από αυτές που υπολογίζονται στατιστικά, λαμβάνοντας υπόψιν την παραγωγή αποβλήτων και τη διαχείρισή τους. Αυτό θα ήταν δυνατό να αποδοθεί είτε σε ένα συνδυασμό υποεκτίμησης από πλευράς μοντέλων και υπερεκτίμησης των εισροών πλαστικών, είτε στο γεγονός ότι κατά την παραμονή τους στο περιβάλλον τα πλαστικά αλληλεπιδρούν με αυτό με τρόπους που καταλήγουν στο να «κρύβεται» μέρος τους. Για παράδειγμα, λόγω της πυκνότητάς τους, ή της επικάθισης βιολογικών παραγόντων, τα πλαστικά μπορούν να κινηθούν κατακόρυφα εντός της υδάτινης στήλης και να καταλήγουν να επιπλέουν ή να βυθίζονται. Η επίδραση του υπέρυθρου (UV) κλάσματος της ηλιακής ακτινοβολίας, της θερμότητας και των μικροοργανισμών μπορούν μα οδηγήσουν σε φωτο-, θερμο- ή βιοαποδόμηση, ενώ η μηχανική καταπόνηση μπορεί να καταλήξει στο θρυμματισμό σε μικρότερα κομμάτια. Μικρού μεγέθους πλαστικά σωματίδια μπορούν να εισέλθουν στους ωκεανούς ως έχουν παραχθεί (πρωτογενή), ωστόσο, ο θρυμματισμός συντελεί στο σχηματισμό δευτερογενών μικροπλαστικών, με μέγεθος μικρότερο των 5 mm, και νανοπλαστικών (<1 μm). Όλα τα πλαστικά έχουν αρνητικές επιπτώσεις για το περιβάλλον και την ανθρώπινη υγεία, αλλά τα μικροπλαστικά και νανοπλαστικά δύνανται να εισέλθουν στους οργανισμούς μέσω πολλών οδών και να έχουν πιο επιβαρυντικές επιδράσεις στους αποδέκτες οργανισμούς.

Για το λόγο αυτό, είναι ιδιαιτέρως σημαντική η κατανόηση της τύχης των πλαστικών και

μικροπλαστικών στο θαλάσσιο περιβάλλον, των διεργασιών που τα επηρεάζουν και των αλληλεπιδράσεών τους. Ο σκοπός της παρούσας διατριβής είναι να επιχειρήσει να εξετάσει τις διεργασίες αυτές, καθώς προκύπτουν στο θαλάσσιο περιβάλλον, έτσι ώστε τόσο ο ρόλος, όσο και ο βαθμός συνεισφοράς τους στην τύχη των πλαστικών να κατανοηθεί καλύτερα. Αυτό έγινε δυνατό μέσα από μια σειρά πειραμάτων σε επίπεδο μικρόκοσμων, μεσόκοσμων και πεδίου. Έτσι επιτεύχθηκε η παρακολούθηση των πολυμερών, αλλά και των αλληλεπιδράσεών τους με την ακτινοβολία και τους θαλάσσιους οργανισμούς, καθώς και ο καθορισμός της βάσης της πλαστικόσφαιρας της νοτιοανατολικής Μεσογείου, που εγκαθίσταται και επηρεάζει τα πλαστικά. Η κλιμακούμενη φύση των πειραμάτων επέτρεψε την εξέταση του κατά πόσο δύναται να προσομοιωθεί το θαλάσσιο περιβάλλον και να αναχθούν τα αποτελέσματα από μικρότερης κλίμακας πειράματα σε αυτό.

Κατά το πείραμα μικρόκοσμων, δευτερογενή μικροπλαστικά από πολυαιθυλένιο χαμηλής (LDPE) και υψηλής πυκνότητας (HDPE) επωάστηκαν με δυο θαλάσσιες κοινότητες. Η μία ήταν άγρια (Souda) και η άλλη εγκλιματισμένη στη χρήση πλαστικών σαν αποκλειστική πηγή άνθρακα (Agios). Κατά τις 120 ημέρες του πειράματος, αναπτύχθηκε βιοφίλμ στην επιφάνεια των μικροπλαστικών υπό και τις δυο συνθήκες, αποκαλύπτοντας ότι και οι δυο κοινότητες διέθεταν την ικανότητα να επιβιώσουν με τα γηρασμένα πλαστικά σαν αποκλειστική πηγή άνθρακα. Εξέταση των πλαστικών σωματιδίων με FTIR (φασματοσκοπία μετασχηματισμού υπέρυθρου Fourier) έδειξε χημική φύσης αλλαγές που συνάδουν με τη βιοαποδόμηση. Ανάλυση δυναμικής σκέδασης φωτός (DLS) επέτρεψε την παρατήρηση πλαστικών σωματιδίων μεγέθους από 56 nm ως 4.5 μm και επιβεβαίωσε εντός των μικρόκοσμων τη βιοϋποβάθμιση και το βιοθρυμματισμό, διεργασίες προαπαιτούμενος για τη βιοαποδόμηση.

Με αποδεδειγμένη τη μη απαίτηση προηγούμενου εγκλιματισμού για την εκμετάλλευση των πλαστικών από τους μικροοργανισμούς, σφαιρίδια πολυπροπυλενίου (PP) με και χωρίς πρότερη τεχνητή γήρανση επωάστηκαν σε μεσόκοσμους με μη εγκλιματισμένες θαλάσσιες κοινότητες υπό ημιρεαλιστικές περιβαλλοντικές συνθήκες για 180 ημέρες. Βακτηριακή επικόλληση και ανάπτυξη βιοφίλμ παρατηρήθηκαν και υπό αυτές τις συνθήκες. Αλλαγές στην επιφάνεια των σφαιριδίων που παρατηρήθηκαν με φασματοσκοπία μετασχηματισμού υπέρυθρου Fourier ολικής αποσβένουσας ανάκλασης (ATR-FTIR) αποκάλυψε ότι και υπό αυτές τις πειραματικές συνθήκες τα πολυμερή υφίσταντο μεταβολές λόγω της ηλιακής ακτινοβολίας και της δράσης των μικροοργανισμών. Μικροσκοπικά σωματίδια δεν ήταν δυνατό να εντοπιστούν κατά την ανάλυση με δυναμική σκέδαση φωτός (DLS). Μετρήσεις ζ-δυναμικού και της υδροδυναμικής διαμέτρου των κολλοϊδών σωματιδίων που περιέχονταν στο θαλασσινό νερό των μεσόκοσμων υπονόησαν ότι τα όποια μικροπλαστικά και

νανοπλαστικά παράχθηκαν κατά την επώαση εγκλωβίστηκαν σε θαλάσσια συσσωματώματα. Αξιοπεριέργως, παρατηρήθηκε διαφορά φάσης ανάμεσα στο μεσόκοσμο που περιείχε τα παρθένα κι εκείνον που περιείχε τα γηρασμένα σφαιρίδια. Δείχθηκε έτσι ότι ενώ τα γηρασμένα πολυμερικά υποστρώματα είναι άμεσα διαθέσιμα προς βιοαποδόμηση, ώστε να απομακρυνθεί το γηρασμένο στρώμα προς την αποκάλυψη εκ νέου παρθένου υλικού, τα παρθένα πολυμερή πρέπει πρώτα να γηρανθούν μέσω αβιοτικών διεργασιών προτού να είναι βιοδιαθέσιμα στις θαλάσσιες κοινότητες.

Η κατακόρυφη κίνηση των πλαστικών σωματιδίων εντός της υδάτινης στήλης εξετάστηκε κατά την επώαση δειγμάτων για 300 ημέρες στον κόλπο της Σούδας. Μελετήθηκαν 5 τύποι πλαστικών φιλμ (PS, PET – πυκνότερα / LDPE, HDPE, PP – ελαφρύτερα από το θαλασσινό νερό), και 3 τύποι πλαστικών σφαιριδίων (LDPE, HDPE, PP), πριν και μετά από γήρανση. Εξετάστηκε η συσσώρευση βιοεπικαθίσεων στην επιφάνεια των δειγμάτων. Ταυτόχρονα, καθορίστηκε η ταχύτητα βύθισής τους χρησιμοποιώντας μια καινοτόμο ημιεμπειρική μεθοδολογία. Μελετήθηκε επίσης η ταχύτητα βύθισης των ίδιων δειγμάτων μετά από αφαίρεση των βιοεπικαθίσεων, ώστε να εξεταστεί η επίδρασή της στα πλευστικά χαρακτηριστικά των δειγμάτων. Η απομάκρυνση των βιοεπικαθίσεων από δυο ισχυρές καταιγίδες επέτρεψε την παρακολούθηση της απομάκρυνσης και της επανεπικάθισης των βιολογικών παραγόντων και την καλύτερη κατανόηση της επίδρασής της επί της βύθισης και της συσχέτισής της με την ταχύτητα βύθισης. Η πυκνότητα και το σχήμα των δειγμάτων επηρέασαν σημαντικά την συμπεριφορά βύθισης των πλαστικών, ενώ η γήρανση δεν έπαιξε καθοριστικό ρόλο στην τύχη βύθισης των σφαιριδίων. Κατά τον τρόπο αυτό καταρτίστηκαν ημι-εμπειρικές σιγμοειδείς μαθηματικές σχέση για την περιγραφή τόσο του ρυθμού ανάπτυξης των βιοεπικαθίσεων, όσο και της μεταβολής της ταχύτητας βύθισης.

Τα ίδια δείγματα πλαστικών που χρησιμοποιήθηκαν για τα προηγούμενα χρησιμοποιήθηκαν για την ανάλυση της σύστασης και της διαδοχής της βακτηρίασής και μυκητιακής κοινότητας μέσω της αλληλούχισης νέας γενιάς (NGS), σε συνδυασμό με τις χημικές αλλαγές τις επιφάνειάς τους, προκειμένου να διαπιστωθεί τυχόν βιοαποδομητική δραστηριότητα. Οι βακτηριακές κοινότητες βρέθηκε να είναι πιο ποικιλόμορφες και μεταβαλλόμενες, με κυρίαρχες βαθμίδες τα *Proteobacteria* και τα *Bacteroidetes.* Τα *Ascomycota*, που και στη βιβλιογραφία απαντώνται συχνά και έχουν βιοαποδομητικές ικανότητες, ήταν κυρίαρχα στις μυκητιακές κοινότητες, που αποδείχθηκαν σταθερότερες. Η βιοαποδόμηση δεν επιβεβαιώθηκε σε αυτή την εργασία. Η επίδραση μιας από τις καταιγίδες που επηρέασαν και τα πλευστικά χαρακτηριστικά των δειγμάτων επηρέασε και τα δείγματα που εξετάστηκαν πριν τη συγγραφή του σχετικού με τις κοινότητες κεφαλαίου, επιτρέποντας την εξέταση της επίδρασης της τυχαιότητας και επί της δομής των μικροβιακών κοινοτήτων. Ο τύπος του πολυμερούς δεν έπαιξε σημαντικό ρόλο στον καθορισμό της

πλαστικόσφαιρας, σε αντίθεση με τη φάση ανάπτυξης του βιοφίλμ και της τυχαίας επίδρασης της απομάκρυνσης των βιοεπικαθίσεων από την καταιγίδα.

Εν κατακλείδι, δείχθηκε ότι οι μικρόκοσμοι και οι μεσόκοσμοι αποτελούν αποτελεσματικά εργαλεία μελέτης της βιοαποδόμησης των πλαστικών, καθώς ο μικρός τους όγκος επιτρέπει την εμφάνιση συγκεντρώσεων αρκετά υψηλών για τη μελέτη παραμέτρων που υπό συνθήκες άπειρης αραίωσης στη θάλασσα δεν θα ήταν εντοπίσιμες. Το κυκλικό μοτίβο γήρανσης και απογήρανσης από τους μικροοργανισμούς επιβεβαιώθηκε και στις τρεις πειραματικες κλίμακες που χρησιμοποιήθηκαν. Θίχθηκε η αβεβαιότητα που εισάγεται από τη μέτρηση του βάρους ως μέθοδος εκτίμησης της βιοαποδόμησης, απουσία πρότερης και ενδελεχούς προεπεξεργασίας των δειγμάτων. Δείχθηκε η καθοριστική επίδραση των βιοεπικαθίσεων στην πλευστική συμπεριφορά πλαστικών δειγμάτων διάφορων μεγεθών και πυκνοτήτων, η οποία μέχρι στιγμή είχε μόνο υποτεθεί. Η νοτιοανατολική μεσογειακή πλαστικόσφαιρα, και δη το μυκητιακό κλάσμα της, μελετήθηκε για πρώτη φορά, εντείνοντας την ανάγκη περεταίρω μελέτης, καθώς εντοπίσθηκαν πιθανοί αποδομητές των πλαστικών. Ωστόσο, η βιοαποδόμηση δεν ήταν δυνατό να δειχθεί αναμφίβολα κατά το πείραμα πεδίου. Είναι, επομένως, δυνατό να υποτεθεί ότι η βιοαποδόμηση στο θαλάσσιο περιβάλλον είναι ελάχιστη. Τέλος, τα αποτελέσματα από τη μια κλίμακα στην άλλη μπορούν να μεταφερθούν, πάντα όμως με πολλή επιφύλαξη.

Chapter 1. Introduction

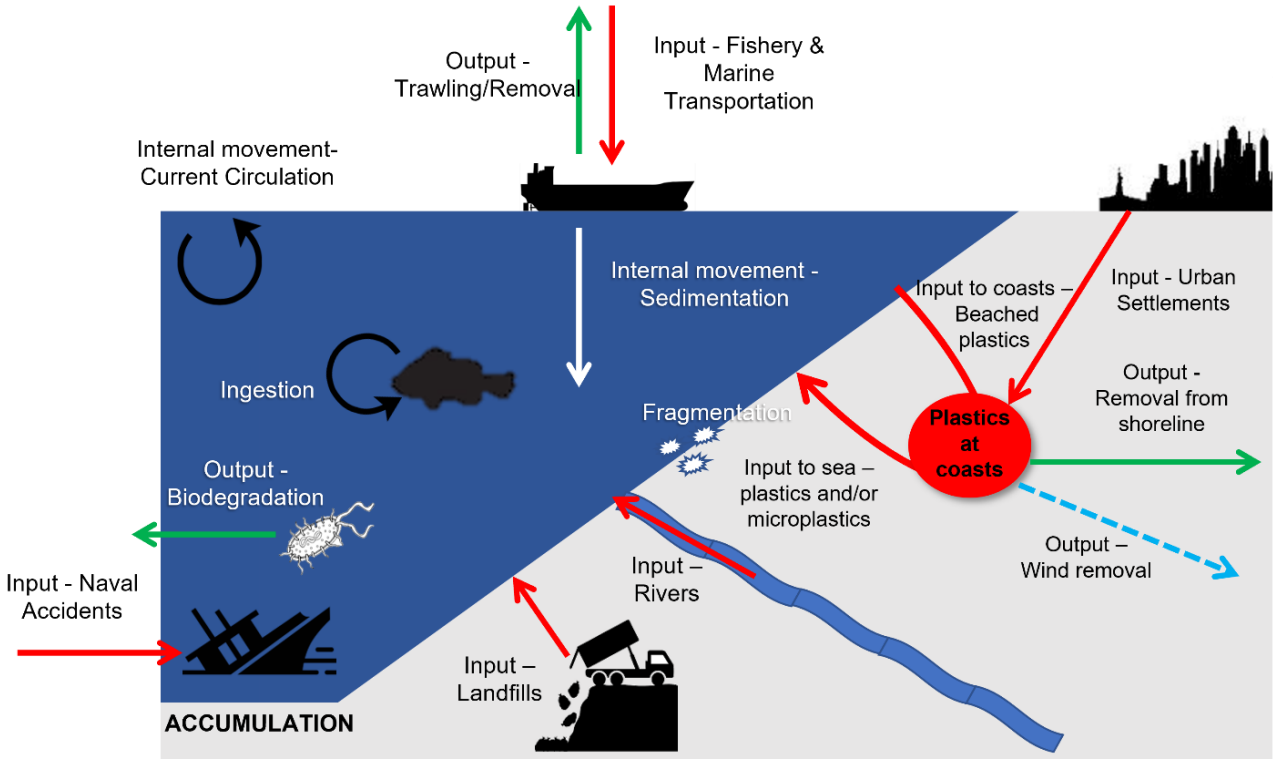

The evolution of all life on earth is largely connected to the existence of natural polymers; polynucleotides, proteins, polysaccharides, to name just a few (Kulkarni et al., 2012). Polymerization is the process of bonding a large number of small identical molecules (monomers) in order to create large molecular chains (polymers). Instinctively, humans turned to their familiar pattern of repeating monomers when designing synthetic materials to fulfil their needs, and thus, a little more than a century ago, celluloid and bakelite, the first synthetic polymers, were invented.

1.1. Plastics

Plastics are high molecular weight polymers, with molecular chains of thousands or hundreds of thousands of repeating monomers (Edmondson and Gilbert, 2017). For instance, polyethylene is the polymerization product of methylene (-CH_2-). Traditionally, plastics are fossil-based. It is estimated that 8% of the global petroleum production is directed towards the production of plastics (Thompson et al., 2010). Recently, the production of plastic from biomass (bioplastics or bio-based) was introduced, as a sustainable and greener alternative, but it is still in its infancy (García-Depraect et al., 2021a). 5.9 MT of biobased plastics were produced in 2021, corresponding to 1.5 % of the 390.7 MT of oil-based plastic production (PlasticsEurope, 2022). The addition of compounds (additives) altering the properties of plastics is common practice, since pure polymers do not usually exhibit the behaviour expected by the users. Plasticizers, fillers, stabilizers, flame retardants and colorants are some of them (Coleman, 2017) and are estimated to make up 6% of the total plastics production (Streit-Bianchi et al., 2020).

Plastics can be categorized in two large groups. Thermosetting plastics or thermosets, namely phenolic, epoxy and other resins, form permanent structures under the effect of heat or ultraviolet (UV) radiation. Thermoplastics, such as polyethylene (PE), polypropylene (PP) polystyrene (PS) and polyethylene terephthalate (PET), can be melted and shaped with the application of heat without loss of properties. (Myer Kutz, 2015).

While in the early stages of their development the use of plastics was not widespread, material shortages during World War II and the following acclimatization of the public to their applications and convenience, resulted in the use of 460 MT in 2019. Future scenarios predict that the yearly plastic demand could increase within the range of 827 MT to 1231 MT by 2060 (OECD, 2022; Streit-Bianchi et al., 2020).

1.2. Types of plastic polymers

The large number of plastic polymers available at the moment is utilized for every possible

application, from durable construction to short-lived packaging materials.

1.2.1. Polyethylene (PE)

PE is a long chain aliphatic hydrocarbon with three main molecular structures: low-density polyethylene (LDPE), linear low-density polyethylene (LLDPE) and high-density polyethylene (HDPE) (Figure 1.1). Polymerization of ethylene to produce PE can occur in one of the following five ways: High-pressure processes, Zieglere-Natta processes, the Phillips process, the Standard Oil (Indiana) process or the Metallocene processes. The properties of the resulting polymer can vary greatly, depending on the degree of branching, molecular mass distribution (MMD), the residual comonomers or impurities lingering in the polymer, the degree of compounding or crosslinking. PE is characterized by densities lower than that of water (900 – 960 kg m^{-3}), durability, moderate tensile strength, good chemical and electrical resistance. It is opaque or semi-opaque, but it can be transparent when in the form of thin films. As a rule, the density of the polymer is used to express branching, and therefore the different structures (Ronca, 2017). At the same time, its density implies that it does not sink in water. In its three forms, PE represented 26.4 % of the annual plastic production in 2021 (OECD, 2022).

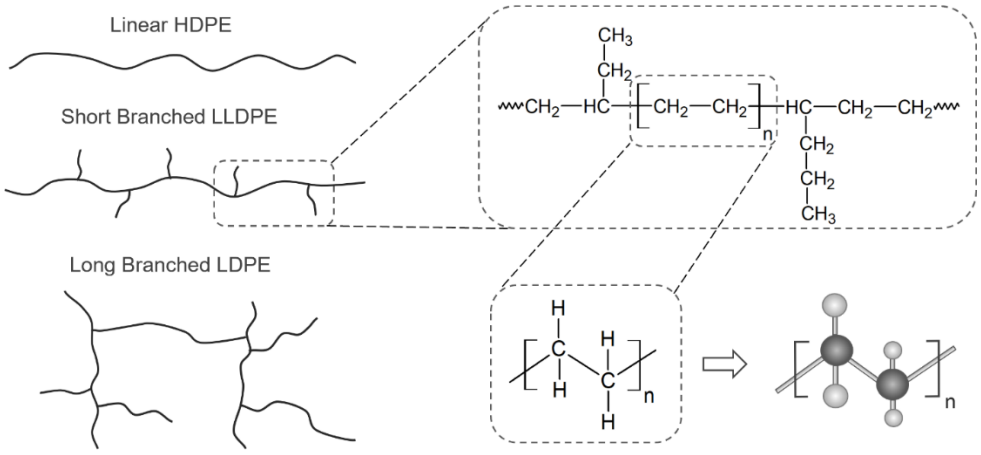

Figure 1. 1: PE molecular structures (http://polymerdatabase.com).

1.2.2. Polypropylene (PP)

PP is a linear hydrocarbon polymer similar to PE. The polymeric chain of PP contains a methyl group attached to every second carbon of the backbone. Several bulk, slurry and gas phase technologies

have been developed for the polymerization of propene (or propylene) to produce PP, with all of them relying heavily on the selection of a metallocene or Zieglere-Natta catalyst. Depending on the spatial arrangement of the methyl groups, three stereoisomers of PP have been identified: isotactic PP (all the methyl groups on the same side of the polymeric backbone), syndiotactic PP (methyl groups on alternating sides of the polymeric backbone) and atactic PP (randomly arranged methyl groups). The arrangement of the methyl groups, along with polydispersity and nucleation, affects the properties, crystallinity, and applications of the polymer. Typically, the density of PP (550 – 943 kg m^{-3}) is lower than that of PE. It possesses similar chemical resistance and electrical properties. The tertiary carbon atoms in the backbone of PP, however, make the polymer susceptible to oxidation, leading to the degradation in lower molar mass compounds (Gahleitner and Paulik, 2017). Nowadays, PP is very widely used, especially for packaging, and in 2021 corresponded to 19.3 % of the total plastic production (OECD, 2022).

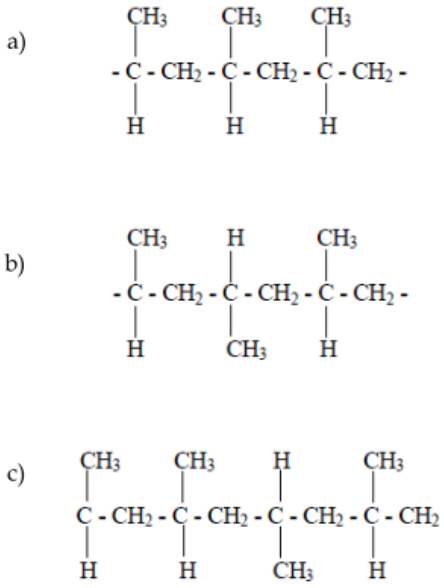

Figure 1. 2: The stereoisomers of PP: (a) isotactic, (b) syndiotactic, (c) atactic (Ariff et al., 2012).

1.2.3. Polyvinyl Chloride (PVC)

PVC is the product of the polymerization of vinyl chloride. It is highly unstable without the addition of additives and stabilizers, and due to the presence of chlorine atoms in the polymeric chain, hazardous for the environment. It is mainly produced by solution polymerization processes and some syndiotacticity can observed, resulting in up to 10% crystallinity. Given the high number of potential additives and the fact that the polymerization method used can affect the final product, the properties

of PVC vary greatly, however its density is consistently higher than 1000 kg m^{-3} (Gilbert and Patrick, 2017), and PVC sinks in water. PVC made up 12.9% of the annual plastic production in 2021 (OECD, 2022).

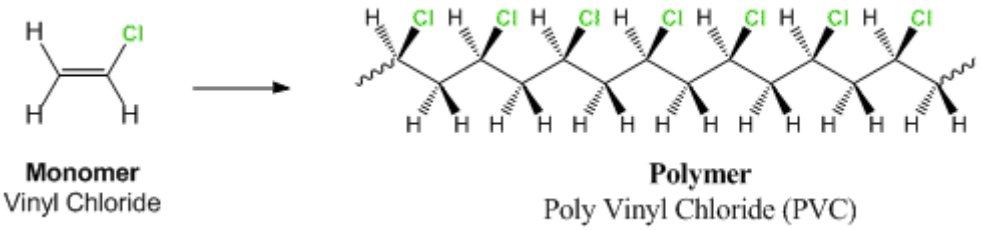

Figure 1. 3: The polymerization of vinyl chloride into PVC (adapted from https://www.chemtube3d.com/_pvcf).

1.2.4. Polyethylene Terephthalate (PET)

PET is produced by ethylene glycol and terephthalic acid in a three-step process: after the initial pre-polymerization, a step-wise growth polycondensation (esterification or transesterification) and a solid-state polymerization follow. PET is stiff, thermally stable, unaffected by many chemicals, but it is prone to hydrolysis. It can be amorphous (transparent, density ~1290 - 1390 kg m^{-3}) or semi-crystalline (opaque, density ~1370-1400 kg m^{-3}). Both structures sink in water (Nisticò, 2020). PET comprised 6.2 % of the global annual production of plastics in 2021 (OECD, 2022).

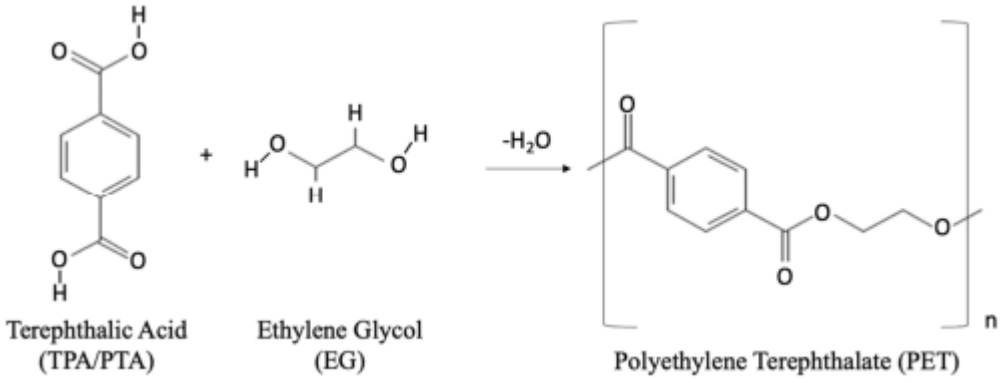

Figure 1. 4: The synthesis of PET by terephthalic acid and ethylene glycol (Benyathiar et al., 2022).

1.2.5. Polystyrene (PS)

PS is an aromatic thermoplastic, the polymerization product of styrene (or ethenylbenzene,

vinylbenzene, phenylethane). Depending on the polymerization process it can be either hard and transparent in its pure form, or soft and white like a foam, if expanded (expanded polystyrene - EPS). PS is most commonly produced via mass, solution or suspension polymerization. It can be found in various stereo-regular forms with several crystallinities. Due to the aromatic benzene ring, PS can be involved in several chemical reactions, including chlorination, hydrogenation, nitration or sulfonation reactions, resulting in discoloration and chain rupture. The density of unmodified PS is 1054 kg m^{-3}, while EPS can be found with densities a low as 10 kg m^{-3}, therefore, while the former sinks in water, the latter floats. It is characterized by excellent electrical and thermal insulation properties, transmits all visible light and has a high Refractive Index (1.592) (Satterthwaite, 2017). In 2021, PS accounted for 5.3 % of the global annual plastic production (OECD, 2022).

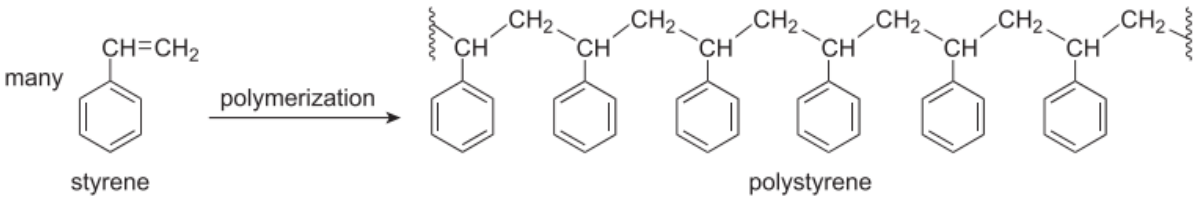

Figure 1. 5: Styrene polymerization into PS (Satterthwaite, 2017).

1.3. Plastic waste

Worldwide, 49 % of the generated plastic waste ends up in landfills, 19 % is incinerated and only 9 % is recycled (OECD, 2022). In the EU, 29.5 MT of plastic waste was collected in 2020. Mixed collection systems contributed 15 MT, while 14.5 MT originated from separate waste collection systems. A 44 % of the annual plastic production consisted of packaging materials, which are mainly characterized by their single use status. Packaging, along with electrical and electronic equipment (WEEE) and waste from container parks are commonly collected separately. For that reason, elevated recycling levels (65 % as opposed to 5%) were observed, instead of energy recovery (57 % as opposed to 27 %) or landfilling (38 % as opposed to 8 %). More specifically, separate collection of packaging waste resulted in 80-fold higher recycling levels. Unfortunately, Greece is still behind in terms of plastic waste management, with landfilling as the main waste treatment (73 %) and recycling only 25 % of its plastic waste (PlasticsEurope, 2022).

A staggering 22 % of the global plastic waste is mismanaged, with a predicted decrease of up to 15 % by 2060 (OECD, 2022). Less developed countries significantly contribute to the production of plastic waste, due to their limited potential for the application of proper collection and management schemes. Incredibly, twenty countries contributed 83 % of the total mismanaged plastic waste

(Jambeck et al., 2015).

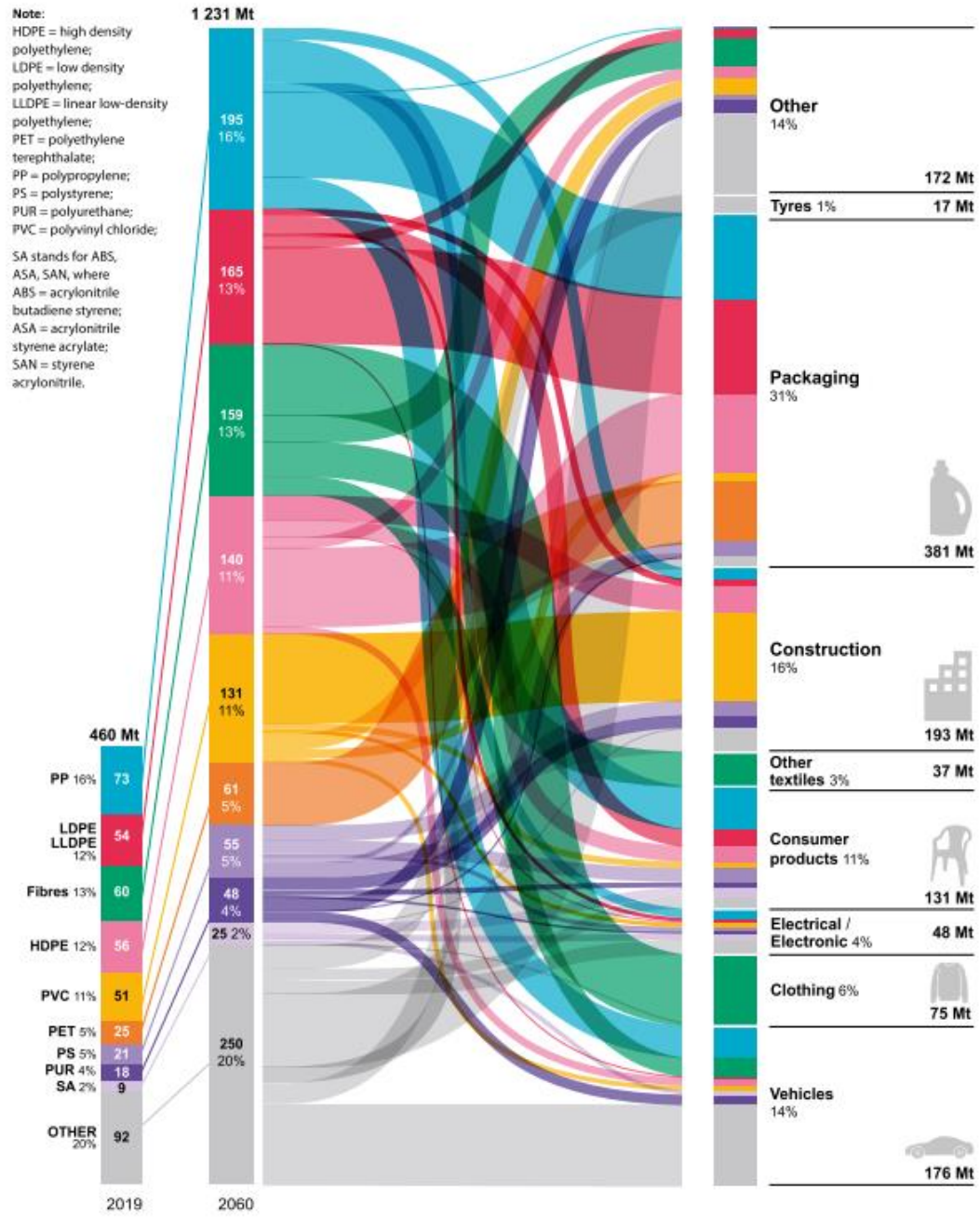

Figure 1. 6: Plastic use in 2019 and 2060 (projection) by polymer type and application (OECD, 2022).

1.4. Fate of plastics in the marine environment

1.4.1. Plastic marine debris (PMD)

The total primary plastic production between 1950 and 2015 has been estimated to amount to 8300 million metric tons. At the same time 6300 Mt of plastic waste has been generated, 4900 Mt of which

have been accumulated in landfills and the environment (Geyer et al., 2017a). Plastic waste originating from the land (open dumping sites, wind and riverine runoff) contributes up to 80 % of the marine plastic debris (Andrady, 2011; Geyer et al., 2017b; Jambeck et al., 2015; Koelmans et al., 2014; Law, 2017). Sea based plastic pollution has been connected with the fishing and tourism sectors (18% of total PMD) and transport accidents and industrial runoffs (Andrady, 2011; Dabrowska et al., 2021). It is considered that 4.8 to 12.7 Mt of plastic waste was introduced in the oceans in 2010 (Jambeck et al., 2015), while the total amount of floating plastics ranges between 93 Mt and 236 Mt (Van Sebille et al., 2015). Taking into account that these quantities could be underestimated by up to 4 or even 16 times, due to the sampling method applied (trawl surveys), 0.4-4 Mt of floating plastic waste has been estimated to exist in the ocean (Lebreton et al., Wayman and Niemann, 2021). At the same time, the concentration of marine plastic waste is expected to keep accumulating, unless measures are taken to limit plastic use and disposal (Ellen MacArthur Foundation, 2017). Plastic waste has been detected in every environmental system, even in the most secluded areas, such as the Antarctica, the Mariana Trench or the top of mount Everest (Caruso et al., 2022; Napper et al., 2020; Peng et al., 2020). It has been even proposed that plastics are a key factor in deciding the transition into a new geological era, the Anthropocene (Zalasiewicz et al., 2016).
It is obvious that the gap between the estimated inputs of floating marine plastic waste and the plastic actually found in the marine environment is huge. Therefore, the question “where is all the plastic?” arises.

1.4.2. Plastic marine debris estimations

The combination of overestimated quantities of plastic entering the marine environment and underestimated quantities of floating plastic could in part explain the disparity between marine plastic inputs and model outputs. The amount of plastic entering the environment has not been adequately quantified. The estimations provided in the literature are based on statistical calculations of municipal waste production and official data of waste management, which may not always be accurate (Jambeck et al., 2015). At the same time, models focusing on marine plastic have been using field sampling results as inputs (Cózar et al., 2014; Eriksen et al., 2014; Van Sebille et al., 2015). These data originate from a limited number of surveys focusing on areas with expected extraordinarily high or low concentrations and do not reflect the values in-between (Lacerda et al., 2019; Sebille et al., 2020). Additionally, they are of heterogeneous nature and often non-comparable since they are greatly affected by the sampling and analysis methods applied by the researchers (Anthony L. Andrady, 2017; Cózar et al., 2014; Law, 2017). It has been highlighted that the most widely used

sampling method, manta nets, cannot collect, and therefore, account for, the smaller fraction of micro- and nanoplastics (Gigault et al., 2016). Thus, a vast amount of floating plastic is ignored by the models, and the resulting underestimations occur.

1.4.3. Removal of plastics from the marine environment

The decrease of plastic concentrations in the marine environment can be attributed to numerous processes taking place throughout their residence time. Breakdown due to mechanical stress, washing up on shores and vertical movements within the water column are the most common mechanical processes. Abiotic degradation is the result of the ultraviolet (UV) fraction of the solar radiation (photodegradation) or the heat from the environment (thermodegradation), while biodegradation refers to the process of plastic deterioration and assimilation by living organisms (Andrady, 2011).

1.4.3.1. Beaching of floating plastic

Plastics can be transported horizontally by currents, winds and waves and finally washed up at beaches (Onink et al., 2021). The removal of plastics to the coastal environment would inevitably lead to lower detection levels in the sea and thus produce lower model outputs.

1.4.3.2. Settling

Benthic systems have been characterized as sinks for unaccounted for plastics (Koelmans et al., 2017). Plastics are indeed the most ubiquitous type of waste found in the deep environments, comprising up to > 90 % of deep water debris (Takada, 2019). Polymers with densities higher than that of seawater (1.035 kg m^{-3}), such as PVC, PS and PET are negatively buoyant, and therefore, expected to settle to the bottom. Numerous studies have been performed on the sinking behaviour of negatively buoyant plastic particles in water in an effort to discern the transport, and subsequently, the fate of these particles in the marine environment. Settling velocities in the range of 86 m day^{-1} to 11 km day^{-1} have been estimated for seawater (Bagaev et al., 2017; Khatmullina and Chubarenko, 2019; Khatmullina and Isachenko, 2017; Kowalski et al., 2016a). It has been demonstrated that factors such as the size, shape and irregularity of the sinking particles affect critical parameters, namely the Reynolds number (Re) and the drag coefficient (C_d), which in turn decide the settling velocity (Chubarenko et al., 2016; Khatmullina and Isachenko, 2017; Kowalski et al., 2016a). Traditional equations, such as these developed by Stokes (1850) and Dietrich (1982a) have been employed, while new equations, empirical and semi-empirical models have been developed

(Francalanci et al., 2021; Nguyen, 2021; Waldschläger and Schüttrumpf, 2019; Yu et al., 2022), to address the inadequate description of plastic particle sinking.

Bottom trawling surveys have revealed that positively buoyant polymers, such as PE and PP, are unexpectedly present in benthic samples (Int-Veen et al., 2021; Kuroda et al., 2020; F. Zhang et al., 2020). Simultaneously, positively buoyant plastics have been found suspended in the water column (Pabortsava and Lampitt, 2020). The residence of positively buoyant plastics in the marine environment allows their interaction with marine organisms which can lead to their subsequent removal in one of the following two ways: On the one hand, plastics can be ingested by aquatic life of all sizes directly or indirectly (Takada, 2019) and incorporated in faecal pellets (Cole et al., 2016) which sink to the deepest parts of the sea as part of the marine snow (Porter et al., 2018). On the other hand, colonization of plastic surfaces by marine biota has the potential to alter their density and hydrophobicity, and as a result their sinking velocity (Cózar et al., 2014; Lobelle and Cunliffe, 2011a; Morét-Ferguson et al., 2010). The development of biofouling leads to increase (Kooi et al., 2017b; Long et al., 2015; Mendrik et al., 2023) or decrease (Kaiser et al., 2017; Nguyen et al., 2020) of the sinking velocity, depending on the characteristics of the environment and the nature of the aggregates formed.

The evidence that plastics settle to the lower layers of the ocean, regardless of their inherent density, is abundant. It has not yet been definitively decided, however, whether plastics reaching the benthos remain there, or whether some mechanisms, for instance bioturbation (Näkki et al., 2017) or bottom shear stress (Ballent et al., 2013), can reverse this process and allow the plastics to be resuspended in the water column (Andrady, 2011). The values of rising velocities of plastic particles in seawater have been estimated between 86 m day^{-1} to 3.7 km day^{-1} (Khatmullina and Chubarenko, 2019; Kooi et al., 2017b; Kukulka et al., 2012; Reisser et al., 2015).

1.4.4. Abiotic Degradation

The degradation of plastics into smaller fragments (microplastics, nanoplastics) which cannot be detected could provide another explanation for the mass balance not being achieved. Degradation is the result of the plastics' interaction with environmental factors; solar radiation, heat, oxygen, water and mechanical stress (S. S. Ali et al., 2021; Andrady, 2011). While mechanical degradation does not result in changes to the molecular weight of the polymer, chemodegradation leads to alterations of the molecular weight (Lambert and Wagner, 2016). The length, composition of the polymeric chain, crystallinity and hydrophobicity determine the susceptibility of each polymer to chemodegradation, since longer chains, absence of heteroatoms in the polymeric backbone, higher crystallinity and

lower hydrophobicity account for increased resistance to degradation. The techniques employed for the production of polymers also affect degradability, since they can result in the presence of unsaturated chromophoric groups, potentially accelerating the initiation of photodegradation, or additives especially integrated in the structure of the polymer to delay degradation (S. S. Ali et al., 2021). Degradation is initiated in the form of photodegradation, with thermo-oxidative degradation and hydrolysis following it (Andrady, 2011). The process of degradation is very slow. The half-lives of common plastics in the marine environment have been estimated in the range between 3.4 (PP) and 1200 years (HDPE). Acceleration of the degradation with UV or heat pre-treatment yielded results in the range 2.3 years (PET) and 530 years (HDPE) (Chamas et al., 2020).

1.4.4.1. Photodegradation

In oxygen rich environments, the interaction of plastic polymers with the UV fraction of the solar radiation leads to optical, namely yellowing due to the production of chiral optical active nanostructures (Elmer-Dixon et al., 2022), and mechanical alterations, such as loss of mechanical properties and embrittlement (Gewert et al., 2015b). The mechanism of photodegradation consists of three steps: initiation, propagation, and termination. For the initiation process, it is required that chromophores, i.e., unsaturated double bonds, are present in the polymeric chain, so that energy is absorbed from the radiation and free radicals are produced from the breakage of C-H bonds. No chromophores are present in the molecular structure of polymers with a C-C backbone, such as PE and PP, and they should be expected to remain unaffected by photodegradation. The presence of impurities or structural abnormalities, however, make the initiation of the photodegradation process possible even for these polymers. In the propagation step, the radicals produced during the initiation step react with oxygen to produce a peroxy radical (ROO•) and at the same time, further radical reactions occur, resulting in auto-oxidation. Thus, chain scission through the Norrish I and II reactions (Singh and Sharma, 2008) and crosslinking take place, increasing or decreasing the molecular weight, accordingly, and causing embrittlement and increase of the active surface of the polymer. Termination occurs when reactions between radicals lead to the production of olefins, aldehydes and ketones containing unsaturated bonds susceptible to further oxidation (Gewert et al., 2015b).

1.4.4.2. Thermodegradation

The thermo-oxidative degradation of plastics requires high temperatures (>100^{o} C) even for the polymer types more susceptible to it (PE, PP), and does not usually occur in marine environment

conditions, unless prior oxidation from the exposure to reactive compounds has occurred (S. S. Ali et al., 2021). The mechanism of thermodegradation is similar to that of photodegradation, with similar by-products. Thermal degradation incorporates two distinct reactions, taking place simultaneously: a random chain scission resulting in molecular weight reduction and a chain-end scission of C-C bonds with volatile products. Naturally, differences between the two processes exist. Thermal degradation can occur at any point of the polymeric chain, not only at a terminal carbon as in photodegradation. Also, thermodegradation takes place throughout the whole sample, and not only on its surface (Singh and Sharma, 2008).

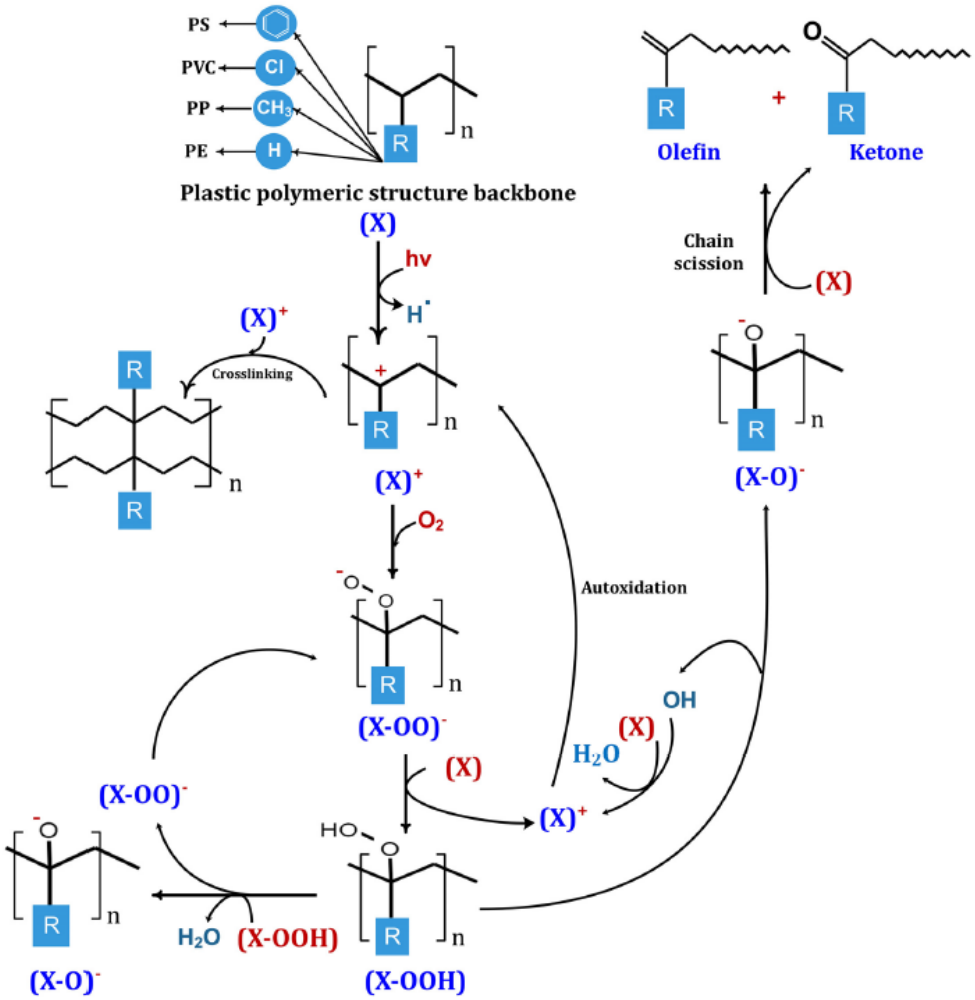

Figure 1. 7: The photodegradation mechanisms of plastics (S. S. Ali et al., 2021).

1.4.4.3. Hydrolysis

Hydrolysis is the reaction of polymers with water producing ionized acids on the polymeric chain. For effective hydrolysis the polymer chain must include hydrophilic, hydrolytically unstable bonds. Polyesters, such as PET, degrade by a simple non-enzymatic, random hydrolytic ester cleavage. The

hydrolysis rate is affected by the molecular weight of the polymer, the mobility and hydrophobicity of the polymer, the chain's stereochemical composition and the concentration of water inside the material. Backbone hydrolysis, especially, is desirable due to the production of low molecular weight products. The hydrolysis process can be accelerated chemically, by ions produced through the reaction itself, or by biological catalysts, i.e., enzymes (S. S. Ali et al., 2021; Singh and Sharma, 2008).

1.4.5. Biodegradation

The biodegradation of traditional fossil based plastics has been considered impossible until very recently (Palmisano and Pettigrew, 1992). Apart from altering the sinking characteristics of plastics, the colonization of their surface and the development of biofilm has been found to facilitate the attachment and proliferation of marine communities with the potential to utilize plastic as a carbon source, called the "plastisphere" (Zettler et al., 2013). Plastic biodegradation is a process which relies on characteristics of the polymer, including molecular weight, shape, size, crystallinity, hydrophobicity and the presence of additives (Ahmed et al., 2018; Yuan et al., 2020). The process of microbial degradation of plastics involves two steps. Initially, microorganisms produce extracellular hydrolytic enzymes (xylanase, lipase, keratinase, protease, chitinase) capable of cleaving the complex polymeric chain into smaller, easily digestible products. These processes are called biodeterioration and biofragmentation (Chandra et al., 2020; R. A. Wilkes and Aristilde, 2017; Yuan et al., 2020). The initial chain scission step can also be performed abiotically, through a pre-treatment step including photodegradation (Gewert et al., 2018; Romera-Castillo et al., 2018; Ward et al., 2019) or mechanical degradation (Ekvall et al., 2019; Enfrin et al., 2020). It was also recently discovered that hydrocarbon degrading bacteria, also degrading PE, possessed the potential to produce reactive oxygen species (ROS) capable of oxidizing the polymer similarly to abiotic processes (Zadjelovic et al., 2022).

When the polymeric chain has been broken down into oligomers, dimers or monomers, the second step of biodegradation is the excretion of intracellular enzymes capable of mineralization into H_20 and CO_2, which are later assimilated by the microorganisms as a carbon source (Lin et al., 2022; Thakur et al., 2023; Zhang et al., 2021).

Microbial taxa with the potential to biodegrade various types of plastic have been identified among bacteria, fungi and recently algae (Ahmed et al., 2018; S. S. Ali et al., 2021; Thakur et al., 2023). Fungi in particular, with the potential to secrete enzymes capable of degrading complex natural polymers, such as lignin (laccases) and polyesters (cutinases), have been identified as effective plastic degraders (Srikanth et al., 2022). Two genera have been highlighted for their plastic degrading capacity: Aspergillus (Esmaeili et al., 2013; Muhonja et al., 2018; Sangeetha Devi et al., 2015; Sarkhel

et al., 2020) and Penicillium (Manzur et al., 2004; Ojha et al., 2017).

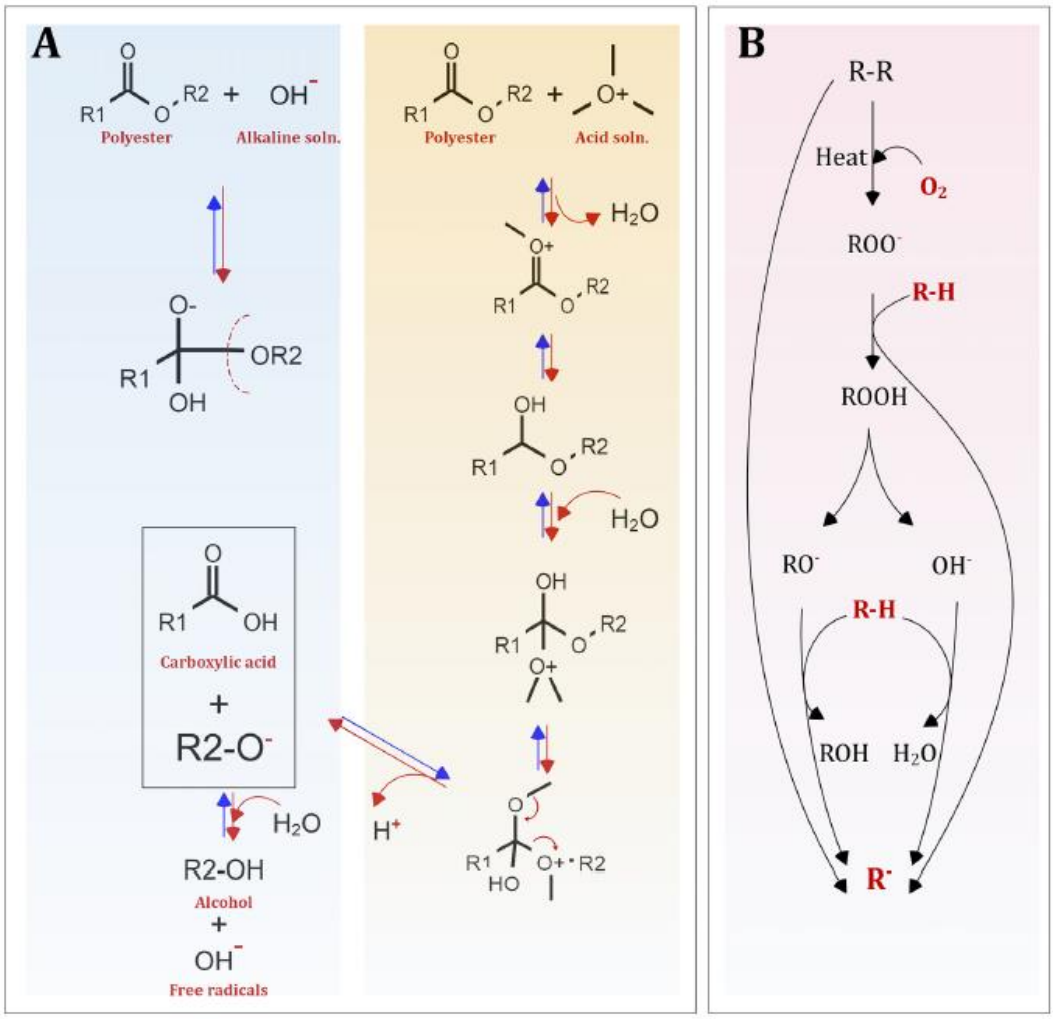

Figure 1. 8: (A) The mechanisms of polyester hydrolysis, (B) the mechanism of polyester thermos-oxidative degradation (S. S. Ali et al., 2021) .

Among the bacterial plastic degraders genera such as the versatile degrader *Pseudomonas*(Balasubramanian et al., 2010; Cox et al., 2018; Taghavi et al., 2021)*, Bacilli* (Auta et al., 2018; Harshvardhan and Jha, 2013; Maroof et al., 2021; Muhonja et al., 2018; Sudhakar et al., 2007; Yang et al., 2014)*, Vibria* (Danso et al., 2018; de Vogel et al., 2021; Raghul et al., 2014; Sarkhel et al., 2020; Sudhakar et al., 2007) and the pioneering PET degrader *Ideonella sakaiensis* (Austin et al., 2018; Palm et al., 2019; Yoshida et al., 2016), can be found.

Most of the putative plastic degraders identified so far have been isolated by soil environments, rather than freshwater or seawater (S. S. Ali et al., 2021). Recently it was estimated than only 25% of the plastic degrading fungi originate from the marine environment, where most plastic waste accumulates (Ekanayaka et al., 2022).

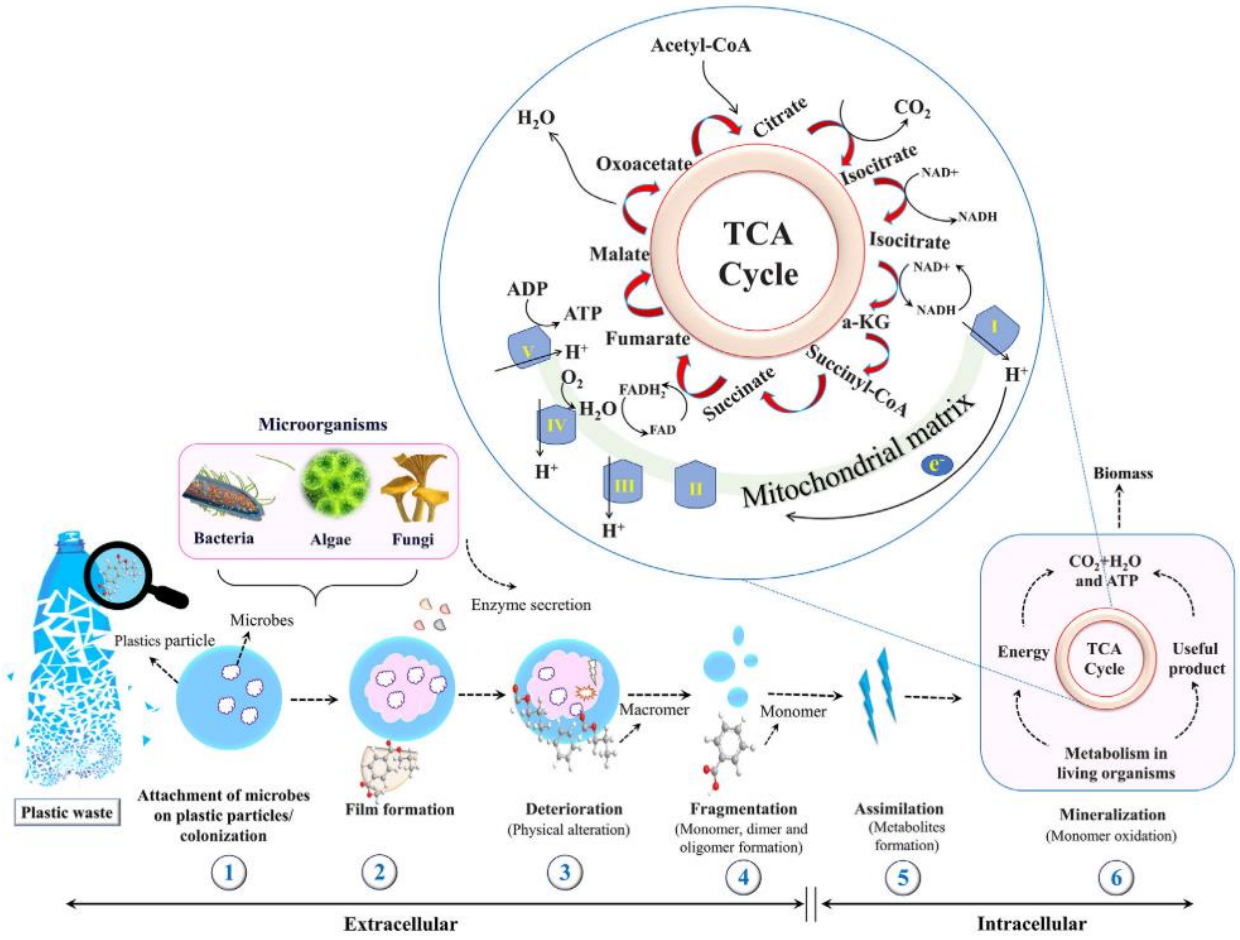

Figure 1. 9: Schematic of plastic biodegradation (Bacha et al., 2023).

The biodegradation of plastics can be monitored by examining changes in the visual, mechanical, thermal or chemical characteristics of the polymers. Microscopy, and more specifically scanning electron microscopy (SEM), is very commonly applied for the visualization of changes to the surface of the samples. Changes in the macromolecular structure of the polymer are observed by spectroscopy, mainly Fourier-transform infrared (FTIR), or chromatographic methods, such as gel permeation chromatography (GPC), high temperature GPC, thin layer chromatography (TLC), gas chromatography–mass spectrometry (GC–MS), high performance liquid chromatography (HPLC), X-ray photoelectron spectroscopy (XPS), and nuclear magnetic resonance (NMR). Thermal gravimetric analysis (TGA), thermogravimetry/derivative thermogravimetry/differential thermal analysis (TG-DTG-DTA), and differential scanning calorimetry (DSC) have been applied for the examination of physicochemical characteristics of the degrading polymer. The biodegrading communities were initially observed microscopically, but the development of next generation sequencing and

metagenomics has provided the scientific community with a clearer picture of the plastic degrading communities and the participating genera. The mineralization of plastics is commonly quantified respirometrically, by the measurement of CO_2 production in closed systems (Matjašič et al., 2021).

1.5. Plastic debris classification

Plastic debris can be categorized based on several criteria: type, colour, origin, intended usage, erosion level, solid state, polymer composition, size. Color, polymer composition and usage are straightforward descriptive concepts. The type of plastic debris can be classified into fragments, pellets, filaments, plastic films, foamed plastic, granules, or styrofoam. The erosion level varies between virgin and weathered, while the solid state can be solid, semi-solid, waxlike, or liquid (Hartmann et al., 2019).

On the basis of size, plastics can characterized as macroplastics, mesoplastics, microplastics or nanoplastics (Hartmann et al., 2019; Hidalgo-Ruz et al., 2012). Despite it being critical for the collection and comparison of plastic size classes, as well as the examination of their properties and adverse effects on the environment, no unanimous verdict has been reached on the matter of plastic debris size (Hartmann et al., 2019). The Joint Group of Experts on the Scientific Aspects of Marine Environmental Protection (GESAMP) have proposed that plastic debris with a nominal size of >25 mm be considered as macroplastics, 5-25 mm mesoplastics, 5 mm – 1 μm microplastics and < 1 μm nanoplastics (GESAMP, 2019). In literature, however, it is possible to encounter alternative definitions. Some researchers have been ignoring the mesoplastic class completely, by dividing it between microplastics and macroplastics (Bergmann et al., 2015; Browne et al., 2007; Moore, 2008). Microplastics have been placed also in size ranges between 1 – 20 μm (Ryan, 2015; Thompson, 2004; Van Cauwenberghe et al., 2015), 62 - 5000 μm (Desforges et al., 2014), <1 mm (Andrady, 2011; Browne et al., 2011; Claessens et al., 2011). Particles as large as 20 μm have been characterized nanoplastics (Wagner et al., 2014). At the same time 335 nm have been also proposed as the largest size for nanoplastics (Koelmans et al., 2017). Based on the industrial definition of nanoparticles, 100 nm have also been used as the maximum value of the nominal diameter of nanoplastics (Bergmann et al., 2015; Mattsson et al., 2015).

The first mention of nanoplastics as a separate class was made by Koelmans et al. in Bergmann et al. (2015). The fact that they were recognized so late, compared to plastic debris and microplastics has to be linked with the fact that their small size made their detection in the marine environment impossible. Analytical techniques used for macro-, meso- and microplastics were generally inadequate at detecting and quantifying microplastics and nanomaterial technologies had to be

applied (Wayman and Niemann, 2021). The separation of nanoplastics from the rest of the plastic debris was vital since their small size stipulates colloid behaviour (Gigault et al., 2018). Their motion is dictated by Brownian motion, rather than shape and density (Hassan et al., 2015). Thus they can remain suspended in the water column and not sink to the bottom or float to the surface of the sea, depending on their buoyancy. At the same time, aggregation plays a major role in the fate of nanoplastics in the marine environment. During their residence in the sea, they aggregate with similar (homoaggregation) or different colloid particles (heteroaggregation) (Oriekhova and Stoll, 2018) to form larger particles with distinct electric and physicochemical properties (aggregates) (Alimi et al., 2018; Mattsson et al., 2018, 2015; Wagner and Reemtsma, 2019), which potentially sink to the bottom (K. Kvale et al., 2020; K. F. Kvale et al., 2020).

Origin-wise, microplastics and nanoplastics can be characterized as primary or secondary. Primary plastic particles have been intentionally produced in this size for commercia use and directly released into the marine environment. They are typically added to personal hygiene products, but they can also originate from leaks or transport accidents of production pellets used in the plastics industry (Friot and Boucher, 2017). Additionally, microfibers released while washing synthetic textiles through wastewater treatment systems into the sea (Gaylarde et al., 2021), as well as particles from vehicle tyres carried by rainwater runoff and rivers are considered primary microplastics (Jan Kole et al., 2017). Secondary plastic particles are the result of the weathering, degradation and subsequent fragmentation of larger plastic debris as they reside in the environment and interact with and within it (Malankowska et al., 2021).

1.6. Analytical Techniques for Microplastic and Nanoplastic detection

For the detection and analysis of microplastics and nanoplastics several techniques can be applied, with microscopy, spectroscopy and thermal degradation being the most widely used. Each method can be applied separately, but a combination of two or more of them has been proposed, to provide exact and accurate results.

1.6.1. Microscopy

Microscopy, in combination with the use of fluorescent dyes, such as Nile Red, has been one of the first methods for microplastic identification. Application of microscopy for plastic particle examination can be very time consuming and since it comprises of visual observation of the samples, it is characterized by low accuracy. Scanning microscopy, in the form of scanning electron microscopy (SEM) or transmission electron microscopy (TEM) enable the observation of plastic particles of very

small sizes. Coupling of SEM/TEM with energy-dispersive X-ray spectroscopy (EDS) can help increase analysis accuracy. The number of sizes which can be analysed thus is limited not only by time availability, but also by the high cost of the equipment (Woo et al., 2021).

1.6.2. Spectroscopy

Spectroscopy has been used in the majority of plastic related literature body. Fourier transform infrared spectroscopy (FTIR) and Raman spectroscopy, combining laser and microscopy technologies, are the two methods widely applied. They involve a non-destructive examination of the chemical composition on the surface of the samples and can provide polymer identification, as well as information on oxidation, and therefore, degradation. FTIR can be used in transmittance, reflectance, or attenuated total reflectance (ATR) mode, with the latter obtaining highly accurate spectra due to the contact of the equipment with the samples, regardless of their surface properties. Raman spectroscopy can also provide information on the crystallinity of the samples. Recently, micro-ATR-FTIR and micro-Raman technologies were developed, enabling the examination of particles as small as 50 μm, and the added benefit of potential for microscope coupling. Raman, reflectance FTIR and ATR-FTIR spectroscopy do not require prior sample pre-treatment and are thus fast. The main disadvantages of spectroscopy involve the increased cost of the equipment and desired high degree of expertise for spectra evaluation. Furthermore, the existence and manipulation of appropriate libraries are crucial for accurate sample examination. Finally, application of ATR spectroscopy requires contact of the probes with the samples, and therefore can result in sample damage (Woo et al., 2021).

1.6.3. Thermal analysis

Thermal analysis can be applied for the identification of polymers, as well as their degradation products. Through differential scanning calorimetry (DSC) the changes in dissolution, crystallization, transition temperatures, and corresponding enthalpy and entropy are examined for polymer identification. Thermogravimetric analysis (TGA), on the other hand, examines the dependence on time and temperature by measuring the weight loss of the sample while heating it at specific rate under given atmospheric and temperature conditions to quantify and identify it. Pyrolysis-gas chromatography mass spectrometry (Py-GC-MS) pyrolyzes plastics into gasses, separates and analyses them by applying GC-MS. The obtained pyrograms can be determined by comparing them to known polymer standards. All three methods are characterized by limitations to the type of polymer which can be analysed (Woo et al., 2021).

1.7. Entry pathways and impacts of plastics in living organisms

Plastics in the air, soil, and water have financial and societal impacts, but more importantly, they interact with organisms of all sizes and classifications, including humans (Werner et al., 2016). Plastic can impact organisms in two ways: directly via ingestion and entanglement (Wright et al., 2013), and indirectly by the adsorption of additives, chemical compounds and pollutants (Bergmann et al., 2015). Microplastics, nanoplastics and plastic-associated additives can enter the human body mainly through ingestion, respiration or even through the skin (Rubio et al., 2020). The fact that the gastrointestinal tract is the main entryway of plastics into the human organisms is not surprising. Microplastic and nanoplastic particles have been not only been detected in seafood, such as mussels, oysters, shrimp and fish (Jinadasa et al., 2023; Kumar et al., 2022) and sea salt (Iñiguez et al., 2017; Karami et al., 2017; Kim et al., 2018; Kosuth et al., 2018), but also in milk, beer and honey (Diaz-Basantes et al., 2020; Kutralam-Muniasamy et al., 2020; Shruti et al., 2020a). Fruit and crops, especially root vegetables, have been found to contain microplastics (Oliveri Conti et al., 2020). Part of the detected microplastics and nanoplastics can be attributed to release from food packaging (Claudia et al., 2022). At the same time, plastic particles have been detected not only in bottled water (Danopoulos et al., 2020; Kankanige and Babel, 2020; Schymanski et al., 2018), but also in tap water (Shruti et al., 2020b; Tong et al., 2020) and ground water (Kumar et al., 2021).

1.7.1. Aquatic life

The marine environment, as a major sink of plastic waste, is the most heavily affected by plastics, including the biota inhabiting it (Lamichhane et al., 2023). Plastics have been found to affect 817 species, 519 of which belong in marine or coastal ecosystems. Plastic entanglement and ingestion affect not only fish, but also birds and marine mammals. Ingestion of plastics results in decreased sense of hunger, food capture ability and digestion. Entanglement, most commonly in lost or discarded fishing gear, also known as ghost nets, compromises the general body condition and mobility, leading to decreased food capture, predator escape and reproduction abilities. Filter feeding and bottom detritus feeding organisms are more likely to indiscriminately consume plastics (CBD, 2016). Micro and nanoplastics have been found to attach on the external organs of organisms, i.e. mussels, and thus enter their bodies (Kolandhasamy et al., 2018).

Plastics contain additives, such as heavy metals, which can be released, causing toxicity (Meng et al., 2021). At the same time, during their residence in the marine environment, plastics can absorb persistent pollutants, such as polycyclic aromatic hydrocarbons (PAHs), polychlorinated biphenyls

(PCBs) or polybrominated diphenyl ethers (PBDEs), concentrate them to orders of magnitude higher concentrations and adsorb them in the bodies of marine organisms, with negative effects, such as hepatic stress, endocrine disruption and carcinogenesis (Jiang et al., 2020; Mato et al., 2001; Rochman et al., 2013). Complex interactions between microplastics and antibiotics have been observed and linked with the expression of antibiotic resistant genes and their implications for human and marine life (Syranidou and Kalogerakis, 2022).

Marine microbial communities consisting of bacteria, fungi, algae, diatoms, among other taxa have been found to successfully colonize plastic marine debris and thrive, forming the so-called "Plastisphere". The plastic attached communities are characterized by complex structures and succession patterns and have been potentially linked with plastic biodegradation (Amaral-Zettler et al., 2020; Robyn J. Wright et al., 2020; Zettler et al., 2013). Plastics floating in the ocean, especially after catastrophic events, namely tsunamis, have been found to act as vectors for the transfer of invasive species, with the potential to alter the equilibrium within the hosting ecosystems (Calder et al., 2014; Goldstein et al., 2014). Microplastics have also been found to affect the permeability and thermal properties of sediments, which could, in turn, affect the well-being of sediment dwelling organisms, especially temperature sex-determined species (Carson et al., 2011). Organisms residing on plastic marine debris could have additional negative effects, since they could be vectors for the transfer of pathogenic species (Beloe et al., 2022; Bowley et al., 2021).

The effects of plastic waste on living organisms are size dependent. Smaller particles, such as nanoplastics, can be ingested by a larger number of organisms, while at the same time, more incorporation pathways are available. Bioaccumulation of microplastics and nanoplastics within marine trophic levels has been supported by the existing literature, however, these findings have not yet been confirmed throughout the generalized trophic network (Miller et al., 2020). Additionally, smaller particle size is linked with higher surface area and subsequent leaching of additives and absorbed pollutants, the bioaccumulation of which, has not yet definitely recognized (Miller et al., 2020; Oliveira and Almeida, 2019). Knowledge on the interactions of nanoplastics with biota is limited and comes mostly from laboratory studies. This is attributed to the lack of measurement techniques in the environment, despite them being able to affect multiple systems within individuals, as well as populations (Gong et al., 2023; Wang et al., 2021; Wayman and Niemann, 2021).

1.7.2. Human health

Studies on the effects of microplastics and nanoplastics on humans are very limited, compared to marine life. Microplastics have been detected in the human body, including human stool (Schwabl et

al., 2019) and placentas (Ragusa et al., 2021). Most of the studies have been performed in vitro (Kumar et al., 2022).

Residence of trapped microplastic particles in the lungs has been connected to pulmonary diseases, namely asthma, pneumonia kai pneumothorax (Prata et al., 2020). It has been found that microplastics and nanoplastics can enter cells (Gratton et al., 2008) and penetrate the gut barrier and enter the circulation ante interfere with iron absorption (Mahler et al., 2012; Rahman et al., 2021). Once out of the gut, microplastics have the potential to cause tissue obstructions (Pedà et al., 2016) and accumulate in the intestine, lungs, and kidneys, altering lipid and energy metabolism and causing oxidative stress and neurotoxicological effects (MohanKumar et al., 2008; Powell et al., 2007). The same researchers also concluded that microplastics can interact with large proteins and interfere with blood circulation, cause intestine immune system modifications and finally, inflammation. Nanoplastic toxicity has been linked with acute inflammation and apoptosis (Choi et al., 2020; Lambert et al., 2017), as well as neurodegeneration and movement impacts in nematodes (Fouad et al., 2018; Li et al., 2017). Plastics can also affect human fertility (D'Angelo and Meccariello, 2021).

The toxicity of microplastics and nanoplastics can also be traced back to their absorption of heavy metals, for instance chromium, the presence of which in the human organism can cause neurological disorders(Liao and Yang, 2020) . Similarly to the effects of absorbed persistent organic pollutants on marine organisms, humans exposed to them via microplastics can suffer cancer (Kumar et al., 2022; Rahman et al., 2021).

Chapter 2. Thesis Objectives

‘


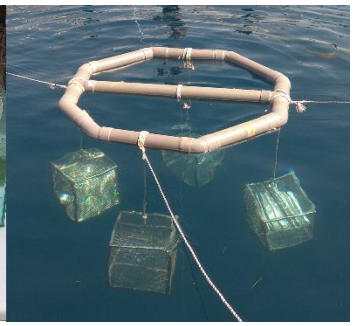

It is obvious that the processes affecting the Global Plastic Budget are numerous and intricately interdependent.

The aim of this work is to examine and deconvolute some of the processes involved in the plastic mass budgets and their interactions, which, despite the rapidly growing body of literature on the topic of plastic pollution, remain mostly obscure. The answers to the following research questions will be sought:

Research question 1: How do the main processes, namely photodegradation, biodegradation, settling and (bio)fragmentation affect the plastics encountered and quantified in the marine environment?

Research question 2: Do interactions between the processes exist? What role does stochasticity play during these interactions?

Research question 3: Is the quantification of the processes possible? Can it be translated into mathematical expressions and model-ready factors?

Research question 4: Which are the key players in the south-eastern Mediterranean plastisphere? Are these communities stable or affected by environmental processes? Does acclimatization play a role in their biodegradation potential?

Research question 5: Is there transferability between different scale experiments? Can laboratory and mesocosm experiments be effectively employed for the examination of such a complex network of processes and their interactions?

To answer these questions, experiments of all scales, from laboratory scale microcosms and mesocosms to field incubation, were designed. Results were produced by the application of traditional plastic pollution analysis techniques (SEM, FTIR, ATR-FTIR, UV-vis spectrometry) in conjunction with novel ones (flow cytometry, next generation sequencing, dynamic light scattering) and advanced data analysis methods.

The main novelty of this dissertation comes with the scale-up approach. Works found in the plastic pollution literature are working in one or two of the scales described here. The transition from a

small, easily controllable microcosm experiment to the mesocosms and finally to the field incubation, while applying similar techniques, wherever that was possible and appropriate, allowed our results to be comparable.

At the same time, considering the vast timescale necessary for the examination of plastic degradation, our experiments are among the longest running which have been performed. The use of several polymer types made it possible to examine their separate behaviour under the same conditions. Most importantly, the use and contrast of virgin and weathered pellets facilitated a "crystal ball" approach, according to which the incorporation of a longer timescale was possible.

The correlation between fouling development and sinking behaviour of plastic samples, including non-spherical mesoplastic films, is studied here for the first time, by employing a novel semi-theoretical approach.

Finally, the composition and succession of the plastic polluted south-eastern Mediterranean has not been examined before. The contribution of the data on fungal taxa to the scientific community is considerable, since marine putative fungal degraders of plastic are understudied and largely ignored, despite their theoretical potential.

Chapter 3. Nanoplastic generation from secondary PE microplastics: Microorganism-induced fragmentation

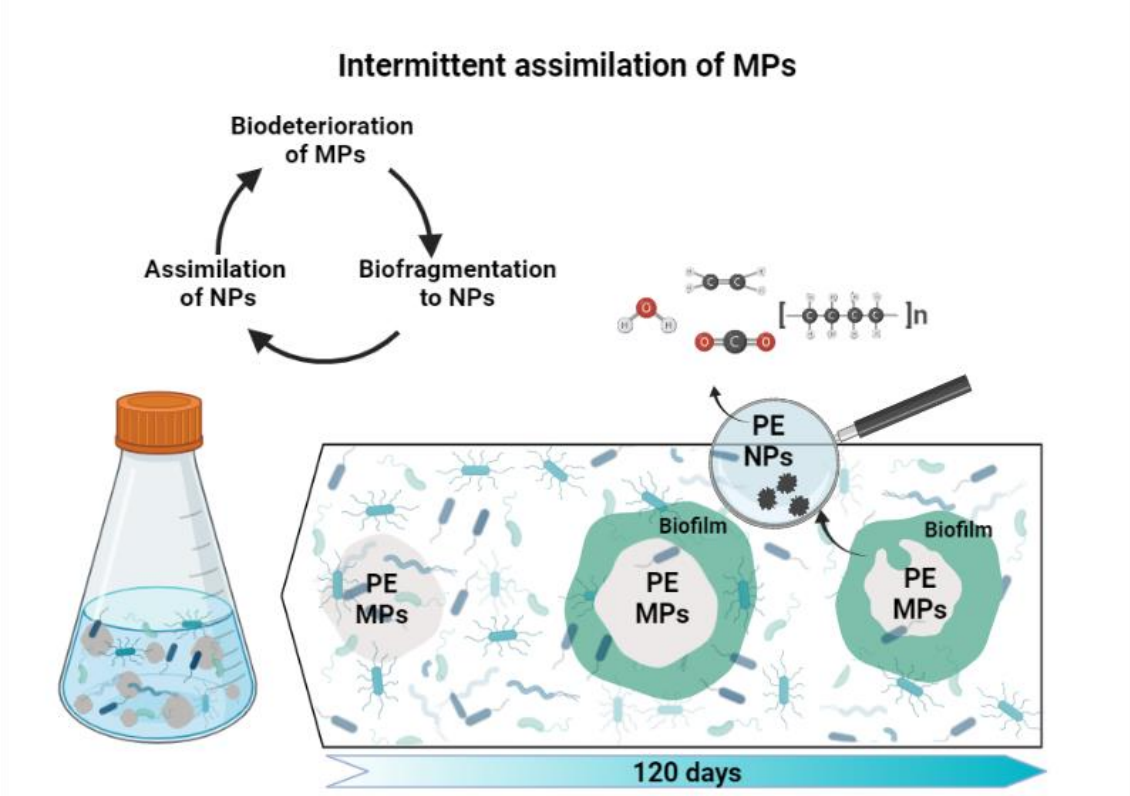

Published as:

Karkanorachaki, K., Tsiota, P., Dasenakis, G., Syranidou, E., Kalogerakis, N., 2022. Nanoplastic Generation from Secondary PE Microplastics: Microorganism-Induced Fragmentation. *Microplastics* 1, 85–101.

3.1. Abstract

Concern regarding the pollution of the marine environment with plastics has been rising in recent years. Plastic waste residing in and interacting with the environment fragments into secondary particles in the micro- and nanoscale, whose negative impacts on the environment are even greater than those of the parent items. In this work, secondary high-density polyethylene (HDPE) and low density polyethylene (LDPE) microplastics were produced by irradiation of virgin films following mechanical fragmentation. The fragments with size ranging from 250 μm to 2 mm were selected for subsequent microcosm experiments. Incubation for 120 days in seawater inoculated with two marine communities, Agios, acclimatized to utilizing plastics as a carbon source, and Souda, as was collected at the Souda bay (Crete, Greece), resulted in biofilm formation by polyethylene (PE) degraders. Monthly FTIR (Fourier-transform infrared spectroscopy) examination of the samples revealed changes in the chemical structure of the surface of the polymers. Dynamic light scattering (DLS) was employed and nano- and microparticles with sizes in the range between 56 nm and 4.5 μm were detected in the seawater of inoculated microcosms. It was thus demonstrated that weathered plastics particles can biodeteriorate and biofragment as a result of biofilm attachment, resulting in the production of nanoplastics due to microbial activity.

3.2. Introduction

Plastics are high molecular weight polymers with excellent chemical and physical properties. Due to improper waste management schemes, accumulation of plastics in marine, freshwater, and terrestrial environments keeps on increasing (Gong and Xie, 2020). A large quantity of plastic particles ends up in the marine environment; 270,000 t of plastics have been estimated to float in the world's oceans, with current convergence areas being most heavily affected such as the ocean gyres, and enclosed water bodies, like the Mediterranean Sea (da Costa et al., 2016; Eriksen et al., 2014).

Plastics contribute to about 80 to 85% of marine litter (Auta et al., 2017) while fragments constitute the majority of marine plastic litter in terms of abundance in the ocean (Cózar et al., 2014). Particle size distributions follow a power law for fragments while the maximum is frequently observed at ~1 mm (Kaandorp et al., 2021). Based on the production process, microplastics (MPs) can be divided into primary when they are fabricated as such and secondary MPs as a result of fragmentation (Malankowska et al., 2021). When plastics are immersed in the marine environment, they undergo ageing and size transformations due to abiotic and biotic processes. Exposure to ultraviolet (UV)

radiation at simulated coastal conditions, followed by mechanical abrasion resulted in the production of thousands of secondary plastic (Song et al., 2017a).

In turn, fragmentation favors biodegradation since it increases the surface to volume ratio (Rummel et al., 2017). Moreover, the fragmented plastics have also reduced molecular weight and therefore biodegradation can more readily occur (Singh and Sharma, 2008). In general, plastic degradation is accomplished by the synergy of abiotic factors and microorganisms (Kumar et al., 2020). Microbial degradation of plastic particles involves steps such as colonization, biodeterioration, biofragmentation, assimilation, and mineralization (I. Ali et al., 2021). Biofilm formation through the microbial adhesion and production of various proteins and polysaccharides results in significant physicochemical alterations on the surface. Biofragmentation of plastics as a result of primarily enzymatic activity follows. Until now, the generation of NPs referred to as particles with the largest dimension below 1 μm, has been demonstrated as part of the degradation of plastic particles mainly due to UV irradiation (Gigault et al., 2016; Sorasan et al., 2021) while no studies have demonstrated the presence of NPs due to microbial activity.

Few studies have demonstrated the ability of marine as well as terrestrial microorganisms to degrade plastics (L. Liu et al., 2021; Raddadi and Fava, 2019), while the information concerning the degradation of weathered plastics is scarce (Auta et al., 2018; Syranidou et al., 2019a). The aim of this study was to investigate the effect of one acclimated (Agios) and one indigenous (Souda) marine community on the physicochemical properties of PE (HDPE and LDPE) secondary MPs in marine microcosms. The colonization process was investigated in conjunction with the monitoring of the impact on the chemical properties of the surface of secondary MPs, toward understanding the generation of and NPs.

3.3. Materials and Methods

3.3.1. Materials/ Generation of secondary MPs

High-density polyethylene (HDPE) and low-density polyethylene (LDPE) films with a thickness of 0.1 mm were obtained from Plastika Kritis S.A. (Heraklion, Greece). They were cut in strips with dimensions 10 cm x 1 cm and exposed to artificial UV-A radiation using 6 Sylvania F36 T8 BLB lamps (emission spectral peak at 365 nm). Irradiation was performed in a closed sand system (Figure 3.1) for a period of time until application of mild mechanical stress would cause fragmentation. The temperature of the system and the amount of radiation were monitored constantly using two Onset HOBO Temperature Light 3500 DP Loggers.

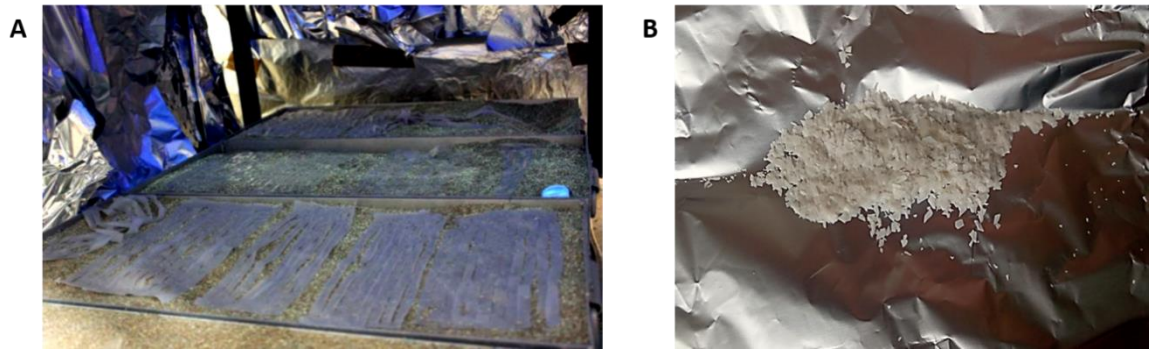

*Figure 3. 1: (**A**) HDPE and LDPE films and (**B**) HDPE secondary microplastics with size 250 μm–2 mm.*

Sufficient fragmentation was observed in HDPE and LDPE films after 5 and 7 months of irradiation, respectively. Complete fragmentation was achieved by the application of mild mechanical stress in rotating borosilicate glass bottles containing sieved sand (Kalogerakis et al., 2017). The plastic fragments went through a size exclusion process, employing two sieves with pore sizes of 2 mm and 250 μm. Fragments of the desired size (250 μm–2 mm) were weighed and separated in 50 ± 2 mg groups. The samples were sprayed with a 70% water~ethanol (completely denatured with 1% ethyl methyl ketone, 1% isopropyl alcohol, 1 g/100 L denatonium benzoate, Merck, Kenilworth, NJ, USA) solution for sterilization and left to dry in an incubator at 37 °C for 3 days prior to placing them in the seawater microcosms.

3.3.2. Biodegradation Assays

3.3.2.1. Marine Communities

Two different marine consortia were used in this study to assess their degradation ability. The community "Agios" is an acclimated consortium, previously developed in previous studies, capable of degrading PE films. The community consists predominantly of the phyla of Proteobacteria (Alphaproteobacteria and Gammaproteobacteria), Bacteroidetes, and Actinobacteria. Additionally, the expression of the *alk*B gene, which has been linked to both hydrocarbon and plastic polymer biodegradation, has been observed (Syranidou et al., 2017c). An indigenous community collected from Souda bay (Crete, Greece) was also exploited. For the isolation of the indigenous community, seawater was collected from Souda bay and was cultured in Erlenmeyer flasks containing 200 mL of DSMZ 453 medium for 7 days at 25 °C in the presence of PE films. The biofilm attached on the films was harvested by gently scraping the surface of the films and cultured anew in DSMZ 453 medium. The community was removed from the culture medium by centrifugation, diluted in sterile seawater, and used for inoculation of the biodegradation experiments ("Souda").

3.3.2.2. Experimental Design

A microcosm experiment was conducted in sterilized flasks in triplicate using HDPE and LDPE secondary MPs as the sole carbon source. A total of twelve flasks per treatment were employed. In each microcosm, 50 mL sterile enriched filtered seawater, 50 mg sterile PE fragments along with the consortia (starting concentration: 10^5 cells mL^{-1}) were added. Sampling occurred at the end of each month by permanently removing 3 flasks per treatment. The experiment was conducted in 25 °C in darkness, under continuous shaking at 120 rpm and lasted for 4 months. Abiotic controls, containing sterile enriched filtered seawater and sterile PE fragments, were incubated for the same period of time in the dark, so as to avoid photodegradation.

3.3.2.3. Viable Cell Concentration and Extracellular Polymeric Substances

Pieces of 250 μm plankton mesh were used for the capture of the PE secondary MPs from the flasks. All the particles retained within the mesh were subsequently washed with 2% *w*/*v* sodium dodecyl sulfate (SDS) in order to remove the biofilm from the surface. The biofilm cells were serially diluted and spread on rich medium plates (DSMZ 453) in order to estimate the cell concentration, along with protein measurements. The concentration of proteins was determined according to the modified Lowry Protein Assay Kit protocol (LOWRY et al., 1951).

3.3.3. FTIR

The chemical structure alterations of the samples were examined using Fourier-transform infrared spectroscopy (FTIR). A small quantity of each sample (3–5 mg) was incorporated in KBr pellets in a 1:10 ratio. The spectra were obtained using a Frontier FTIR spectrometer (PerkinElmer, Waltham, MA, USA) and analyzed using Spectrum software (PerkinElmer, Waltham, MA, USA). For each sample 64 scans were performed, with a scan resolution of 4 cm^{-1} in the 4000–450 cm^{-1} absorbance range. Chemical changes on the surface of the microplastics were monitored monthly, by calculating the following indices using the absorbance values from the respective spectra (Anthony L Andrady, 2017):

$$Keto\ Carbonyl\ Bond\ Index\ (KCBI) = \frac{A_{1715}}{A_{1465}} \quad (1)$$

$$Ester\ Carbonyl\ Bond\ Index\ (ECBI) = \frac{A_{1740}}{A_{1465}} \quad (2)$$

$$Vinyl\ Bond\ Index\ (VBI) = \frac{A_{1650}}{A_{1465}} \quad (3)$$

$$Internal\ Double\ Bond\ Index\ (IDBI) = \frac{A_{908}}{A_{1465}} \quad (4)$$

3.3.4. Nanoparticle Detection–Light Scattering

The presence of plastic particles of micro or nano scale in the microcosms was investigated monthly using dynamic light scattering (DLS), with a SALD-7500nano particle analyzer (Shimadzu, Japan). Following the measurement of a blank sample of fresh seawater, a volume of 5 mL of seawater from the mesocosms was analyzed using WingSALD II version 3.1.1 in terms of both volume and number of particles every month. DLS results are reported as particle diameter in μm versus number of particles or volume of particles. While the former allows for maximum concentration sensitivity, the latter provides information on larger particles that are not well represented in the samples in terms of number.

3.3.5. Data Analysis

Statistical analysis of the data was implemented using R version 4.0.0 (R Core Team, Vienna, Austria) in the environment RStudio version 1.3.959. Data normality was conducted using the Shapiro–Wilk test. Depending on data normality, the Kruskal–Wallis non-parametric test and one-way ANOVA were used to detect statistically significant differences between samples. The package ggplot2 was used for data visualization.

3.4 Results

3.4.1. Biofilm Populations on PE Secondary Microplastics

Biofilm populations on the surface of the secondary microplastics increased from the 10^5 cells mL^{-1} initially added to the microcosms. Cell abundances in the microcosms inoculated with the acclimated Agios community were consistently higher than those inoculated with the Souda community (Figure 3.2). The growth observed after 30 days of incubation was statistically significant; the Agios community achieved an average of 1.44 logCFU mL^{-1} increase (Figure 3.2B) when utilizing HDPE microplastics as sole carbon source. For LDPE, average increases of 0.93 logCFU mL^{-1} (Souda community) and 2.26 logCFU mL^{-1} (Agios community) could be observed in 30 days (Figure 3.2C,D). The only exception to that pattern was exhibited by the Souda community in microcosms containing HDPE microplastics. While in the first 30 days the cell growth was minimal, statistically significant

growth was noted between the 30th and 60th day, reaching an average increase of 1.3 logCFU mL^{-1}. A decrease of 0.74 logCFU mL^{-1} was followed by an almost equal increase of 0.71 logCFU mL^{-1} to a final average viable cell concentration of 6.45 ± 0.15 logCFU mL^{-1} at the end of the incubation period (Figure 3.2A). The acclimated Agios community behaved similarly, regardless of the type of MPs provided as carbon source. Viable cell concentrations increased for 60 days, reaching maximum average values of 7.29 ± 0.44 logCFU mL^{-1} and 7.58 ± 0.52 logCFU mL^{-1} when incubated with HDPE and LDPE respectively. For the remainder of the experiment a decrease of cell concentrations led to final values of 6.61 ± 0.16 logCFU mL^{-1} for LDPE microcosms and 6.11 ± 0.29 logCFU mL^{-1} for LDPE microcosms (Figure 3.2B,D). Souda community cell populations increased until the 90th day up to 6.70 ± 0.76 logCFU mL^{-1}, when a decrease to a final concentration of 6.24 ± 0.38 logCFU mL^{-1} was observed (Figure 3.2C). Viable cell concentration evolution over time was statistically significant among all treatments.

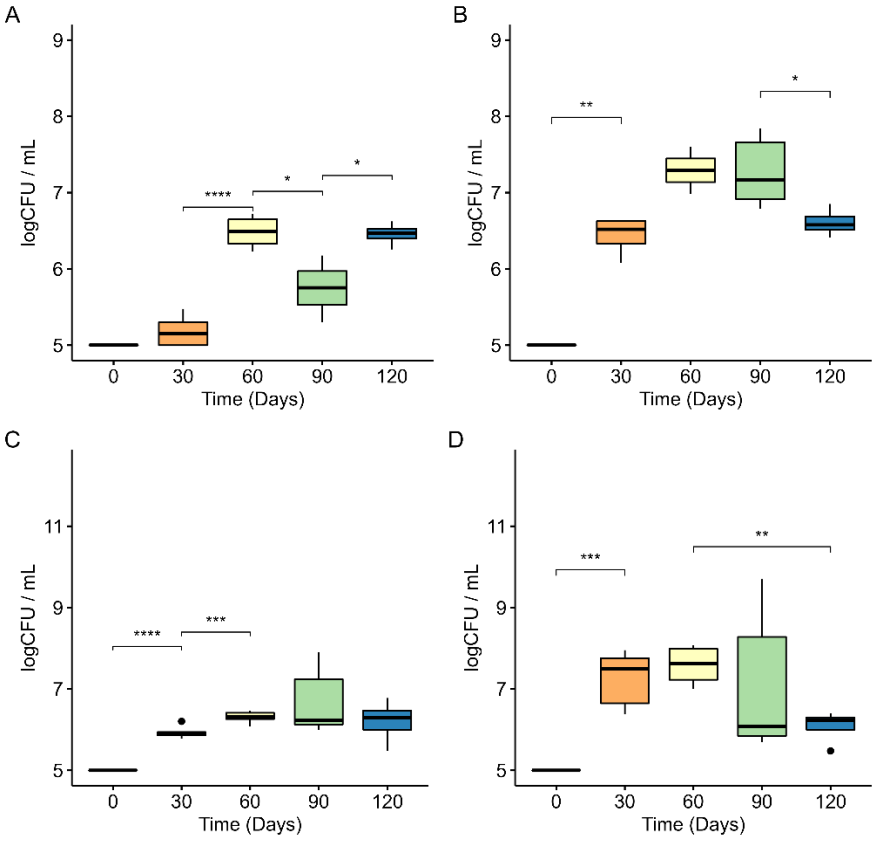

*Figure 3. 2: The abundances of Souda biofilm community on (A) HDPE and (C) LDPE secondary MPs and the abundances of Agios biofilm community on (B) HDPE and (D) LDPE secondary MPs over time. Stars indicate significance levels: * for p < 0.05, ** for p < 0.01, *** for p < 0.001.*

Exopolymeric protein concentrations on secondary MPs shown in Figure 3.3 do not exhibit similar patterns as the biofilm cells. They fluctuate in a similar manner on HDPE microplastics and by the end of the incubation period a definite decrease can be observed. On the other hand, protein concentrations on LDPE microplastics behave not only differently than those on HDPE, but also between the two treatments, reaching marginally higher values than those initially measured at the end of the cultivation period. More specifically, average protein concentrations on the surface of the HDPE secondary microplastics (73.8 ± 3.8–165.2 ± 27.5 μg mL^{-1}) were consistently almost one order of magnitude higher than those on LDPE (10.0 ± 1.6–20.7 ± 6.8 μg mL^{-1}). The high average protein concentrations observed for the Souda community (165.2 ± 27.5 μg mL^{-1}; Figure 3.3A) and for the Agios community (143.7 ± 15.6 μg mL^{-1}; Figure 3.3B) on HDPE microplastics after 30 days of incubation were followed by a steep decrease on the 60th day (73.8 ± 3.8 μg mL^{-1} for the Souda community and 82.4 ± 14.3 μg mL^{-1} for the Agios community). The increase in protein concentration that can be noted on the 90th day (105.7 ± 1.7 μg mL^{-1} for the Souda community and 82.5 ± 14.3 μg mL^{-1} for the Agios community) does not restore the concentrations to the initially measured maximum values. The average values decreased further in the time resulting in final protein concentrations of 93.0 ± 10.1 μg mL^{-1} for the Souda community and 90.3 ± 3.3 μg mL^{-1} for the Agios community. The proteins on the surface of LDPE samples incubated with the Souda community decreased, as previously seen on HDPE, however more gradually from 13.2 ± 1.5 μg mL^{-1} on the 30th day to 10.0 ± 1.6 μg mL^{-1} on the 60th day (Figure 3.3C). From that point on, average concentrations increased marginally to 10.8 ± 1.6 μg mL^{-1} on the 90th day and finally reached 14.1 μg mL^{-1} at the end of the experiment. The average protein concentrations measured on LDPE microplastics, following incubation with the Agios community exhibited a gradual increase from 14.6 ± 2.2 μg mL^{-1} on the 30th day to 19.2 ± 1.3 μg mL^{-1} on the 90th day and finally decreased to 14.8 ± 2.1 μg mL^{-1} at the end of the experiment (Figure 3.3D). It should be noted that the differentiation of protein concentration values was not statistically significant between samplings. The differences observed between the two LDPE treatments were statistically significant ($p = 0.002$), but this was not the case for HDPE ($p = 0.808$). Finally, the different PE types affected the protein concentration on the surface in a statistically significant manner; comparison between HDPE and LDPE samples for the Souda community revealed statistically significant differences ($p = 0.0003$ and $p = 6.8 \times 10^{-6}$).

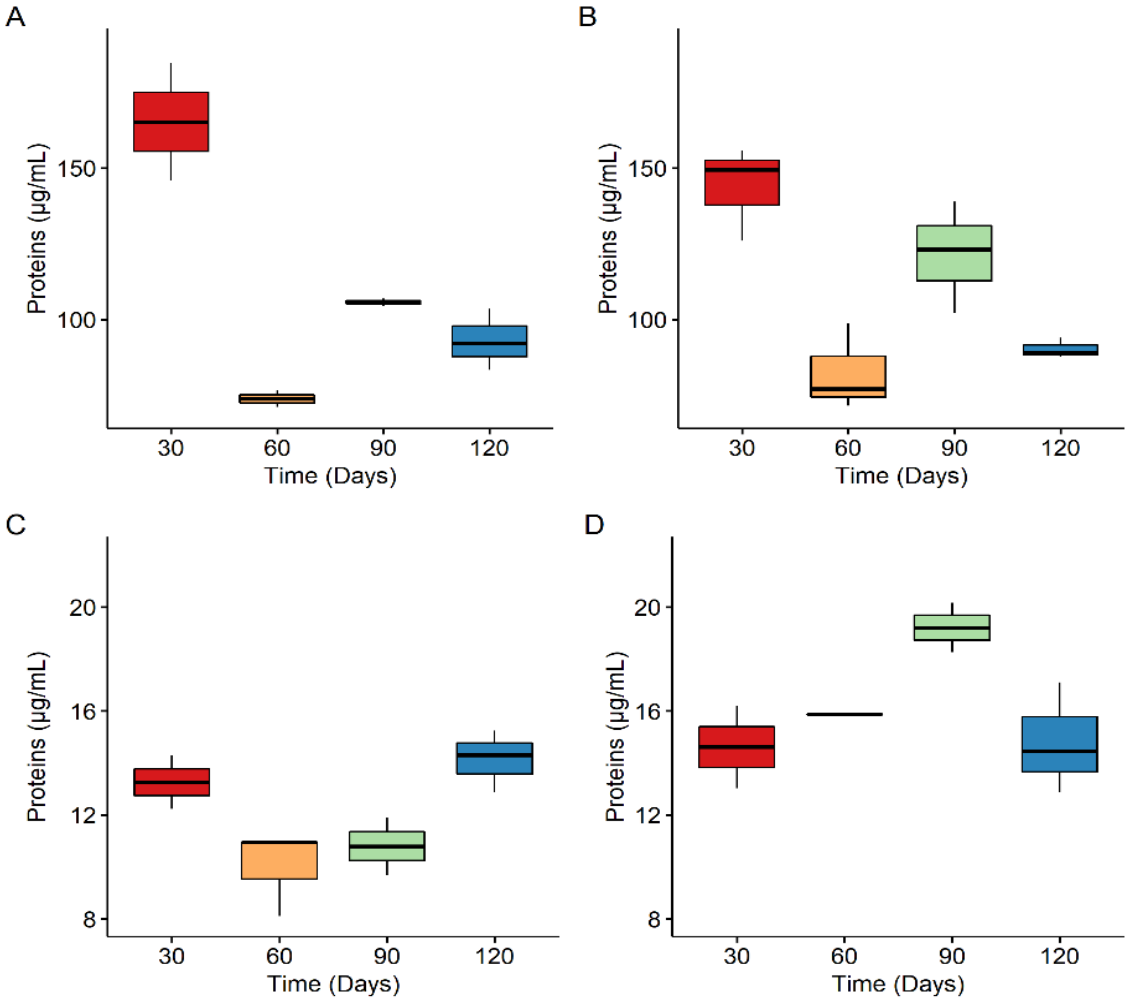

Figure 3. 3: The concentration of proteins within the Souda biofilm community on (A) HDPE and (C) LDPE secondary MPs and the concentration of proteins within the Agios biofilm community on (B) HDPE and (D) LDPE secondary MPs over time.

3.4.2. FTIR

The FTIR spectra of secondary LDPE microplastic samples at the beginning of the incubation period (Weathered_LDPE) and after 90 and 120 days of incubation with each community (LDPE_3months_S, LDPE_4months_S, LDPE_3months_A, LDPE_4months_A) are shown in Figure 3.4. As seen the broad stretching hydroxyl (O-H) peak visible in the range 3200–3600 cm^{-1} of the LDPE microplastics was smoothed as incubation progressed, regardless of the community. The carbonyl (C=O) peak at 1708 cm^{-1} was sharpened and higher absorbance values were observed as incubation progressed. Finally, the carbon oxygen (C-O) peak at 1163 cm^{-1}, which cannot be detected on the initial LDPE microplastics, was most visible after 90 days of incubation with both the Souda and Agios community, and was smoothed out on the 120th day.

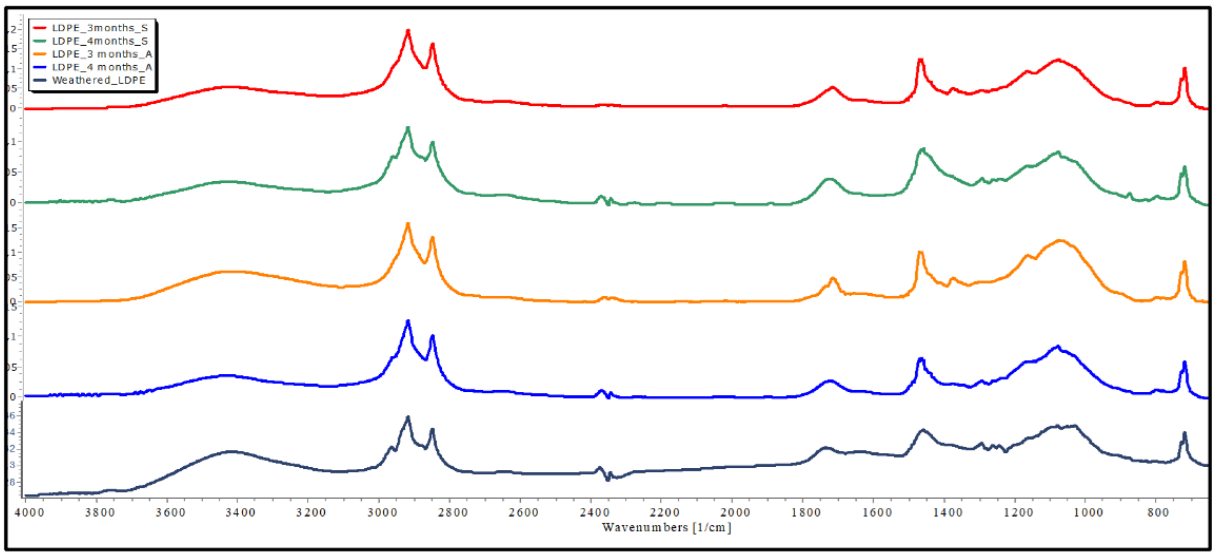

Figure 3. 4: The FTIR profiles of LDPE secondary MPs prior and after exposure to Souda and Agios communities.

HDPE microplastics initially used for the microcosms had an average keto carbonyl bond index (KCBI) value of 0.89 ± 0.00 (Figure 3.5A,B). A maximum increase was observed after 30 days for samples incubated with the Souda community (KCBI = 0.98 ± 0.006; Figure 3.5A) as well as for samples incubated with the Agios community (KCBI = 0.96 ± 0.02; Figure 3.5B). Further incubation resulted in a marginal drop to final average values of 0.92 ± 0.008 for the Souda community (Figure 3.5A) and 0.93 ± 0.02 for the Agios community (Figure 3.5B). LDPE microplastics, with an average initial KCBI value of 1.36 ± 0.00 (Figure 3.5C,D), exhibited notable decrease after 30 days of incubation with both communities; 0.87 ± 0.11 for Souda (Figure 3.5C) and 0.84 ± 0.13 for Agios (Figure 3.5D). The average KCBI values of LDPE microplastics incubated with the Souda community fluctuated before attaining the final average value of 0.90 ± 0.00 (Figure 3.5C). On the other hand, incubation with the Agios community did not alter the LDPE microplastics significantly, from a keto carbonyl bond index point of view, since the average values were almost stable. After 120 days KCBI was 0.85 ± 0.03 (Figure 3.5D). The differences observed between the HDPE and LDPE microplastic samples after the incubation with the two communities were statistically significant (p = 0.014 for Souda community and p = 0.0008 for Agios community, respectively).

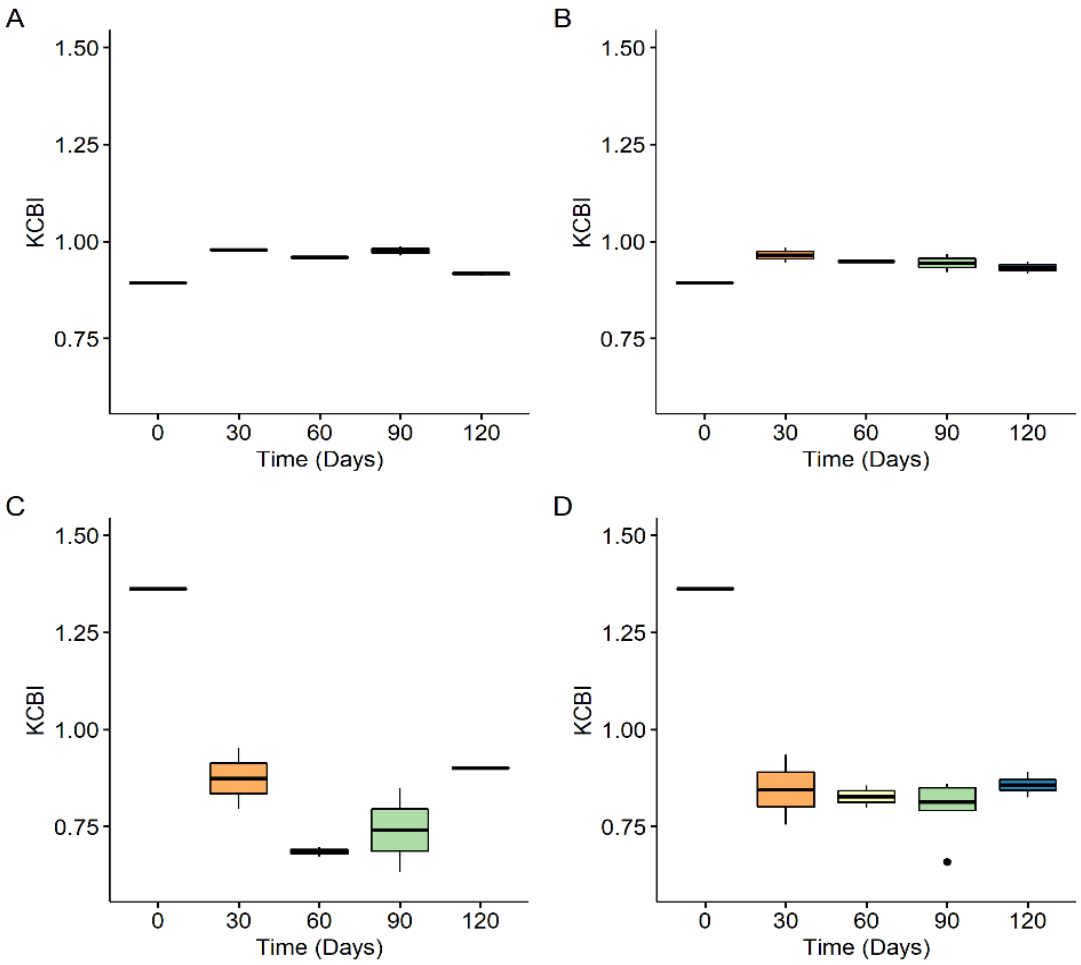

Figure 3. 5: The KCBI of (A) HDPE and (C) LDPE secondary MPs inoculated with the Souda community and the KCBI of (B) HDPE and (D) LDPE secondary MPs inoculated with the Agios community.

A 30-day incubation with any of the two communities employed was proven sufficient for the chemical alteration of the surface of the HDPE microplastics, from an ester carbonyl bond index (ECBI) point of view (Figure 3.6A,B). The initial average ECBI value of 0.88 ± 0.00 of the microplastics at the time of incubation was succeeded by 0.97 ± 0.008 for samples incubated with the Souda community (Figure 3.6A) and 0.96 ± 0.03 for samples incubated with the Agios community (Figure 3.6B). The average ECBI values for Souda community-incubated HDPE microplastics fluctuated until the final value of 0.90 ± 0.009, while for the Agios community incubated samples, a clear pattern of decrease until a value of 0.92 ± 0.02 was observed. As far as the LDPE microplastics were concerned, almost no change can be observed from the initial average value of 0.80 ± 0.00 in the first 30 days (Figure 3.6C,D). The minimum average ECBI values were observed on the 60th day of incubation; 0.62 ± 0.02 for the LDPE microplastics incubated with the Souda (Figure 3.6C) community and 0.72 ± 0.07 for LDPE microplastics incubated with the Agios community (Figure 3.6D). Increase in the

average ECBI values over the following 60 days resulted in final values which were slightly higher than the original ones; 0.85 ± 0.00 for the samples from the Souda community microcosms (Figure 3.6C) and 0.84 ± 0.04 for the samples from the Agios community microcosms (Figure 3.6D). The *p-values* from the Mann–Whitney U test revealed that the differences observed between the two polymers were statistically significant for both communities (p = 0.0003 for Souda and $p = 7.75 \times 10^{-5}$ for Agios).

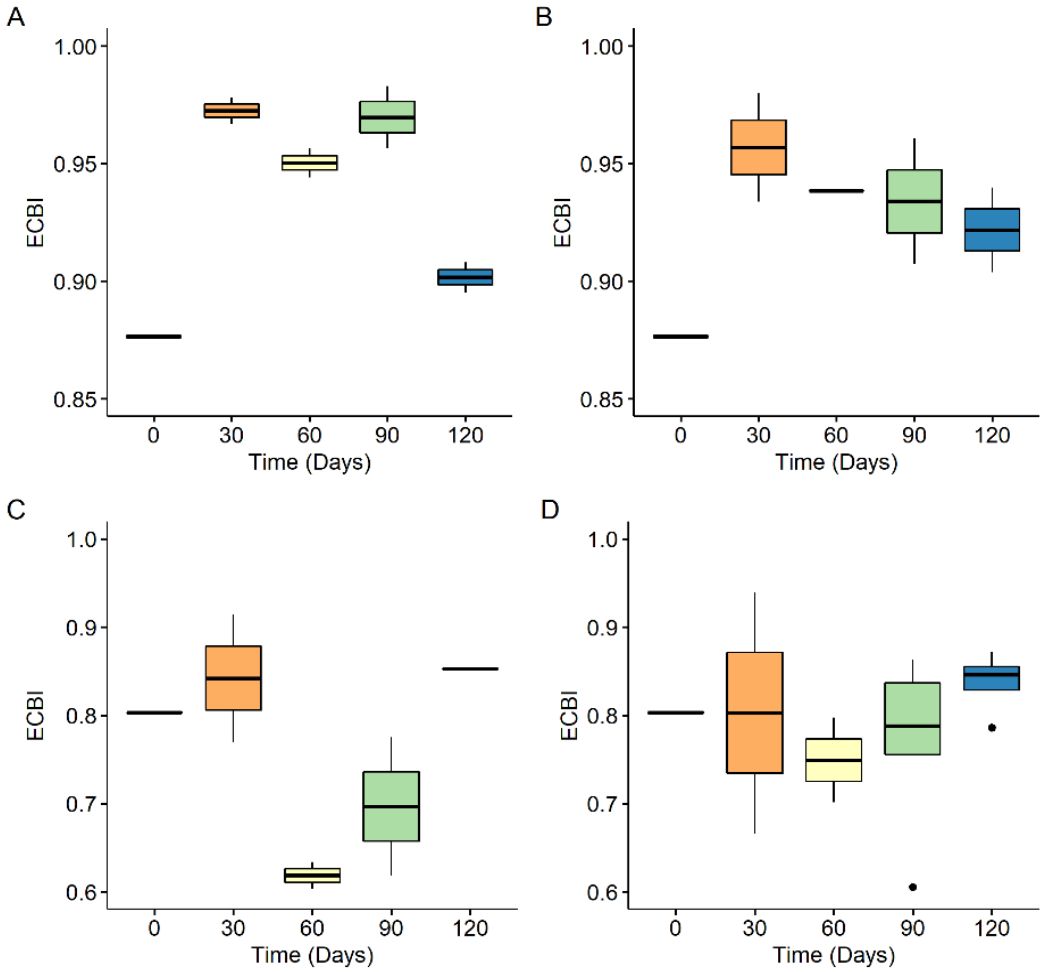

Figure 3. 6: The ECBI of (A) HDPE and (C) LDPE secondary MPs inoculated with the Souda community and the ECBI of (B) HDPE and (D) LDPE secondary MPs inoculated with the Agios community.

Incubation of both secondary microplastic types contributed to the development of internal double bonds on the polymers' surfaces. During the first 30 days in the microcosms, all average internal double bond index (IDBI) values increased from an initial value of 0.83 ± 0.00 for HDPE and 0.36 ± 0.0 for LDPE. More specifically, incubation with the Souda community resulted in an average IDBI value of 0.95 ± 0.008 for HDPE samples (Figure 3.7A) and 0.82 ± 0.17 for LDPE samples (Figure 3.7C),

while incubation with the Agios community yielded average values of 0.93 ± 0.05 for HDPE (Figure 3.7B) and 0.79 ± 0.22 for LDPE (Figure 3.7D). From that point on, however, each polymer exhibited different behavior. The average IDBI of HDPE microplastics incubated with the Souda community was stabilized until the 90th day and on the 120th day, a decrease to a value of 0.87 ± 0.01 was observed (Figure 3.7A). Incubation with the Agios community resulted in a gradual decrease of the average IDBI value to a final 0.89 ± 0.02 (Figure 3.7B). After incubation with the Souda community, LDPE microplastic samples' IDBI values exhibited an increasing pattern, until the final value of 1.01 ± 0.00 (Figure 3.7C). In the treatment of the Agios community, LDPE microplastics gradually reached a final average value of 1.07 ± 0.02 (Figure 3.7D). It is notable that both LDPE treatments resulted in their maximum average values on the 90th day, with very high standard deviations (1.62 ± 0.53 for Souda-incubated samples and 0.96 ± 0.29 for Agios- incubated samples). No statistically significant differences could be discerned between polymer types or communities.

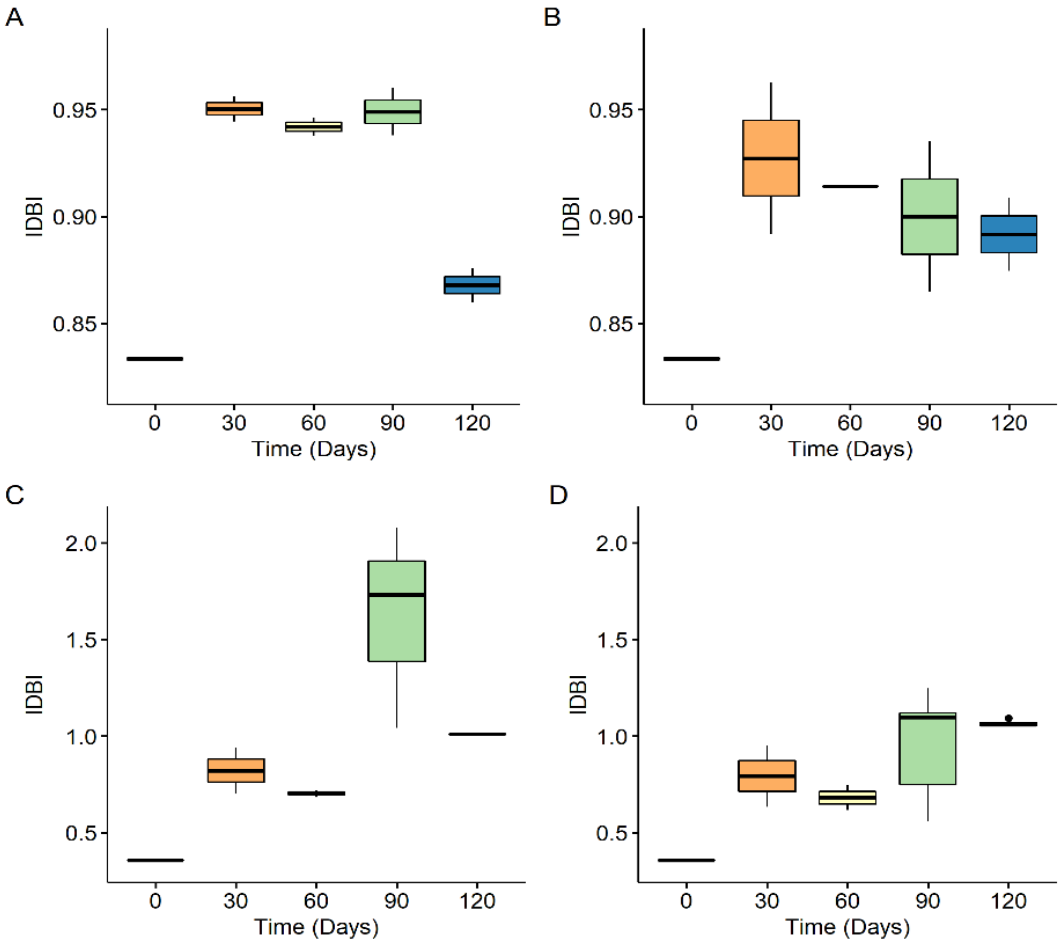

Figure 3. 7: The IDBI of (A) HDPE and (C) LDPE secondary MPs inoculated with the Souda community and the IDBI of (B) HDPE and (D) LDPE secondary MPs inoculated with the Agios community.

Artificial UV irradiation affected the two types of PE in a similar manner, but to a dissimilar extent. The average vinyl bond index (VBI) value of HDPE upon initiation of the experiment was 0.89 ± 0.00, while that of LDPE was 0.14 ± 0.00. Incubation with the two marine communities led to increased detection of vinyl bonds for all treatments (Figure 3.8). Incubation with the Souda community resulted in average VBI values of nearly 1.00 from the 30th to the 90th day of the experiment, which finally decreased to 0.92 ± 0.003 at the end of the incubation period (Figure 3.8A). The average value of 0.99 ± 0.04 was achieved after 30 days of LDPE incubation with the Agios community. It decreased gradually to a final average value of 0.94 ± 0.03 on the 120th day (Figure 3.8B). The initial increase in average VBI values was more distinct, reaching 0.82 ± 0.17 after a 30-day incubation with the Souda community (Figure 3.8C) and 0.78 ± 0.20 with the Agios community (Figure 3.8D). For the remainder of the experiment, average VBI values of LDPE microplastics incubated with the Souda community fluctuated until the final value of 0.80 ± 0.00 was attained (Figure 3.8C). The fluctuations for Agios community-incubated samples were less pronounced, with a final average value of 0.76 ± 0.05 (Figure 3.8D). Statistically significant differences could be observed between the two polymers for each community (p = 0.0003 for the Souda community and $p = 1.63 \times 10^{-5}$ for the Agios community).

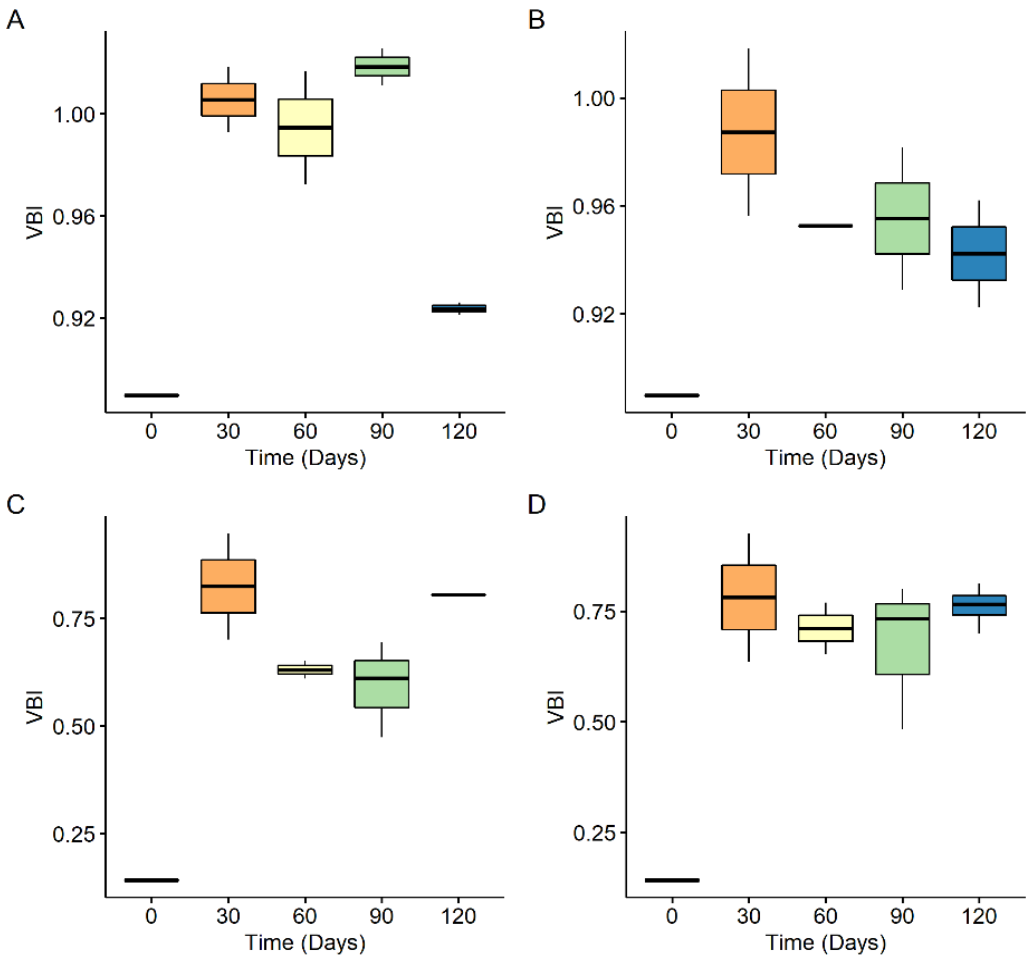

Figure 3. 8: The VBI of (A) HDPE and (C) LDPE secondary MPs inoculated with the Souda community and the VBI of (B) HDPE and (D) LDPE secondary MPs inoculated with the Agios community.

Generally, in the first 30 days the FTIR indices of all treatments increased, from 4.8% (ECBI of LDPE incubated with the Souda community) to 483.1% (VBI of LDPE incubated with the Souda community). Following the initial abrupt increase, the ECBI of HDPE MPs incubated with the Souda community fluctuated until a 7% decrease took place between the 90th and 120th day. On the other hand, MPs after incubation with the Agios community steadily declined throughout the experiment. ECBI values of LDPE MPs followed a similar pattern of increase on the 30th day, which was followed by decrease on the 60th day. For the remainder of the experiment, the value of the ECBI index increased, until both treatments reached approximately the same value. The IDBI refers to C=C bonds in the polymeric chain while the VBI refers to terminal C=C bonds. Interestingly, examination of IDBI and VBI of HDPE MPs showed that regardless of incubation community, the values of the two bond indices followed the same pattern of increase in the first 30 days, stabilization between the 30th and 90th day and decrease in the last 30 days. The total percentile differentiation of the two indices was

equal in both treatments (13.5% for Souda incubated samples and 11.0% for Agios incubated samples), indicating that double bonds were created in the polymeric chains in an identical manner, despite the incubation with different communities. That was not the case with LDPE MPs. While the two indices followed the same pattern until the 60th day of incubation with the Souda community, they followed opposite directions until the termination of the experiment. The VBI of Agios community incubated samples did not change after the initial increase of the first 30 days. The IDBI however, progressively increased, despite minute fluctuations. The only exception to that pattern of increase was the KCBI of both LDPE treatments. After 30 days of incubation, a decrease of more than 30% was noted, accompanied by simultaneous slight increase in ECBI. Carbonyl index decrease resulted from the incubation of HDPE and LDPE with fungi, with the change being more definite for LDPE samples after 30 days (Ojha et al., 2017). The KCBI value of weathered LDPE microplastics prior to inoculation was 34% higher than that of HDPE.

3.4.3. Size Distribution of Generated Nanoplastics

In this section, the size distribution of the micro- and nanoparticles generated from the microplastics used are presented. Generally, the particle size distribution of HDPE particles by volume shifted to the right as incubation progressed with either community. The temporal diameter differentiation of secondary HDPE particles as a function of their volume is shown in Figures 3.9A,B. Examination of samples from the abiotic control showed average diameters of 5.357 ± 0.209 μm, with a modal value of 3.548 μm. After 30 days of incubation with the Souda community the mean diameter of the LDPE particles contained in the liquid was 0.814 ± 1.128 μm, with a modal value of 0.102 μm. On the 60th day, the mean diameter diminished to 0.654 ± 0.945 μm, with a higher modal value of 0.129, while on the 90th day, both mean and modal diameters increased with respective values of 3.172 ± 0.906 μm and 0.412 μm. At the end of the experiment, further increase was observed, with a final mean diameter of 28.937 ± 0.533 μm and a modal diameter of 54.923 μm (Figure 3.9A). Incubation with the Agios community resulted in gradual increase in the mean diameter of the plastic particles, from 6.144 ± 0.584 μm on the 30th day to 56.976 ± 0.402 μm on the 120th day. Interestingly, the highest modal value was observed on the 90th day, with a value of 110.467 μm (Figure 3.9B). The diameter by volume of LDPE particles was generally higher than that of HDPE. The particle size distribution of LDPE secondary MPs incubated with the Souda community did not shift significantly over time. An initial mean diameter of 56.390 ± 0.255 μm was initially measured, close to the modal diameter (54.923 μm). On the 60th day, the mean diameter increased to 82.604 ± 0.259 μm, with a modal value of 87.513. On the 90th day the diameter started to decrease (mean = 51.621 ± 0.279 μm, modal =

54.923 μm), to finally attain the minimum mean value of 26.564 ± 0.488 μm and a modal diameter of 43.510 μm (Figure 3.9C). Incubation of LDPE microplastics with the Agios community shifted the particle size distribution to the left. After 30 days nanoparticles of a mean diameter of 6.144 ± 0.584 μm (modal = 17.138 μm) were produced. The mean diameter increased until 66.639 ± 0.426 μm until the 90th day (modal = 110.467 μm) and finally decreased to 56.976 ± 0.402 μm, with a close modal of 54.923 (Figure 3.9D).

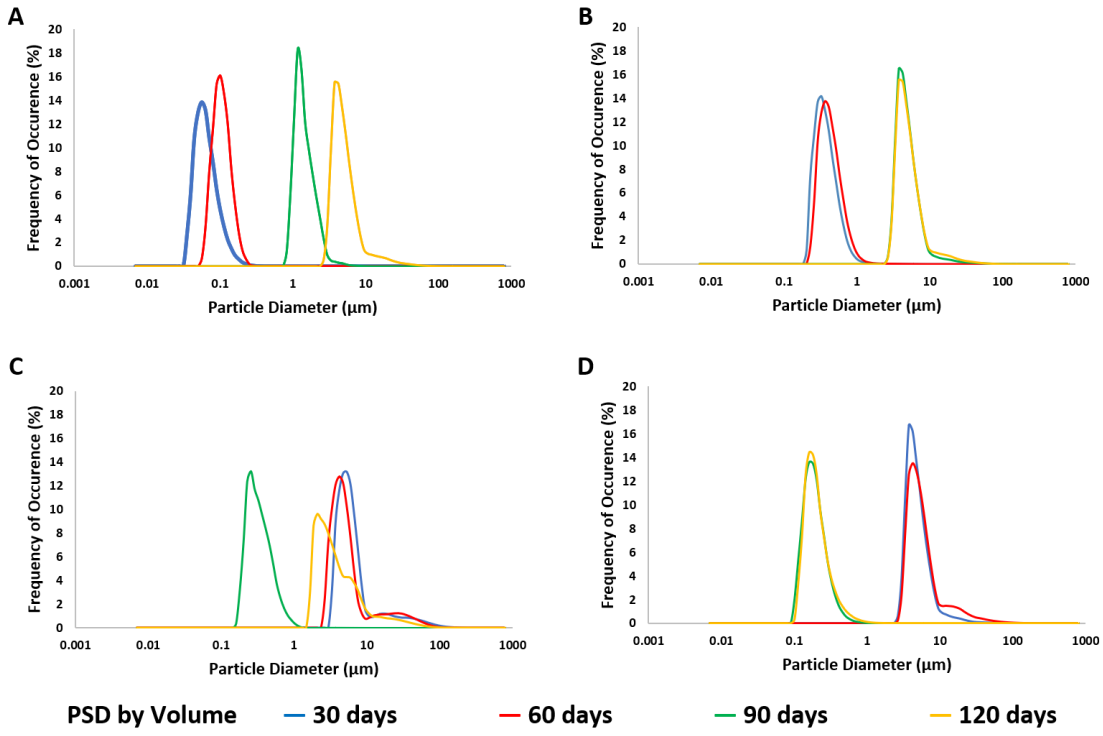

Figure 3. 9: The particle size distribution of (A) HDPE and (C) LDPE secondary MPs inoculated with the Souda community and of (B) HDPE and (D) LDPE secondary MPs inoculated with the Agios community by volume of particles as measured by dynamic light scattering.

The distribution of HDPE particle size by number shifted decisively to the right, regardless of incubation community. The mean diameter by number after Souda community incubation for 30 days was 0.062 ± 0.157 μm, with a modal value of 0.056 μm. The diameter increased progressively until the end of the experiment, when maximum mean and modal values of 1.345 ± 0.142 μm and 1.122 μm were measured (Figure 3.10A). Increase in particle diameter by number was observed after the incubation of HDPE microplastics with the Agios community, as well. Distinctively, the mean particle diameter was 0.353 ± 0.154 μm (modal = 0.282 μm) after 30 days and reached 4.945 ± 0.203 μm on the 120th day. Notably, the modal diameter value did not change between the 90th and 120th day

and was stable with a value of 3.548 μm (Figure 3.10B). The diameter of LDPE particles fluctuates throughout the experiment, but a shift of the distribution to the left can be observed, more distinctly in the case of Agios community-incubated samples (Figures 3.10B,D). LDPE particles of a mean diameter of 6.531 ± 0.297 μm and a modal diameter of 4.467 μm were detected in samples from the 30th day of incubation with the Souda community. On the 60th day, the mean particle diameter was 5.579 ± 0.313 μm with an equal modal diameter of 4.467 μm. A steep increase of diameter was observed on the 90th day (mean = 0.314 ± 0.168 μm, modal = 0.224 μm), followed by an increase to a mean diameter of 3.836 ± 0.321 μm, with a modal value of 2.239 μm (Figure 3.10C). The diameter of LDPE particles incubated with the Agios community fluctuated, however in a dissimilar manner. The mean particle diameter was 4.670 ± 0.171 μm (modal = 3.548 μm) on the 30th day. One month later, a higher mean diameter equal to 5.594 ± 0.250 μm, with a modal diameter of 4.467 was observed, only to decrease steeply in the next sampling, to a minimum mean diameter of 0.182 ± 0.161 μm (modal = 0.178 μm). Samples from the end of the experiment exhibited slightly higher diameters, with a mean value of 0.192 ± 0.168 μm and a modal diameter of 0.178 μm (Figure 3.10D).

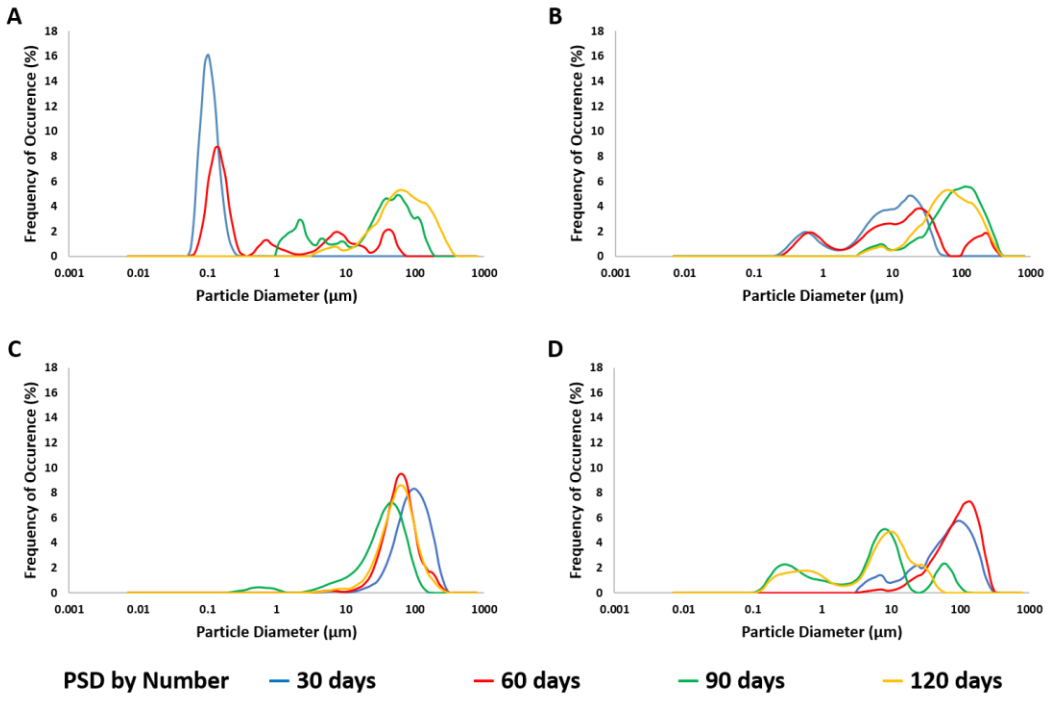

Figure 3. 10: The particle size distribution of (A) HDPE and (C) LDPE secondary MPs inoculated with the Souda community and of (B) HDPE and (D) LDPE secondary MPs inoculated with the Agios community by number of particles.

3.5. Discussion

3.5.1. Changes of Incubated Secondary Microplastics

It has been shown that among a variety of plastics polymers, PE was the material less facilitating to biofilm development and fragmentation (Gerritse et al., 2020). Biofilm development on the surface of PE particles, however, has been associated with biodegradation (Ganesh Kumar et al., 2020; Balasubramanian et al., 2010; Gilan et al., 2004; Yans et al., 2018). Microorganisms recruit the extracellular enzyme reservoir to enable the biodeterioration and biofragmentation of solid substrates (García-Depraect et al., 2021b). In this experiment, viable cells and protein concentrations were examined as a measure of biofilm formation and microbial activity, while FTIR and DLS were employed to detect polymer-related changes.

Our results highlight the significance of the time factor in the process of PE biodegradation. The first 30 days of incubation were crucial to the evolution of the system parameters. Between inoculation and the first sampling, viable cell concentrations increased in all treatments. With the exception of microcosms containing HDPE incubated with the Souda community, that increase was intense and statistically significant. As expected, the highest cell concentrations were recorded for the acclimated Agios community, regardless of polymer type used as a substrate (Syranidou et al., 2017c). Cell abundances which initially increased and decreased over time were estimated indirectly via the measurement of increased protein concentrations during the biodegradation of LDPE by bacterial strains (Yans et al., 2018). The elevated cell abundances were consistent with the high protein concentrations noted at the same sampling. In microcosms containing HDPE secondary MPs, the highest protein concentrations were also achieved after 30 days of incubation.

Between the first and the 30th day, the most severe changes in FTIR indices were also observed. Increases of FTIR indices similar to those shown here have been reported previously during biodegradation experiments (Manzur et al., 2004; Sangeetha Devi et al., 2015; Sudhakar et al., 2008; Yans et al., 2018). It appears that the branched molecular structure of LDPE, which facilitated the incorporation of oxygen atoms in the polymeric chain during the irradiation period (Chamas et al., 2020; Martínez-Romo et al., 2015), also made it easier for the keto carbonyl bonds to dissolve. The increase in VBI can also be connected to the creation of oligomers with terminal C=C bonds via the Norrish II mechanism (Eyheraguibel et al., 2017). The decrease of the majority of the indices over time can be an indication of weathered polymer consumption by the marine communities. This idea is reinforced by the FTIR spectra (Figure 3.3), where the hydroxyl peak of the material used for incubation is less prominent after 90 and 120 days. Changes of FTIR indices during the biodegradation of LDPE have been reported before (Harshvardhan and Jha, 2013), while increase of

vinyl bonds was related to the biodegradation of a mixture of plastics by marine communities (Syranidou et al., 2019a).

Comparison of all index values for the Souda and Agios communities reveals that changes occurring as a result of incubation with the Agios community were gradual and more stable, while those from the Souda community tended to be more dynamic. This result indicates that the biofilm produced from the already acclimated Agios community was more stable, and therefore more predictable and suitable for long-term incubation of samples, with the purpose of polymer mineralization (Sudhakar et al., 2008). The Agios community, previously developed and successfully employed by the authors for the biodegradation of naturally weathered polyethylene and polystyrene samples, has been found to contain elevated abundances of the *alk*B gene (Syranidou et al., 2017a, 2017c). The presence of hydrocarbon-degrading microorganisms containing the *alk*B gene has been linked to the potential biodegradation of plastics (Delacuvellerie et al., 2019).

3.5.2. Nanoplastics Generation and Fate

Incubation of secondary MPs with the two marine communities also resulted in the generation of NPs in the seawater. The size of the detected nanoparticles was consistently lower than the cutoff of the filter used to separate the secondary MPs to be included in the experiment (250 μm). In detail, NPs with size ranging from 56 nm to 355 nm were detected after 30 days of incubation in the seawater of the three out of the four microcosms, supporting the scenario of biofragmentation of PE secondary MPs. It is important to mention that no NPs were detected in the seawater from the abiotic controls at the beginning of the experiment or after 120 days of incubation in the dark. It is, therefore, not possible to attribute the generation of NPs to photodegradation or mechanical stress. Biofragmentation is a depolymerization step which includes the catalytic cleavage of already degraded MPs into smaller units (Amobonye et al., 2021). These intermediate materials are low molecular weight fragments such as monomers and short-chain oligomers. For example, linear alkane hydrolysis products due to PE biodegradation have been detected while the carbon chain length differed depending on the species of bacteria (Montazer et al., 2018). These compounds can be classified as NPs if their larger dimension is below 1 μm (Gewert et al., 2015b; Sorasan et al., 2021). Moreover, surface corrosion of the MPs takes place following microbial adhesion on the surface (Montazer et al., 2018).

The presence of NPs was more prolonged and the fragments were smaller in microcosms containing HDPE secondary MPs as carbon source. Given the chemical structures of LDPE and HDPE, that was unexpected. This result is linked to the fact that after incubation both the KCBI and the ECBI of HDPE

MPs were consistently higher than those of LDPE microplastics (Bardají et al., 2020). The dissolution of carbonyl bonds within the polymeric structure could be the mechanism behind chain scission and the subsequent production of NPs (I. Ali et al., 2021; Zeenat et al., 2021). Depolymerization occurring during chain scission is considered to initiate assimilation of the short-chain oligomers to complete mineralization (Choe et al., 2021). That implies that NP particles could have been produced in the LDPE microcosms, as a result of the removal of branches of the polymer chain. However, they could not be detected during DLS analysis, as they had been consumed by the bacteria in the seawater. This observation is similar to the fate of byproducts from the biodegradation of petroleum hydrocarbons in the marine environment.

The occurrence of NPs in the natural environment has been extensively highlighted, including the potential toxic effects on biota (I. Ali et al., 2021; Alimi et al., 2018; Alprol et al., 2021; Chae and An, 2016; Cole and Galloway, 2015; Mattsson et al., 2018). Despite the ever-increasing number of studies on NPs, research of their generation is completely novel. That can be attributed to the fact that this phenomenon has been mostly ignored until now. Moreover, the development of standardized protocols is of utmost importance. The effect of organisms on their production and fate has not been elucidated yet. Understanding of the sources and production of NPs through studies like this, would provide further insight on the impacts that might occur from their presence in the environment. Thus, a wide spectrum of studies should be completed, in order to identify the processes and mechanisms that govern the generation of secondary nanoparticles under various environmental conditions.

3.6. Concluding remarks

The presence of plastics of all scales in the environment has been linked to a number of processes and interactions, which have not been fully studied despite the ever-increasing volume of relevant publications. This work presents the potential for secondary MPs colonization and subsequent biodegradation by marine communities, by demonstrating their proliferation in microcosms with HDPE and LDPE as the sole carbon source. Structural changes on the surface of the polymers were consistent with biodeterioration, while the products of biofragmentation were for the first time identified as nanoplastics due to microbial activity. Always keeping in mind, the implications that might arise from the increased toxicity of nanoplastics, this work aspires to constitute a stepping stone toward the biological mitigation of the plastic pollution problem. Finally, it is crucial that efforts be made to understand and include the microbially produced NPs in the plastic mass balance models.

Chapter 4. Intertwined synergistic abiotic and biotic degradation of polypropylene pellets in marine mesocosms

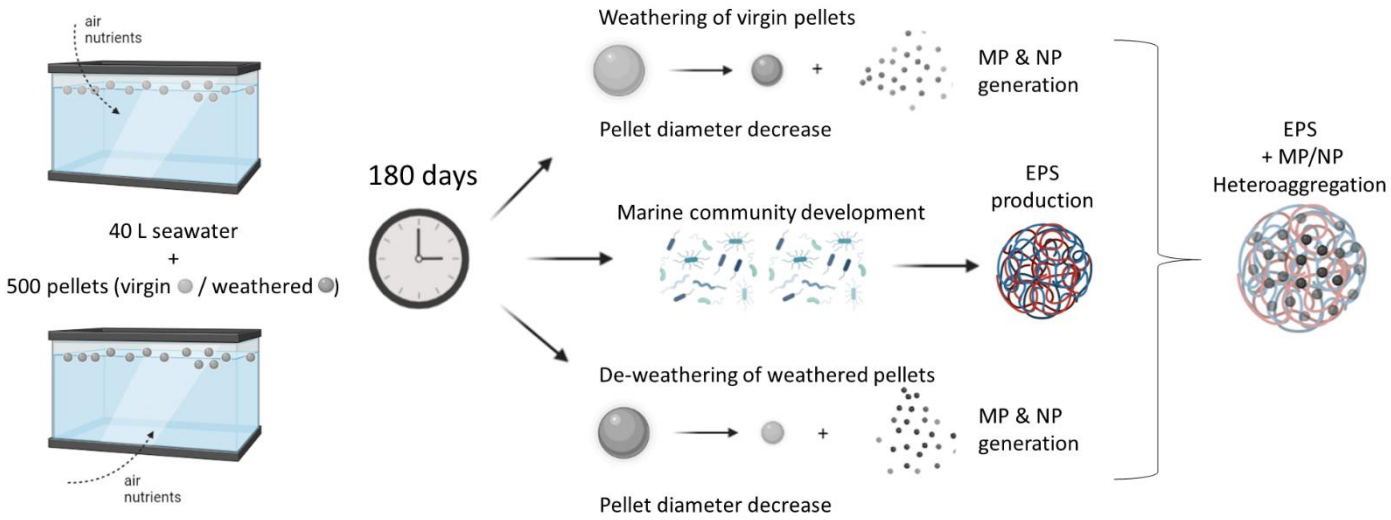

Published as:

Karkanorachaki, K., Syranidou, E., Maravelaki, P.-N., Kalogerakis, N., 2023. Intertwined synergistic abiotic and biotic degradation of polypropylene pellets in marine mesocosms. *Journal of Hazardous Materials*, 457, 131710.

4.1. Abstract

The accumulation of plastic waste in the oceans has caused growing concern for its effects on marine life. The interactions of plastics with environmental factors have been linked to fragmentation to micro- and nanoparticles with different properties and consequences, but the mechanism of fragmentation has not been fully understood yet. In this work, we investigate the combined effect of biotic and abiotic factors towards the degradation of virgin and artificially weathered polypropylene (PP) pellets after a long-term incubation period in marine mesocosms. The surface chemical alterations and deterioration of the polymer, in conjunction with the attachment and evolution of marine bacterial communities, the development of biofilm and exopolymeric substances (EPS), as well as the colloidal properties (zeta-potential and hydrodynamic diameter) of the mesocosms were studied. The surface area of both types of pellets decreased over time, despite no concrete weight change being observed. Cell growth, EPS production and colloid particle size were correlated to the loss of area. Therefore, we propose that surface area could be effectively monitored, instead of weight loss, as an alternative indicator of polymer degradation in biodegradation experiments. Changes in the chemical structure of the polymer, in addition to the evolution of the biological factors, implied that a complex degradation process alternated between two phases: an abiotic phase, when UV irradiation contributes to the deterioration of the polymer surface layers and a biotic phase, when marine communities degrade the weathered polymer surface to reveal the underlying layer of virgin polymer. Finally, microscopic particles, produced as a result of the decrease in pellet area, promoted the aggregation of colloidal particles. The role and impacts of these colloidal particles in marine ecosystems are yet as unidentified as that of micro- and nano-sized plastic particles and call for further investigation.

4.2. Introduction

Plastic production has been constantly increasing since the introduction of bakelite more than a century ago. The worldwide production of plastics in 2019 was 368 Mt, while 57.9 Mt were produced in the EU alone. In 2018, 25% of the 29.1 Mt of post-consumer plastic waste collected in the EU was not recycled or used for energy recovery (PlasticsEurope-Association of Plastics Manufactures, 2020), but was led to landfills, eventually contributing, along with other land-based sources, to 80% of the plastic pollution of the marine environment (Jambeck et al., 2015; Koelmans et al., 2014). The resulting accumulation of plastics floating in the ocean has been estimated between 93-236 thousand metric tons (Van Sebille et al., 2015) and it has been predicted that it will continue accumulating, until action is taken to reduce the production of plastics and plastic waste (Ellen MacArthur

Foundation, 2017).

The residence of plastic polymers in the marine environment can lead to their physicochemical degradation and subsequent fragmentation, under the effect of solar radiation, heat, mechanical stress, and biological factors (Alimi et al., 2022a). Thus, secondary particles are produced: microplastics with diameter smaller than 5 mm (Andrady, 2011; Arthur et al., 2009), and nanoplastics, typically smaller than 1000 nm (Bergmann et al., 2015; Gigault et al., 2018).

There has been growing evidence of the adverse effects of microscopic plastic particles on marine biota, either by damaging them physically, or due to their intrinsic toxicity and sorption of heavy metals and organic compounds (Chae and An, 2016; Sana et al., 2020). Micro- and nanoplastics are characterized by high surface-to-volume ratios, which allow for attachment and prosperity of marine organisms. Thus, new, complex ecosystems, called the "plastisphere", are created, suggesting that the impacts of plastics may not be entirely negative (Wright et al., 2020; Zettler et al., 2013). The composition, functions and interactions within the plastisphere are currently being investigated (Amaral-Zettler et al., 2020; Roager and Sonnenschein, 2019), with the intention of identifying organisms with the capacity to biodegrade plastic polymers (Matjašič et al., 2021). The presence of microbial biofilm on the surface of three types of oil-based plastic polymers has been found to induce changes in crystallinity, stiffness and surface roughness of the plastics, even after a 2-week period of time (McGivney et al., 2020). Very recently, the extracellular production of reactive oxygen species (ROS) by the marine bacterial genus *Alcanivorax* was found to potentially result in oxidation of PE samples, much like abiotic weathering (Zadjelovic et al., 2022).

The presence of plastic in the ocean has recently been associated with increased concentrations of dissolved organic carbon. At the same time, biological processes, such as biofilm attachment or aggregation, can affect the mobility of microscopic plastic particles, and therefore, the forms of bioavailable carbon in the water column (Karkanorachaki et al., 2021; Oriekhova and Stoll, 2018; Praetorius et al., 2020).

Despite the fact that weathering has been identified as a parameter that should be included in micro- and nanoplastic studies, it is rarely considered (Alimi et al., 2022a). Also, the properties of secondary micro- and nanoplastics differ greatly from the parent particles as well as engineered nanoparticles that are commonly used for the study of their behavior in the marine environment (Gigault et al., 2021). The use of uniform spherical polystyrene beads (Chen et al., 2018; Galgani et al., 2019; Mao et al., 2020; Shiu et al., 2020) acts as a step towards shedding light to the processes occurring in actual marine conditions. More realistic samples which include secondary micro- and nanoplastics, have barely been used (Kaiser et al., 2019).

The purpose of this work was to monitor and investigate the fate of microplastics in the marine environment. In contrast to most relevant literature, we study the weathering of microplastics as the combined effect of abiotic (UV radiation) and biotic (biofilm) factors. UV radiation is not the sole factor determining abiotic degradation; it is, however, of the utmost importance. Temperatures in the marine environment are low, and therefore, thermodegradation is not expected to play a significant role in the degradation process. At the same time, C-C backbone polymers lack heteroatoms in their polymeric chain, and therefore, hydrolysis is not expected to greatly contribute to their degradation, unless prior photodegradation has occurred (S. S. Ali et al., 2021; Gewert et al., 2015a). Mechanical fragmentation does occur in the marine environment, if it is very close to the shoreline, however, prior exposure to UV radiation intensifies its effect (Song et al., 2017b). The novelty of this work also entails the use of production pellets, as opposed to easily degrading microbeads or thin films, in the sense that size-wise they are closer to the items usually found in the marine environment. More specifically, virgin and artificially weathered polypropylene (PP) pellets resided in marine mesocosms for 6 months, while the polymer changes and the interactions between the PP pellets and microorganisms were examined throughout this period. The selection of PP was made based on its high demand of almost 10 Mt in the EU in 2019. This polymer type is most commonly used for packaging, and it constitutes a large portion of the annually produced plastic waste ending up in the oceans (Plastics Europe, 2020). Due to its chemical structure, PP is considered as highly resistant to biodegradation (Gewert et al., 2015). In these mesocosm experiments the time-dependent removal of weathered layer from the surface of the pellets was monitored. A consecutive pattern has been observed whereby the weathering of polymer surface is followed by the removal of the weathered polymer layer by microorganisms until the layer of virgin polymer is revealed and then the process is repeated with the weathering of the polymer surface. This process was studied in correlation with biological parameters in order to determine the fate of the secondary particles produced and the role that secondary micro- and nanoplastics play in the formation of marine aggregates.

4.3. Materials and Methods

4.3.1. Experimental Setup

Additive free polypropylene (PP) production pellets acquired from Plastika Kritis S.A. (Heraklion, Greece) were used for this experiment, as is (virgin) or following artificial aging (weathered). For accelerated weathering, the pellets were subjected to ultraviolet radiation for 4 months inside a metal box with reflective walls. The 6 Philips TUV 8W FAM/10X25BOX lamps used for that purpose

emitted light in the area 240-260 nm (UV-C). During the irradiation period, the pellets were mixed on a weekly basis, to ensure consistent weathering of the surface of all the pellets. The box was ventilated to avoid temperature rise and the consequent aging due to thermo-oxidation. The radiation levels, as well as the temperature were monitored using a HOBO Temperature Light 3500 DP Logger.

Two glass tanks were placed in a sheltered outdoor location at the Technical University of Crete campus (35.533369, 24.070092) from October 2019 to April 2020. A six-month period was considered an adequate interval of time, based on the duration of similar experiments from the literature. With the exception of Brandon et al. (Brandon et al., 2016) and Biber et al. (Biber et al., 2019), similar natural UV exposure experiments lasted between 2 and 6 months (Cai et al., 2018; Kalogerakis et al., 2017; Karlsson et al., 2018; Mao et al., 2020; Zhu et al., 2020). Following collection at Souda bay (35.500161, 24.062723), 40 L of seawater were filtered through a 250 μm mesh plankton net and placed in each tank. Water quality parameters were measured and used as baseline. A total of 10 g of virgin and 10 g of weathered (approximately 500 particles) pellets were placed in the designated mesocosms ("virgin mesocosm" and "weathered mesocosm"). At the beginning of the experiment, the average Feret diameter of the virgin and weathered particles used was 4.13 ± 0.17 mm and 4.11 ± 0.15 mm, respectively. Prior to placement in the mesocosms, the pellets were sterilized using a 70% solution of deionized water - ethanol (completely denatured with 1% Ethyl methyl ketone, 1% isopropyl alcohol, 1 g/100 L Denatonium benzoate, Merck). Aeration, as well as water circulation, were achieved by using 3 air-stones attached to a fish tank air-pump in each tank (Sera Diaphragm pump Air 275). Air flow was modulated constantly to achieve dissolved oxygen values according to the measured baseline. Radiation and temperature in each tank and the surrounding environment were logged using a HOBO Temperature Light 3500 DP Logger. Water loss due to evaporation was consistently restored to the initial volume of 40 L, using deionized water, in order to maintain the salt content of the mesocosms. Water loss due to evaporation was consistently restored to the initial volume of 40 L, using deionized water, in order to maintain the salt content of the mesocosms.

Monitoring of the water evaporation and aeration and any adjustments needed (deionized water addition, air-pump or air-stone replacements) were performed on a daily basis. Water temperature, pH, total suspended solids (TSS) and the electrical conductivity (E.C.) were measured weekly. The rest of the water quality parameters were analyzed on sampling days. Nutrients were added, if necessary, when nitrate depletion was observed to reach the baseline values determined for the seawater exactly after the mesocosms were installed. Nutrients were added in the form of a 10:1

KNO_3 and KH_2PO_4 solution until the concentration of nitrates reached the baseline level. The experimental procedure flowchart can be found in Figure S1.

4.3.2. Sampling and Sample Preparation

At the end of each month, 40 pellets were removed from each tank. The pellets were washed in 15 mL falcon tubes containing a solution of 10 mL of deionized water and 5 drops of Tween80 (removed biofilm from pellets) and placed on a mechanical mixing table (120 rpm). After 3 days, the pellets were removed, and gently scrubbed with a soft toothbrush for the removal of any residual biofilm traces. Washing with deionized water was performed for the removal of residual Tween80, followed with washing with >98% ethanol for dehydration. Next pellets were dried at 45 ^{o}C for 3 days. The removed biofilm from pellets was stored at -20^{o}C for further analysis, while the clean pellets were placed in aluminum jars.

During each sampling, 50 mL of liquid from the center of each tank were also collected (water column), to be used for further analysis (nutrient and protein concentration, dynamic light scattering, zeta potential and hydrodynamic particle diameter).

4.3.3. Dynamic Light Scattering

Dynamic light scattering (DLS) was employed to investigate the presence of micro- and nanoplastics in the water column. Analysis was performed with a SALD-7500nano particle analyzer (Shimadzu, Japan). Seawater (5 mL) from the mesocosms was examined on sampling days, in terms of volume and number of particles using the WingSALD II version 3.1.1 software. The samples were filtered through the same 250 μm mesh plankton net initially used for the seawater to remove large suspended particles. Fresh seawater was used as a blank sample. The Refractive Index value for PP was set to RI_{PP} = 1.49. Calibration of the instrument was performed with 20 μm, 100 μm, 200 μm and 500 μm polystyrene beads (NIST traceable size standards 3000 Series, Thermo Scientific) prior to analysis. The zeta-potential of water column samples from the mesocosms was examined as a measure of the stability of any colloidal formations, as well as the hydrodynamic diameter of the existing colloids. Measurements were performed at a temperature of 25 ^{o}C on a Nano ZS90 ZetaSizer (Malvern Instruments Ltd., UK), using the DTS1070 and DTS0012 disposable cuvettes for zeta-potential and size measurements, accordingly. The Refractive Index value was set to $RI_{colloids}$ = 1.18 (Stramski and Woźniak, 2005). A 1 L beaker of seawater was incubated in the same conditions as the mesocosms for the same period as the mesocosms and the zeta potential and hydrodynamic diameter of the colloid particles were measured, to determine the contribution of PP particles to the

aggregation process.

4.3.4. Biological Measurements

Biofilm attachment was quantified by staining the surface of 3 pellets with Crystal Violet (1% aqueous solution, Sigma-Aldrich), as already described (Lobelle and Cunliffe, 2011). Protein measurements were used as an indicator of the exopolymeric substances (EPS) produced during the formation of biofilm on the polymeric surfaces. The concentration of proteins in water column samples, as well as in the removed biofilm from pellets samples were measured monthly, as a complementary biofilm quantification method. A volume of 20 μL of sample was added in a disposable cuvette containing 1 mL of Quick Start™ Bradford 1x Dye Reagent (Bio-Rad, USA). After 30 minutes of incubation in the dark, the optical density of the solution was measured at 595 nm. Concentrations were quantified using a freshly made bovine serum albumin (BSA) standard curves (0-500 μg/mL). All optical density measurements were performed on a Shimadzu Uvmini-1240 spectrophotometer. The number of cells in the plastisphere was studied using flow cytometry. The cells were harvested by centrifugation (13.2 rpm for 20 min), resuspended in 1 mL of phosphate buffer solution (PBS, 0.1 M, pH=7.4), and fixed with methanol-free formaldehyde (final concentration of 4%) for 15 min. Following washing with excess PBS and an additional centrifugation step (13.2 rpm for 20 min), the cells were resuspended in 998 μL of PBS. The samples were stained with 2 μL of 1X Thiazole Green (10,000X Biotium) and incubated in the dark for 20 min, before being analyzed with a Beckman-Coulter CytoFLEX flow cytometer. Instrument gain for analysis was set to FSC = 300, SSC = 150, FITC = 50 and the primary threshold level was set to SSC = Automatic. Samples were measured at a flow rate of 30 μL/min and the measurement was terminated once 10.000 events had been recorded. A blank sample of 998 μL of PBS stained with 2 μL of 1X Thiazole Green was used for the elimination of background noise.

4.3.5. ARISA PCR

DNA was extracted in duplicates from the removed biofilm from pellets and water column samples, using the CTAB protocol for the extraction of bacterial genomic DNA (Moore et al., 2004). The isolated genomic DNA was resuspended in 50 μL TE buffer and the DNA concentration was measured on a Qubit 4.0 fluorometer (Invitrogen, Thermo Fisher Scientific, USA), using the Qubit dsDNA high sensitivity assay. The investigation of the community diversity between samples was evaluated by automated method of ribosomal intergenic spacer analysis (ARISA) PCR. The ITS1 region of rRNA was amplified using the ITSF (5-GTCGTAACAAGGTAGCCGTA-3) and ITSReub (5-GCCAAGGCATCCACC-3) primers, which target the 16S-23S rRNA intergenic transcribed spacers (Cardinale et al., 2004). PCR was performed using the KAPA HiFi HotStart PCR Kit (Kapa Biosystems,

USA), in a 25 μL mixture containing 0.75 μL of deoxynucleotide triphosphates, 0.75 μL of each of the forward and reverse primers, 0.5 μL KAPA HiFi HotStart DNA Polymerase (1 U/μL), 5 μL KAPA HiFi Fidelity Buffer (5X) and 1-5 μL DNA (depending on the measured concentrations). The cycling conditions for the PCR reaction were: one denaturation phase at 95 ˚C for 3 min, followed by 40 cycles at 98 ˚C for 20 s, 65 ˚C for 15 s, 72 ˚C for 2 min, and a final extension at 72 ˚C for 4 min. The PCR product along with the 15/1500 bp markers and the ladder contained in the Agilent DNA 1000 Assay Kit was loaded on a DNA 1000 chip (Agilent Technologies, Belgium). The chip was run on an Agilent 2100 Bioanalyzer.

4.3.6. ATR-FTIR

The chemical structure of the pellet surfaces over time was examined by studying the functional groups, using Attenuated Total Reflection – Fourier-Transform Infrared spectroscopy (ATR-FTIR). Analyses were performed on a Nicolet™ iS50 FTIR Spectrometer equipped with a diamond ATR accessory (Thermo Scientific, USA). Spectra were obtained with Thermo Scientific's OMNIC software. Four clean pellets from each tank were examined from two sides every month. Spectrum acquisition was done after 32 scans for absorbance numbers between 4000 and 400 cm^{-1}, with a scan resolution of 4 cm^{-1}. A background scan was performed at the beginning of each session and repeated after approximately 30 minutes, to ensure the quality of the acquired spectra. Changes of the surface chemical structure were monitored by the calculation of a number of indices related to the degradation of plastic polymers, namely the keto carbonyl (KCBI), ester carbonyl (ECBI), vinyl (VBI) and carbonyl (CI) indices (Albertsson et al., 1987; Rajakumar et al., 2009). The index values were calculated from the peak intensity at specific wavenumbers (I_{xxxx}), as shown in Table 4.1.

Table 4. 1: Calculation of indexes from ATR-FTIR spectra absorbance values.

Index	Calculation Formula
keto carbonyl (KCBI)	$\mathrm{KCBI} = \frac{I_{1715}}{I_{974}}$
ester carbonyl (ECBI)	$\mathrm{ECBI} = \frac{I_{1740}}{I_{974}}$
vinyl (VBI)	$\mathrm{VBI} = \frac{I_{1640}}{I_{974}}$
carbonyl (CI)	$\mathrm{CI} = \frac{I_{1740}}{I_{1460}}$

4.3.7. Pellet Weight and Area Measurements

A total of 10 sets of virgin and 10 sets of weathered pellets, each set consisting of 5 pellets, were weighed prior to placement in the mesocosms using a 5-digit digital laboratory scale. From these measurements, the average gravimetric weight for one individual pellet, as well as the standard deviation, were calculated. After each sampling the collected pellets were randomly separated in groups of five and weighed. The averages and standard deviations were calculated and statistically analyzed. Washed pellets were photographed using a Leica MC190HD camera attached to a Leica MZ7s stereoscope. The diameter of all collected pellets was measured using ImageJ version 1.52i version and the area was calculated using the surface area equation for a sphere (πD^2).

4.3.8. Data analysis

Statistical analysis, as well as the principal component analysis (PCA) were carried out using R version 4.0.0 (R Core Team, 2021) in the environment R Studio version 1.3.959. Shapiro-Wilk's test was used for the examination of data normality and subsequently the Kruskal-Wallis non-parametric test was applied for the detection of statistically significant differences between samples. Correlation matrices were created using the *cor.mtest* function, while correlation plots were created using *corrplot* (Wei, T. and Simko, 2017).

The analysis of ARISA fragments was performed using the Bioanalyzer software. Fragments that differed by less or equal to 3 bp were considered identical and fragments with Fluorescence Units over 150 were considered for further analysis (Ramette, 2009). PCA of the biofilm communities was performed using the function *prcomp* and *fviz_pca* from the package "factoextra" (Kassambara and Mundt, 2020). Ellipses in the PCA graph grouped the different treatments with a confidence level of 0.95. Data visualization was implemented using the *ggplot2* package.

4.4. Results

4.4.1. Mesocosm seawater characterization

The state of the water column in the emulated pelagic zone was assessed through the examination of the following parameters.

4.4.1.1. Radiation and Water Quality Measurements

Radiation monitoring revealed that the virgin mesocosm was exposed to a total of 1.33×10^7 Lux of radiation throughout the experiment, while the weathered mesocosm to 1.56×10^7 Lux. The results of the water quality parameter measurements prior to nutrient supplementation are shown in Table S1.

4.4.1.2. Nanoparticle detection – Light Scattering

Monthly examination of mesocosm seawater samples did not reveal the presence of plastic particles in the nano- (<1 μm) and micro- (<1 mm) scale.

4.4.1.3. Zeta-potential and Colloid Hydrodynamic Diameter

The absolute values of zeta-potential (Figure 4.1a) in mesocosms were higher than the seawater (7.2 ± 0.8 mV) throughout the experimental period. After a constant increase of 150 days, a maximum value of 16.2 ± 0.5 mV was observed in the mesocosm seawater samples from the virgin mesocosm followed by a decrease to 11.9 ± 0.9 mV. The zeta-potential in the weathered mesocosm also increased for 120 days to reach a maximum of 14.0 ± 0.4 mV. Zeta-potential in the weathered mesocosm reached a value of 11.0 ± 1.1 mV at the end of the experiment. The zeta potential of the control sample containing no PP pellets at the end of the experiment was -7.4 ± 0.346 mV.

Marine colloids are organic or inorganic particles present in the marine environment with dimensions large enough to possess supermolecular structure and properties, but at the same time small enough to sediment quickly in the absence of aggregation (Buffle et al., 1998). The hydrodynamic diameter of marine colloids contained in the system consistently increased in both mesocosms as shown in Figure 4.1b. Interestingly, for the first 60 days of the experiment, the two mesocosms followed almost identical patterns, and differentiated afterwards. During the last 30 days, the hydrodynamic diameter of colloid particles decreased in both treatments, achieving final values of 1437.0 ± 174.5 nm and 1150.0 ± 204.0 nm in the virgin and weathered mesocosm, respectively. The hydrodynamic diameter of marine colloids in the control sample not containing PP pellets on the 180th day was 442.7 ± 97.3 nm.

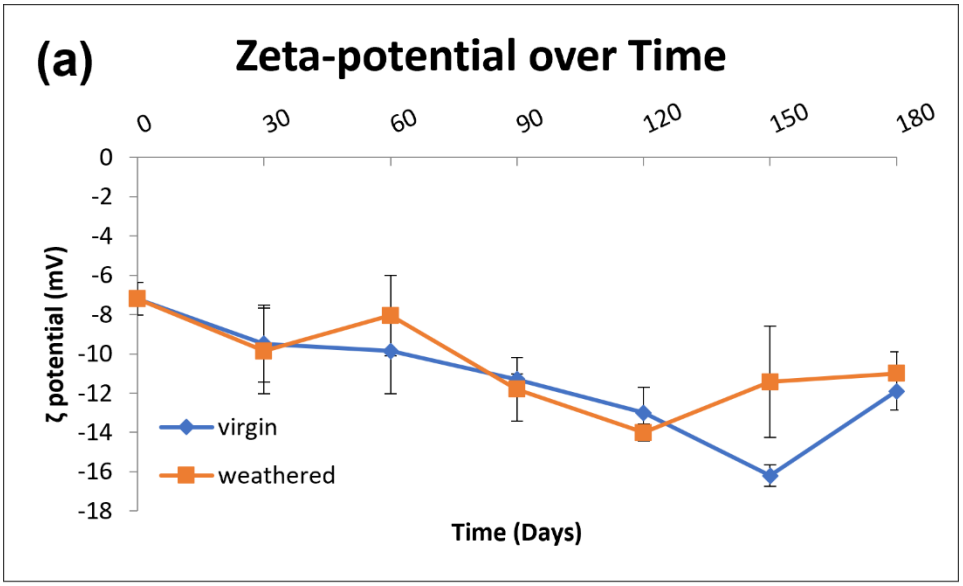

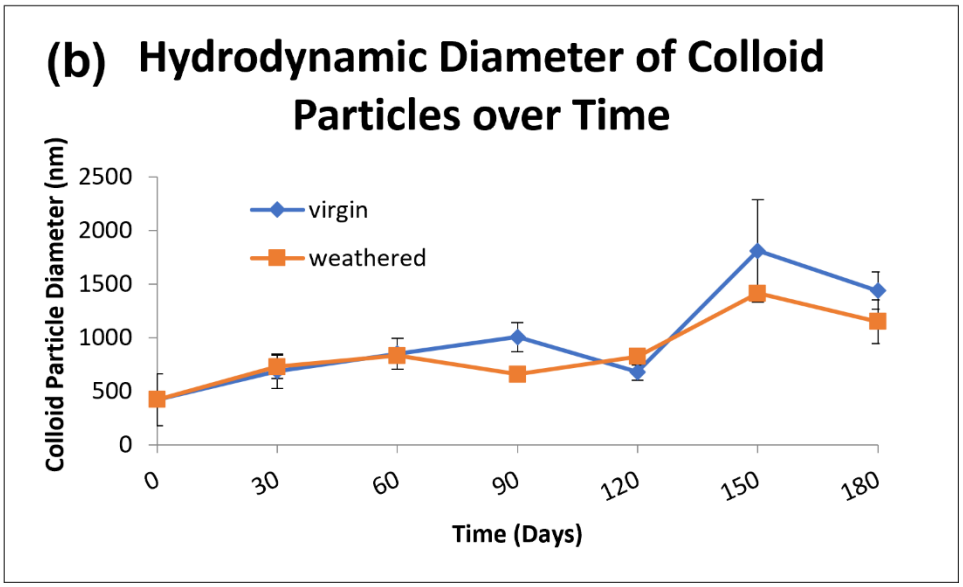

Figure 4. 1: (a) Zeta-potential in the water column samples of the virgin and weathered mesocosm over time, (b) Hydrodynamic diameter of colloid particles in the mesocosm seawater samples of the virgin and weathered mesocosm over time.

4.4.2. Free living and plastic colonizing microbial communities in the mesocosms

4.4.2.1. Biofilm Development

Biofilm was detected on the surface of the pellets - 30 days after the initiation of the experiment (Figure 4.2). The absorbance values fluctuated with time in both mesocosms. Even though the absorbance was consistently higher in removed biofilm from weathered pellets samples; however, no statistically significant differences were observed. More specifically, an initial increase from the value of 0.50 ± 0.042 on the surface of the virgin pellets to a maximum value of 1.10 ± 0.343 over the first 30 days was followed by a decrease to 0.66 ± 0.210 for the next 60 days. The observed 1.05 ± 0.55 of day 150 finally regressed to 0.87 ± 0.426 at the end of the experiment. Similarly, for weathered pellets, an absorbance of 0.86 ± 0.280 was measured after 30 days. A steep increase to 1.88 ± 0.480 was observed on the 60th day, reaching 1.97 ± 0.242 on the 90th day. After 120 days the minimum absorbance value of 0.84 ± 0.279 was measured, wherefrom the maximum value of 2.04 ± 0.896 of the final measurement was achieved after 60 days.

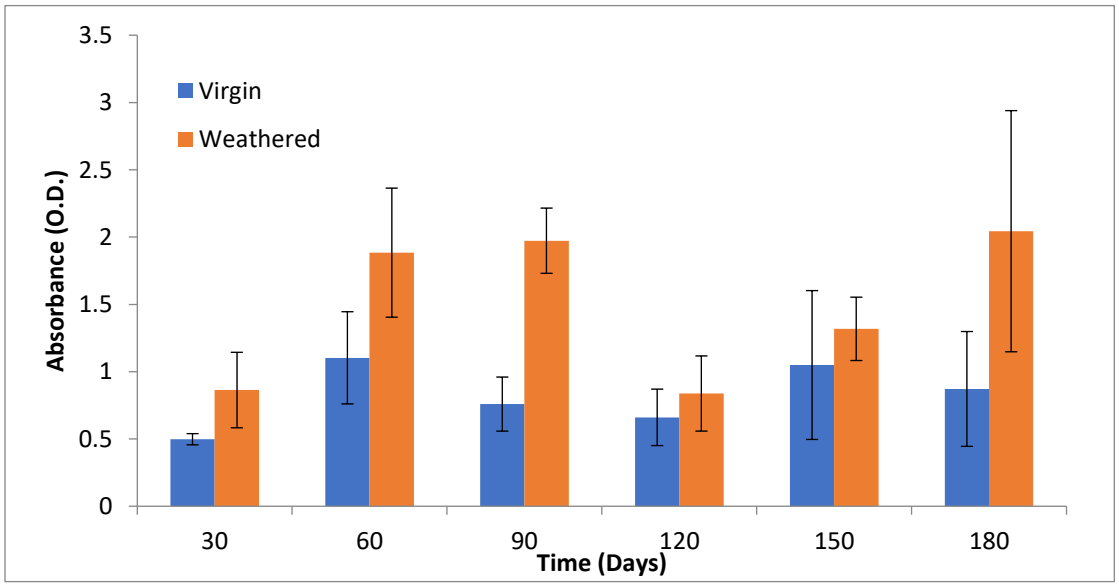

Figure 4. 2: Biofilm accumulation on pellet surfaces over time, as indicated by the absorbance (optical density) of Crystal Violet- stained samples.

An estimation of the EPS within the biofilm and in the mesocosm seawater was performed by measuring the protein concentrations on the surface of the pellets, as well as in the seawater samples respectively. After the initial attachment, the proteins on the pellet surfaces were mostly stable, regardless of weathering degree, ranging between 961.6 – 1071.0 μg/cm^2 on the virgin and between 1250.9 – 1537.4 μg/cm^2 on the weathered pellets (Figure S2). Interestingly, both maximum values were observed after 150 days of incubation. Despite the absence of statistically significant differences

between the two mesocosms, the consistently higher protein concentration on the weathered pellets is in agreement with the aforementioned biofilm measurements. A gradual increase of protein concentrations in the seawater samples was noticed (Figure S3); from the initial 319.1 μg/mL of the seawater used for filling the tanks, to 527.8 μg/mL and 562.2 μg/mL in the virgin and weathered mesocosm, respectively. It can be seen that the protein concentrations in the weathered mesocosm are consistently higher than the virgin mesocosm, in agreement with the previous biofilm and protein measurements.

4.4.2.2 Cell Concentration and Community Diversity

Given that sufficient time for acclimatization, biodegradation of C-C backbone plastics within marine biofilm matrices is possible (Syranidou et al., 2017, 2019), the number of sessile cells is an important factor in the polymer deterioration process. Initial biofilm attachment was accompanied by the growth of $1.01x10^7$ and $2.15x10^7$ cells/cm^2 on the surface of the virgin and weathered pellets, respectively (Figure 4.3). The slight reduction of cells observed after 60 days of incubation ($5.02x10^6$ cells/cm^2 for virgin and $7.35x10^6$ cells/cm^2 for weathered pellets) was followed by gradual increase in the last 30 days of the experiment, despite the marginal decrease observed in the virgin mesocosm ($1.06x10^8$ cells/cm^2 for virgin and $6.26x10^7$ cells/cm^2 for weathered pellets). Quantification of free cells in the mesocosm revealed them to be significantly lower. Starting from $2.2x10^3$ cells/mL in the seawater initially used, they increased up to $1.8x10^4$ cells/mL and $5.6\ x10^4$ cells/mL for virgin and weathered pellets, respectively.

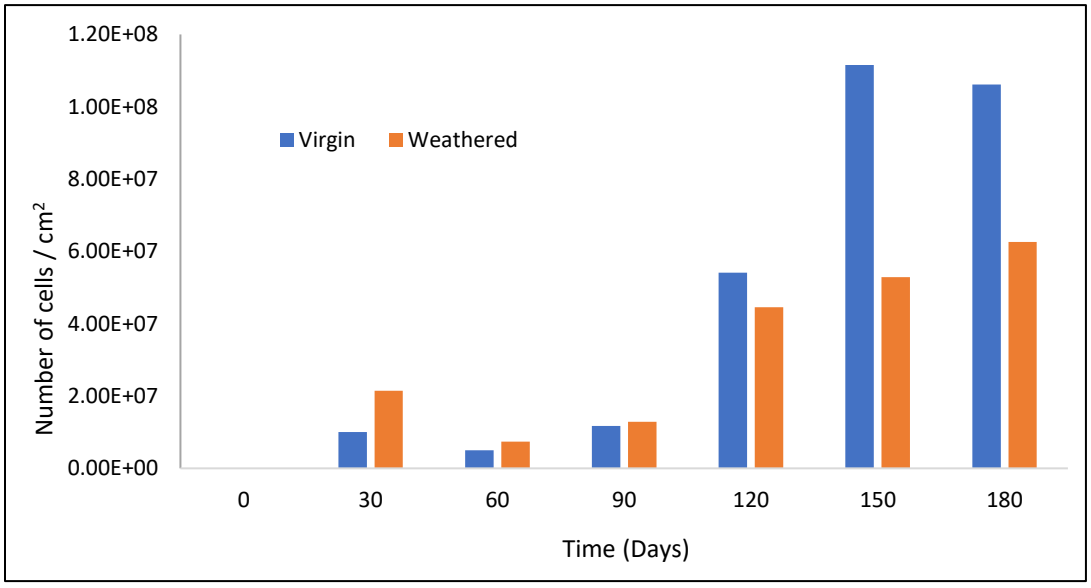

Figure 4. 3: The number of cells on the surface of the pellets from the two mesocosms over time.

The composition of the community was compared using non-metric multidimensional scaling (NMDS) in terms of time (first 3 versus last 3 months), as well as the surface condition of the pellets acting as a substrate. The analysis was performed in two stages: first for the samples from the mesocosm seawater, to assess the free-living communities, and the biofilm which was removed from the pellets, and then for the biofilm samples alone. It was revealed that 6 months was not sufficient time for the planktonic and biofilm communities to differentiate in a substantial manner (Figure S7a). The samples from the second half of the experiment are more dispersed, indicating separation of the community from the one initially added. However, no statistically significant differences can be observed between the two groups (Figure S7b). When pellet weathering is used as a separating factor, it can be noted that planktonic and biofilm communities are overlapping, irrespective of pellet substrate weathering (Figure S7c). When the biofilm communities are examined separately, a distinct clustering exists and the difference between the two sets of samples are statistically significant (Figure S7d). Therefore, the non-metric multidimensional scaling comparisons provided indications that polymer weathering can act as a driving force for community evolution.

4.4.3. Polymer Properties

4.4.3.1. ATR- FTIR

An incubation period of 60 days in the mesocosm resulted to drastic oxidation of the surface of virgin PP pellets (Figure 4.4a and Figure S4). The broad peak between 3600 and 3000 cm^{-1} is attributed to the O-H stretching from the introduction of hydroxyl groups (OH) on the chemical structure of PP. The peaks at 1642 cm^{-1} and 1150 cm^{-1} correspond to the C=O stretching, and to C-O bond stretching, respectively. After 90 to 120 days of incubation the peaks were still present, however less pronounced, while at the end of the experiment the polymer structure was closer to that of the virgin polymer of day 0. The FTIR Indices calculated for the virgin pellets (Figure 4.5) confirm that there were changes in the chemical structure of the surface of the polymer not only between the start and the end of the experimental period, but also between days 90 and 180. It can be observed that the differences occurring during that time affected the indices related to carbonyl groups, namely KCBI, ECBI and CI (Figure 4.5a, 4.5b and 4.5d), in a statistically significant manner (*p-value* < 0.01).

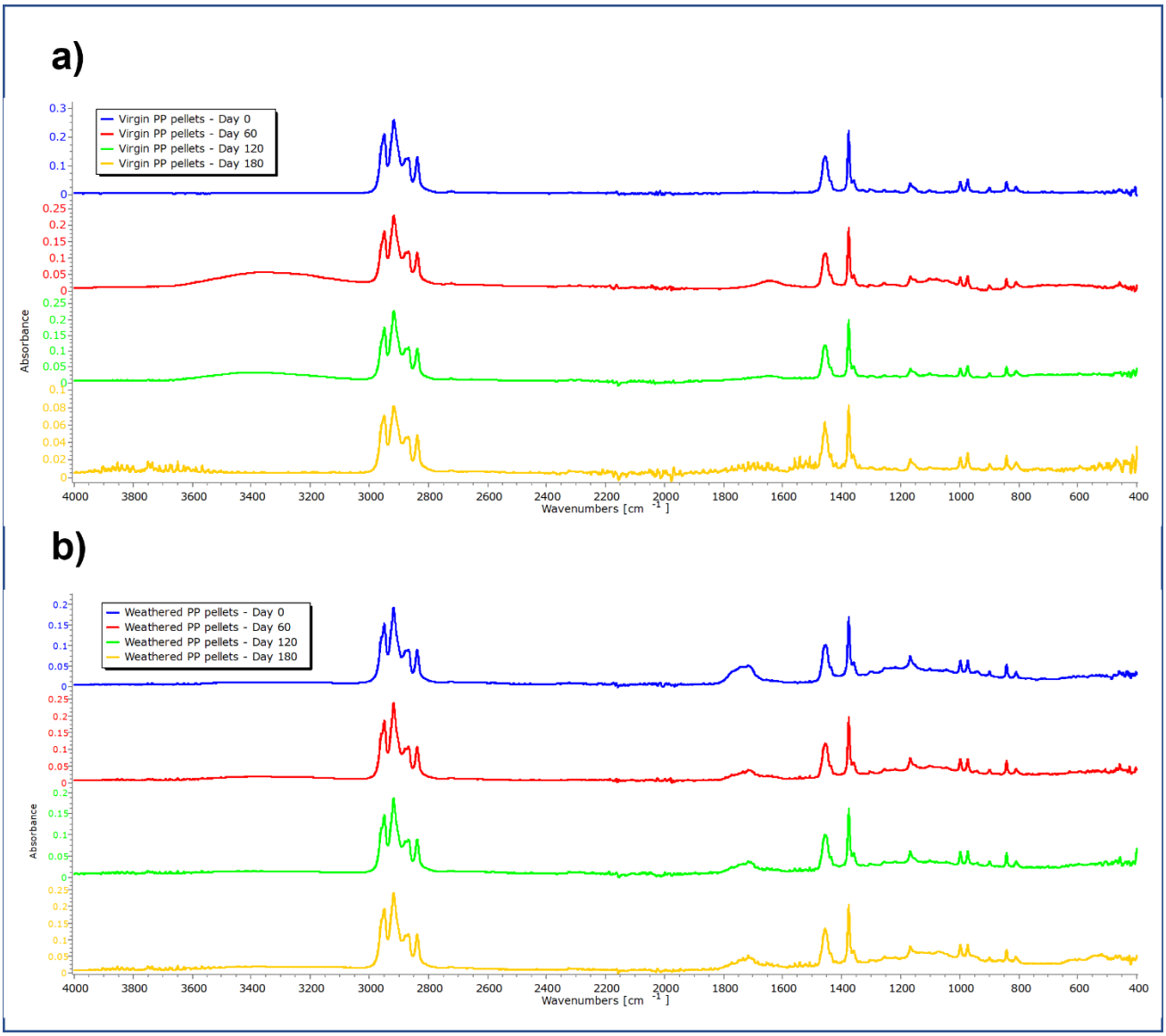

Figure 4. 4: ATR-FTIR spectra on days 0, 60, 120 and 180 of: (a) virgin pellets; (b) weathered pellets.

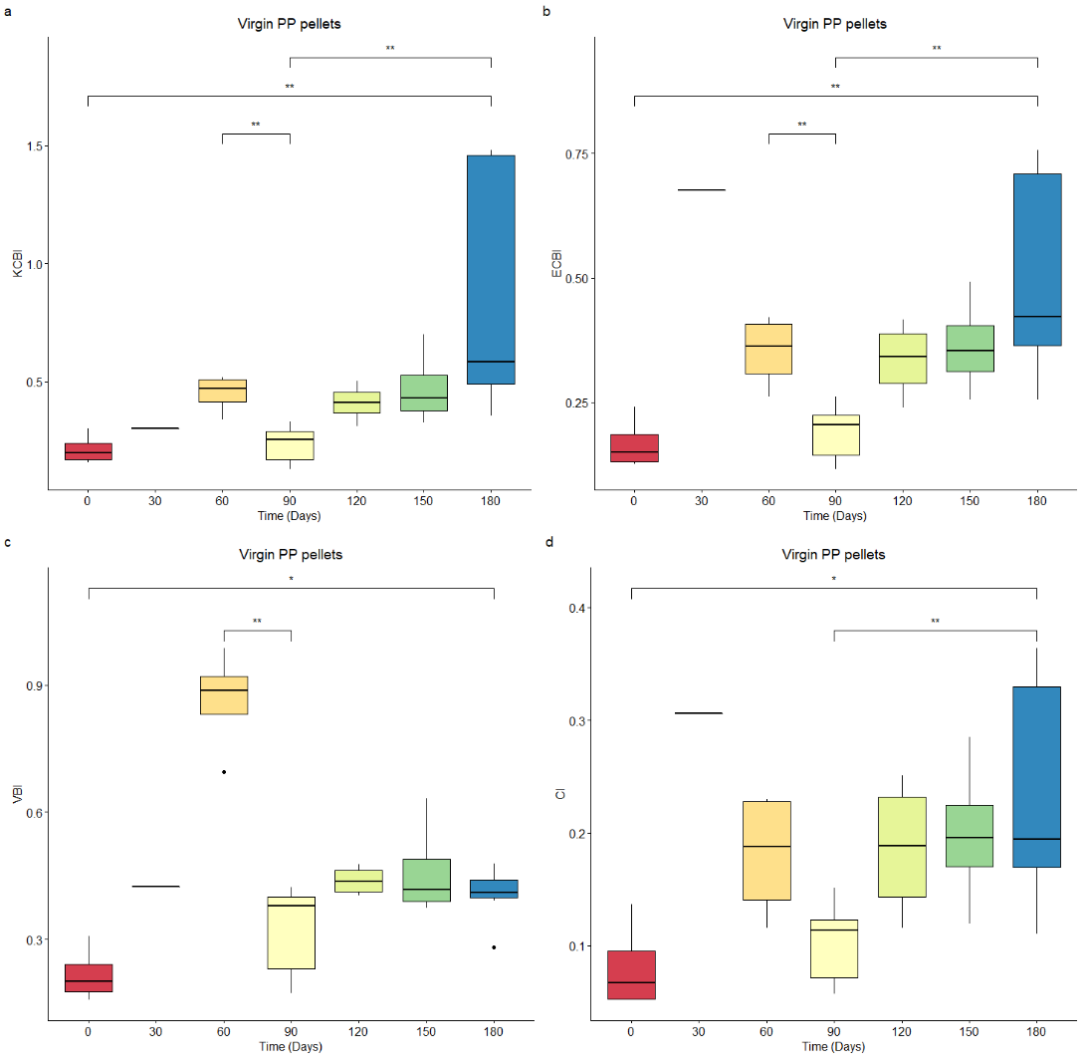

Figure 4. 5: ATR-FTIR indices of virgin pellets over time: (a) Keto carbonyl bond index; (b) Ester carbon bond index; (c) Vinyl bond index; (d) Carbonyl index. Stars indicate significance levels: one star for p-values <0.05, two stars for p-values <0.01.

The spectra for weathered samples (Figure 4.4b and Figure S5) reveal how mesocosm incubation affected the already changed structure of the pellets. The broad conjugated C=O stretching aldehyde peak at 1717 cm^{-1} was less pronounced after 60 days and was reamplified in the second half of the experiment, while it also became sharper over time. A C-O stretching ether band peak (1100 cm^{-1}) was present on day 60, almost disappeared on day 180 and was again detected at the end of the experiment. The C=O stretching and C-O stretching peaks detected due to oxidation of the virgin PP pellets were present in the weathered pellet spectra, as well, but following a pattern similar to the 1100 cm^{-1} peak; receding on day 120 to reappear at the end of the experiment. The tendency of the weathered pellets to return to the virgin state in the first half of the experiment, to then follow

oxidation patterns similar to the virgin pellets can be observed in Figure 4.6. KCBI, ECBI and CI values decrease until day 90 and then increase for the rest of the experimental period. VBI values, however, increase steeply in the first 30 days, decrease until the 90th day and then slowly increase again, indicating the accentuated presence of double bonds in the chemical structure of the pellet surfaces. From day 90 until the end of the experiment the polymer was substantially oxidized, similarly to the "virgin mesocosm" samples, as can be seen by the significance levels (*p-values* < 0.05) in Figures 4.6a, 6b and 6d. Finally, it can be observed in Figure 4.6c that significant differences in VBI values exist not only between days 90 and 180 (*p-value* < 0.01), as happens with the rest of the indices, but also between days 0 and 30 (*p-value* < 0.05), 30 and 60 (*p-value* < 0.05) and throughout the experiment (*p-values* < 0.01).

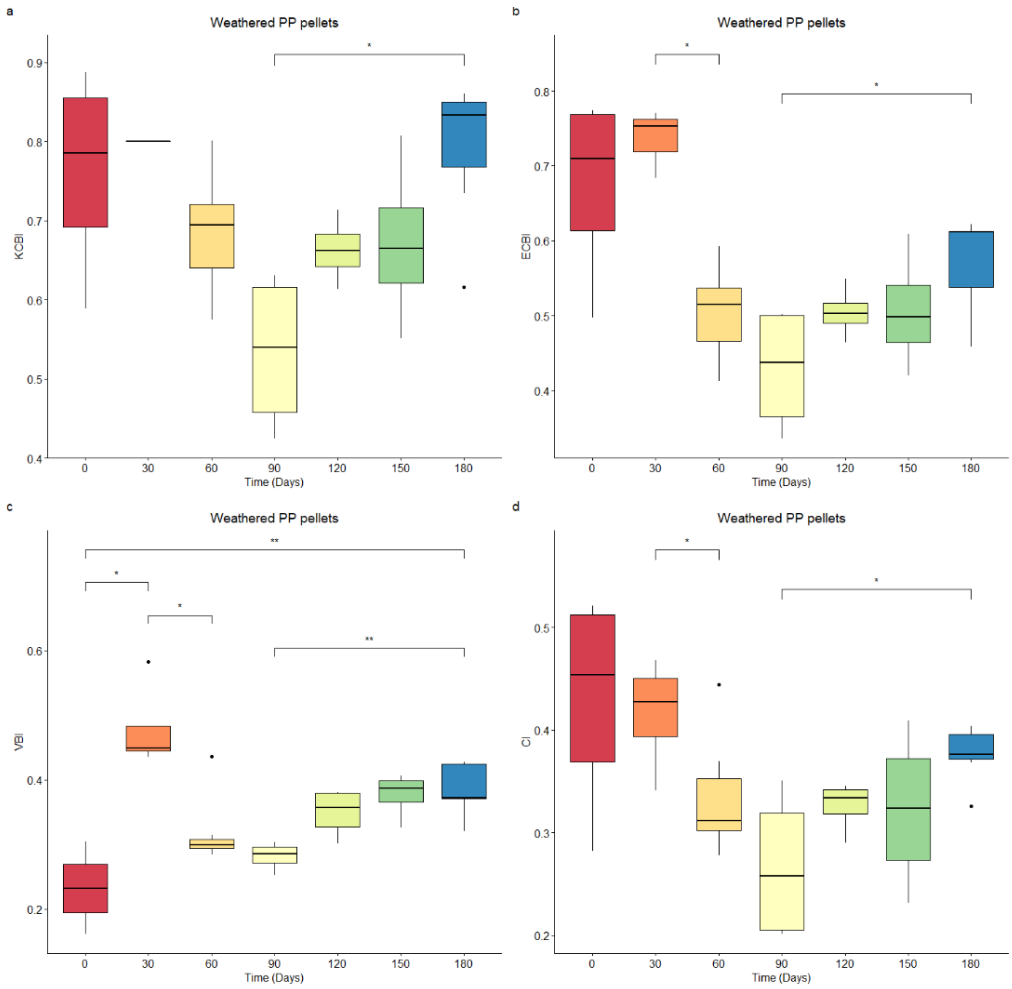

Figure 4. 6: ATR-FTIR indices of weathered pellets over time: (a) Keto carbonyl bond index; (b) Ester carbon bond index; (c) Vinyl bond index; (d) Carbonyl index. Stars indicate significance levels: one star for p-values <0.05, two stars for p-values <0.01.

4.4.3.2. Pellet Area and Weight

Over the 180-day incubation period, the area of the virgin pellets decreased by 20.8%, while that of the weathered pellets 26.3% (Table 4.2). This decline occurred mainly in the first half of the experiment for the virgin pellets (14.9%), and during the second half (22.7%) for the weathered pellets. However, the weight of the pellets fluctuated throughout the 180 days. The individual weight measurements with the respective averages and the 95% confidence intervals can be observed in Figure S6.

Table 4. 2: Average (n=10) single pellet area and weight over time.

Time	Area (cm^2)		Weight (mg)	
(Days)	Virgin	Weathered	Virgin	Weathered
0	0.54 ± 0.045	0.53 ± 0.039	24.23 ± 0.979	22.53 ± 1.563
30	0.51 ± 0.043	0.53 ± 0.091	25.06 ± 0.368	22.62 ± 1.046
60	046 ± 0.076	0.52 ± 0.118	24.87 ± 1.126	23.44 ± 0.670
90	0.46 ± 0.045	0.51 ± 0.123	-	-
120	0.45 ± 0.215	0.48 ± 0.131	24.92 ± 1.272	24.46 ± 0.450
150	0.44 ± 0.101	0.42 ± 0.125	25.26 ± 1.251	23.10 ± 0.676
180	0.425 ± 0.111	0.39 ± 0.101	24.97 ± 0.897	23.67 ± 1.005

4.4.3.3. PCA – Correlations

Principal component analysis was performed using 18 variables, corresponding to the parameters examined throughout the experiment: time ("Days"), O.D. after the application of Crystal Violet dye on the samples ("Crystal_Violet_OD"), protein concentration on the pellet surface and the water column ("Proteins" and "Proteins_Liquid"), number of cells, pellet area, pellet weight, FTIR indices, zeta-potential, colloid particle size, temperature, conductivity, dissolved oxygen, total nitrogen and NO_3. The PO_4 concentrations were omitted since the values were consistently below the detection limit. A total of 12 principal components (PC) were required for the explanation of the variance between the samples. The first three components, PC1, PC2 and PC3 contributed to the variance by 40.1 %, 18.5 % and 14.8 %, respectively. Interestingly, a time-dependent sample clustering can be observed (Figure 4.7). The increased length of the vectors for the FTIR indices emphasizes the effect of radiation during the initial stages of incubation. Samples from days 90 and 120 overlap lower on the PC2 axis, while the samples from the last 60 days of the experiment cluster towards the direction of the biological parameter vectors.

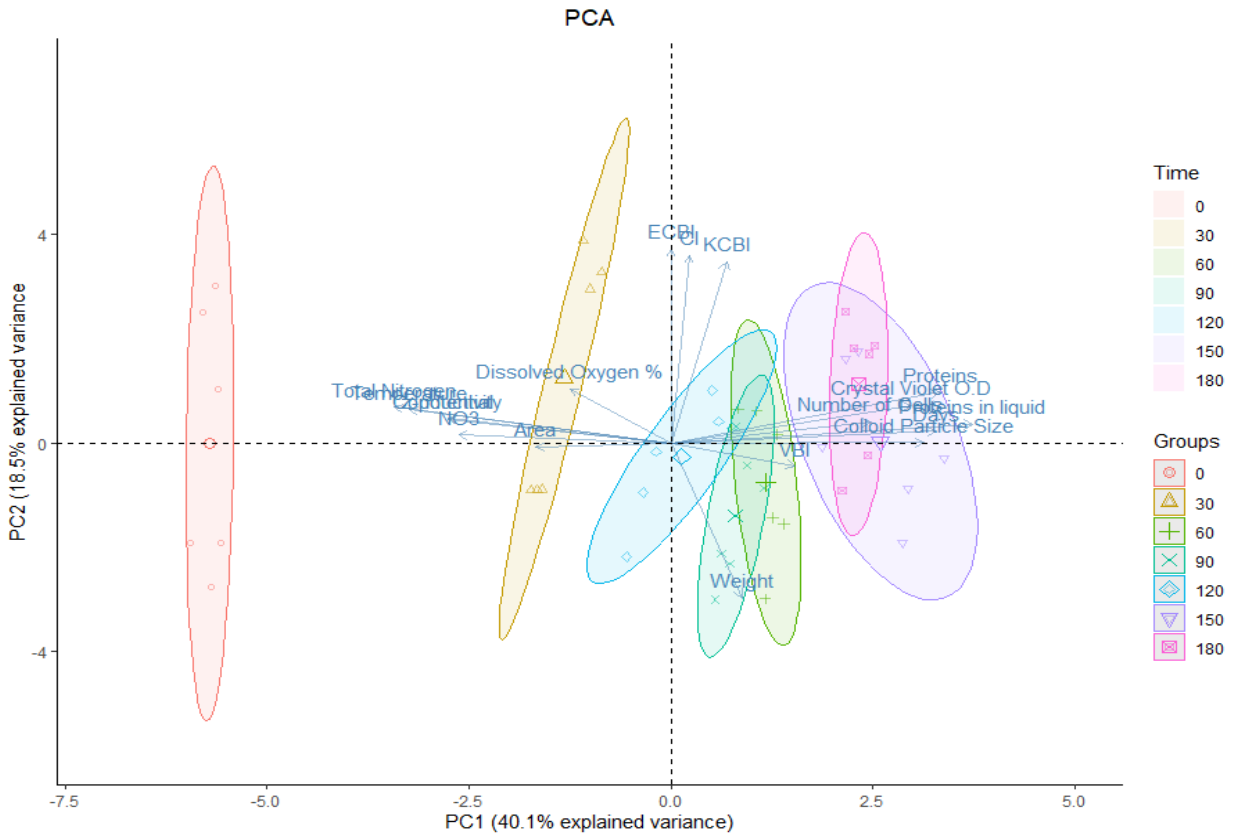

Figure 4. 7: Principal component analysis biplot.

The correlations between the aforementioned parameters reveal significant results (Figures S8a and S8b). The biological parameters are correlated with environmental factors and nutrient availability, more intensively in the weathered mesocosm. Even though in the virgin mesocosm the area of the pellets is negatively correlated to all of the biological parameters examined, nevertheless, in the weathered mesocosm the negative correlation only applies to the number of cells within the biofilm. In accordance with the PCA results (Figure 4.7), FTIR indices are not correlated to the biological parameters. Differences can also be observed upon the examination of the correlations of zeta-potential and colloid particle sizes with the biological parameters; they are strongly correlated in the virgin mesocosm, but in a weaker manner than in the weathered mesocosm.

4.5. Discussion

The fate of virgin and artificially weathered PP pellets in the marine environment was studied in mesocosms. Micro- and mesocosm experiments can serve as valuable tools, especially when concentration measurements are involved, to overcome limitations arising from the infinite dilution

of microscopic particles in the sea. In the experiment described here, this was also facilitated by high concentrations of microplastics, which could, however, be potentially found in the sea, especially in the Mediterranean Sea, second to pollution only to the oceanic gyres (Suaria et al., 2018). A total of 18 parameters related to the polymer, biological factors and the mesocosm seawater as well as their interactions were monitored, to comprehensively describe the degradation process and elucidate the interplay among these parameters.

4.5.1. The fate of secondary microplastics

The hydrodynamic diameter of the colloid particles in the mesocosm seawater increased over time, while the surface area of the examined pellets (computed as πD^2) decreased due to solar radiation and the interaction with the attached cells (Rummel et al., 2017). It seems that the generated microparticles induce the formation of larger aggregates over time in the mesocosm seawater. Aggregation is generally considered a significant process that determines the fate of microplastics (MPs) in the aquatic environment (Besseling et al., 2017). In fact, two phases of the experiment (0-90 days and 90-180 days) can be observed, where the colloid diameter is concerned, in line with the other measurements (number of cells in the biofilm and changes of surface chemistry). During the last 60 days of the experiment, the size of the colloid particles is higher than the corresponding one in the seawater used to fill the tanks for the virgin and weathered mesocosms. At the same time, it is noteworthy that during the period when the largest colloid particles can be detected in the water column, the zeta-potential is between -11 mV and -16.2 mV. Particle aggregation, however, is considered to be occurring spontaneously in the neutral range between -10 and 10 mV (Clogston and Patri, 2011). This counterintuitive observation could be attributed to the kinetic energy added to the mesocosms by the aeration system. According to the Derjaguin-Landau-Verwey-Overbeek (DLVO) theory (Verwey et al., 1946), this kinetic energy could assist the particles in overcoming the electrostatic repulsion energy barrier into the region where van der Waals attractive forces lead them to aggregate into larger particles. The post-aggregation zeta-potential decrease has been mentioned by Zhang et al. (2019), while the decrease in colloid hydrodynamic diameter observed in the last 30 days of the experiment is also consistent with the findings of Pacek et al. (2007), who noted the de-aggregation of silica agglomerates when particle size exceeded 3 μm.

It can be safely assumed that micro- and nanoparticles were generated in the mesocosms and this is related to the area loss of the pellets (Ali et al., 2021; Andrady et al., 2019; Lambert and Wagner, 2016; Mattsson et al., 2018; Piccardo et al., 2020; Song et al., 2017). The number of secondary MPs has been linked to the extent of aging of weathered fragments; the more aged pellets produce more particles when exposed to irradiation (Sorasan et al., 2022). However, sub-millimetric PP particles

could not be detected in the mesocosm seawater using dynamic light scattering particle analysis, which can be attributed to the low concentrations of the particles in the seawater (ter Halle et al., 2017). The development of biofilm may act as photo-protective barrier (Rizzo et al., 2021). The produced MPs could have been retained inside the biofilm matrix immediately after their release from the pellets, thus not leading to an increase of their concentration due to degradation.

Another and most probable reason might be that the secondary particles have been encompassed in the EPS from which the marine colloidal particles present in the liquid consist of, as part of the hetero-aggregation process (Oriekhova and Stoll, 2018; Praetorius et al., 2020). In aquatic environments, several environmental factors such as pH, ionic strength and the presence of natural organic matter influence the behavior of microplastics and nanoplastics (NPs) and thus govern the extent of their aggregation potential (Sharma et al., 2021). High initial concentrations of nutrients and proteins were determined in the natural seawater used for the experiment. These concentrations can be traced back to the characteristics of the area from which the seawater was collected. Souda is an enclosed bay receiving the runoff of Moronis river passing through fertilized agricultural areas. The river transfers high loads of nitrogen enriching the ecosystem (Dasenakis et al., 2012). The higher levels of nutrients could pose the threat for eutrophication in the mesocosms. That did not occur, however, and it might have played a role in the rapid increased aggregation observed in the mesocosms. The process of aggregation can also be greatly affected by particle size. Alimi et al. (2022b) found that smaller particles (28 nm) tended to aggregate more effectively than larger ones (220 nm) in artificial seawater, natural water as well as in the presence of $CaCl_2$ and sodium alginate. The marine EPS can interact with NPs leading to the formation of a diverse biomolecular coating on the surface of NPs, known as eco-corona and/or to the development of aggregates with entrapped NP particles (Junaid and Wang, 2021). The presence of plastic polymer nanoparticles, namely polystyrene and polymethyl methacrylate, has been found to assist the faster and more effective aggregation of organic matter in water samples and leads to the formation of microgels (Chen et al., 2018; Shiu et al., 2020). Moreover, the biofilm could induce the NPs generation as part of the biofragmentation process (Karkanorachaki et al., 2022) and these sticky particles have a high potential not only to interact with the existing aggregates but also to strongly contribute to the formation of new ones (Michels et al., 2018). Polystyrene nanoparticles have also been linked to higher polysaccharidic and proteinaceous gel concentrations in mesocosm experiments and the increased excretion of highly proteinic EPS (Galgani et al., 2019, Shiu et al., 2020), in accordance with the increase in protein concentrations in the seawater of both our mesocosms. This resulted in the entrapment of microplastics into the gel particulates, as proteins contain positively charged sections that are capable of interacting with the

negatively charged particles (Pradel et al., 2023). The incorporation of microscopic plastic particles in extracellular polymers, microgels and marine colloidal particles can lead to changes in size and density and subsequently the sinking velocity of the hetero-aggregates (Galloway et al., 2017; Kaiser et al., 2019, 2017; Kooi et al., 2017; Rummel et al., 2017). Thus, micro- and nanoplastics can be vertically transferred via the sinking of marine snow towards the seafloor (K. Kvale et al., 2020; K. F. Kvale et al., 2020; Porter et al., 2018). Having sunk, plastics can act as an additional bioavailable organic carbon source, stimulating microbial growth (Chae et al., 2020; Galgani et al., 2019; Romera-Castillo et al., 2018; Zhu et al., 2020). As a result, the aggregation with organic particles could determine the fate of MPs by altering their sinking behavior (Leiser et al., 2020) as well as their ecological impact (Junaid and Wang, 2021). Due to the constant aeration of the tanks, settling was prevented and the observation of "marine plastic snow" was not possible.

Despite the area loss, it was not possible to detect weight reduction of the pellets. That could be attributed to the statistical calculation of the weight of the pellets described in section 2.7, which was dictated by the difficulty to individually identify each pellet for weighing before and after incubation. The behavior of the pellet weight also could be explained by the oxidation of the polymer, since the introduction of oxygen in the polymeric chain could lead to weight increase. Finally, salt crystals or biological material could be trapped in cracks or holes resulting from the degradation material. Thus, any weight decrease that might otherwise have been observed, could be offset by the additional non-polymeric material. In order to avoid potential bias and at the same time, effectively estimate the surface process of polymeric degradation, we propose that area loss should be used instead of weight reduction as an indicator of polymeric degradation. Given the precision required for the quantification of such miniscule changes, analytical techniques, such as BET, should be further developed and applied.

4.5.2. Effect of biofilm on the surface

Weathered pellets were found to be more susceptible to biofilm attachment and development than their virgin counterparts. Variations in the extent of biofilm, observed for both the virgin and weathered pellets, indicate cycles of attachment and detachment, possibly due to the fact that the pellet surface is limited and cannot facilitate indefinite growth (Karkanorachaki et al., 2021). Cell numbers in the first phase (0-90 days) of the experiment are generally higher in the weathered mesocosm, but in the second phase, this situation is reversed. It is therefore evident that weathered pellets are initially the preferred substrate for cell growth. With time, virgin pellets are preferred instead. The surface of the virgin polymer is deteriorating with time which may facilitate cell

attachment in the same way as the weathered pellets at the beginning of the experiment. At the same time, the upper surface layer of the weathered pellets, which was damaged by the UV radiation and allowed for the sustainment of cells, is removed, thus revealing the virgin part of these pellets. The number of cells, which is strongly negatively correlated to the area of the pellets ($r = -0.74$ for the virgin and $r = -0.84$ for the weathered samples), supports this hypothesis. In general, increased biofilm quantities and cell growth were detected when the polymeric surface is most deteriorated which is consistent with the aforementioned hypothesis and supported by published literature (Rummel et al., 2017).

Plastisphere communities are considered to be different from the free-living bacteria in the marine environment (Dussud et al., 2018; Frère et al., 2018), as well as from those developing on natural particles (Crespo et al., 2013). Our findings indicate that this is not always the case. When the samples were not segregated based on the weathering of the PP pellets provided as substrate, the communities attached on the surface of the pellets were not significantly different compared to the planktonic ones. This observation can be supported by the assumption that the time provided was not adequate for substantial community differentiation. The process of community acclimatization for plastic polymer biodegradation is a time-dependent process (Yang et al., 2020). Long acclimatization times are required by the marine communities before biodegradation begins, while on the other hand, the effects of the biotic and abiotic degradation demand time in order to be detectable. A six-month acclimatization period has been reported (Syranidou et al., 2017), which is equal to the total duration of our experiment. The diversity between marine communities on virgin and weathered pellets, however, confirmed that biofilm formation is also a substrate-dependent process (Yang et al., 2020). In the marine environment, where other processes which could delay the biofilm build-up or diminish the effect of solar radiation are present, these effects might be visible after periods of time longer than those reported here. For that reason, the degradation times of polymers have been placed on the scale of decades or even centuries (Chamas et al., 2020).

Photooxidation acts as an effective pretreatment for the biodegradation of the highly resistant PP pellets (Aravinthan et al., 2016; Esmaeili et al., 2013; Roy et al., 2008). The chain scission and cross-linking caused by the UV radiation counterbalance the presence of tertiary carbon atoms in the backbone of the polymer, therefore making it more susceptible to microorganisms. Furthermore, marine microorganisms have been found capable of producing reactive oxygen species (ROS), namely superoxide, upon incubation with PE, another polyolefin with a C-C backbone. It is speculated that interactions with ROS result in unspecific chain oxidation, similar to that occurring from abiotic weathering (Zadjelovic et al., 2022). Residence of virgin pellets in the marine mesocosm for 60 days

resulted in the alteration of the physicochemical properties of the surface (increase of all the FTIR indices). Carbonyl groups appear in the spectra, indicating abiotic degradation (Gewert et al., 2015). Increase in the values of the indices conveys the tendency of the virgin particles to converge with their weathered counterparts, possibly under the effect of natural light (Veerasingam et al., 2020). The rapid decrease observed in the next 30 days suggests microbial consumption of the weathered layer. The oxidation process has been found to be limited to the upper surface layer of the polymer (Andrady et al., 2021). Therefore, we expect that a new "virgin" layer was exposed, allowing the cycle to recommence. This "consumption" phase coincided with the steep increase of the number of cells within the biofilm on the surface of the virgin pellets.

The pattern of weathered layer consumption and re-weathering detected for the virgin pellets was observed in weathered pellet samples, as well. A decrease of all carbonyl-related indices can be detected over the first phase of the experiment (90 days). In the second phase of the experiment the indices increased anew. Additionally, during the first phase of the experiment, the number of biofilm cells was higher than that from the virgin samples. Therefore, the difference in community abundance is to a significant degree driven by the chemical structure of the pellet substrate, and more specifically by the weathering degree of the pellets (Yang et al., 2020*).* At the time of the first sampling, cell abundances are slightly higher in both biofilms from virgin and weathered pellets. That could be in part attributed to the assimilation of residual monomers in the case of virgin pellets (Klaeger et al., 2019), and low molecular weight compounds easily available after the irradiation of weathered PP pellets. When the monomers have been used up by the microorganisms, cell abundances in the biofilm attached to the weathered pellets are higher (60-90 days). Only after the virgin pellets had had sufficient time to be oxidized did the microorganisms actively resume multiplying in the biofilm attached to the initially virgin polymers. A combination of the larger surface area of the virgin pellets and the fact that recent oxidation would lead to higher concentrations of ready-to-assimilate low molecular weight products resulted in the higher cell densities observed in the second phase of the experiment. Two separate phases were identified that occur in a sequential manner: the initial polymer deterioration due to the interactions with the environment, followed by the removal of the degraded polymer layer by microorganisms and the exposure of a "new fresh" layer. The closed system design, as well as the limited duration of the experiment, could negatively affect the universality of our concluded timeframe. However, this is the first time that the two-phased pattern of weathering and consumption is reported, and the critical point in time for the observed phase shift to occur coincides on the 90th day in both mesocosms.

Assuming the release of a plastic particle in the marine environment, a prolonged period of solar

irradiation, especially in conjunction with mechanical abrasion caused by waves, would result in alterations in the chemical structure and polymeric chain integrity. Biofouling removal from the surface of plastic particles while they remain in the marine environment (Karkanorachaki et al., 2021), would also lead to additional exposure to solar radiation. Residence times of plastics in the sea have been estimated to be longer than 200 days (Hinata et al., 2017), much more than the approximately 90 days indicated by our findings to be needed for phase transition. Furthermore, beaching of a plastic particle at the end of the residence time, could accelerate the weathering process (Corcoran et al., 2009) before the particle is resuspended in the water column (Onink et al., 2021). Once resuspended, surface weathering would favor the attachment of marine communities on the particle (Huang et al., 2022) and the subsequent consumption of the weathered upper layer, due to processes such as biofragmentation or biodegradation (Amobonye et al., 2021; Taghavi et al., 2021). The biological "polishing" of the plastic particle (Syranidou et al., 2017a) would lead to the exposure of the virgin polymer, less attractive to biofilm formation and microbial degradation, and thus more susceptible to abiotic weathering via solar UV radiation. Long residence times, even more so with intervals of beaching and resuspension, could therefore facilitate the cycles of weathering and polishing phases up to the point where the particle would completely disappear. This "disappearance" could be attributed to the assimilation and mineralization of the polymer by the marine communities, the incorporation of generated micro- and nanofragments to colloidal structures or a combination of both.

The idea that traditional petroleum hydrocarbons-based plastics can be biodegraded within a specific time scale is still very young but unraveling the mechanism and the parameters involved in the process could help us elucidate a largely unknown part of their fate in the marine environment. As shown by the PCA (Figure 4.7), the process is governed by numerous factors, environmental and biological, with time being the most influential. The direction of the oxygen-related ATR-FTIR index vectors indicate that they contribute greatly and almost exclusively to the second principal component. Thus, it can be confirmed that the abiotic degradation due to UV radiation takes place independently of environmental interferences or biological processes.

Finally, understanding the biologically induced transport and removal processes of plastics of all sizes in the environment could change the way we see the world from a biochemical standpoint. The fraction of plastic waste more susceptible to leaching possesses the potential to be seen as a nutrient-enriching factor rather than a pollutant and could lead to a reimagining of the carbon cycle, specifically considering the anthropogenic factor (Chiellini et al., 2007). More research is needed, however. One the one hand, examination of more polymer types under various conditions is

necessary. On the other hand, the effects of the presence of additional man-made substances on the marine carbon cycle should be identified.

5. Concluding remarks

Polymer degradation of C-C backbone plastic pellets, expressed as area reduction, as well as chemical structure changes, is combined with the examination of biological and mesocosm seawater parameters, with the aim of elucidating the fate of microplastics in the marine environment. The interactions of both virgin and artificially weathered PP pellets with environmental and biological factors (18 in total) were monitored, so that the effect of weathering and marine biota could be examined. Most of the parameters analyzed in this work highlight that a period of 90 days is critical for the achievement of degradation in the case of virgin polymers. ATR-FTIR analysis in conjunction with community analysis proved valuable in revealing that the weathering degree of the pellet surface acts as the determining factor of the biofilm community attachment and composition. Following the release of a plastic item in the marine environment, two distinct succeeding phases can be discerned in the interaction among polymer, environment, and biofilm. The first is the weathering phase, during which the polymer surface gradually deteriorates, mainly due to the abiotic effect of UV radiation. As a result, the biofilm attachment and development are facilitated, causing the initiation of the de-weathering phase, whereby the biofilm communities start removing the weathered layers of polymer. To conclude, after a critical degree of surface deterioration, consecutive cycles involving microbial removal of the weathered layer, exposure of “fresh” virgin layer and re-deterioration of this “fresh” fraction are repeated until the complete disappearance of the plastic particles. Finally, the critical role of aggregation in the entrapment and long-term suspension of micro- and nanoplastics in the water column was recognized.

Chapter 5. Sinking characteristics of microplastics in the marine environment

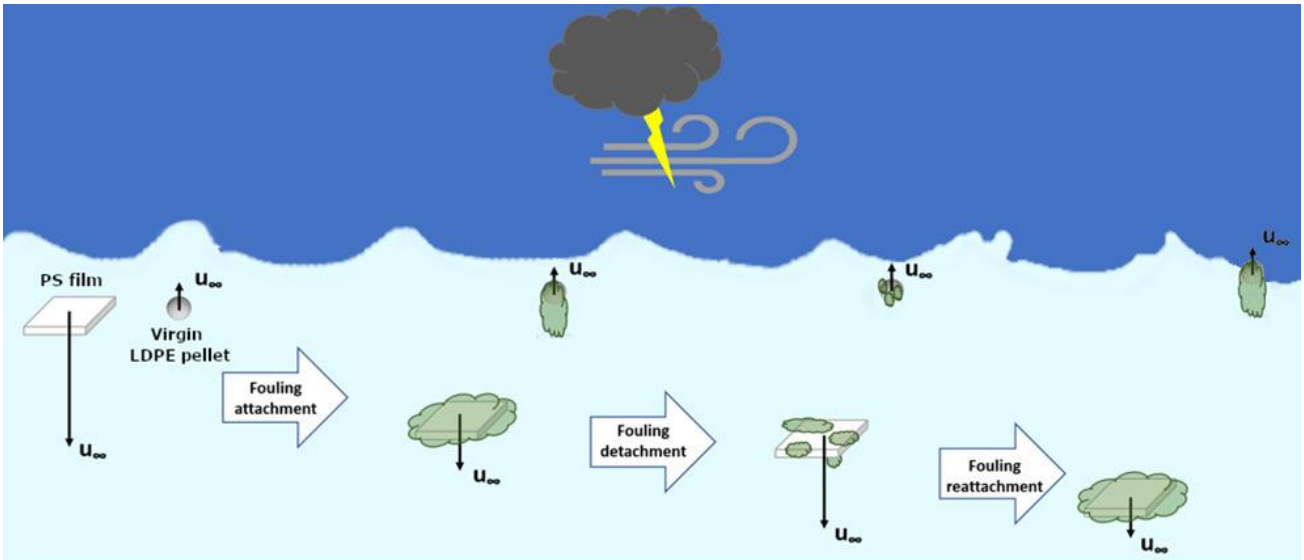

Fouling attachment and reattachment affect the sinking velocity of larger plastic samples, while the sinking velocity of pellets remains unchanged. The removal of fouling during extreme weather effects could potentially lead to reversal of this process and the start of a new fouling reattachment process.

Published as:

Karkanorachaki, K., Syranidou, E., Kalogerakis, N., 2021. Sinking characteristics of microplastics in the marine environment. *Science of the Total Environment* 793, 148526.

5.1. Abstract

Plastic pollution is presently one of the most widespread and minimally understood problems. Vast quantities of plastics that have entered the marine environment should be detected floating on the sea surface are seemingly missing from the global budget. A vertical transfer process should be able to explain the imbalance in mass, as well as the findings of buoyant plastics at the bottom of the sea. These processes are of paramount importance to modelling efforts on the fate of plastics and microplastics in the marine environment. In order to fill this gap and develop correlations that could be used in modelling activities, we have designed and performed a 300-day long field experiment to monitor the interactions between microplastics (pellets and films) and the marine environment for five types of plastic polymers. Fouling, changes in diameter, gravimetric weight and sinking velocity were monitored and the correlations between them were studied using principal component analysis (PCA). Density, fouling and sample form (strip or pellet) were found to greatly affect the sinking characteristics of the polymers, leading to an increase or decrease in the sinking velocity. Finally, mathematical expressions for the estimation of fouling attachment and the sinking velocity with respect to time for each type of plastic were determined from the experimental data.

5.2. Introduction

The detection of plastic waste in the marine environment can be dated back as the early 1970s. It was not, however, until recently (Andrady, 2011) that its ubiquity forced the scientific community to actively acknowledge the problem and engage in its study. A staggering amount of plastic, namely 4.8 to 12.7 million metric tons of plastic is estimated to enter the marine environment annually via land or sea (Cózar et al., 2014; Geyer et al., 2017a). It has been calculated that more than 65% of the polymers produced, including polypropylene (PP) and polyethylene (PE) in its various forms (Geyer et al., 2017; Plastics Europe and Conversion Market & Strategy GmbH, 2019), have densities lower than that of seawater. It would, therefore, be expected that most of the plastic entering the marine environment should be found floating on the surface of the seas, while bottom samples should contain only negatively buoyant polymers, namely polystyrene (PS) and polyethylene terephthalate (PET). Estimations of slightly more than 250,000 tons of floating plastics in the ocean (Eriksen et al., 2014), prove that this is not the case, since a vast amount of plastics is “missing”. Seafloors have indeed been found to act as sinks for part of the missing plastic (Koelmans et al., 2017; Van Cauwenberghe et al., 2013). Recent work attributed the discrepancies observed to processes including biofouling, marine snow, stranding, settling, burial and degradation to microplastics (Lebreton and Andrady, 2019; Porter et al., 2018; Wang and Liu, 2019).

Understanding the vertical transport of plastics in the marine environment and the processes affecting it is imperative for constructing a realistic mass balance that would in the long run enable the mitigation of plastic pollution. The sinking velocity of production pellets (Ballent et al., 2012), laboratory-produced particles of various polymer types, sizes and shapes (Kowalski et al., 2016b), sub-millimeter particles (Kaiser et al., 2019), fibers (Khatmullina and Isachenko, 2017) and microplastic-plankton aggregates (Long et al., 2015) have been examined, but only recently the sinking characteristics of films were studied, which represent a large portion of the collected plastic pollution samples (Van Melkebeke et al., 2020). An overview of the relative literature is presented in Table 5.1. The interactions between plastic particles and biofouling have long been suspected to affect their density, hydrophobicity and sinking velocity (Cózar et al., 2014; Lobelle and Cunliffe, 2011b; Morét-Ferguson et al., 2010). Recently these theories were validated, showing that the attachment of fouling organisms either increased or decreased the sinking velocity of plastic particles (Kaiser et al., 2017; Long et al., 2015), even more so if the fouling organisms belong in the macro-scale (Fazey and Ryan, 2016).

Despite the fact that research teams keep on advancing our knowledge on the fate of plastic pollution in the marine environment, the processes which influence it are rarely known to us. The knowledge gap concerning the sinking of plastics in the sea can be filled with extensive experimentation in the field and subsequent data analysis. This study aims to be the first multi-polymer examination of the sinking characteristics of plastics in a long-term time dependent matter in actual marine conditions at the Eastern Mediterranean Sea. The identification of the parameters that are most influential on the sinking behavior of the polymers was pursued, so that a set of modeling-ready mathematical expressions is produced describing the evolution of sinking velocity and the fouling attachment rate.

Table 5. 1: Reported sinking velocities of microplastics.

Polymer	Size	Density	Source	Sinking Matrix	Measurement Methods	Velocity	Study
~ 180 high density pellets	< 5 mm	> seawater	Strandlines	Still saltwater	Filming of pellet settling in column	2.0×10^{-2} - 7.0×10^{-2} ms^{-1}	Ballent et al. (2012)
PE, PP, hard plastics, sheets, lines and foams	0.5-207 mm	< seawater	Density separated oceanic Manta Trawl Samples	Filtered Seawater	Rise in Cylinder	1.0×10^{-3}- 4.4×10^{-2} ms^{-1}	Reisser et al. (2015)
Fragments Lines	0.5-5 mm	< seawater	Density separated oceanic Manta Trawl Samples	Filtered Seawater	Rise in Cylinder	$(6.0 \pm 1.0 \times 10^{-3})$ - $(1.9 \pm 0.6 \times 10^{-2})$ ms^{-1}	Kooi et al. (2017)
PS, PA, PMMA, PET, POM, PVC	0.5 mm ± 0.01 mm	998, 1010, 1026 kgm^{-3}	Industrial pellets broken into smaller particles	Filtered Distilled Water and Seawater	Settling in Cylinder	$6 - 91 \times 10^{-3}$ ms^{-1}	Kowalski et al. (2016)
PS, PE	~ 1mm cylinders	1050, 955 kgm^{-3}	Seawater incubated fouled samples (0-14 weeks)	Filtered Seawater	Sinking in Cylinder	$(9.0 \times 10^{-2} – 1.5 \times 10^{-2})$ - $(1.2 \times 10^{-2}$-$1.7 \times 10^{-2})$ ms^{-1}, no sinking for PE	Kaiser et al. (2017)
PCL and various materials	0.17 - 5 mm	1131, 1130 - 1168 kgm^{-3}	Artificially produced spherical and cylindrical granules, aged fishing lines	Distilled Water	Sinking in column	5×10^{-3} - 1.3×10^{-3} ms^{-1}	Khatmullina & Isachenko (2017)
Irregularly shaped PA, PMMA, PET particles	6-251 µm	1140, 1190, 1390 kgm^{-3}	Laboratory produced particles	Filtered Seawater	Shadowgraphy method in cuvette	6.4×10^{-6} - 1.0×10^{-1} ms^{-1}	Kaiser et al. (2019)

PE, PP, PS (EPS), PVC, PET, and PPA pellets, fragments, fibers and foams	300 µm - 5 mm	830 - 1368 kgm^{-3}	Artificially produced	Distilled Water	Sinking in column and particle imaging velocimetry	6.5 $x10^{-3}$ - 3.1 $x10^{-1}$ ms^{-1} (rising) and 3.9 $x10^{-3}$ - 1.8 $x10^{-1}$ ms^{-1} (sinking)	Waldschläger & Schüttrumpf (2019)
PET, HDPE, PP, PS, PE, PVC granules, films, fibers	0.63 mm - 3.48 mm	950 - 1432 kgm^{-3}	Microplastics from municipal plastic waste	Deionized Water, Ethanol	Sinking in column and imaging	4.5 $x10^{-3}$ - 1.52 $x10^{-1}$ ms^{-1}	Van Melkebeke et al. (2020)
PU	50 - 500 µm	1195 kgm^{-3}	Laboratory produced particle aggregates after incubation	filtered river water	Optical Measurement of CEll Colonization (OMCEC)	1.9 $x10^{-5}$ - 3.0 $x10^{-3}$ ms^{-1}	Nguyen et al. (2020)
PET, PP, PVC	5mm squares	0.9-1.4 kgm^{-3}	Laboratory produced from household items after incubation in the field	River water	Settling in column	2.3 $x10^{-2}$ - 5.6 $x10^{-2}$ ms^{-1}, no sinking for PP	Miao et al. (2021)

* Abbreviations: PE – polyethylene, PP – polypropylene, PS – polystyrene, PA – polyamide, PMMA – polymethyl methylacrylate, PET – polyethylene terephthalate, POM - polyoxymethylene, PVC – polyvinyl chloride, PCL – polycaprolactone, EPS – extended polystyrene, PPA - polyphthalamide, HDPE – high density polyethylene, PU – polyurethane

5.3. Materials and Methods

5.3.1. Polymer Types

The most widely used types of polymer were selected to be studied, so that they would represent the polymers most commonly encountered in the marine environment (Plastics Europe and Conversio Market & Strategy GmbH, 2019). Three types of virgin production pellets were purchased from Plastika Kritis S.A. (Heraklion, Greece): Low Density Polyethylene (LDPE), High Density Polyethylene (HDPE), Polypropylene (PP). HDPE in the form of $CaCO_3$ enriched film with a thickness of 30 μm was also obtained from Plastika Kritis S.A. In addition, films of LDPE (30 μm), PP (30 μm), PS (500 μm) and PET (36 μm) were kindly provided by A. Hatzopoulos S.A. (Thessaloniki, Greece).

5.3.2. Artificial Aging of Pellets

In order to investigate the effect of weathering to the change of sinking characteristics of the polymers, 100 g of each pellet type were artificially aged. The pellets were exposed to ultraviolet (UV-C) radiation in a specifically modified system. Initially, the walls of a metal box were covered with aluminum foil, so that any radiation absorption from the box could be eliminated. The aluminum foil was placed in a way that air flow would not be obstructed, thus allowing the temperature of the chamber to be constant. For the photo-weathering process 6 lamps emitting in the 240-260 nm area (Philips TUV 8W FAM/10X25BOX) were used, powered by an agarose gel transilluminator (Vilber Lourmat TFX-20 MX). The cover of the transilluminator was removed and replaced by a Pyrex-glass surface, upon which the pellets were placed. The pellets remained in the chamber for a period of 4 months, during which they were periodically stirred, in order to ensure uniform weathering. The radiation and the temperature to which the pellets were exposed inside the chamber were logged using a HOBO Temperature Light 3500 DP Logger.

5.3.3. Experimental Setup

The behavior of virgin and weathered LDPE, HDPE and PP pellets, and LDPE, HDPE, PP, PS and PET films in the marine environment, as well as their interactions with the indigenous marine communities was studied *in situ*. The selected area in Eastern Mediterranean Sea was in Souda bay, Crete, Greece (35.480077, 24.111419). The duration of the experiment was 300 days (18 June 2019 to 18 April 2020). A floating octagonal platform was constructed from polyvinyl chloride (PVC) pipes

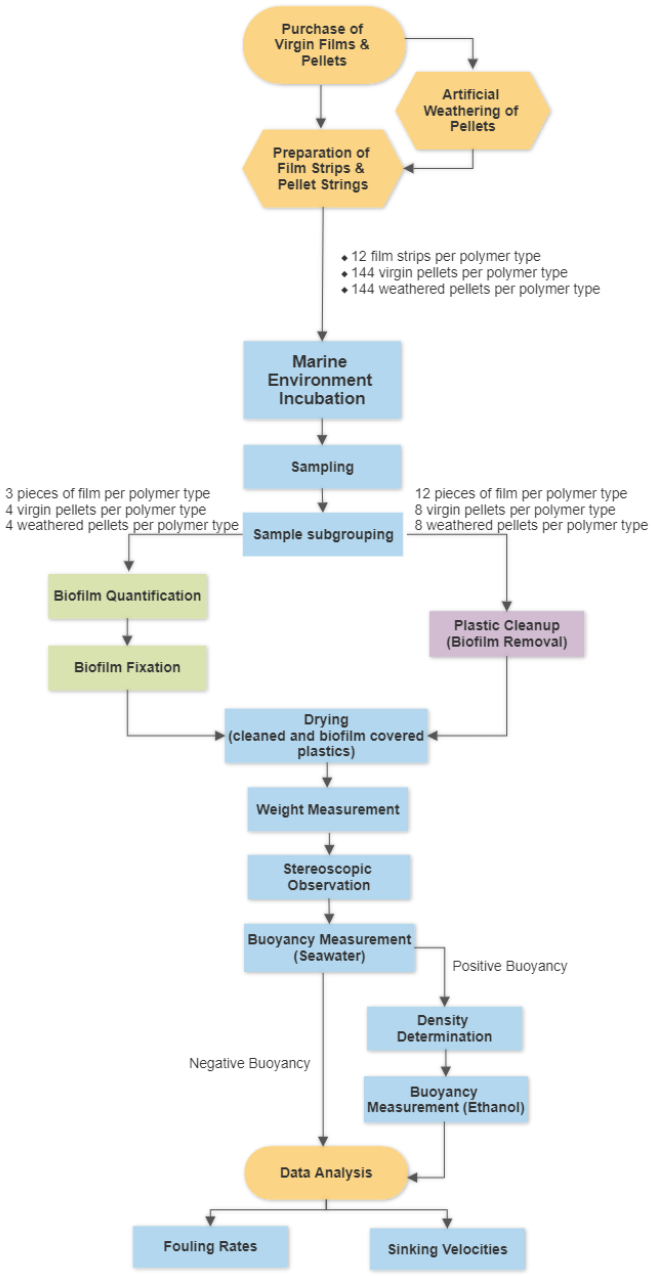

Figure 5. 1: Flow chart of the processes followed.

(diameter = 0.125 m) filled with polyurethane foam. The platform was used as a floating device upon which four stainless steel cages were tied, containing the plastic samples attached to stainless steel wire (Figure S9).

Three forms of polymer samples were used:

- 30 cm x 2 cm strips from the virgin films with holes for the stainless wire
- Strings with 12 virgin pellets, each with a hole in the middle, allowing the stainless wire to pass through them

- Strings with 12 weathered pellets, each with a hole in the middle, allowing the stainless-steel wire to pass through them (Figure S9).

For each positively buoyant polymer type (LDPE, HDPE, PP) a designated cage was created, containing 12 strings of virgin pellets, 12 strings of weathered pellets, as well as 12 virgin polymer film strips. The fourth cage contained 12 strips for each negatively buoyant polymer type (PS and PET).

5.3.4. Water Quality Measurements

Radiation and temperature in the surrounding environment were continuously measured using a HOBO Temperature Light 3500 DP Logger. Monitoring of the physicochemical characteristics of the water of the area in which the experimental setup was installed aimed at ascertaining that the system is characteristic of the southeast Mediterranean environment, in terms of water quality. Furthermore, systematic measurements proved that the presence of the nearby aquaculture did not affect the water quality of the area. Finally, the effect of the experimental setup itself on its surroundings was assessed, so that any negative impact could be mitigated. Water quality parameters were examined on the day of the experimental setup deployment for an establishment of a water quality baseline. The same parameters were analyzed for seawater from the vicinity of the experimental platform on each sampling day (Table S1).

5.3.5. Sampling and Sample Preparation

At the end of each sampling period, one strip of LDPE, HDPE and PP, as well as one string of virgin and one string of weathered pellets were removed from the cages and moved to the lab in sterilized glass jars filled with seawater. Sampling for HDPE was halted prematurely, due to the loss of the metal cage containing the samples, as the result of extreme wind velocities affecting the area of study. For PS and PET, one strip of each polymer was removed during each sampling. Once collected from the marine environment, the samples were kept in the dark at 4^{o}C for analysis. At the same time, seawater was collected in sterilized bottles for water quality analysis.

Prior to analysis, the samples were separated in two subgroups; one intended for examination with the fouling and biofilm attached and one without them. For that reason, the original film strips were cut in 15 square pieces (2 cm x 2 cm). Three 2 cm x 2 cm pieces and 4 pellets of each kind were washed with Phosphate Buffer Solution (0.1 M, pH = 7.4) and fixed with 2% formaldehyde for 2h. Washing with deionized water was followed by washing with serial deionized water – ethanol solutions (25%, 50%, 75%, 90%) (completely denaturated with 1% Ethyl methyl ketone, 1%

isopropyl alcohol, 1 g/ 100 L Denatonium benzoate, Merck). The polymer samples with the fixed biofilm and macrofouling were dried for 3 days at 45 ^{o}C. Special attention was given in order to eliminate biomass and polymer loss during the washing process.

The remaining 12 pieces of film strip and 8 pellets underwent washing for the removal of the attached biofilm and biofouling. Initial washing with Tween80 in Falcon tubes left on a mechanical mixing table (120 rpm) for 3 days, was followed by washing with Sodium dodecyl sulfate (SDS) for 2h with simultaneous vortexing and gentle scrubbing. The cleaned polymers were dried at 45 ^{o}C for 3 days.

5.3.6. Biofilm Quantification

Quantification of the attachment of biofilm on sample surface was performed by measuring the optical density per sample surface (n=3) as previously described (Lobelle and Cunliffe, 2011b). Briefly, the samples were air dried for 45 min and stained with 1% aqueous solution of Crystal Violet (Sigma-Aldrich). Then, the samples were washed three times with sterile seawater and air dried for 45 min. Finally, the samples were placed in 2mL Eppendorf tubes with 1 mL of 95% ethanol for 10 min and the optical density was measured at 595 nm using a Shimadzu UVmini-1240 spectrophotometer. For comparison purposes, all values were expressed per polymer surface area (O.D./cm^2).

5.3.7. Buoyancy

For the estimation of the sinking velocity of both cleaned and fouled samples, a 2 L glass volumetric cylinder was used for the simulation of the water column (Kaiser et al., 2017). Measurements were performed in a temperature-controlled environment (25^{o}C) after enough time had passed for thermal equilibrium to be achieved among ambient air, measurement matrix and samples. This way thermal stability of the water column was ascertained. Seawater was filtered through a 250 μm mesh plankton net for the removal of particles and large organisms. Seawater conductivity was measured (57.5 mS/cm) for the calculation of a seawater salinity of 38.3 ppt using method 2520B (Jenkins, 1982). The cylinder, with an approximate height of 45 cm, was filled up to 40 cm and on the outer surface, marks were made every 5 cm. Measurements were conducted on a heavy-duty laboratory bench and care was taken so that no external vibrations could possibly affect the sinking behavior of the examined samples.

For this measurement, 3 square 2 cm x 2 cm pieces and 3 pellets from each set were examined. The plastic particles were first immersed in the seawater to eliminate the presence of air bubbles, which could affect their buoyancy, and then were allowed to settle in the water column. In the event that

secondary motions (not on the vertical axis) occurred during settling, the measurement was discarded and repeated. The time elapsed every 5 cm was counted using a timer. In order to avoid the effect of acceleration and deceleration to the measured sinking velocity, the upper and lower 5 cm were not used in the calculations. The sinking velocity achieved in the first 10, 15, 20, 25 and 30 cm was calculated. The value at which the velocity stabilized was marked as the terminal velocity, and this was the value used for further analysis.

Realization of the sinking velocity experiments in a glass volumetric cylinder with a diameter of 8.3 cm could introduce measurement bias, owing to the effect of the cylinder walls on the sinking samples. For that reason, a number of corrections had to be implemented. According to Chhabra et al. (2003), the terminal velocity achieved by a sinking sphere of diameter d in a liquid of kinematic viscosity v in the absence of walls (u_∞ - terminal boundless sinking velocity) can be expressed a function of the sinking velocity (u) of the same sphere in the same liquid in a tube of diameter D, using a wall factor f:

$$u_\infty = \frac{u}{f} \quad (5.1)$$

The wall factor f is a function of the Reynolds number (Re=ud/v) and the sphere-to-tube diameter ratio λ=d/D. Calculation of the Reynolds number for the conditions of our experiments revealed Re>4000, therefore it is safe to assume that the flow in the cylinder was turbulent. Under this flow regime, the wall factor f can be considered independent of the Reynolds number and it can be expressed as:

$$f = (1 - \lambda^2)(1 - 0.5\lambda^2)^{0.5} \quad (5.2)$$

The shape of the film samples used for sinking velocity measurements was square, consequently equations (5.1) and (5.2) could not be used for the calculation of u_∞. Instead, the volume-equivalent sphere diameter (d_s) was calculated and then used in the expression of λ (λ=d_s/D) and f (Chhabra, 1996):

$$f = 1 - 1.28\lambda \quad (5.3)$$

The density of the original LDPE, HDPE and PP strips and pellets was lower than that of seawater. For that reason, it was impossible for them to sink in the seawater. To estimate the terminal sinking velocity of the aforementioned low-density samples, the sinking velocity (u_{EtOH} and $u_{EtOH,\infty}$) of the samples (LDPE, HDPE, PP) was measured in ethanol (99.5% denatured with 1% Ethyl methyl ketone, 1% Isopropyl alcohol, 1g/100L Denatonium benzoate EMSURE, Merck), following the procedure mentioned earlier for seawater. Additionally, we measured the sinking velocity of the cleaned PS and PET, as well as virgin and weathered PS pellets in seawater and ethanol. Dividing the sinking velocities in the absence of walls in the two liquids for PS and PET, in film and pellet form, a

correlation factor ζ was estimated for pellets and square samples relating the sinking velocities in the two liquids:

$$u_{\infty} = -\frac{u_{EtOH,\infty}}{\zeta} = -\frac{u_{EtOH}}{\zeta f} \qquad (5.4)$$

The minus sign was introduced to indicate that the direction of the sinking sample movement, driven by the difference in densities, is opposite to the one imposed by the gravitational force. The u_{∞} values calculated by this procedure were used for all the low-density samples, while for the high-density samples, the actual sinking velocities measured in seawater.

Finally, the estimation of the densities of these samples was done through the immersion in a series of successive deionized water and ethanol mixtures.

5.3.8. Stereoscopic observation

Changes in the surface, as well as biofilm attachment on the polymers were observed monthly with a Leica MZ7s stereoscope equipped with a Leica MC190HD camera. Additionally, the diameter of the pellets was calculated from the photographs taken, using the ImageJ version 1.52i software. Examination of pellet diameters using Shapiro normality test revealed that they do not follow normal distribution, therefore Mann-Whitney U tests were performed to examine whether the decrease observed between virgin and weathered pellets of each type was statistically significant.

5.3.9. Gravimetric Weight

Prior to being placed in the metal cages, the plastic samples were weighed with a 5-digit digital laboratory scale. Each individual strip and the predetermined sets of 12 pellets were weighed after the creation of holes for the insertion of the metal wire, a process which would affect the weight.

After sampling, the set of three 2 cm x 2 cm pieces cut from the polymer strips strip and the 4 pellets with the fixed biofilm and macrofouling were weighed. Similarly, the rest of the strip and the 8 remaining pellets from each string were weighed after gentle washing and drying. Care was taken so that no weight loss would take place during washing and drying. The weights with and without biofilm and macrofouling were grossed up to a 2 cm x 30 cm strip or 12 pellets, so that comparisons with the original weight would be possible.

5.3.10. Data analysis

Statistical analysis of the data and principal component analysis (PCA) on the factors affecting the sinking velocity of the polymer samples was performed with R version 4.0.0, in the environment R

Studio Version 1.3.959. Data normality was examined using the Shapiro-Wilk test. Since the samples followed in their majority non-normal distributions, the Kruskal-Wallis non-parametric test was used to examine whether there existed statistically significant differences to the samples, while the correlation of the samples was studied using the Spearman's rank correlation coefficient. PCA is a data analysis method that mathematically transforms the original data into independent variables. Each variable represents a portion of the data variance, and combinations of them can be examined in relation to the percentage of the variance that can be represented. The function *prcomp* was used for the PCA analysis and the graphs were created using *ggbiplot* contained in the *ggpplot2* package. Combined explained variation of 75% or higher were considered adequate. Curve fitting for the sinking velocities and fouling growth was performed for each type of plastic using MATLAB R2014a. The precise 95% confidence intervals of the nonlinear model were computed by MATLAB using functions *fitnlm* and *predict*.

5.4. Experimental Results

It is important to stress that the HDPE samples resided in the marine environment for 58 days less than the rest of the samples. It is, therefore, unforeseen whether the HDPE samples would behave in a manner similar to LDPE and PP, should they have had the opportunity to reside in the sea for the remaining experimental time. This fact seems to be highly important, as HDPE appears to be the most heavily affected by fouling organisms of the five types of polymers examined.

5.4.1. Water Quality

With the exception of the fourth sampling (30-11-2019), when elevated chemical oxygen demand (COD) and Total Nitrogen values could possibly be attributed to a random source point pollution incident, the parameters remain more or less stable and within a close range of the baseline values (Table S2).

5.4.3. Stereoscopic Observation

At the end of the experiment, apart from the biofilm, a number of macrofouling organisms attached to the surface of the polymers. The marine communities on the polymers were distinct, and their composition was dynamic, following succession patterns that depended on time and the weather conditions. Namely, PP and PET strips were mainly covered by biofilm, LDPE, HDPE and PS acted as the substrate for the growth of eukaryotic organisms such as marine plants, diatoms, macroalgae, bryozoa, barnacles, insects and cephalopod eggs. Photos of the polymers, depicting the attachment

of biofilm and fouling agents can be seen in Figure S10.

Monthly stereoscopic observation of the samples confirmed the macroscopic observations, with biofilm layers on the surface of PP and PET strips and a combination of biofilm and macroorganisms on the surface of the pellets and the rest of the polymer strips (Figure S11).

The diameter of the plastic pellets, as calculated from the images acquired from the stereoscope camera, is shown in Table S3. Pellet diameter systematically decreased over time. More specifically, a 17.3% decrease in diameter was observed for virgin LDPE pellets. The decrease was more prominent in case of weathered pellets since 25.6% decrease exhibited in the weathered pellets of this polymer type. Similarly, the diameter of the virgin PP pellets decreased by 15.5% over the 300-day period, while the weathered PP pellets were almost one fourth of their initial size, with a 25.8% decrease in diameter. A 16.5% decrease of diameter was observed for virgin pellets and a comparable 13.4% for weathered pellets. Interestingly, weathering is a factor affecting diameter decrease only in the case of HDPE pellets ($p=0.008$).

5.4.4. Gravimetric Weight

The weight difference (in g) was calculated for each sample, in both cleaned and fouled state (Figure S12). Among the cleaned polymer strips, the most notable weight reduction was observed for PS (0.8g after 202 days). A reduction of 0.009 g, 0.009 g, 0.053 g and 0.088 g for PP PET, HDPE and LDPE respectively. Weathered pellets were significantly more susceptible to deterioration than their virgin counterparts. More specifically, while weathered LDPE pellets showed a weight reduction of 0.050 g, the weight reduction for the virgin form of the material was 0.030 g. Similarly, virgin HDPE pellets demonstrated a weight reduction of 0.015 g, as opposed to the 0.036 g of the weathered HDPE pellets. The difference in weight reduction for PP pellets was less distinguished, nonetheless following the pattern observed for the other two types of polymers, with the virgin and weathered pellet weight reduction being 0.018 g and 0.024 g, respectively.

5.4.5. Fouling growth

Fouling growth contributed to the increase of the weight of the polymer samples used. Polymer strips were more significantly affected, with weight increases of 1.13 g for PET, 1.67 g for LDPE, 2.36 g for PP, 11.3 g for PS and 11.5 g for HDPE. The discrepancies between virgin and weathered pellets can be observed here, as well, with the growth on the latter being appreciably heavier than that on the former. Characteristically, the weight increase for virgin LDPE pellets was 0.084 g, and 0.187 g for the weathered pellets. Virgin HDPE and PP pellets were less attractive to fouling organisms, with

0.207 g and 0.249 g increases in weight, whereas increases of 0.522 g and 0.605 g were observed for the weathered ones.

5.4.6. Relationship for fouling versus time

Fouling growth was modeled as a function of time. Only the first 152 days were considered for this process, since the extreme weather events that followed caused serious fouling removal. Although the fouling process proceeded, it produced irregularities that should not be taken into account. Among the various mathematical expressions to fit to the growth of fouling on the surface of plastic films and plastic pellets, a simple S-shaped curve was selected. The logistic function (sigmoid curve) given by Equation 13 below, was considered as the most appropriate due to its simplicity and asymptotic characteristics.

$$Y = \frac{a}{1 + e^{-b(X-c)}} \quad [5.5]$$

where a, b and c are constants and represent the unknown parameters to be estimated by nonlinear least squares from the experimental data. The values of the three constants calculated for each polymer type, as well as the coefficient of determination (R^2) and the root mean square error (RMSE) of each fitted curve, are presented in Table 5.2. As seen in Table 5.2, the fouling growth is well explained by the sigmoid curve (R^2 >0.9 in most of the cases). It can be observed that it is a time dependent process, not significantly affected by the polymer type or extent of weathering. The shape, however, seems to affect the maximum amount of fouling per surface unit that can be accumulated on plastic particles, since the values of parameter a are consistently higher for film samples.

Table 5. 2: Sigmoid curve constants for the mathematical expressions of fouling growth on plastic polymer samples.

Polymer Type	Degree of Weathering	**a** [mg cm^{-2}]	**b** [day^{-1}]	**c** [day]	R^2	RMSE
LDPE film	virgin	0.086	0.301	110.9	0.891	0.019
HDPE film	virgin	2.982	0.034	203.9	0.999	0.0207
PP film	virgin	16.883	0.0440	333.5	0.995	0.010
PS film	virgin	121.790	0.0257	521.9	0.932	0.044
PET film	virgin	0.280	0.0340	241.6	1.000	0.001
LDPE pellets	virgin	0.037	0.024	98.9	0.903	0.007
	weathered	0.054	0.082	75.3	0.633	0.025
HDPE pellets	virgin	0.071	0.148	85.3	0.985	0.006
	weathered	0.218	0.137	170.4	0.981	0.019

PP pellets	virgin	0.076	0.356	39.7	0.733	0.028
	weathered	0.080	0.378	157.5	0.694	0.027

As an example of the curve fitting for HDPE film samples, the model estimates, the experimental data and the 95% confidence intervals of the model predictions are shown in Figure 5.2. All the remaining fitted curves corresponding to the estimated parameters in Table 5.2 can be found in the Supplementary materials (Figures S14 – S23).

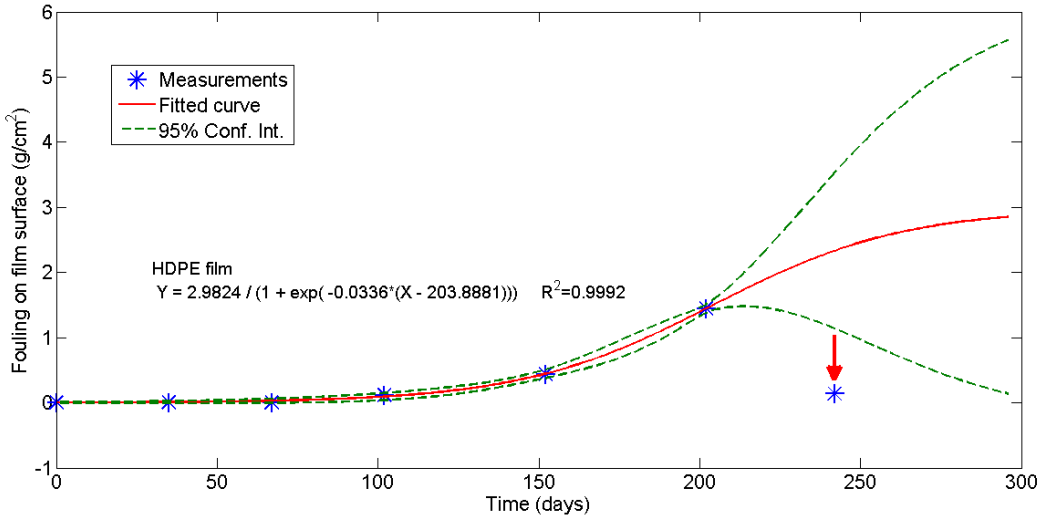

Figure 5. 2: Curve fitting of fouling growth on HDPE films over time. The red arrow points to an "outlier" which was not included in the fitting process as it was measured following an extreme weather event.

5.4.7. Biofilm Development

Crystal violet binds to nucleic acid and protein molecules and is therefore a measure of the biofilm attached on the surface of the polymer samples examined. The biofilm on the polymer strips constantly increased (Figure S13), in contrast to the attachment of macrofouling organisms, which were removed from the polymer surface, as a consequence of strong winds affecting the area of study. Notably, PET being the polymer less affected by fouling macro-organisms, exhibits the highest Optical Density per cm^2 at the end of the experiment (35.2 Optical Density per cm^2). LDPE, PS and PP followed with an Optical Density of 27.8, 26.6 and 22.6 per cm^2, respectively, while the Optical Density per cm^2 was 20.6 for HDPE after 242 days in the marine environment.

Biofilm accumulation on the surface of plastic pellets was consistently lower, compared to that observed on the surface of the polymer films, suggesting that the polymer shape influences the biofilm development. When exposed to the marine environment, films appear as a more attractive

substrate in comparison with the virgin and weathered pellets. The maximum values of Optical Density per cm^2 for virgin pellets were 2.5 for PP, 5.0 for LDPE and 6.6 for HDPE, as opposed to the respective values of 4.9 for LDPE, 6.6 for PP and 7.2 for weathered HDPE pellets. The quantity of biofilm on weathered pellets was increasing for the duration of the experiment, with only weathered LDPE pellet biofilm accumulation demonstrating a tendency to plateau after 242 days in the marine environment. The biofilm on virgin pellets, however, gradually decreased on PP and remained stable on LDPE, in accordance with the observations on fouling, thus indicating a tendency for biofilm detachment. The biofilm on virgin HDPE pellets continued accumulating. This may be attributed to the enhanced suitability of HDPE as a biofilm attachment. During the first 202 days of exposure to the marine environment, the virgin HDPE, LDPE and PP, as well as the weathered HDPE and LDPE pellets exhibited the same pattern of biofilm development. However, the biofilm redevelopment, following its removal by extreme wind and wave activity, was distinct for each pellet type.

5.4.8. Sinking Velocity

The sinking velocity of the polymers in the cleaned and fouled state was studied, as a function of time. Examination of the effect the cylinder in which the measurements were performed, revealed that in the case of pellets it was negligible ($f>0.99$). The ratio ζ of the terminal boundless sinking velocity in ethanol and seawater for the PS pellets tested was calculated. The value was equal to 4.52 ± 0.52 and it was used to estimate the sinking velocities of LDPE, HDPE and PP pellets used for the experiment. For the square film pieces the factor f ranged between 0.61 and 0.88. From the values of the ratio ζ of each piece, a mean value of 2.14 ± 0.77 was estimated and used for further calculations.

5.4.8.1. Positively buoyant polymers

Please note that in this section, the minus symbol of the values indicates the direction of the terminal boundless sinking velocities (rising) of the positively buoyant polymer samples. The use of the terms *increase* or *decrease* will therefore refer to the absolute value of the terminal boundless sinking velocities.

5.4.8.1.1. Film samples

The estimated terminal boundless sinking velocities over time for LDPE films are shown in Figures 5.3A and 5.3D. Starting from the same initial sinking velocity (-3.96×10^{-3} ms^{-1}), fouled and cleaned film pieces exhibit completely distinct sinking behaviors. Towards the end of the experiment, the sinking velocities of the fouled samples were up to three orders of magnitude higher than those of

their cleaned counterparts. Fouled LDPE film samples rose to the surface with ever-increasing sinking velocities that reached a mean peak value of -3.23 ms^{-1} on the 242th day. Fouling removal due to the extreme wind conditions that affected Souda Bay just before the 300th day resulted a terminal boundless sinking velocity of -1.67 ms^{-1}. Cleaned LDPE film samples, on the other hand, manifested slight discrepancies that could well be attributed to experimental errors, with terminal boundless sinking velocities ranging between -6.06 $x10^{-3}$ ms^{-1} and -2.52 $x10^{-3}$ ms^{-1}.

Similarly, the absolute value of the terminal boundless sinking velocity of the fouled HDPE film pieces at the time of the final sampling, with a mean value of -3.23 ms^{-1}, was three orders of magnitude higher than that of the virgin pieces of the same polymer (-3.96 $x10^{-3}$ ms^{-1}). Due to the loss of the samples because of the bad weather conditions, it is unclear whether the fouling from the polymer surface would have been removed and how that would affect the sinking behavior of the samples. Identically to the cleaned LDPE samples, the terminal boundless sinking velocity of the pieces of cleaned HDPE varied marginally with the passage of time (Figures 5.3B and 5.3E).

Examination of the fouled PP film pieces (Figures 5.3C and 5.3F) demonstrated that, akin to LDPE and HDPE samples, biofouling buildup affected the terminal boundless sinking velocity. From an initial value of -2.46 $x10^{-3}$ ms^{-1} in the virgin state, at the 202th day the fouled samples reached and in general maintained a mean sinking velocity of -2.22 ms^{-1} to -1.99 ms^{-1} at the end of the experimental period. The cleaned samples behaved equivalently to the LDPE and HDPE pieces, with negligible variations from the virgin polymer pieces (Figure 5.3F), thus the sinking velocities of the cleaned films may be considered approximately stable throughout the duration of the experiment.

As expected, higher variations are observed in the sinking velocities of the samples as fouling build-up progresses with time. This can be attributed to the non-identical nature and degree of biofouling on each of the three pieces examined. Characteristically, PP samples, that were mainly covered by biofilm and less macrofouling organisms, present the smallest standard deviations in the terminal boundless sinking velocities; 6.90 x 10^{-2} ms^{-1} to 6.81 x 10^{-1} ms^{-1}, as opposed to 4.97 x 10^{-1} ms^{-1} to 1.11[1] ms^{-1} for LDPE and 9.01 x 10^{-1} ms^{-1} to 9.88 x 10^{-1} ms^{-1} for HDPE. Comparison of fouled versus the cleaned samples of each film type using the Mann-Whitney u test revealed that fouling attachment led to statistically significant sinking lower/higher behaviors.

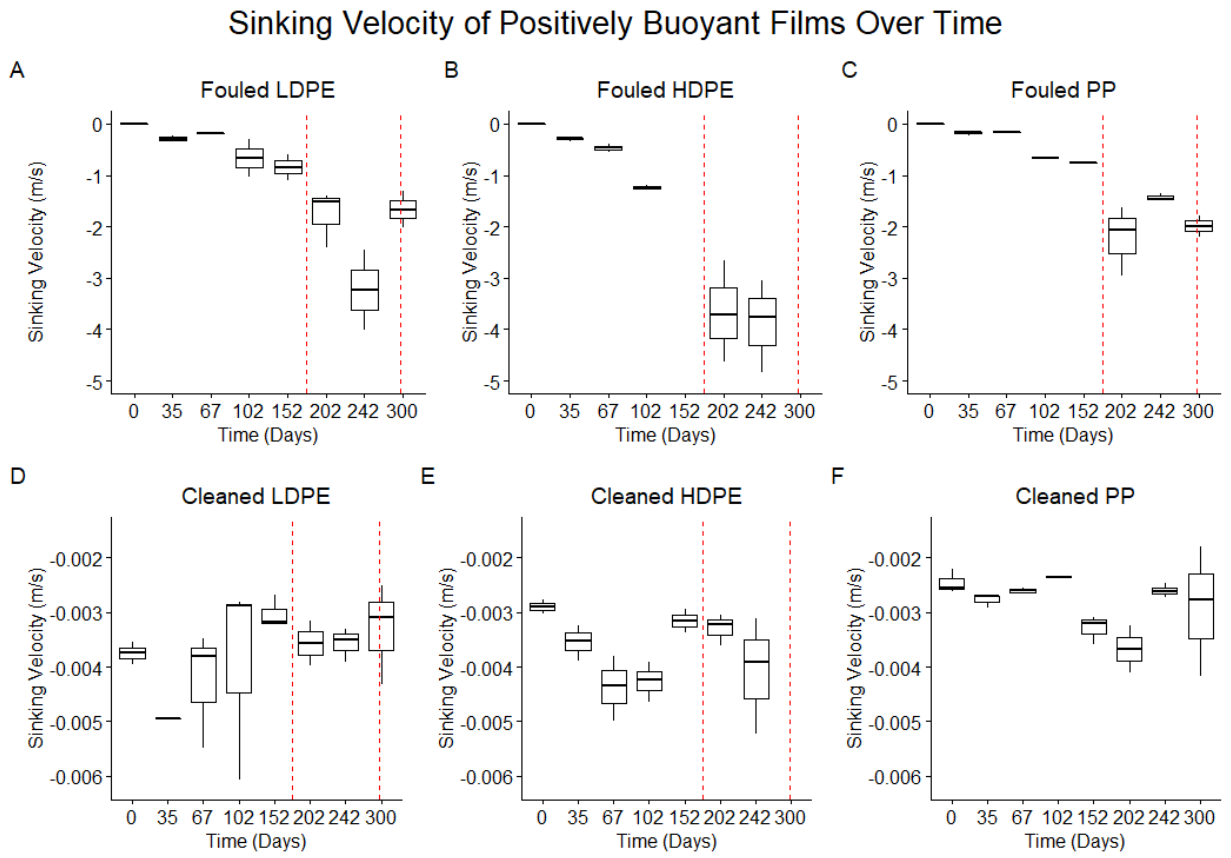

Figure 5. 3: Sinking velocity of positively buoyant film samples over time (ms-1). The broken red lines indicate days with extreme wind velocities.

5.4.8.1.2. Pellet samples

The terminal boundless sinking velocities of virgin and weathered pellets in the fouled and cleaned state were also calculated for all three types of polymers. Opposite to the drastic changes in sinking velocity observed for film pieces of LDPE, HDPE and PP, the sinking behavior of pellets barely diversified over time, even after biofouling development. The terminal boundless sinking velocity of fouled virgin and weathered LDPE pellets (Figures 5.4A and 5.4G) slightly increased by the end of the 300-day period (from -3.03 x10^{-2} ms^{-1} to -2.25 x10^{-2} ms^{-1} and from -2.50 x10^{-2} ms^{-1} to -1.79 x10^{-2} ms^{-1}), after undergoing some fluctuation. Despite the minimal variation, cleaned pellets of the same polymer (Figures 5.4D and 5.4J) underwent even smaller changes; for virgin pellets, from -3.03 x10^{-2} ms^{-1} to -3.22 x10^{-2} ms^{-1} and for weathered ones from -2.50 x10^{-2} ms^{-1} to -2.82 x10^{-2} ms^{-1}. Notably, the fouled weathered pellet samples from day 242, when the terminal boundless sinking velocity seems to be at its most diverse, were characterized by intense biofouling growth.

Cleaned HDPE pellets (Figures 5.4E and 5.4K) exhibit as minimal fluctuations of terminal boundless sinking velocities as LDPE pellets. The initial value of -3.73 x10^{-2} ms^{-1} of the cleaned virgin HDPE

samples transitioned to -4.15 x10^{-2} ms^{-1}. Cleaned weathered HDPE pellets floated to the surface with a velocity of -3.11 x10^{-2} ms^{-1} at the start of the experimental period, as opposed to -3.50 x10^{-2} ms^{-1} after 242 days in the marine environment. When it comes to fouled HDPE pellets (Figures 5.4B and 5.4H), however, the observed differences were slightly more pronounced. Higher variations over time can be observed, especially in the case of the fouled weathered samples. The initial terminal boundless sinking velocity of -3.11 x10^{-2} ms^{-1} calculated for the untreated sample, increased to -6.33 x10^{-2} ms^{-1} after 152 days and -6.25 x10^{-2} ms^{-1} after 242 days.

Cleaned virgin PP pellets (Figure 5.4F) exhibit slight variation (-3.50 x10^{-2} ms^{-1} on day 0 to -3.53 x10^{-2} ms^{-1} after 300 days), whereas the sinking velocity of cleaned weathered PP pellets (Figure 5.4L) was characterized by a slight decrease (-3.67 x10^{-2} ms^{-1} in the beginning versus -2.94x10^{-2} ms^{-1} at the end of the experiment). Interestingly, the standard deviations calculated for cleaned PP pellets (n=3), were the highest among cleaned pellet samples. The terminal boundless sinking velocity of fouled PP pellets generally tended to increase over time after a nominal initial decrease up to day 152 for the virgin and day 102 for the weathered samples (Figures 5.4C and 5.4I). The extremely harsh winds that affected the area of study on day 175 led to an increase of velocity that also amplified by the effect of the second gale, just before the last sampling.

Finally, the differences observed between fouled and cleaned pellet samples were statistically significant in most of the examined cases, except virgin PP and weathered LDPE pellets. LDPE and PP pellet samples displayed similar behavior in their virgin and weathered state. Statistical differences could be detected only in the case of HDPE (*p-value* = 0.03).

5.4.8.2. Negatively buoyant polymers

The terminal boundless sinking velocity of cleaned PS and PET was not greatly affected by their time in the marine environment. Despite the marginal tendency of their sinking velocity to increase, it can be stated that they remained unchanged over time (Figures 5.5C and 5.5D). That is not the case for the fouled plastic film pieces. Both PS and PET samples (Figures 5.5A and 5.5B) exhibited an initial steep increase of sinking velocity, followed by an equally steep decrease and plateauing phase close to the point of not sinking from day 67 to 300. The values of the terminal boundless sinking velocity at the end of the experiment were 6.87 x10^{-5} ms^{-1} and 2.03 x10^{-4} ms^{-1}, for PS and PET, accordingly. Intriguingly, in spite of the similar sinking behavior of the two polymers, the observed differences between cleaned and fouled samples were statistically significant only in the case of PET.

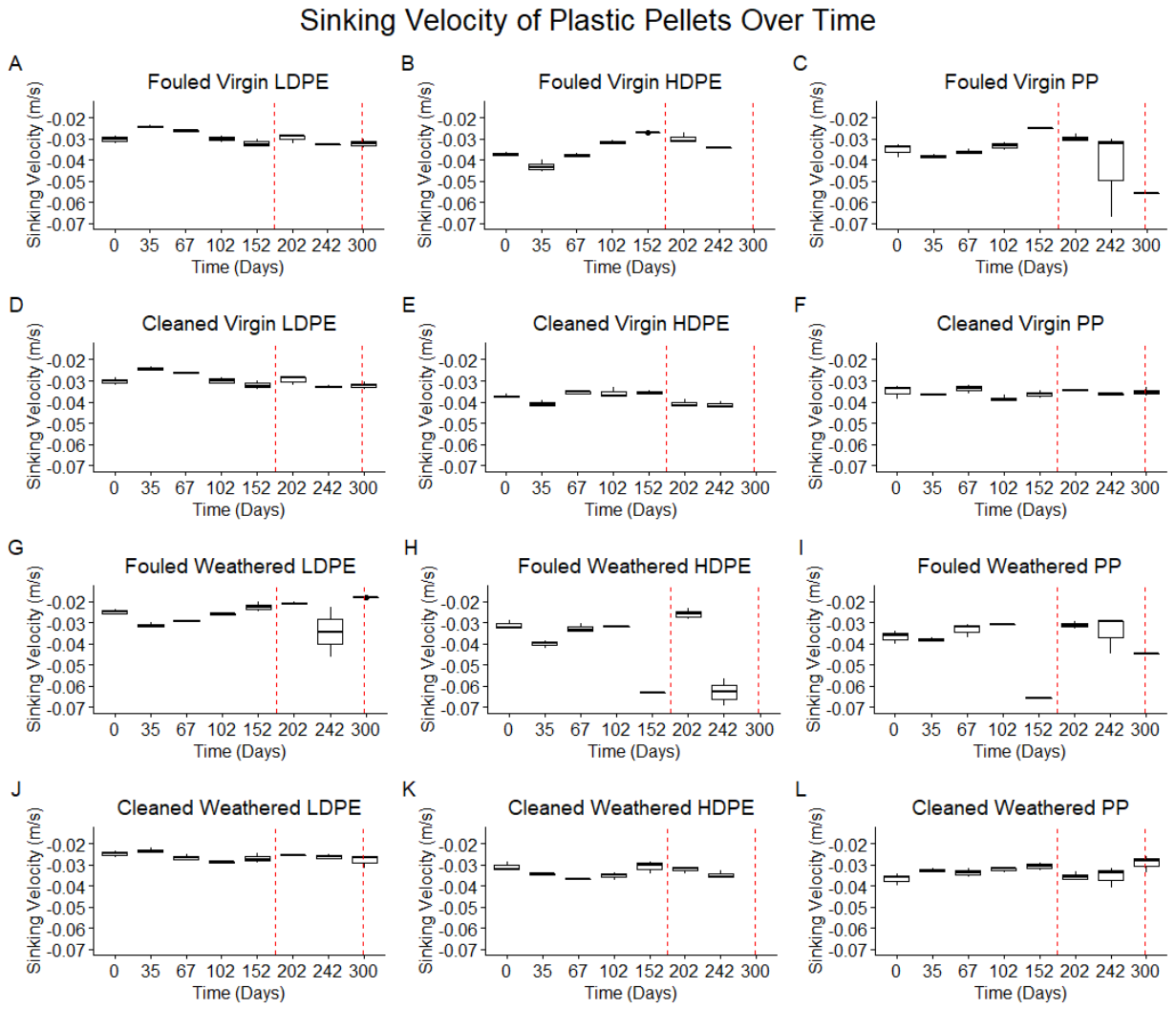

Figure 5. 4: Sinking velocity of positively buoyant film samples over time (ms-1). The broken red lines indicate days with extreme wind velocities.

5.4.9. Relationship for sinking velocity versus time

The velocity of all samples, regardless of shape, degree of weathering or the presence of fouling organisms can be adequately described by a sigmoid curve (logistic equation) of the form

$$u_{\infty} = \frac{a}{1 + e^{-b(t-c)}} \quad [5.6]$$

Where u_{∞} is the terminal sinking velocity in the absence of walls (ms^{-1}); a, b and c are unknown constant parameters; and t is the time (days). The values of the estimated parameters a, b and c for the evolution over time of the terminal sinking velocities for each sample are shown in Table 3 together with the coefficient of determination (R^2) and the root mean square error (RMSE). It can be observed that, the selected sigmoidal expressions fit the data very well. In general, the values for parameter a, which represents the maximum sinking velocity, tended to be higher for fouled samples.

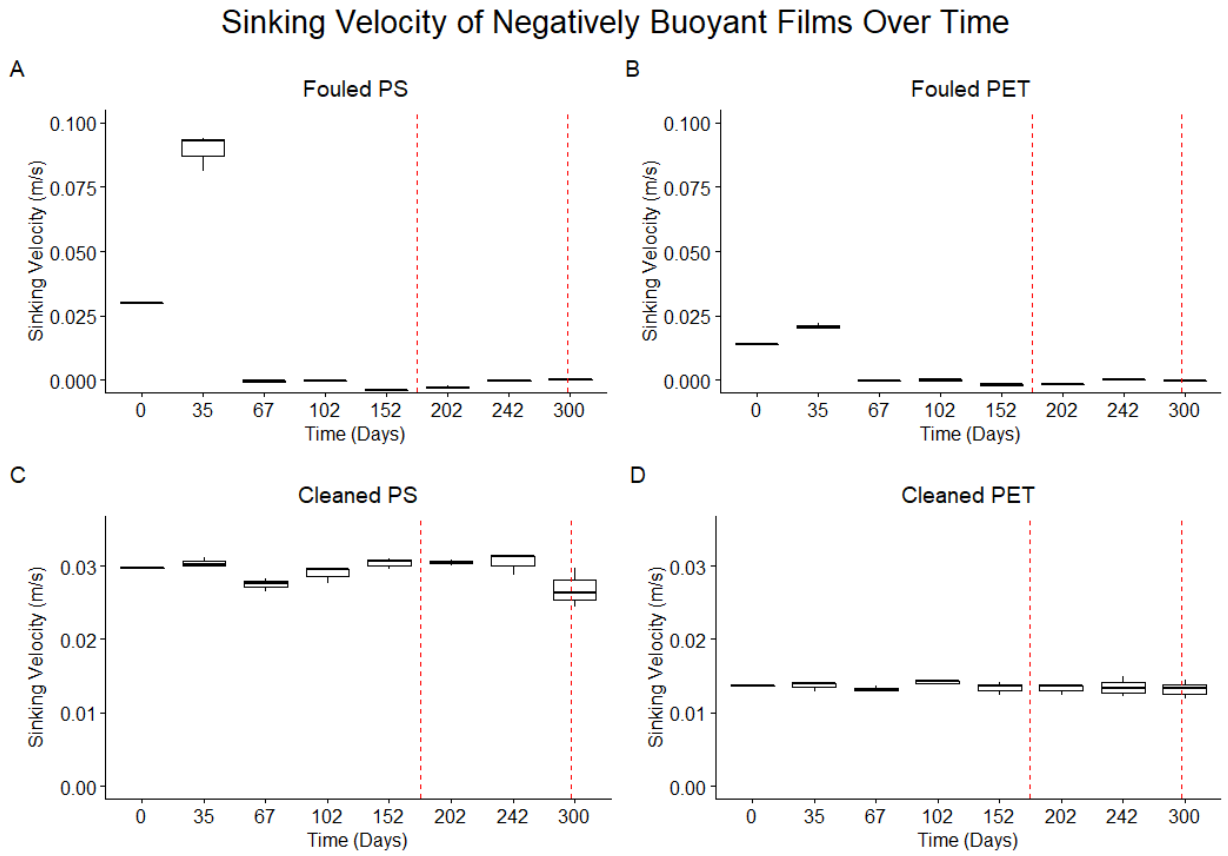

Figure 5. 5: Sinking velocity of negatively buoyant film samples over time (ms-1). The broken red lines indicate days with extreme wind velocities.

Finally, with the exception of weathered HDPE and PP pellets, it can be seen that fitting of the data of fouled samples was more effective with R^2 values well over 0.70.

As an example of the curve fitting for HDPE film samples, the model estimates, the experimental data and the 95% confidence intervals of the model predictions as computed with MATLAB are shown in Figure 5.6. All the remaining fitted curves corresponding to the estimated parameters in Table 5.3 can be found in the Supplementary materials (Figures S24 – S44).

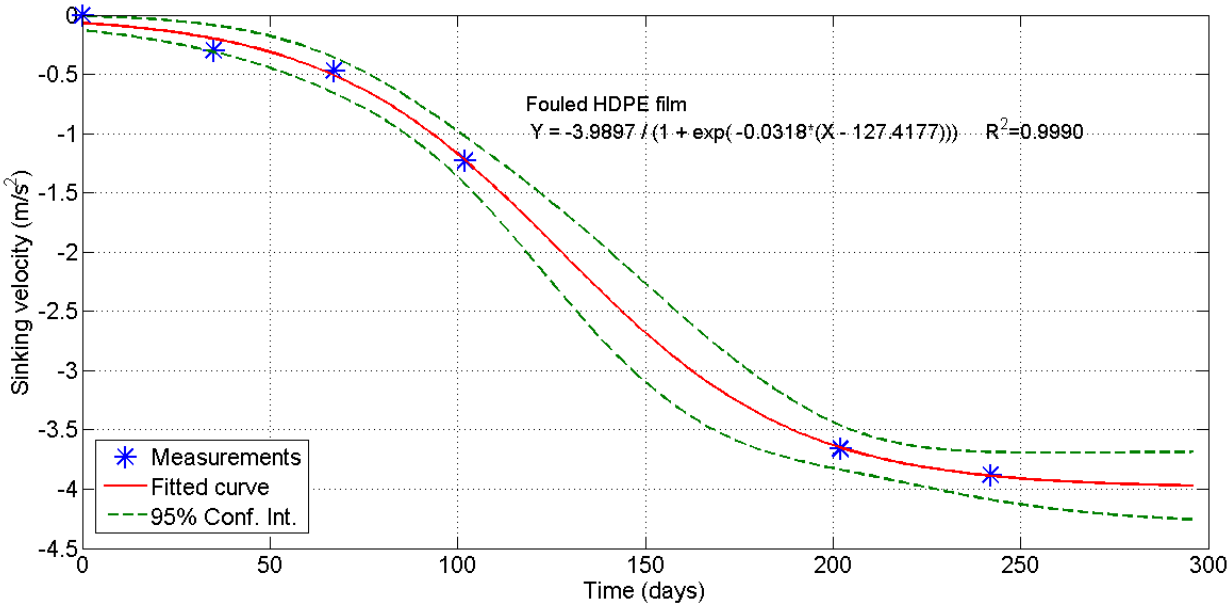

Figure 5. 6: Fouled HDPE film sinking velocity over time data curve fitting.

Table 5. 3: Sigmoid curve constants for the mathematical expression of sinking velocities over time.

Sample			**a** [m s^{-1}]	**b** [day^{-1}]	**c** [day]	**R^2**	**RMSE**
Films	**LDPE**	Cleaned	-0.1155	-0.0015	-2110.0	0.62	$4.3*10^{-4}$
		Fouled	-1.8019	0.0253	136.5	0.94	$2.1*10^{-1}$
	HDPE	Cleaned	-0.0042	0.0377	-18.9	0.89	$2.8*10^{-4}$
		Fouled	-3.9897	0.0318	127.4	0.99	$7.0*10^{-2}$
	PP	Cleaned	-0.1281	0.0021	1894.2	0.70	$3.2*10^{-4}$
		Fouled	-1.9372	0.0291	141.6	0.87	$3.7*10^{-1}$
	PS	Cleaned	0.0305	0.0740	-47.7	0.99	$5.8*10^{-5}$
		Fouled	6.2079	-0.2283	-23.4	0.97	$2.0*10^{-3}$
	PET	Cleaned	0.0383	-0.0002	-2915.5	0.97	$4.0*10^{-5}$
		Fouled	0.2200	-0.2310	-11.7	0.96	$1.2*10^{-3}$
Virgin Pellets	**LDPE**	Cleaned	-0.0321	0.0200	-19.6	0.88	$1.4*10^{-3}$
		Fouled	-0.0342	-0.0057	397.8	0.88	$1.5*10^{-3}$
	HDPE	Cleaned	-1.1406	0.0006	5466.2	0.70	$1.7*10^{-3}$
		Fouled	-2.2651	-0.0028	-1408.0	0.80	$3.3*10^{-3}$
	PP	Cleaned	-0.0356	0.1646	49.3	0.52	$9.0*10^{-4}$
		Fouled	-2.4241	0.0015	2862.4	0.77	$4.4*10^{-3}$
Weathered Pellets	**LDPE**	Cleaned	-0.0265	0.4500	30.5	0.85	$6.7*10^{-4}$
		Fouled	-1.0584	-0.0023	-1473.3	0.97	$9.1*10^{-4}$

	HDPE	Cleaned	-0.0356	0.0614	-31.3	0.88	$1.0*10^{-3}$
		Fouled	-0.1096	0.0057	175.2	0.70	$1.1*10^{-2}$
	PP	Cleaned	-0.5049	-0.0260	122.51	0.91	$8.3*10^{-2}$
		Fouled	-1.9795	-0.0012	-3688.9	0.67	$2.1*10^{-3}$

5.4.10. Principal Component Analysis

The variables incorporated in the PCA model were sinking velocity, gravimetric weight difference, polymer density, time expressed as Days, biofilm O.D. per cm^2 and the area of the sample. Initially, all types of polymer films were examined simultaneously. It was thus revealed (Figure S45) from the heavy clustering of the heavier and the lighter polymers, that the polymers should be examined separately, in terms of density, for the results to be illuminating. Correspondingly, polymer pellets will be examined separately by type (Figure S46).

Two principal components were not sufficient for the examination of cleaned LDPE, HDPE and PP films (61.8% of the variance explained), although it can be observed from the dispersion of the samples that time is a factor significantly affecting their sinking characteristics (Figure S47). For cleaned PS and PET films, on the other hand, a two-dimensional analysis explains 89.0% of the sinking behavior. Time dependent progression can be observed in this case, too. Examination of the totality of fouled film samples in Figure S48 reveals that sinking velocity and fouling attachment and weight difference are strongly correlated. The samples will once more be examined separately, for the thorough investigation of the factors affecting their sinking behavior. Dispersion of the samples on the PCA biplot for LDPE, HDPE and PP films (Figure S49) shows that the strongly correlated time and biofilm attachment are the main factors affecting their sinking characteristics. Time-dependent clustering can be observed for PS and PET (Figure S50), with samples loosely clustered. Density seems to be the factor linearly driving any differences observed between samples.

Two principal components make up for 99.3% of the observed variance in the behavior of virgin (Figure S51) and 76.0% of weathered polymer pellets (Figure S52). Three time-dependent clusters can be observed for virgin pellet samples, regardless of polymer type. Clustering can be observed for weathered pellets, as well, with a time-dependent progression of the samples, along an area-density axis. Examination of the pellet samples per polymer type reveals that the main parameter influencing the sinking behavior of LDPE pellets is density (Figure S53). Clustering observation shows that the sinking characteristics of the samples, which were similar during the first 152 days, in the course of time differentiated, and towards the end of the experiment, were close to their initial state. It is, therefore, evident that fouling, greatly affecting density and weight differences, rather than

weathering, was the main factor leading this process. In the case of HDPE (Figure S54), the contribution of weight difference to the sinking characteristics is more pronounced than LDPE, especially for fouled samples, as expected. Examination of the clustering patterns leads to the same conclusion as for LDPE; while initially all samples behaved in a similar manner, the passage of time led to segregation which is more noticeable between fouled and cleaned pellet samples. Furthermore, even HDPE pellets, which remained in the marine environment for almost two months less than the rest of the samples, follow the pattern of re-exhibiting the initial sinking characteristics after some time. Finally, PP pellets behaved similarly, as shown in Figure S55.

5.5. Discussion

All surfaces (including plastics) in the marine environment, can act as substrates for the attachment and growth of marine life (Rogers et al., 2020). However, the role of fouling attachment, detachment and reattachment to the fate of marine plastics has been widely recognized, yet it has only been demonstrated by Ye and Andrady (1991) and for a period of about half a year. Biofouling, consisting of the initial microbial biofilm (Kirstein et al., 2019; Oberbeckmann and Labrenz, 2020) to macrofauna and macroflora (Bravo et al., 2011; Bryant et al., 2016) can affect the sinking characteristics of plastics and hence, their fate in the marine environment. The structure of microbial communities colonizing the plastic surfaces is not affected by the type of substrate (Oberbeckmann et al., 2016). Location, season and the availability of nutrients, however, have been shown to affect the composition of them (Oberbeckmann et al., 2017), as well as parameters related to the substrate itself, such as surface hydrophobicity and roughness (Rummel et al., 2017). All the samples of this study resided in the marine environment under exactly similar conditions, yet the attached macro-communities were visibly distinct among polymer types. We can, therefore, support the hypothesis that the attaching macrofouling communities were in some way affected, on a phenotypic level, by the plastic substrate. Removal of fouling can lead to a reversal of sinking characteristics, causing sinking plastics to float and *vice versa* (Anthony L Andrady, 2017). In accordance, this phenomenon was also observed in this work after the accidental removal of macrofouling organisms due to extreme weather events (very strong winds) occurred during the experimental period. We hypothesize, therefore, that PET and PP samples, which were mainly covered by biofilm, exhibited less variations in sinking behavior towards the end of the experiment, due to the fact that the removal of biofilm is more challenging than that of macrofouling organisms.

The mathematical expressions provided in Table 5.2 estimate the fouling growth on the surface of a microplastic film or pellet exposed to marine environment and they are suggested for exploitation in

modelling studies concerning the fate of microplastics in the east Mediterranean region as well as in areas with similar environmental conditions. The sigmoid form of the fouling growth curves indicates the existence of three distinct phases: an adjustment phase, during which marine organisms slowly attaches on the surface of the plastics; a rapid growth phase and a plateau, determined by surface availability and intermittent shearing of excessive biofouling. A percentage of the attached fouling was removed from the surface of the samples in the period between the 150th and 200th day. Moreover, the metal cage containing the HDPE samples was lost after the 242nd day of the experiment. Both events can be attributed to extreme weather events, mere specifically gales. On the 23rd of December 2019 (175th day) and on the 15th of April 2020 (297th day) wind velocities of up to 75km/h (9 Bf) affected the area of study. For that reason, in long term experiments, the effect of weather conditions should be taken in consideration. Fouling removal due to extreme winds or wave activity should be considered as a break point. Regrowth after that point should follow the sigmoid curves we have proposed, but with different initial conditions as some degree of fouling should remain attached on the surface and it should be taken into account.

Weathered plastic pellets exhibit a decrease in hydrophobicity (Gewert et al., 2015b). The more hydrophilic a substrate is, the more susceptible it is to biofilm attachment. Although, no changes in fouling growth were observed between virgin and weathered pellets exposed to marine environment in our study. That leads to enhanced biodegradation potential and further tendency to remain suspended in the water column or sink (Michels et al., 2018) in comparison to virgin polymeric materials. The weathering process, naturally occurring in the marine environment (Jahnke et al., 2017), can thus be linked to changes in the sinking characteristics of plastics. PCA of our results revealed that density and sinking velocity are highly correlated, and therefore one could potentially be used as an indicator of the other.

It can be observed by the gravimetric weight results that although weight difference is used as an indicator of polymer deterioration, it is not an effective way of estimating sinking rates, as it does not change in a time-dependent manner. As seen by the pellet diameter measurements, the change in dimensions could act as an indicator, instead. It was presented, however, as a measure of the attachment of macroorganisms, and was one of the parameters affecting the sinking behavior of the samples. At the end of the experiment, the polymers exhibited sinking characteristics similar to those observed during their first days in the marine environment. This behavior can be attributed to the observed partial removal of fouling. The variability in sinking behaviors observed in this study is consistent with the work of Kaiser et al. (2017), and can possibly be explained when the non-uniform fouling is taken into consideration, along with the community succession and the removal of fouling

by extreme weather events. Furthermore, HDPE, one of the types of polymer more susceptible to colonization, can be clearly distinguished by the increase of weight due to the growth of fouling organisms.

In this work, we propose a new method for estimating the velocity at which a positively buoyant particle would move towards the water surface, in case it is present or released underwater. That is achieved by using actual sinking velocity measurements in a different liquid matrix (ethanol). This way, the estimation of theoretical dimensionless diameters and sinking velocities (Dietrich, 1982b) widely used in literature (Kaiser et al., 2019; Kooi et al., 2017a; Kowalski et al., 2016b) can be avoided. We believe that our approach of combining theory and experimental measurements can lead to more accurate estimation of terminal sinking velocities of microplastics in the marine environment. Van Melkebeke et al. (2020) have showed that the terminal sinking velocities of microplastics can be 3-4 times lower than those theoretically calculated. Moreover, the estimation of the wall factor f suggests that sinking experiments in a typical 2 L glass volumetric cylinder produce extremely accurate results for particles which can be assumed spherical, even for diameters in the 4 mm area ($f>0.99$). It was also showcased, that it can be used for larger, even square in shape pieces, when corrections have been applied ($0.61 < f < 0.88$).

Examination of the vertical movement of field-incubated plastic samples in the water column leads to a number of noteworthy observations. Distinct behaviors could be discerned among film samples of different buoyancy (negative / positive), as well as between the two shapes (films / pellets) of the same polymer type. Samples cleaned of biofilm and macrofouling organisms exhibited minimal change of sinking velocity, regardless of polymer type or shape. Thus, polymer structures are not easily affected by non-acclimated microorganisms to the specific polymers (Raddadi and Fava, 2019). Moreover, the miniscule differences in sinking velocity agree with the results of Syranidou et al. (2019). This team observed decreasing sinking velocities of cleaned PS pieces collected from the marine environment and incubated with acclimated PS-degrading marine communities for six months and increasing sinking velocities for samples with biofilm still attached on their surface. The values of terminal boundless sinking velocity, in the range of 10^{-3} – 10^{-2} ms^{-1}, are within the order of magnitude of that calculated for each virgin polymer. The values presented here also are in agreement with sinking velocity values from numerous literature sources with diverse sample types, in terms of polymer type, origin and size, as can be seen in Table 5.1. The possibility that the observed variance in these values is a result of invisible biofilm residues which were not removed from the sample surface or experimental error cannot be excluded.

Substantial differences can be noted between cleaned and fouled film samples, which in the majority

of cases were found to be statistically significant. Our results demonstrate the necessary time for substantial alterations of sinking velocities to occur is density dependent when microplastics are exposed to the Eastern Mediterranean marine environment and fouling organisms; up to 100 days for polymers with densities lower and 35 for polymers with densities higher than that of the surrounding seawater. The elapsed time as well as the nature and quantity of the fouling developed, however, was not enough for changes from negative to positive sinking velocities or *vice versa*. Chubarenko et al. (2016) estimated that 10-15 years are needed for sinking of negatively buoyant plastics to occur. Nonetheless, results from other sources have been contradictory. Positive buoyancy plastic items have been observed in benthic sediments. Additionally, sinking is an explanation for the missing quantities of plastics from mass budgets (Cózar et al., 2017; Van Cauwenberghe et al., 2013; Woodall et al., 2014). It was found by Fazey and Ryan (2016) that a period of up to 66 days was sufficient for LDPE and HDPE film samples to exhibit negative buoyancy. Kaiser et al. (2017) demonstrated that after 42 days in marine water, the sinking velocity of PS particles increased by 81%, and macrofouling organisms attached to LDPE to the extent that sinking occurred during that time. Modelling of the sinking behavior of plastic particles has even predicted periods of time as short as 24-26 days (Kooi et al., 2017b). The dissidence among researchers can be attributed to local environmental, trophic and weather conditions, as well as experimental methods. Increase of up to three orders of magnitude (-10^{-3} ms^{-1} to -10^{0} ms^{-1}) was estimated for the terminal boundless sinking velocity of positively buoyant film samples. This can be attributed to the presence of water within the fouling biomass, since water can lead to a decrease in drag force and therefore to an increase in sinking velocity (Long et al., 2015). The decrease observed for the terminal boundless sinking velocities of negatively buoyant film samples (10^{2} ms^{-1} to 10^{-5} ms^{-1}) was more pronounced, also achieved in shorter times (67 days) and maintained throughout the experiment. These changes could in time lead to the presence of heavy polymers, such as PS and PET, suspended in the water column or even floating, as it has already been observed in the field.

The terminal boundless sinking velocities of fouled pellets marginally changed over time. With the exception of virgin LDPE pellets, minor increase was observed for the first 35 days, followed by consistent decrease until the first incidence of extreme weather. Fouling removal resulted in disruption of this decrease, leading to increased terminal boundless sinking velocities, higher standard deviations among triplicate samples, as well as worse curve fitting. With the exception of HDPE (*p-value* = 0.03), no statistical differences were observed between the sinking behavior of virgin and weathered pellets made of LDPE and PP.

It is worth mentioning that the sinking behavior of fouled pellets was decisively distinct from that of

fouled film pieces. This can be attributed to the size and shape (Kowalski et al., 2016b; Ryan, 2015; Van Melkebeke et al., 2020) and in consequence the excess area of the films available for colonization by fouling organisms. Macrofouling organisms have increased porosity and as a result, are more permeable by the surrounding water. Water penetration is believed to have resulted in the density alteration of the examined samples and therefore to the observed differences in sinking velocities.

Modelling of the sinking behavior of plastics in the marine environment has been investigated the last years, however, many questions are yet to be answered. Predicting the fate of plastics has proven challenging (Khatmullina and Chubarenko, 2019), despite the existing amount of work (Ballent et al., 2013, 2012; Chubarenko et al., 2016; Kooi et al., 2017a; Nguyen et al., 2020). In this work, we intend to bridge the gap between the field and the model, by proposing equations to describe the shift in sinking velocity over time, as an alternative to already existing quadratic linear regression models (Kaiser et al., 2019). The extent and locality of the examined dataset may impose a number of limitations. However, sigmoidal expressions were proposed for the correlation of the sinking behavior of plastics with time since it considers the following factors. The initial lag in sinking velocity change, until enough macrofouling developed to affect the plastics, is taken into consideration. Moreover, the observed stabilization of the values of the terminal sinking behaviors after a certain amount of time, is also very well approached by the sigmoidal form of the curves. As can be seen in Table 5.3, the majority of the R^2 values of our proposed fitting were above 0.80. Given the environmental origin of our samples, even the few cases when the fitting did not very well express our data points, can be considered acceptable.

Finally, multivariate analysis of our data using PCA confirmed the critical role that fouling and density play in the determination of the sinking characteristics of plastics in the marine environment. Further work can be performed in this direction, by including more parameters, for instance surface roughness, hydrophobicity or the structure of the marine community attached on the plastic samples, in order to provide a spherical view of the factors affecting plastic sinking velocities.

5.6. Concluding remarks

In this work, the time evolution of the sinking velocity of five polymer types residing in Eastern Mediterranean Sea was examined, using a newly proposed combination of field and laboratory experiments, and data analysis. The critical effect of fouling growth and its relationship to the shape and size of the particles was established. The importance of extreme weather events that have the ability to alter the quantity of biofouling attached, was experimentally recognized for the first time in conjunction with the implications that might arise on the vertical movement and distribution of

plastics in the water column. Significant alterations of the sinking behavior of microparticles occurred after incubation of approximately 100 days and 35 days for polymers with densities lower and higher than that of the surrounding seawater respectively. Sigmoidal equations were proposed for describing the sinking of particles over time in the marine environment that could be further exploited in modeling studies.

Chapter 6. Extreme weather events as an important factor for the evolution of plastisphere but not the degradation process

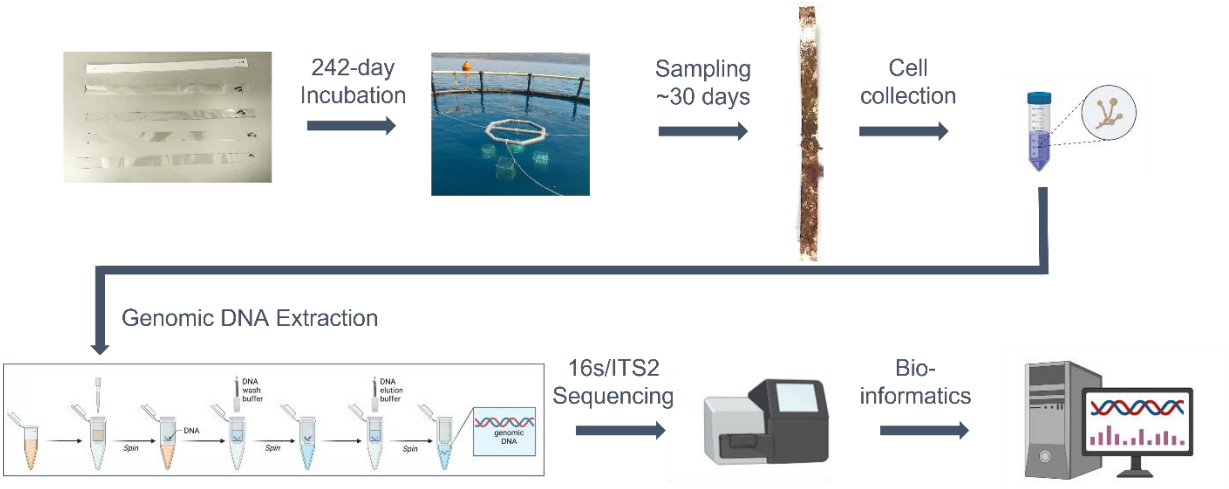

In Preparation

6.1. Abstract

Marine plastics, with their negative effects on marine life and the human health, have been recently recognized as a new niche for the colonization and development of marine biofilms. Members of the colonizing communities could possess the potential for plastic biodegradation. Thus, there is an urgent need to characterize these complex and geographically variable communities and elucidate the functionalities. In this work, we characterize the fungal and bacterial colonizers of 5 types of plastic films (High Density Polyethylene, Low Density Polyethylene, Polypropylene, Polystyrene and Polyethylene Terepthalate) over the course of a 242-day incubation in the south-eastern Mediterranean and relate them to the chemical changes observed on the surface of the samples via ATR-FTIR. The 16s rRNA and ITS2 ribosomal regions of the plastisphere communities were sequenced on four time points (35, 152, 202 and 242 days). The selection of the time points was dictated by the occurrence of a severe storm which removed biological fouling from the surface of the samples and initiated a second colonization period. The bacterial communities, dominated by *Proteobacteria* and *Bacteroidetes*, were the most variable and diverse. Fungal communities, characterized mainly by the presence of *Ascomycota*, were not significantly affected by the storm. Neither bacterial nor fungal community structure were related to the polymer type acting as substrate, while the surface of the plastic samples underwent weathering of oscillating degrees with time. This work examines the long-term development of Mediterranean epiplastic biofilms and is the first to examine how primary colonization influences the microbial community re-attachment and succession as a response to extreme weather events. Finally, it is one of the few studies to examine fungal communities, despite them containing putative plastic degraders.

6.2 Introduction

Increasing plastic demand and production, combined with improper waste management, have resulted in the estimated presence of 140 MT of plastics in the ocean (OECD, 2022). The Mediterranean Sea, characterized by low water exchange rate, high degree of economic activity and population density around its shores, has been identified as one the most plastic polluted regions of the planet (Cózar et al., 2015; Suaria et al., 2016), with model simulations indicating that 5 – 10 % of the global plastic mass is accumulated in the Mediterranean basin (Van Sebille et al., 2015). Residing in the marine environment, plastics interact with their surroundings, namely heat, radiation, mechanical forces or living organisms. As a result, plastics undergo chemical alterations and can possibly fragment into micro- (< 5 mm) or even nanoplastics (< 1 μm) (Andrady, 2011; Frias and Nash, 2019). Apart from potentially harming marine life and the human health (Sangkham et al.,

2022), plastics, through their hydrophobicity, can act as substrates for the attachment and development of distinct complex communities called the plastisphere (Zettler et al., 2013).

Despite the fact that oil based plastics have traditionally been considered non-biodegradable, it has been found that members of the plastisphere possess the potential for plastic degradation (Amobonye et al., 2021; Gambarini et al., 2022). Biodegradation could act as an attractive alternative to the existing plastic waste management schemes, such as landfilling, recycling or energy recovery, which have not yet been optimized (Kibria et al., 2023). Bacterial and fungal strains, such as *Pseudomonas sp., Bacillus sp.* and *Aspergillus sp.* have been recognized as plastic degraders (Amobonye et al., 2021; Singh Jadaun et al., 2022). Insect gut microbiome associated communities have also been successfully linked with the biodegradation of plastics (J. Zhang et al., 2020). Polyethylene (PE) is the most frequently used plastic polymer, followed by polypropylene (PP), polyvinylchloride (PVC) and polystyrene (PS) (PlasticsEurope, 2022). The biodegradation of the recalcitrant C-C backbone polymers has been investigated. The applications of PVC are long-term, in contrast to polyolefins, from which single-use products are mainly manufactured and therefore, contribute substantially to the plastic pollution (PlasticsEurope, 2022). For that reason, the highest number of biodegradation studies are referring to PE, followed by PP and PS (Singh Jadaun et al., 2022). Polyethylene terephthalate (PET) degradation using microorganisms and their enzymes has also been specifically examined (Qi et al., 2022).

The potential for plastic biodegradation has sparked the interest of researchers worldwide. The characterization of marine communities thriving on plastic surfaces has been the object of many recent studies (Kwee et al., 2022). Research has been mainly focused on prokaryotic, rather than eukaryotic community analysis (Koh et al., 2023; Robyn Joanna Wright et al., 2020). This can be explained by the increased complexity of eukaryotic genetic material and in consequence the increased difficulty in the application of sequencing techniques and data interpretation, but also the lack of substantial reference material and database entries (Tender et al., 2017). Plastics collected from the marine environment with unknown residence times have been frequently used for plastisphere analysis, as well as samples specifically introduced for this purpose to the environment for known periods of time (Robyn Joanna Wright et al., 2020). Deployment times are in general short, but deployments of up to 308 (Tender et al., 2017) or 719 days (Agostini et al., 2021) have been reported.

It has been demonstrated that free-living microorganisms differ from those attached on plastic surfaces (Kirstein et al., 2018; Oberbeckmann et al., 2016, 2014). The effect of numerous environmental drivers, such as substrate type, geographic location, time, or biofilm maturation, on

plastisphere composition have been studied. Plastic associated communities can be defined by geographic location (Catão et al., 2021; Lacerda et al., 2020; Mothes et al., 2021) and season (Oberbeckmann et al., 2016). Substrate-related factors such as charge, hydrophobicity and roughness have been found to affect community attachment (Cai et al., 2019) and composition (Rummel et al., 2017), however there has been no definite consensus on whether the plastic type is a community defining parameter. For instance, Mincer et al. (Mincer and Zettler, 2016), Oberbeckman et al. (Oberbeckmann et al., 2016) and Witt et al. (Witt et al., 2011) agree that substrate type is irrelevant to the community structure, while Frère et al. (Frère et al., 2018), Hansen et al. (Hansen et al., 2021) and Pinnell and Turner (Pinnell et al., 2019) found substrate-specific differences. Biofilm composition and maturation, usually expressed in temporal terms, has been the most extensively examined parameter. Both the initial, as well as the long-term community composition have been studied. Initial colonizers, namely Proteobacteria, as well as the most commonly detected genera, such as Bacteroidetes, Firmicutes and Cyanobacteria, have been identified (Roager and Sonnenschein, 2019).

For this study, 5 types of plastic films (LDPE, HDPE, PP, PS and PET) were incubated in Souda Bay (Crete, Greece) for 300 days. The chemical alterations of the polymeric structure throughout the experiment duration were examined monthly using ATR-FTIR, in conjunction with the plastisphere composition at four critical time points, in relation to a severe storm event. Both the bacterial and fungal community structure was examined, through the application of next generation sequencing (NGS) of the 16s rRNA and ITS2 ribosomal regions. In this work the non-linear observation of biofilm development is studied for the first time. The removal, reattachment and redevelopment of plastic residing communities on the examined substrates allowed us to investigate the hypothesis whether the previous existence of biofilm plays a determining role in the community succession. Finally, the understudied fungal plastisphere of the south-eastern Mediterranean is examined for the first time.

6.3. Materials and methods

6.3.1. Experimental setup

Five types of oil-based plastic polymers in film form were used: LDPE, $CaCO_3$ enriched HDPE, PP, PS and PET. HDPE films was purchased from Plastika Kritis S.A. (Heraklion, Greece), while the rest were contributed by A. Hatzopoulos S.A (Thessaloniki, Greece). The thickness of the film varied from 30 μm (LDPE, HDPE, PP) and 36 μm (PET) to 500 μm (PS).

A total of 12 film strips (surface area of each side: 30 cm x 2 cm) were prepared from each film type. Holes were made along each strip, to allow the insertion of stainless-steel wire. The wire was used to

secure the strips in place inside four (4) metallic cages which would allow the submersion of the plastic film strips in the sea, while also protecting them from being washed away by currents and waves. LDPE, HDPE, and PP were each incubated in their designated cages. PS and PET were placed together in the fourth cage, due to their distinct characteristics (colour, thickness, and hardness) that made it impossible for the two polymers to be confused.

6.3.2. Field incubation and sampling

An octagonal floating device was constructed from polyvinyl chloride (PVC) pipes (d = 0.125 m) after filling them with polyurethane foam. The use of the foam trapped air inside the pipes and at the same time acted as water insulation, thus guaranteeing constant floatation of the device. The four cages containing the plastic films were tied diametrically on opposite sides of the device, to ensure balanced loading. The polymer films were incubated in Souda Bay, Crete, Greece (35.480077, 24.111419) for 300 days (18/06/2019 - 18/04/2020).

Samplings were performed on the 35th, 67th, 102nd, 152nd, 202nd, 242nd and 300th day, respectively. During each sampling, one strip from each film type was permanently removed from the metallic cage, stored in pre-sterilized glass jars, and transferred to the lab.

On the 175th day the incubation site was affected by strong winds, with speeds up to 75 km/h (9 Bf). The resulting wave activity contributed to the removal of the biofilm which had developed on the surface of the samples. Biological deposition on the polymeric surface resumed when the weather conditions allowed it. Thus the biofilm on the surface of the polymers can be classified as follows: the biofilm on the polymers on the 35th day (before the storm, initial maturation– BI), the biofilm on the polymeric surface before the storm (before the storm, final maturation – BM), the biofilm initially reattaching after the storm (after the storm, initial maturation – AI) and finally, the biofilm on the polymers after sufficient time has elapsed for its re-maturation (after the storm, final maturation – AM). Loss of the cage containing the HDPE samples due to intense wave prior to the 300th day sampling led to the selection of the 242nd day as the final date of sampling. Thus, it was possible to analyze the community of all polymer types on the same timeline.

6.3.3. Sample preparation

At the time of analysis, the plastic films were cut in 15 (fifteen) 2 cm x 2 cm square pieces. On three (3) randomly selected pieces, the biofilm was fixed to be examined with scanning electron microscopy (SEM). The fixation process consisted of initial washing with phosphate buffer solution (PBS, 0.1 M, pH = 7.4), followed by fixation with a 2% formaldehyde solution in deionized water. The

fixed samples were then washed in deionized water for the removal of the formaldehyde, and serial ethanol (completely denatured with 1% Ethyl methyl ketone, 1% isopropyl alcohol, 1 g/100 L Denatonium benzoate, Merck) ~ deionized water solutions (25%, 50%, 75%, 90%). The samples were finally dried at 45 ^{o}C for 72 hours. Careful sample handling ensured that no biofilm would be removed from the surface of the plastics pieces.

The biofilm was removed from the rest of the polymer squares (12) by gentle scraping the surface with sterilized loops. The biofilm from each piece was stored in –20 ^{o}C for further analysis. The plastic squares were washed further by placing them on a mechanical mixing table (120rpm) for 3 days in 50 mL falcon tubes containing 40 mL of a Tween80 ~ deionized water solution. At the end of the 3rd day, the wash liquid was stored in –20 ^{o}C, while the plastic squares underwent a final washing; they were placed in 50 mL falcon tubes containing 10% Sodium dodecyl sulphate (SDS) and vortexed at high speed. After two hours, the plastic squares were removed from the tubes and dried at 45^{o}C for 72 hours.

6.3.4. Attenuated total reflection - Fourier transform infrared spectroscopy (ATR-FTIR)

The functional groups on the surface of the virgin and biofilm-free polymers over time were identified using ATR-FTIR. Two sides from 4 (four) biofilm-free square film samples of each type were analysed after each sampling. A Nicolet iS50 FTIR spectrometer equipped with a diamond ATR accessory (Thermo Scientific, USA) was used to acquire spectra. Spectrum visualization and processing was performed with the OMNIC software (Thermo Scientific, USA). A total of 32 scans was acquired for each sample, in the spectral range of 4000cm^{-1} – 400cm^{-1}, with a scanning resolution of 4 cm^{-1}. Spectra were analysed using Spectragryph software version 1.2.16 (Menges, 2022). From the absorptions at specific wavenumbers of each spectrum, the values for five indices were calculated: The keto carbonyl (KCBI), ester carbonyl (ECBI), vinyl bond index (VBI), internal double bond index (IDBI) and carbonyl (CI) indices (Albertsson et al., 1987; Rajakumar et al., 2009). The calculation values for each polymer can be found in Table S1.

6.3.5. Scanning electron microscopy (SEM)

The surface of the polymers, as well as the structure of the attached biofilm and community were observed under a scanning electron microscope. Virgin polymer samples and biofouled samples collected on the 242nd day were coated with 20 nm of gold using a SCD 050 sputter coater (Bal-Tec). Scanning electron microscopy was performed with a JSM-6390LV SEM (Jeol, USA).

6.3.6. Biofilm quantification and genomic DNA extraction

Prior to washing, the biofilm was quantified on the surface of three (3) of the plastic square pieces, following the protocol of (Lobelle and Cunliffe, 2011b). Biofilm quantity was then expressed as optical density per surface area (O.D./cm^2).

For the extraction of the genomic DNA, the DNeasy PowerSoil Pro Kit (Qiagen, Germany) was used, according to the manufacturer's instructions. The resulting DNA concentration was measured on a Qubit 4 fluorometer (Invitrogen, Thermo Fisher Scientific, Waltham, MA, USA), using the Qubit dsDNA high sensitivity assay.

6.3.7. 16s RNA and ITS2 amplicon sequencing and data processing

The V3-V4 regions of the 16s rRNA gene and the ITS2 ribosomal region were sequenced for bacterial and fungal communities. Sequencing was performed in 3 biological replicates on an Illumina NovaSeq PE250 (2 x 250 bp) system by Novogene (UK) Company Ltd. (Cambridge, UK), using the bacterial primers 341F/806R (5'-CCTAYGGGRBGCASCAG-3' / 5'-GGACTACNNGGGTATCTAAT-3') and fungal primers ITS3/ITS4 (5'-GCATCGATGAAGAACGCAGC-3' / 5'-TCCTCCGCTTATTGATATGC-3').

Bioinformatics analysis was performed in R version 4.0.0 (R Core Team, 2021) in the R Studio environment version 1.3.959. The DADA2 pipeline was employed for the analysis of the resulting fastq files using the corresponding R package (Callahan et al., 2016). For ITS data, cutadapt version 3.7 (Martin, 2011) in conjunction with Python version 3.11.0a4 (van Rossum, 1995) was used to remove primers and barcodes prior to further analysis. Chimeric sequences, mitochondria and chloroplasts were removed. Taxonomy assignment was performed using the SILVA version 138 (Quast et al., 2013; Yilmaz et al., 2014) database for the 16s rRNA region and UNITE database (Nilsson et al., 2019) for the ITS2 region. The DECIPHER R package (Wright, 2016) was used for multiple amplicon sequence variant (ASV) alignment and the phangorn R package version 2.8.1 (Schliep, 2011) was used for the construction of a phylogenetic tree. The sequence table produced by DADA2, the sequence taxonomies, the phylogenetic tree, along with the sample metadata were imported in the phyloseq R package version 1.38.0. The resulting phyloseq object was used for downstream analysis.

The R package microeco (C. Liu et al., 2021) was used for further analysis. To eliminate the influence of sequencing depth on community diversity, bacterial samples were rarefied to 56096 reads and fungal samples to 15336 reads. Alpha diversity was evaluated using the observed number of taxa, as well as the Shannon and Simpson indices for diversity and evenness. Kruskal-Wallis rank sum test and one-way ANOVA were performed to examine the significance of the observed differences. The

attached communities were ordinated with non-metric multidimensional scaling (NMDS) based on the Bray-Curtis distance with the R package vegan (Oksanen, JariJari Oksanen, F. Guillaume Blanchet, Michael Friendly, Roeland Kindt, Pierre Legendre, Dan McGlinn et al., 2020). Pairwise PERMANOVA (999 permutations) using the Bray-Curtis distance was conducted to examine the statistical significance among substrates and biofilm phase. The significant bioindicator taxa across groups were identified using Linear discriminant analysis Effect Size (LEfSe) (Segata et al., 2011). Redundancy analysis (RDA) was applied to distinguish the environmental factors affecting the observed variation among samples. Metabolic function prediction for the bacterial communities was realized using Tax4Fun (Aßhauer et al., 2015). PlasticDB (Gambarini et al., 2022) was utilized to identify putative biodegraders among the identified taxa.

6.4. Results

6.4.1. Attenuated total reflection - Fourier transform infrared spectroscopy (ATR-FTIR)

Chemical alterations could be observed over time in the ATR-FTIR spectra of all polyolefins examined. More specifically, a wide peak corresponding to OH- stretching carboxylic acids appeared in the 3000-3650 cm^{-1} regions of the spectra of LDPE, HDPE, and PP. Stretching C=C bonds appeared over time in the form of weak peaks at 1610 cm^{-1} for LDPE and PP samples and a peak at 1650 cm^{-1} corresponding to C=O stretching was detected for HDPE samples. C-O stretching bonds could be identified at 1050 cm^{-1} and at 1100 cm^{-1} in the spectra of the three polymers. For PP a peak at 907 cm^{-1} could be detected, corresponding to the deformation of carboxylic acid and the C-H deformation of aldehydes and vinyl groups. The spectrum of LDPE can be seen in Figure 6.1, along with the values of the KCBI, ECBI, VBI, IDBI and CI over time. Those of HDPE and PP in Figures S56 and S57, respectively. The ATR-FTIR spectra of the cleaned PS (Figure S58) and PET (Figure S59) samples did not reveal any change to the chemical structure of the polymers.

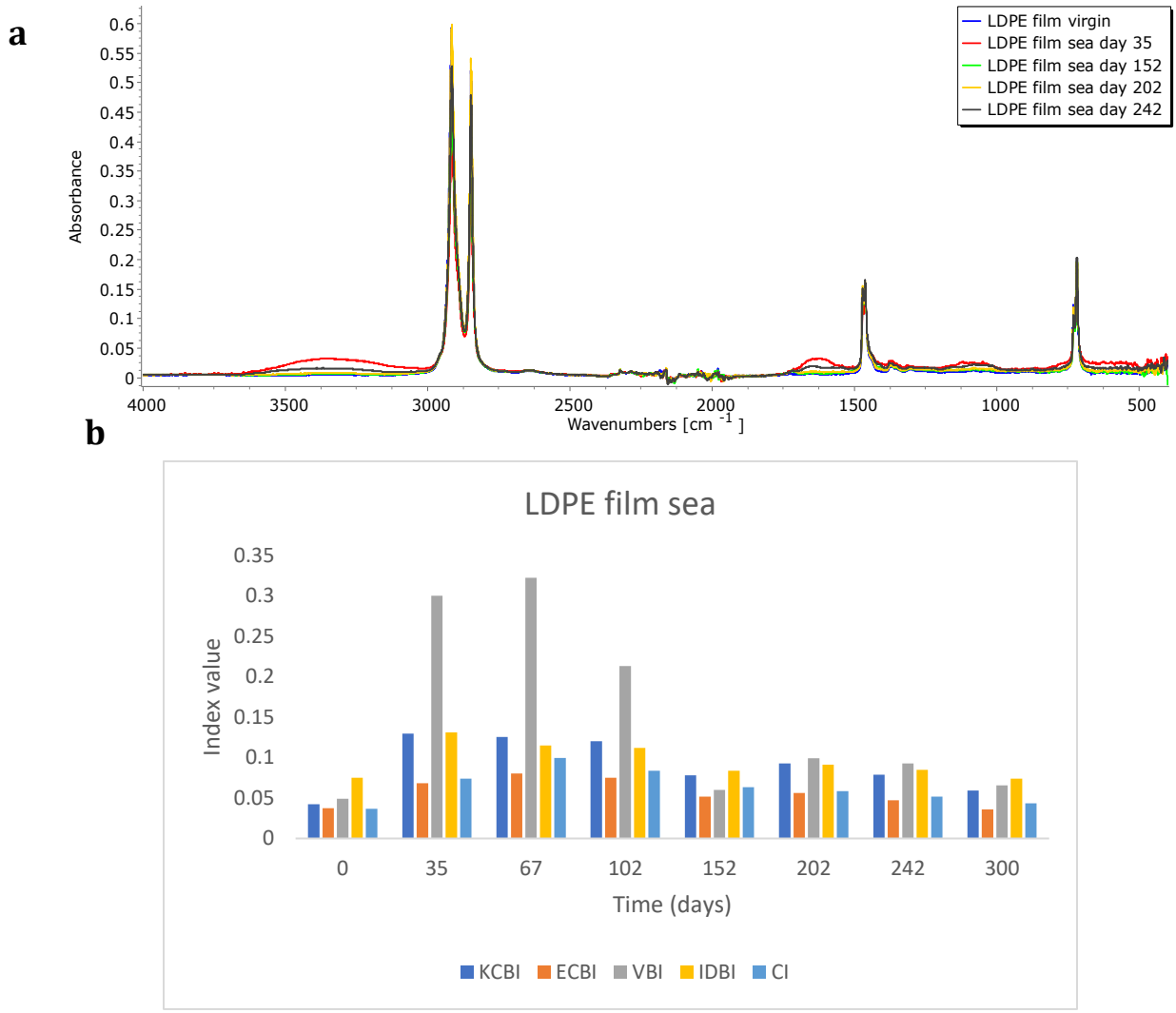

Figure 6. 1: (a) ATR-FTIR spectra of LDPE samples over time. (b) Index values for LDPE over time.

6.4.2. Scanning electron microscopy

The surface of the plastic samples facilitated the attachment of macroscopic organisms such as marine plants, macroalgae, insects, barnacles, and cephalopod eggs. Marine algae development could also be observed by the naked eye. SEM images allowed the microscopic inspection of the biofilm structure and other fouling agents attached on the samples. Along with the ever-present EPS structures (Figure 6.2a), marine fungal hyphae (Figure 6.2b) and numerous diatom species (Figure 6.2c, 6.2d, 6.2e) were present on all polymer types. The mineral exoskeletal formations of bryozoans (Figure 6.2f) were also identified on all samples. Coccolithophores (Figure 6.2g) were present on LDPE and PS samples, while calcareous worm tubes (Figure 6.2h) were photographed on HDPE, PS and PET.

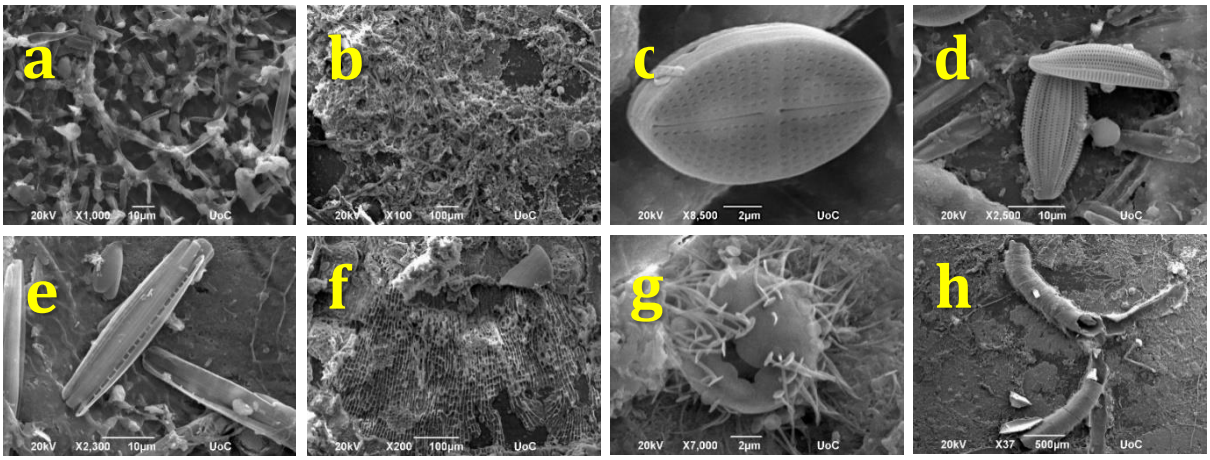

Figure 6. 2: (a) EPS structure on PET sample, (b) fungal hyphae on LDPE sample, (c) diatom on PP sample, (d) diatom on PS sample, (e) diatom on PS sample, (f) mineral exoskeletal bryozoan formation on HDPE sample, (g) coccolithophore on PS sample, (h) calcareous worm tube on HDPE sample.

6.4.3. Southwestern Mediterranean bacterial and fungal plastisphere communities

The examination of the communities was performed before and after the removal of biofilm by a storm on the 175th day. Two occasions were selected: early after the biofilm development and prior to its removal by the natural event. Therefore, analysis was performed on samples of all polymer types collected on the 35th (Before Initial – BI), 152nd (Before Mature – BM), 202nd (After Initial – AI) and 242nd (After Mature – AM) day. A total of 57 bacterial and 52 fungal samples were successfully sequenced, producing a total of 5692212 and 4835711 raw reads, respectively. After rarefaction, 7481 unique bacterial and 6367 unique fungal taxa remained for analysis.

6.4.3.1. Community composition

At the phylum level (Figure S60) *Proteobacteria* dominated the bacterial communities (43.9% - 98.5%), followed by *Firmicutes* (0.75% - 24.2%), *Actinobacteria* (0.3% - 51.5%) and *Bacteroidetes* (0.1% - 18.1%). The prevalence of *Actinobacteria* is especially pronounced in samples collected before the removal of biofilm (BI), while *Bacteroidetes* are highly abundant in the mature biofilm samples before the removal due to extreme wind and wave activity (BM). *Firmicutes*, on the other hand, were notably prevalent in biofilm samples collected after the re-establishment of the biofilm (AI and AM). The 10 most abundant bacterial genera for each polymer per biofilm phase can be seen in Figure 6.3. The prevalence of *Acinetobacter* (39.1% - 88.7%) in mature biofilms can be observed, both in samples collected before the removal and after the redevelopment of biofilm (AM and BM), regardless of the substrate type. *Pseudomonas* is very common (7.8% - 32.1 %) among the genera on

the surface of HDPE, PET, and PP during the second cycle of biofilm development (AM). The genus *Cutibacterium*, although present in the composition of all BI communities, is more abundant in PS and PET samples. Similarly, the genus *Ralstonia*, despite barely being detected in mature biofilms on any polymer type, is quite common in the BI communities developing on the surface of HDPE (3.5% - 11.3%), LDPE (3.5% - 5.6%) and PS (2.6% - 10%). The percentage of genera represented in "Others" is higher in both BI and AI, when compared with BM and AM.

Ascomycota is the dominant fungal phylum (82.4% - 99.5%), followed by *Basidiomycota (*0.4% - 3.5%) (Figure S61). At the genus level, *Aspergillus* was found to be the most abundant (2.1% - 87.4%), followed by *Engyodontium* (0.8% - 70.5%), *Candida* (0.1% - 52.6%) and *Nacaseomyces* (0.1% - 34.7%). The relative abundance of *Engyodontium* is higher in mature communities (AM and BM). Relative abundances of low representation genera listed as "Others" in initial fungal communities (AI and BI) can also be observed (Figure 6.4).

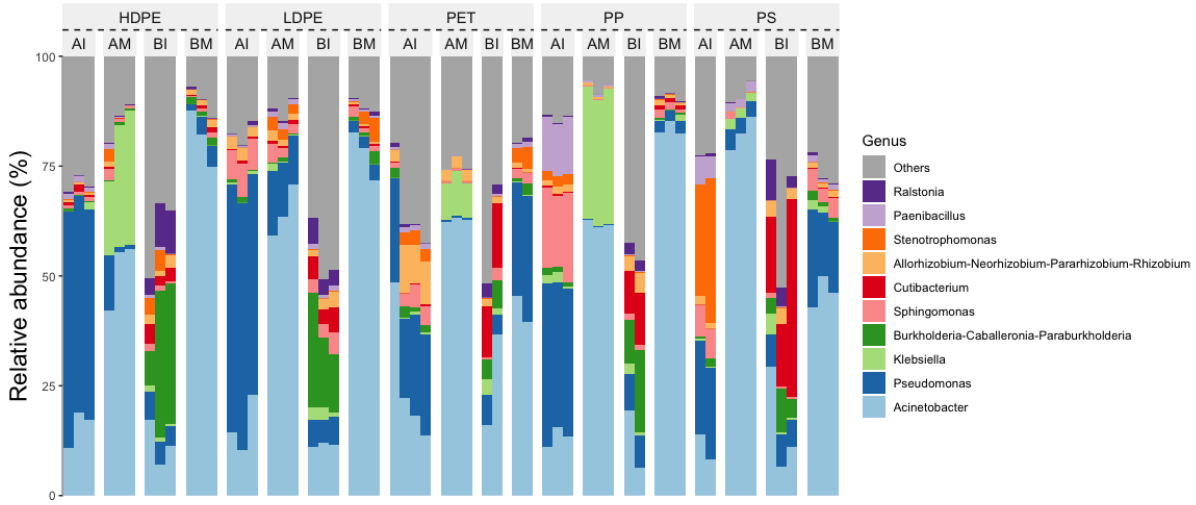

Figure 6. 3: Relative abundance of bacterial genera present in bacterial biofilm collected from the surface of each polymer type, associated with fouling phase (AI, After removal Initial; AM, After removal Mature; BI, Before removal Initial; BM, Before removal Mature).

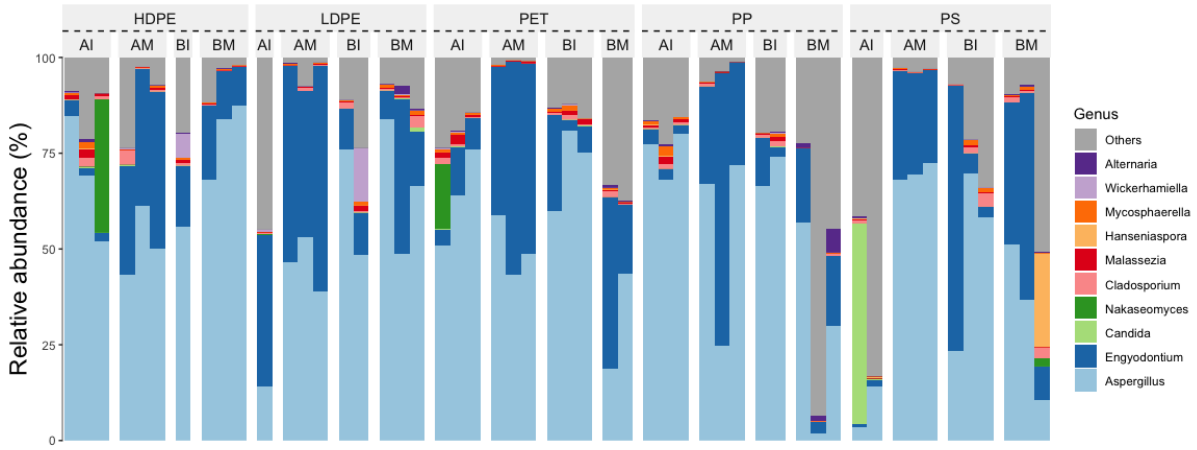

Figure 6. 4: Relative abundance of fungal genera in fungal assemblages collected from the surface of each polymer type, associated with fouling phase (AI, After removal Initial; AM, After removal Mature; BI, Before removal Initial; BM, Before removal Mature).

6.4.3.2. Bacterial and fungal community diversity

The polymeric substrate did not affect the community alpha diversity (Figure S62). The number of observed bacterial ASVs on the surface of the different polymers were higher than the number of observed fungal ASVs. Bacterial diversity, expressed as the Shannon Index value, did not vary significantly among the various polymeric surfaces. For fungi, the community diversity was lower on PP and higher on PS. Statistically significant differences were not detected for either bacterial or fungal communities in terms of diversity, evenness, or richness, when the polymer type is the distinguishing factor (Table S4). The communities displayed significant dissimilarities, however, when examined with reference to the phase of the fouling community (Table S5). More specifically (Figure S63), the bacterial community initially developing on the polymers after few days of their deployment in the marine environment (BI) was more diverse, characterized by a higher number of observed ASVs, as well as a higher Shannon Index value. As the attached community thrived for prolonged period (BM), the values of both alpha diversity indexes decreased. Recolonization of fouling agents after the bad weather (AI) resulted again in an increase, despite not reaching the initial levels (BI). Further maturation of the bacterial community (AM) brought forth further limitation of the bacterial community, with diversity almost equal to that observed prior to the biofilm removal. The early fungal community (BI) was characterized by 250.1 ± 79.8 observed taxa and a Shannon Index value of 1.9 ± 0.6. Upon maturation (BM), fungal diversity was lower (observed = 136.1 ± 66.0, Shannon Index= 1.4 ±0.6). The community diversity increased anew after the reattachment of fouling agents (AI), without however reaching the exact values of the BI samples (observed = 231.7 ± 55.1, Shannon = 2.1 ± 0.7). The final mature community (AM) diversity was the lowest we encountered

(observed = 90.4 ± 37.2, Shannon Index = 1.0 ± 0.4).

Non-metric multidimensional scaling (NMDS) revealed the distinct composition of bacterial communities among biofilm phases (Figure 6.5a). Some overlap of the mature communities (BM and AM) can be observed, while the two freshly developed bacterial assemblages are clustered in a very clear way. The effect of the polymer type acting as a substrate is negligible in community composition. PERMANOVA analysis further supports this result since all of the pairwise comparisons between polymer types were statistically insignificant ($P > 0.07$). At the same time, pairwise comparisons between biofilm phases generated statistically significant results in all cases ($P < 0.001$). The overlap of fungal communities observed in the NMDS plot (Figure 6.5b), regardless of substrate type or biofilm phase was also supported by PERMANOVA. More specifically, pairwise comparisons between substrate types did not produce statistically significant results ($P > 0.112$). Comparisons between the biofilm phases also did not reveal any statistically significant differences between the communities ($P > 0.197$).

The number of unique bacterial ASVs for each polymer type, as well as each biofilm phase was determined. A total of 630 ASVs were detected on all substrates, while the highest number of unique ASVs was detected on the surfaces of PET samples (Figure S64a). The situation was quite different when it came to fungal community attachment on plastic substrates. Only 100 ASVs were shared among all substrate types, with most unique ASVs being observed on PS (Figure S64b). A total of 544 bacterial taxa were present in all biofilm phases. Initial biofilms presented with higher unique ASV numbers, which decreased with biofilm maturation (Figure S64c). A miniscule 104 fungal ASVs were common among all four biofilm stages. Fungal communities were similarly characterized by high initial unique ASV abundances which were reduced as the biofilm matured (Figure S64d).

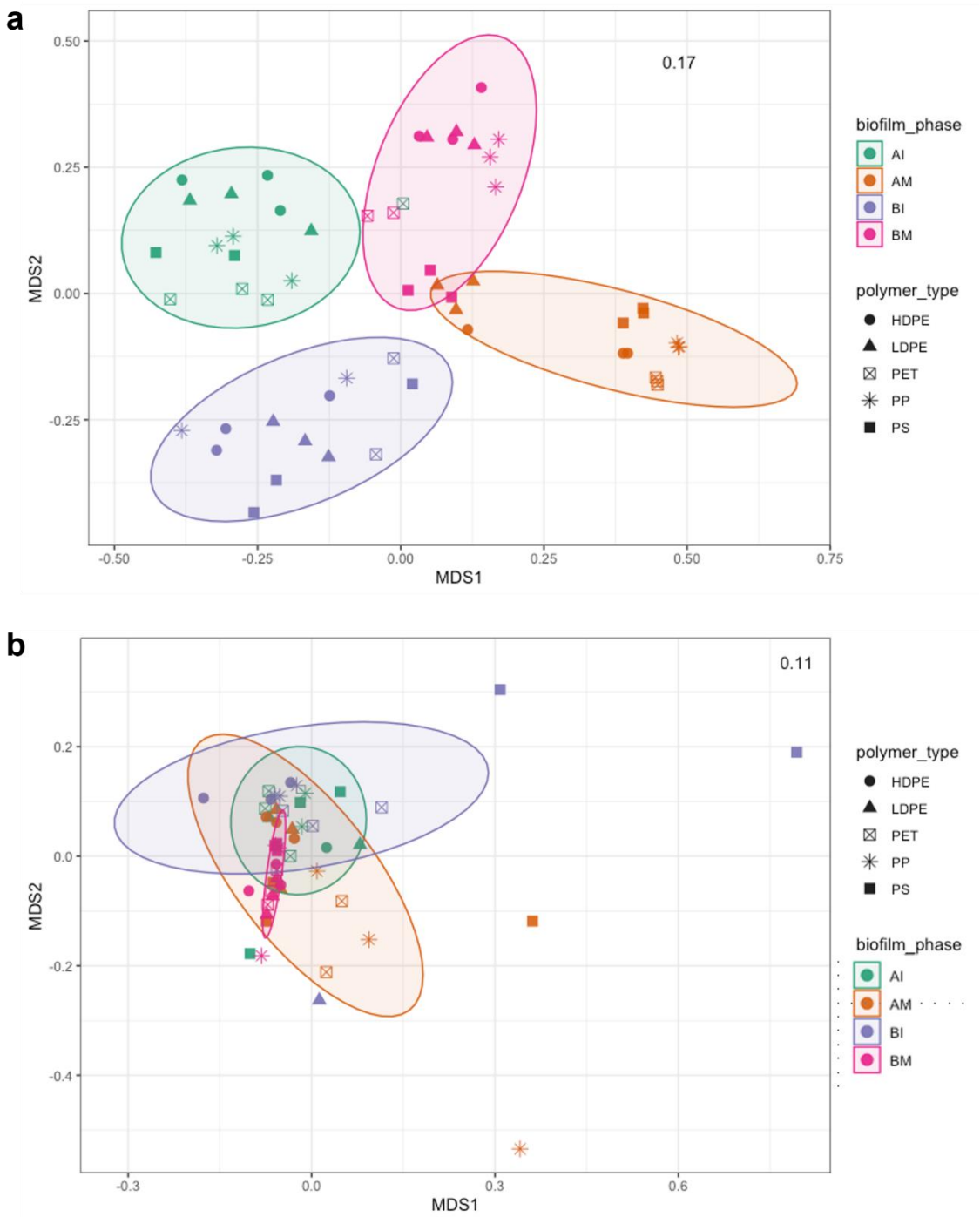

Figure 6. 5: NMDS ordination of Bray-Curtis distances of a) bacterial and b) fungal communities.

6.4.3.3. Biomarkers

LefSe analysis allowed the identification of biomarkers of the separate biofilm phases. Despite the statistically significant differences in the composition of the bacterial and fungal communities

studied in this work, few taxa could be exclusively identified per biofilm phase, thus acting as biomarkers of each biofilm phase. Interestingly, only taxa corresponding to the initial phases of biofilm development could be determined. The class *Actinobacteria* was characteristic of the bacterial biofilm initially developing on the surface of the polymers (BI), while the phylum *Firmicutes* of the first stages of biofilm re-development after its removal (AI) (Figure S65). The fungal phylum *Basidiomycota* discriminated the AI biofilm stage from the other three (Figure S66).

6.4.3.4. Community differentiation factors

Redundancy analysis (RDA) showed how environmental factors were related to the community development on the plastic samples. More information on the examined factors, with a focus on biofilm quantification and sinking characteristics of the samples were provided by Karkanorachaki et al. (Karkanorachaki et al., 2021). Well defined clustering can be observed in the biplot for the bacterial samples (Figure S67). The number of cells in the biofilm influences the BI, AI, and AM samples. This is not the case for the BM samples, however. The density of the polymer was the significant factor in separating PET and PS in BM samples, as expected, but that does not apply for the other groups of samples. The alterations of chemical structure of the sample surfaces with time, expressed as ATR-FTIR indices, affected the community as well. For fungal samples (Figure S68) no clear clustering can be observed and none of the parameters examined has a significant effect on the samples' behaviour.

6.5. Discussion

The semi-enclosed Mediterranean Sea has been identified as one of the most heavily polluted areas by plastic and microplastic waste worldwide (Cózar et al., 2015; Eriksen et al., 2014; Suaria et al., 2016). Given its oligotrophic status (Krom et al., 2004), available substrates such as plastics allowing for secure attachment and nutrient utilization (Song et al., 2023), and at the same time acting as a potential carbon source are easily colonized by marine organisms; thus the Mediterranean "plastisphere" is formed (Amaral-Zettler et al., 2020; Zettler et al., 2013). This work constitutes the examination of the composition of the plastisphere communities throughout the longest-term *in-situ* incubation in the Mediterranean Sea of 5 types of plastic films, in relation with polymer substrate and biofilm stage. The removal and re-establishment of biofilm by extreme wind and wave activity during the 242-day duration of the experiment, allowed for the first time the systematic examination of community succession in the perpetually dynamic manner which characterizes natural ecosystems. Biofilm presence has been linked with surface changes in the physicochemical properties of PE, PP

and PS beads (McGivney et al., 2020). Incubation of LDPE, HDPE and PP in the Mediterranean Sea resulted in structural changes to their surface. The presence of oxygen containing moieties in the polymeric chains of the samples, namely carboxylic acids and carbon oxygen bonds, could be attributed to photodegradation, the result of the effect of solar radiation (Gewert et al., 2015a). Incremental increase of the vinyl bond (VBI) and internal double bond index (IDBI) values in the initial stages of the incubation period indicates biodegradation (Harshvardhan and Jha, 2013), while their decrease over the next stages can be attributed to further biological dissolution of the unsaturated bonds (Chamas et al., 2020). This pattern of bond formation and dissolution, as the result of biological process has previously been observed in marine microcosm and mesocosm degradation experiments (Chapter 4). The highest values of all indices were observed for PP samples, followed by LDPE and HDPE, as expected by the structure of the respective polymeric chains (Chamas et al., 2020; Gewert et al., 2015a; Syranidou et al., 2023). Signs of degradation process, however, could not be detected on the surface of PS and PET samples, which remained unchanged throughout the experiment. PS is considered very susceptible to photooxidation and there has been evidence of its biodegradation (Ho et al., 2018). At the same time, neither photooxidation, nor hydrolysis, the main degradation mechanisms of PET in marine environments (Gewert et al., 2015a), were observed. It can be inferred that the development of biofilm and biofouling on the surface of the samples was acting as a shield the polymers from the effect of their immediate environment (hydrolysing water and UV radiation). Bacterial biofilms have been found to cause changes to the properties of polymers, such as the roughness, stiffness and crystallinity, similar to these caused by photooxidation (McGivney et al., 2020). Furthermore, reactive oxygen species (ROS) produced by the hydrocarbon degrading bacterium *Alcanivorax* has been hypothesized to cause abiotic-like oxidation of PE (Zadjelovic et al., 2022). It might be prudent to assume, however, that the observed result could be a combination of biotic and abiotic processes (Chapter 4) (Karkanorachaki et al., 2023). The initial oxidation of the polymer, resulting in hydrophilicity and surface to volume ratio modifications, and therefore more effective biofilm attachment, was caused initially by radiation from the sun (Takada, 2019). After the establishment of the marine community biofilm, biotic processes dominate the degradation mechanism. The enrichment of the "Xenobiotics Biodegradation and Metabolism" pathway in the predicted BI community metabolic function (Figure S69) could possibly be linked with the decrease in the values of the ATR-FTIR indices, since chain scission products from PE weathering have been found to enrich hydrocarbon degrading bacteria, with the potential to degrade plastics, as well (Erni-Cassola et al., 2020).

Images acquired by SEM revealed the complexity of the south-eastern Mediterranean plastisphere.

The presence of exopolymeric substance matrices, fungal hyphae, diatoms, and calcareous formations by marine organisms imply the development of a multi-level network of interactions. Diatoms and bacterial biofilms have been recognized as the main plastic colonizers, however that might be the result of the limited number of works on marine fungi and other eukaryotic communities (Amaral-Zettler et al., 2020). Mixed diatom and bacterial biofilm structures have previously been detected on polyethylene and biodegradable plastic bags showing degradation signs, following incubation in the Mediterranean Sea for 15 and 33 days (Eich et al., 2015). In the Caribbean Sea, marine incubation of six types of plastics for six weeks revealed the presence of bacteria, as well as diatoms, dinoflagellates, red, green, and brown algae, parasitic ciliates and apicomplexans (Dudek et al., 2020). Confocal laser scanning microscopy (CLSM) on everyday plastic item samples incubated in Vineyard Sound (Massachusetts, U.S.A.), revealed high initial diatom abundances, which subsequently were reduced by the introduction of more colonizers (Zhao et al., 2021). Microplastic sample communities from the North Pacific Gyre were dominated by bacilli and pennate diatoms, while coccoid bacteria, centric diatoms, dinoflaggelates, coccolithophores and radiolarians were also detected (Carson et al., 2013). Plastic associated communities from 68 microplastics collected from Australian marine and coastal environments were more diverse, with a variety of diatom genera, coccolithophores, bryozoans, barnacles, bacteria, cyanobacteria, fungi, a dinoflagellate, an isopod, a marine worm and marine insect eggs (Reisser et al., 2014).

A large volume of the existing literature on the subject of plastisphere composition is based on "snapshots" of the communities, as the plastics are commonly sampled from the marine environment, with no knowledge of the prior history of the examined samples (Robyn Joanna Wright et al., 2020). Despite the fact that it is possible to get an inkling of the weathering degree of a plastic sample spectroscopically (Ioakeimidis et al., 2016) or by microscopic examination of fragmentation and cracking (Meides et al., 2022), it is impossible to actually know its residence time in the marine environment or the history of biofilm formation and community succession. A closer inspection of the bacterial and fungal communities attached on the polymers via NGS reveals that the epiplastic community composition is dynamic and time dependent. Plastic colonization in the marine environment is a matter of minutes, with maturation being achieved after approximately 9 days (Erni-Cassola et al., 2020; Latva et al., 2022). Maturation of biofilm is a dynamic process and can involve several phases (Jacquin et al., 2019). *Bacteroidetes* (Latva et al., 2022) and *Proteobacteria*, namely *Gammaproteobacteria* (Jin-Woo Lee, Ji-Hyun Nam, Yang-Hoon Kim, Kyu-Ho Lee, 2008; Pollet et al., 2018) and *Alphaproteobacteria* (Wright et al., 2021), are recognized as the early stage colonizers. *Proteobacteria* (genera *Acinetobacter, Pseudomonas, Klebsiella, Sphingomonas,*

Burkholderia) was the main observed bacterial phylum in all time points of this work, with *Bacteroidetes* being also abundant, especially in biofilm matrices of prolonged exposure. The succession of *Proteobacteria* by *Bacteroidetes* in marine samples from India was observed with biofilm maturation (Sushmitha et al., 2021). The sessile lifestyle and macromolecule utilization capacity of *Bacteroidetes* can be assumed to be favoured by the development of a stable ecocorona, thus enabling the fresh enrichment of *Bacteroidetes* in the later stages of colonization (Latva et al., 2022). *Firmicutes* have been previously identified in laboratory scale enrichment studies using indigenous marine Mediterranean communities (Syranidou et al., 2019c, 2017b, 2017a). *Actinobacteria*, most famously the genus *Rhodococcus* (Gilan and Sivan, 2013), have also been detected in polymer-attached marine biofilms (Hansen et al., 2021; Oberbeckmann et al., 2016). Previous assemblages from plastic particles residing in the Mediterranean Sea indicated increased *Cyanobacteria* abundances (Dussud et al., 2018), in accordance with our findings. Interestingly, the genus *Vibrio*, which has been reported to dominate plastic-residing bacterial communities (Amaral-Zettler et al., 2020), was not among the most abundant taxa observed here. Fungal communities have not yet been studied extensively (Robyn Joanna Wright et al., 2020). Saprotrophic *Ascomycota* (genera *Aspergillus, Engyodontium, Candida, Cladosporium*), the dominant phylum in the examined fungal communities, and *Basidiomycota* were highly abundant in samples from three distinct aquatic ecosystems (Kettner et al., 2017), the western South Atlantic and the Antarctic Peninsula (Lacerda et al., 2020) and certain cave system samples (Latva et al., 2022). The clear prevalence of *Ascomycota* over *Basidiomycota* could in part be attributed to amplification bias introduced by systematic length differences of the ITS2 region (Bellemain et al., 2010), but it could also be related to regional dominance of the phylum (Lacerda et al., 2020).

No agreement has been reached among researchers on whether the polymer type acting as substrate affects the attached microbial community composition. On the one hand, it has been found that there is a clear distinction between polyolefin (PP, PE) and PS attaching microbial communities (Frère et al., 2018), as well as among PE, PP and PS (Amaral-Zettler et al., 2015; Hansen et al., 2021) and polyolefins and PVC (Pinto et al., 2019). Metanalysis of the existing literature is in agreement with our conclusion that no significant community differentiation exists among the different plastic polymers (Oberbeckmann and Labrenz, 2020; Wright et al., 2021). Genomic and proteomic examination of marine biofilms on PE, PS and wood concurred that the type of plastic did not affect the community composition (Oberbeckmann et al., 2021). The degree of weathering of the polymeric substrate, however, has been recognized as a community structure driving force (Erni-Cassola et al., 2020). Geographic location has been instead identified as a determining factor of the plastisphere

composition (Basili et al., 2020; Kettner et al., 2017; Oberbeckmann et al., 2021), along with other environmental factors, such as salinity and nutrient concentrations (Oberbeckmann et al., 2017).

The time-dependent nature of the community succession has been elucidated from field experiments aiming to create accurate time series (Robyn Joanna Wright et al., 2020). Field experiments, however, can be disrupted by external factors and therefore are usually short-term and focus mainly on the initial stages of epiplastic community assemblage and succession. The incidence of a severe storm on the 175th day of incubation in Souda Bay did not interrupt our experiment, but remarkably allowed us to examine for the first time the bacterial and fungal succession of the mature epiplastic community in two time points before and after the removal of the initial biofilm. The decrease in alpha diversity observed in both instances, before the removal and after the re-establishment and re-maturation of the biofilm, implies the tendency of the systems to be move towards less diverse and more stable conditions, regardless of the starting point or the weathering degree of the polymer acting as substrate. The alpha diversity of fungal communities we observed was consistently lower than those of bacterial communities, and the differences observed were less pronounced. This observation can in part be attributed to amplification bias during the ITS region sequencing (Bellemain et al., 2010), as well as the fact that fungal hyphae contributed to the more secure attachment of fungi on the polymeric surface. Additionally, fungal growth rates are significantly lower than bacterial (Rousk, 2011). Therefore, the 42 days elapsing between the AI and AM samplings might prove insufficient time for quantifiable changes in the fungal community composition. These assumptions can also be supported by the fact that no clear clustering can be observed in the RDA biplot.

Already a large number of bacterial, fungi and other microorganisms of marine origin have been linked with plastic biodegradation (Amobonye et al., 2021; Oberbeckmann and Labrenz, 2020; Roager and Sonnenschein, 2019; Singh Jadaun et al., 2022; Wright et al., 2021). Hydrocarbon degraders, such as *Alcanivorax borkumensis* (Delacuvellerie et al., 2019; Zadjelovic et al., 2022), have been found to degrade polyethylene. No members of the hydrocarbon degrading communities, suspected to also degrade plastics, have been greatly represented among our samples. Utilization of PlasticDB (Gambarini et al., 2022) data allowed the cross reference of the 10 most common among the identified genera with proven plastic degraders. *Pseudomonas sp.*, a versatile xenobiotics degrader, has been identified as a plastic degrader (R A Wilkes and Aristilde, 2017). Several species of the genus *Pseudomonas* have been reported as degraders of LDPE (*P. aeruginosa, P. chlororaphis, P. cintronellolis, P. fluorescens, P. monteilii, P. putida, P. syringae, P. protegens*), HDPE (*P. aeruginosa, P. fluorescens), PP (P. azotoformans), PS (P. aeruginosa, P. putida, P. linii) and PET (P. aestusnigri, P.*

oleovorans, P. mendocina). Stenotrophomonas species have been found to potentially degrade polyolefins, such as LDPE (*S. humi, S. maltophilia*), HDPE and PP (S. *panacihumi*). The genus *Acinetobacter* contains *A. baumannii,* listed as a putative LDPE and PET degrader, as well as *A. pittii* (degrading LDPE) and *A. johnsonii* (degrading PS). *Paenibacillus* has been assumed to degrade HDPE, LDPE (*P. macerans)* and PS (P. urinalis). *Rhizobium viscosum,* and *Klebsiella pneumoniae* are considered among the degraders of LDPE and HDPE, accordingly). When it comes to fungi, a plethora of *Aspergillus* species have been identified as putative plastic degraders (**LDPE**: *A. clavatus, A. flavus, A. fumigatus, A. japonicus, A. nidulans, A. niger, A. nomiae, A. oryzae, A. terreus, A. brasiliensis*, **HDPE**: *A. flavus, A. niger, A. terreus, A. tubingensis*, **PET**). Finally, *Cladosporium cladosporioides* has been proclaimed to degrade PET. Comparison of our communities to the genome of PET degrading *Ideonella Sakaiensis*, however, did not reveal active shared metabolic pathways (Gambarini et al., 2022). Interestingly, most of the aforementioned plastic degraders have been isolated by soil or landfill sites, raising questions on our ability to isolate plastic degraders from the marine environment, or even whether marine organisms possess the capacity to degrade plastics.

Pathogenic taxa, as well as antibiotic resistant genes, have been detected among the plastic colonizers. The increased transfer potential of the pathogenic taxa enriched biofilms could be linked with negative implications for the health of not only humans, but also of marine ecosystems (Bowley et al., 2021; Kaur et al., 2022; Syranidou and Kalogerakis, 2022). The most abundant bacterial species among the ones detected in this work, and more specifically the *A. baumannii*, which has been linked with LDPE and PET degradation, is a well-known drug resistant human pathogen (Antunes et al., 2014). The genera *Pseudomonas* and *Klebsiella* are also known as potential pathogens (Silby et al., 2011; Ullmann, 1998), with *P. aeruginosa* causing 10% of nosocomial infections in most European hospitals (Bentzmann and Plésiat, 2011). *Burkholderia* contains human, animal, as well as plant pathogenic species (Nowak and Coenye, 2008). *Stenotrophomonas, Paenibacillus* and *Ralstonia* have the potential to be pathogenic to humans (Adegoke et al., 2017; Grady et al., 2016; Ryan and Adley, 2014). *Aspergillus* species cause allergies and pulmonary diseases (Barnes and Marr, 2006), while *Clodosporium* has been linked to plant pathogenicity, and recently to coastal plants (Liu et al., 2017).

6.6. Concluding Remarks

Plastisphere community composition field studies have so far been mostly short term and focused on the initial stages of biofilm formation and maturation. Plastics, however, are recalcitrant compounds and can reside in the marine environment for decades, if not centuries. Long residence times allow for multiple interactions of plastic waste with environmental factors, which would lead

to the random removal and reattachment of marine biofilms. Climate change has been predicted to globally bring forth severe weather events, such as storms or even hurricanes, which would cause the ocean residing plastic surface cleaning and recolonization. The stochastic rather than simply time dependent consideration of colonization allowed the examination of the effect of a pre-existing biofilm on (a) the south-eastern Mediterranean marine community composition and succession and (b) the polymer itself. While the extent of degradation of the polymer was found to fluctuate throughout the experimental period, the plastisphere community showed a tendency for less diverse, more stable compositions. It is important to mention that the community composition of bacterial biofilms did not eventually converge with prolonged attachment; instead, they were significantly different. To elucidate whether significant community structure change occurs over time, the unchanging fungal communities should be studied deeper and in more long terms experiments, especially given their prolonged growth rates. The potential for both biodegradation and pathogenicity were also identified. This work highlights the necessity for comprehensive and stochasticity-including examination of the plastisphere. That, in conjunction with polymer deterioration monitoring could eventually lead to the detection of plastic degrading members of the plastisphere and a biological solution to the global problem of plastic pollution.

Chapter 7. Conclusions and Recommendations

In this dissertation, the four most important processes of plastic degradation and the interplay among them were examined, so that the question "where is the plastic we cannot detect?" would be answered. At the same time, it was explored whether real world conclusions drawn from the results of micro- and mesoscale experiments can be considered accurate.

- The theoretical hypothesis that prior abiotic degradation of polymers allows their faster and more effective colonization and degradation by microorganisms was confirmed.
- Attachment of colonizers and development of biofouling is correlated with the sinking characteristics of microplastics and non-spherical film mesoplastics. Size, density, and biofilm accumulation affected the sinking behavior. Sigmoid curves can explain both biofouling development and sinking velocity changes.
- Mixed marine bacterial communities possess the potential to thrive in a plastic-rich, otherwise carbon-starved environment. A short period of time is required for the acclimatization of the microorganisms to the consumption of plastic-derived carbon.
- Bacterial and fungal taxa with the potential to degrade plastics are present in the south-eastern Mediterranean plastisphere. The fungal community of the area was studied for the first time.
- Biodegradation of weathered plastics under favorable conditions is a faster process than is generally thought. The generation of micro- and nanoplastics in the microcosm experiments indicated that biofragmentation had occurred in 30 days of incubation. Biofragmentation, followed by bio-assimilation, is a prerequisite for biodegradation. The FTIR spectra of the samples also indicated chemical alterations of the polymers concurrent with biodegradation, confirming that conclusion.
- Heteroaggregation is a determining factor in the underestimations of microplastics and nanoplastics in the marine environment.
- A cyclical pattern of weathering and biological de-weathering, allowing for repetition of the process was implied by all our experiments. The altering characteristics of both the biological factors studied and the polymers were similar in all experimental scales. The transferability hypothesis is, therefore, confirmed, assuming similar experimental and data analysis methodologies are applied.

While this thesis contributes significantly to the aim of understanding the problem of plastic pollution, as a first step towards its eventual solution, more work needs to be done in future, if complete elucidation is to be achieved. The escalation of this work could proceed as follows:

- Repetition of incubations with additional polymers, including bio-based and biodegradable plastics, with longer experimental periods.
- Determination of the effect of micro- and nanoplastic aggregation and sinking on the formation of marine snow and the carbon cycle.
- Examination of additional stochastic factors affecting the colonization and degradation of plastics.
- Performance of metagenomic analysis to study the community composition in depth and confirm or disprove the activation of biodegradation and enzyme production genes in the sample-colonizing communities.
- Bioreactor incubation, where the manipulation of controlled conditions would enhance and accelerate the biotic and abiotic degradation and fragmentation.
- Genetic engineering plastic degrading bacteria towards the production of desired compounds.

The results presented here can be utilized further in two manners: Theoretically, via the incorporation of the relationships and factor values provided in plastic pollution models and practically, by designing and implementing optimized pilot scale plastic degrading systems towards the solution of the plastic pollution problem.

About the author

Aikaterini Karkanorachaki received her environmental engineering diploma from the School of Environmental Engineering (Technical University of Crete, Greece) and a Master's degree in Waste Management from the same school. In 2018 she was awarded a scholarship for her doctorate research from the State Scholarship Foundation (I.K.Y.). She has extensive experience in laboratory and field experimentation, gained by working for FP-7 and H2020 EU-funded (BIOCLEAN, WATER4CROPS, INMARE, MINAGRIS), ERA-MIN2 (nanoBT), as well as nationally funded research programmes. She has authored 4 publications in peer reviewed journals, and co-authored 6, resulting in 478 citations (Scopus). She has presented in numerous international and national conferences and attended international training courses on sample preparation (2017), microbiome sequencing and data analysis (2021) and marine microplastic pollution (2022). She is a member of Cost Action Priority (CA20101). Her research interests include plastic pollution monitoring in marine and soil matrices and plastic biodegradation by microbial communities.

Publications

PhD Journal Publications

Karkanorachaki, K., Syranidou, E., Maravelaki, P.N., Kalogerakis N., 2023. Intertwined synergistic abiotic and biotic degradation of polypropylene pellets in marine mesocosms. *Journal of Hazardous Materials* 457, 131710.

Karkanorachaki, K., Tsiota, P., Dasenakis, G., Syranidou, E., Kalogerakis, N., 2022. Nanoplastic Generation from Secondary PE Microplastics: Microorganism-Induced Fragmentation. *Microplastics* 1, 85–101.

Karkanorachaki, K., Syranidou, E., Kalogerakis, N., 2021. Sinking characteristics of microplastics in the marine environment. *Science of the Total Environment* 793, 148526.

Other Journal Publications

E. Syranidou, K. Karkanorachaki, D. Barouta, E. Papadaki, D. Moschovas, A. Avgeropoulos, N. Kalogerakis, 2023. Relationship between the Carbonyl Index (CI) and fragmentation of polyolefin plastics during aging. Environmental Science and Technology, 57, 21, 8130-8138.

E. Syranidou, **K. Karkanorachaki**, F. Amorotti, A. Avgeropoulos, B. Kolvenbach, N.-Y. Zhou, F. Fava, P. F.-X. Corvini, N. Kalogerakis, 2019. Biodegradation of mixture of plastic films by tailored marine consortia. *Journal of Hazardous Materials* 375, 33-42.

K. Karkanorachaki, S. Kiparissis, G. C. Kalogerakis, E. Yiantzi, E. Psillakis, N. Kalogerakis, 2018.

Plastic pellets, meso-and microplastics on the coastline of Northern Crete: Distribution and organic pollution. *Marine Pollution Bulletin* 133, 578-589.

P. Tsiota, **K. Karkanorachaki**, E.Syranidou, M. Franchini, N. Kalogerakis, 2018. Microbial degradation of HDPE secondary microplastics: preliminary results. *Proceedings of the international conference on microplastic pollution in the Mediterranean Sea*, 181-188.

E. Syranidou, **K. Karkanorachaki**, F. Amorotti, M. Franchini, E. Repouskou, M. Kaliva, M. Vamvakaki, B. Kolvenbach, F. Fava, P. F.-X. Corvini, N. Kalogerakis, 2017. Biodegradation of weathered polystyrene films in seawater microcosms*. Scientific Reports* 7(1), 1-12.

E. Syranidou, **K. Karkanorachaki**, F. Amorotti, E. Repouskou, K. Kroll, B. Kolvenbach, P. F.-X. Corvini, F. Fava, N. Kalogerakis, 2017. Development of tailored indigenous marine consortia for the degradation of naturally weathered polyethylene films*. PLoS One* 12(8), e0183984.

N. Kalogerakis**, K. Karkanorachaki**, G. C. Kalogerakis, E. I. Triantafyllidi, A. D. Gotsis, P. Partsinevelos, F. Fava, 2017. Microplastics generation: onset of fragmentation of polyethylene films in marine environment mesocosms. *Frontiers in Marine Science* 4, 84.

International Conference Presentations

Fate of fossil-based plastics and bioplastics in the marine environment, 3rd International Conference on Microplastic Pollution in the Mediterranean Sea, Napoli, 25-28 September 2022 (oral presentation)

Fungal community succession of the south-eastern Mediterranean plastisphere, European Bioremediation Conference VII, Chania, 12-17 June 2022 (poster presentation)

Tempo-spatial dynamics of micro and mesoplastics and PAHs pollution in coastal environments, European Bioremediation Conference VII & 11th International Society for Environmental Biotechnology conference, Chania, 4-9 July 2018 (oral presentation)

National Conference Presentations

Αλληλεπίδραση και υποβάθμιση του HDPE στο θαλάσσιο περιβάλλον: Μια προσέγγιση κλίμακας, 13th Panhellenic Conference of Chemical Engineering, Patras, 2-4 June 2022 (oral presentation)

Αλληλεπίδραση πλαστικών πολυμερών με το θαλάσσιο και παράκτιο περιβάλλον, 12th Panhellenic Conference of Chemical Engineering, Athens, 29-31 May 2019 (poster presentation)

Biodegradation of weathered polyethylene (PE) films in the marine environment, 7th Conference of the Scientific Society Mikrobiokosmos, Athens, 7-9 April 2017 (poster presentation)

REFERENCES

A., G.K., K., A., M., H., K., S., G., D., 2020. Review on plastic wastes in marine environment – Biodegradation and biotechnological solutions. Mar. Pollut. Bull. 150, 110733. https://doi.org/10.1016/j.marpolbul.2019.110733

Adegoke, A.A., Stenström, T.A., Okoh, A.I., 2017. Stenotrophomonas maltophilia as an emerging ubiquitous pathogen: Looking beyond contemporary antibiotic therapy. Front. Microbiol. 8, 1–18. https://doi.org/10.3389/fmicb.2017.02276

Agostini, L., Cezar, J., Moreira, F., Bendia, A.G., Carolina, M., Kmit, P., Waters, L.G., Ferreira, M., Santana, M., Yukio, P., Sumida, G., Turra, A., Pellizari, V.H., 2021. Science of the Total Environment Deep-sea plastisphere : Long-term colonization by plastic-associated bacterial and archaeal communities in the Southwest Atlantic Ocean. Sci. Total Environ. 793, 148335. https://doi.org/10.1016/j.scitotenv.2021.148335

Ahmed, T., Shahid, M., Azeem, F., Rasul, I., Shah, A.A., Noman, M., Hameed, A., Manzoor, N., Manzoor, I., Muhammad, S., 2018. Biodegradation of plastics: current scenario and future prospects for environmental safety. Environ. Sci. Pollut. Res. 25, 7287–7298. https://doi.org/10.1007/s11356-018-1234-9

Albertsson, A.C., Andersson, S.O., Karlsson, S., 1987. The mechanism of biodegradation of polyethylene. Polym. Degrad. Stab. 18, 73–87. https://doi.org/10.1016/0141-3910(87)90084-X

Ali, I., Cheng, Q., Ding, T., Yiguang, Q., Yuechao, Z., Sun, H., Peng, C., Naz, I., Li, J., Liu, J., 2021. Micro- and nanoplastics in the environment: Occurrence, detection, characterization and toxicity – A critical review. J. Clean. Prod. 313, 127863. https://doi.org/10.1016/j.jclepro.2021.127863

Ali, S.S., Elsamahy, T., Al-Tohamy, R., Zhu, D., Mahmoud, Y.A.G., Koutra, E., Metwally, M.A., Kornaros, M., Sun, J., 2021. Plastic wastes biodegradation: Mechanisms, challenges and future prospects. Sci. Total Environ. 780, 146590. https://doi.org/10.1016/j.scitotenv.2021.146590

Alimi, O.S., Farner Budarz, J., Hernandez, L.M., Tufenkji, N., 2018. Microplastics and Nanoplastics in Aquatic Environments: Aggregation, Deposition, and Enhanced Contaminant Transport. Environ. Sci. Technol. 52, 1704–1724. https://doi.org/10.1021/acs.est.7b05559

Alprol, A.E., Gaballah, M.S., Hassaan, M.A., 2021. Micro and Nanoplastics analysis: Focus on their classification, sources, and impacts in marine environment. Reg. Stud. Mar. Sci. 42, 101625. https://doi.org/10.1016/j.rsma.2021.101625

Amaral-Zettler, L.A., Zettler, E.R., Mincer, T.J., 2020. Ecology of the plastisphere. Nat. Rev. Microbiol. 18, 139–151. https://doi.org/10.1038/s41579-019-0308-0

Amaral-Zettler, L.A., Zettler, E.R., Slikas, B., Boyd, G.D., Melvin, D.W., Morrall, C.E., Proskurowski, G., Mincer, T.J., 2015. The biogeography of the Plastisphere: Implications for policy. Front. Ecol. Environ. 13, 541–546. https://doi.org/10.1890/150017

Amobonye, A., Bhagwat, P., Singh, S., Pillai, S., 2021. Plastic biodegradation: Frontline microbes and their enzymes, Science of the Total Environment. Elsevier B.V. https://doi.org/10.1016/j.scitotenv.2020.143536

Andrady, Anthony L., 2017. The plastic in microplastics: A review. Mar. Pollut. Bull. 119, 12–22. https://doi.org/10.1016/j.marpolbul.2017.01.082

Andrady, Anthony L, 2017. The plastic in microplastics: A review. Mar. Pollut. Bull. 119, 12–22. https://doi.org/10.1016/j.marpolbul.2017.01.082

Andrady, A.L., 2011. Microplastics in the marine environment. Mar. Pollut. Bull. 62, 1596–1605. https://doi.org/10.1016/j.marpolbul.2011.05.030

Antunes, C.S., Visca, P., Towner, K.J., 2014. Acinetobacter baumannii : evolution of a global pathogen 292–301. https://doi.org/10.1111/2049-632X.12125

Ariff, Z.M., Ariffin, A., Rahim, N.A.A., Jikan, S.S., 2012. Rheological Behaviour of Polypropylene Through Extrusion and Capillary Rheometry. InTech 29–48.

Aßhauer, K.P., Wemheuer, B., Daniel, R., Meinicke, P., 2015. Tax4Fun: Predicting functional profiles from metagenomic 16S rRNA data. Bioinformatics 31, 2882–2884. https://doi.org/10.1093/bioinformatics/btv287

Austin, H.P., Allen, M.D., Donohoe, B.S., Rorrer, N.A., Kearns, F.L., Silveira, R.L., Pollard, B.C., Dominick, G., Duman, R., Omari, K. El, Mykhaylyk, V., Wagner, A., Michener, W.E., Amore, A., Skaf, M.S., Crowley, M.F., Thorne, A.W., Johnson, C.W., Lee Woodcock, H., McGeehan, J.E., Beckham, G.T., 2018. Characterization and engineering of a plastic-degrading aromatic polyesterase. Proc. Natl. Acad. Sci. U. S. A. 115, E4350–E4357. https://doi.org/10.1073/pnas.1718804115

Auta, H.S., Emenike, C.U., Fauziah, S.H., 2017. Distribution and importance of microplastics in the marine environment : A review of the sources , fate , effects , and potential solutions. Environ. Int. 102, 165–176. https://doi.org/10.1016/j.envint.2017.02.013

Auta, H.S., Emenike, C.U., Jayanthi, B., Fauziah, S.H., 2018. Growth kinetics and biodeterioration of polypropylene microplastics by Bacillus sp. and Rhodococcus sp. isolated from mangrove sediment. Mar. Pollut. Bull. 127, 15–21. https://doi.org/10.1016/j.marpolbul.2017.11.036

Bacha, A.U.R., Nabi, I., Zaheer, M., Jin, W., Yang, L., 2023. Biodegradation of macro- and micro-plastics in environment: A review on mechanism, toxicity, and future perspectives. Sci. Total

Environ. 858, 160108. https://doi.org/10.1016/j.scitotenv.2022.160108

Bagaev, A., Mizyuk, A., Khatmullina, L., Isachenko, I., Chubarenko, I., 2017. Anthropogenic fibres in the Baltic Sea water column: Field data, laboratory and numerical testing of their motion. Sci. Total Environ. 599–600, 560–571. https://doi.org/10.1016/j.scitotenv.2017.04.185

Balasubramanian, V., Natarajan, K., Hemambika, B., Ramesh, N., Sumathi, C.S., Kottaimuthu, R., Rajesh Kannan, V., 2010. High-density polyethylene (HDPE)-degrading potential bacteria from marine ecosystem of Gulf of Mannar, India. Lett. Appl. Microbiol. 51, 205–211. https://doi.org/10.1111/j.1472-765X.2010.02883.x

Ballent, A., Pando, S., Purser, A., Juliano, M.F., Thomsen, L., 2013. Modelled transport of benthic marine microplastic pollution in the Nazaré Canyon. Biogeosciences 10, 7957–7970. https://doi.org/10.5194/bg-10-7957-2013

Ballent, A., Purser, A., de Jesus Mendes, P., Pando, S., Thomsen, L., 2012. Physical transport properties of marine microplastic pollution. Biogeosciences Discuss. 9, 18755–18798. https://doi.org/10.5194/bgd-9-18755-2012

Bardají, D.K.R., Moretto, J.A.S., Furlan, J.P.R., Stehling, E.G., 2020. A mini-review: current advances in polyethylene biodegradation. World J. Microbiol. Biotechnol. 36, 1–10. https://doi.org/10.1007/s11274-020-2808-5

Barnes, P.D., Marr, K.A., 2006. Aspergillosis: Spectrum of Disease, Diagnosis, and Treatment. Infect. Dis. Clin. North Am. 20, 545–561. https://doi.org/10.1016/j.idc.2006.06.001

Basili, M., Quero, G.M., Giovannelli, D., Manini, E., Vignaroli, C., Avio, C.G., Marco, R. De, Luna, G.M., Luna, G.M., 2020. Major Role of Surrounding Environment in Shaping Biofilm Community Composition on Marine Plastic Debris 7, 1–12. https://doi.org/10.3389/fmars.2020.00262

Bellemain, E., Carlsen, T., Brochmann, C., Coissac, E., Taberlet, P., Kauserud, H., 2010. ITS as an environmental DNA barcode for fungi : an in silico approach reveals potential PCR biases 1–9.

Beloe, C.J., Browne, M.A., Johnston, E.L., 2022. Plastic Debris As a Vector for Bacterial Disease: An Interdisciplinary Systematic Review. Environ. Sci. Technol. 56, 2950–2958. https://doi.org/10.1021/acs.est.1c05405

Bentzmann, S. De, Plésiat, P., 2011. Meeting report The Pseudomonas aeruginosa opportunistic pathogen and human infections 13, 1655–1665. https://doi.org/10.1111/j.1462-2920.2011.02469.x

Benyathiar, P., Kumar, P., Carpenter, G., Brace, J., Mishra, D., 2022. Reciclaje de botella a botella de tereftalato de polietileno (PET) para la industria de bebidas: una revisión. Polymers (Basel). 14.

Bergmann, M., Gutow, L., Klages, M., 2015. Marine anthropogenic litter. Mar. Anthropog. Litter 1–447. https://doi.org/10.1007/978-3-319-16510-3

Biber, N.F.A., Foggo, A., Thompson, R.C., 2019. Characterising the deterioration of different plastics in air and seawater. Mar. Pollut. Bull. 141, 595–602. https://doi.org/10.1016/j.marpolbul.2019.02.068

Bowley, J., Baker-Austin, C., Porter, A., Hartnell, R., Lewis, C., 2021. Oceanic Hitchhikers – Assessing Pathogen Risks from Marine Microplastic. Trends Microbiol. 29, 107–116. https://doi.org/10.1016/j.tim.2020.06.011

Brandon, J., Goldstein, M., Ohman, M.D., 2016. Long-term aging and degradation of microplastic particles: Comparing in situ oceanic and experimental weathering patterns. Mar. Pollut. Bull. 110, 299–308. https://doi.org/10.1016/j.marpolbul.2016.06.048

Bravo, M., Astudillo, J.C., Lancellotti, D., Luna-Jorquera, G., Valdivia, N., Thiel, M., 2011. Rafting on abiotic substrata: Properties of floating items and their influence on community succession. Mar. Ecol. Prog. Ser. 439, 1–17. https://doi.org/10.3354/meps09344

Browne, M.A., Crump, P., Niven, S.J., Teuten, E., Tonkin, A., Galloway, T., Thompson, R., 2011. Accumulation of microplastic on shorelines woldwide: Sources and sinks. Environ. Sci. Technol. 45, 9175–9179. https://doi.org/10.1021/es201811s

Bryant, J.A., Clemente, T.M., Viviani, D.A., Fong, A.A., Thomas, K.A., Kemp, P., Karl, D.M., White, A.E., DeLong, E.F., 2016. Diversity and Activity of Communities Inhabiting Plastic Debris in the North Pacific Gyre. mSystems 1, 1–19. https://doi.org/10.1128/msystems.00024-16

Cai, L., Wang, J., Peng, J., Wu, Z., Tan, X., 2018. Observation of the degradation of three types of plastic pellets exposed to UV irradiation in three different environments. Sci. Total Environ. 628–629, 740–747. https://doi.org/10.1016/j.scitotenv.2018.02.079

Cai, L., Wu, D., Xia, J., Shi, H., Kim, H., 2019. Influence of physicochemical surface properties on the adhesion of bacteria onto four types of plastics. Sci. Total Environ. 671, 1101–1107. https://doi.org/10.1016/j.scitotenv.2019.03.434

Calder, D.R., Choong, H.H.C., Carlton, J.T., Chapman, J.W., Miller, J.A., Geller, J., 2014. Hydroids (Cnidaria: Hydrozoa) from Japanese tsunami marine debris washing ashore in the northwestern United States. Aquat. Invasions 9, 425–440. https://doi.org/10.3391/ai.2014.9.4.02

Callahan, B.J., McMurdie, P.J., Rosen, M.J., Han, A.W., Johnson, A.J.A., Holmes, S.P., 2016. DADA2: High-resolution sample inference from Illumina amplicon data. Nat. Methods 13, 581–583. https://doi.org/10.1038/nmeth.3869

Carson, H.S., Colbert, S.L., Kaylor, M.J., McDermid, K.J., 2011. Small plastic debris changes water movement and heat transfer through beach sediments. Mar. Pollut. Bull. 62, 1708–1713. https://doi.org/10.1016/j.marpolbul.2011.05.032

Carson, H.S., Nerheim, M.S., Carroll, K.A., Eriksen, M., 2013. The plastic-associated microorganisms of the North Pacific Gyre. Mar. Pollut. Bull. 75, 126–132. https://doi.org/10.1016/j.marpolbul.2013.07.054

Caruso, G., Bergami, E., Singh, N., Corsi, I., 2022. Plastic occurrence, sources, and impacts in Antarctic environment and biota. Water Biol. Secur. 1, 100034. https://doi.org/10.1016/j.watbs.2022.100034

Catão, E., Pollet, C.P.T., Barry-, C.G.R., Rehel, K., Linossier, I., Turquet, L.J., 2021. Temperate and tropical coastal waters share relatively similar microbial biofilm communities while free- - living or particle- - attached communities are distinct 2891–2904. https://doi.org/10.1111/mec.15929

Chae, Y., An, Y.J., 2016. Effects of micro- and nanoplastics on aquatic ecosystems: Current research trends and perspectives. Mar. Pollut. Bull. 1–9. https://doi.org/10.1016/j.marpolbul.2017.01.070

Chamas, A., Moon, H., Zheng, J., Qiu, Y., Tabassum, T., Jang, J.H., Abu-Omar, M.M., Scott, S.L., Suh, S., 2020. Degradation Rates of Plastics in the Environment. ACS Sustain. Chem. Eng. https://doi.org/10.1021/acssuschemeng.9b06635

Chandra, P., Enespa, Singh, D.P., 2020. Microplastic degradation by bacteria in aquatic ecosystem, Microorganisms for Sustainable Environment and Health. INC. https://doi.org/10.1016/b978-0-12-819001-2.00022-x

Chhabra, R.P., 1996. Wall effects on terminal velocity of non-spherical particles in non-Newtonian polymer solutions. Powder Technol. 88, 39–44. https://doi.org/10.1016/0032-5910(96)03100-2

Chhabra, R.P., Agarwal, S., Chaudhary, K., 2003. A note on wall effect on the terminal falling velocity of a sphere in quiescent Newtonian media in cylindrical tubes. Powder Technol. 129, 53–58. https://doi.org/10.1016/S0032-5910(02)00164-X

Chiellini, E., Corti, Æ.A., Antone, Æ.S.D., Billingham, N.C., 2007. Microbial biomass yield and turnover in soil biodegradation tests : carbon substrate effects 169–178. https://doi.org/10.1007/s10924-007-0057-4

Choe, S., Kim, Y., Won, Y., Myung, J., 2021. Bridging Three Gaps in Biodegradable Plastics: Misconceptions and Truths About Biodegradation. Front. Chem. 9.

https://doi.org/10.3389/fchem.2021.671750

Choi, D., Bang, J., Kim, T., Oh, Y., Hwang, Y., Hong, J., 2020. In vitro chemical and physical toxicities of polystyrene microfragments in human-derived cells. J. Hazard. Mater. 400, 123308. https://doi.org/10.1016/j.jhazmat.2020.123308

Chubarenko, I., Bagaev, A., Zobkov, M., Esiukova, E., 2016. On some physical and dynamical properties of microplastic particles in marine environment. Mar. Pollut. Bull. 108, 105–112. https://doi.org/10.1016/j.marpolbul.2016.04.048

Claessens, M., Meester, S. De, Landuyt, L. Van, Clerck, K. De, Janssen, C.R., 2011. Occurrence and distribution of microplastics in marine sediments along the Belgian coast. Mar. Pollut. Bull. 62, 2199–2204. https://doi.org/10.1016/j.marpolbul.2011.06.030

Claudia, C., La Spina, R., Mehn, D., Fumagalli, F., Ceccone, G., Valsesia, A., Gilliland, D., 2022. Detecting Micro-and Nanoplastics Released from Food Packaging: Challenges and Analytical Strategies. Polymers (Basel). 14. https://doi.org/10.3390/polym14061238

Cole, M., Galloway, T.S., 2015. Ingestion of Nanoplastics and Microplastics by Pacific Oyster Larvae. Environ. Sci. Technol. 49, 14625–14632. https://doi.org/10.1021/acs.est.5b04099

Cole, M., Lindeque, P.K., Fileman, E., Clark, J., Lewis, C., Halsband, C., Galloway, T.S., 2016. Microplastics Alter the Properties and Sinking Rates of Zooplankton Faecal Pellets. Environ. Sci. Technol. 50, 3239–3246. https://doi.org/10.1021/acs.est.5b05905

Coleman, E.A., 2017. 21 Plastics Additives, Second Edi. ed, Applied Plastics Engineering Handbook. Elsevier Inc. https://doi.org/10.1016/B978-0-323-39040-8/00021-3

Cox, R., Lopes, W.A., Jahn, K.L., 2018. Quantitative roundness analysis of coastal boulder deposits. Mar. Geol. 396, 114–141. https://doi.org/10.1016/j.margeo.2017.03.003

Cózar, A., Echevarría, F., González-gordillo, J.I., Irigoien, X., Úbeda, B., 2014. Plastic debris in the open ocean 17–19. https://doi.org/10.1073/pnas.1314705111

Cózar, A., Martí, E., Duarte, C.M., García-de-Lomas, J., Van Sebille, E., Ballatore, T.J., Eguíluz, V.M., Ignacio González-Gordillo, J., Pedrotti, M.L., Echevarría, F., Troublè, R., Irigoien, X., 2017. The Arctic Ocean as a dead end for floating plastics in the North Atlantic branch of the Thermohaline Circulation. Sci. Adv. 3, 1–9. https://doi.org/10.1126/sciadv.1600582

Cózar, A., Sanz-Martín, M., Martí, E., González-Gordillo, J.I., Ubeda, B., Á.gálvez, J., Irigoien, X., Duarte, C.M., 2015. Plastic accumulation in the mediterranean sea. PLoS One 10, 1–12. https://doi.org/10.1371/journal.pone.0121762

D'Angelo, S., Meccariello, R., 2021. Microplastics: A threat for male fertility. Int. J. Environ. Res. Public Health 18, 1–11. https://doi.org/10.3390/ijerph18052392

da Costa, J.P., Santos, P.S.M., Duarte, A.C., Rocha-Santos, T., 2016. (Nano)plastics in the environment - Sources, fates and effects. Sci. Total Environ. 566–567, 15–26. https://doi.org/10.1016/j.scitotenv.2016.05.041

Dabrowska, A., Łopata, I., Osial, M., 2021. The ghost nets phenomena from the chemical perspective. Pure Appl. Chem. 93, 479–496. https://doi.org/10.1515/pac-2020-1102

Danopoulos, E., Twiddy, M., Rotchell, J.M., 2020. Microplastic contamination of drinking water: A systematic review. PLoS One 15, 1–23. https://doi.org/10.1371/journal.pone.0236838

Danso, D., Chow, J., Zimmermann, W., Wei, R., 2018. crossm New Insights into the Function and Global Distribution of 84, 1–13.

de Vogel, F.A., Schlundt, C., Stote, R.E., Ratto, J.A., Amaral-Zettler, L.A., 2021. Correction: Comparative genomics of marine bacteria from a historically defined plastic biodegradation consortium with the capacity to biodegrade polyhydroxyalkanoates (Microorganisms, (2021) 9, 186, 10.3390/microorganisms9010186). Microorganisms 9. https://doi.org/10.3390/microorganisms9040744

Delacuvellerie, A., Cyriaque, V., Gobert, S., Benali, S., Wattiez, R., 2019. The plastisphere in marine ecosystem hosts potential specific microbial degraders including Alcanivorax borkumensis as a key player for the low-density polyethylene degradation. J. Hazard. Mater. 380, 120899. https://doi.org/10.1016/j.jhazmat.2019.120899

Desforges, J.P.W., Galbraith, M., Dangerfield, N., Ross, P.S., 2014. Widespread distribution of microplastics in subsurface seawater in the NE Pacific Ocean. Mar. Pollut. Bull. 79, 94–99. https://doi.org/10.1016/j.marpolbul.2013.12.035

Diaz-Basantes, M.F., Conesa, J.A., Fullana, A., 2020. Microplastics in honey, beer, milk and refreshments in Ecuador as emerging contaminants. Sustain. 12. https://doi.org/10.3390/SU12145514

Dietrich, W.E., 1982a. Settling velocity of natural particles. Water Resour. Res. 18, 1615–1626. https://doi.org/10.1029/WR018i006p01615

Dietrich, W.E., 1982b. Settling velocity of natural particles. Water Resour. Res. 18, 1615–1626. https://doi.org/10.1029/WR018i006p01615

Diversity, C. on B., 2016. Marine Debris: Understanding, Preventing and Mitigating the Significant Adverse Impacts on Marine and Coastal Biodiversity. Technical Series No.83. Secretariat of the Convention on Biological Diversity, CBD Technical Series.

Dudek, K.L., Cruz, B.N., Polidoro, B., Neuer, S., 2020. Microbial colonization of microplastics in the Caribbean Sea. Limnol. Oceanogr. Lett. 5, 5–17. https://doi.org/10.1002/lol2.10141

Dussud, C., Meistertzheim, A.L., Conan, P., Pujo-Pay, M., George, M., Fabre, P., Coudane, J., Higgs, P., Elineau, A., Pedrotti, M.L., Gorsky, G., Ghiglione, J.F., 2018. Evidence of niche partitioning among bacteria living on plastics, organic particles and surrounding seawaters. Environ. Pollut. 236, 807–816. https://doi.org/10.1016/j.envpol.2017.12.027

Edmondson, S., Gilbert, M., 2017. The Chemical Nature of Plastics Polymerization 19–37. https://doi.org/10.1016/B978-0-323-35824-8.00002-5

Eich, A., Mildenberger, T., Laforsch, C., Weber, M., 2015. Biofilm and diatom succession on polyethylene (PE) and biodegradable plastic bags in two marine habitats: Early signs of degradation in the pelagic and benthic zone? PLoS One 10, 1–16. https://doi.org/10.1371/journal.pone.0137201

Ekanayaka, A.H., Tibpromma, S., Dai, D., Xu, R., Suwannarach, N., Stephenson, S.L., Dao, C., Karunarathna, S.C., 2022. A Review of the Fungi That Degrade Plastic. J. Fungi 8, 1–27. https://doi.org/10.3390/jof8080772

Ekvall, M.T., Lundqvist, M., Kelpsiene, E., Šileikis, E., Gunnarsson, S.B., Cedervall, T., 2019. Nanoplastics formed during the mechanical breakdown of daily-use polystyrene products. Nanoscale Adv. 1, 1055–1061. https://doi.org/10.1039/c8na00210j

Ellen MacArthur Foundation, 2017. The New Plastics Economy: Rethinking the Future of Plastics & Catalysing Action. Ellen MacArthur Found. 68. https://doi.org/10.1103/Physrevb.74.035409

Elmer-Dixon, M.M., Fawcett, L.P., Hinderliter, B.R., Maurer-Jones, M.A., 2022. Could Superficial Chiral Nanostructures Be the Reason Polyethylene Yellows as It Ages? ACS Appl. Polym. Mater. 4, 6458–6465. https://doi.org/10.1021/acsapm.2c00877

Enfrin, M., Lee, J., Gibert, Y., Basheer, F., Kong, L., Dumée, L.F., 2020. Release of hazardous nanoplastic contaminants due to microplastics fragmentation under shear stress forces. J. Hazard. Mater. 384, 121393. https://doi.org/10.1016/j.jhazmat.2019.121393

Eriksen, M., Lebreton, L.C.M., Carson, H.S., Thiel, M., Moore, C.J., Borerro, J.C., Galgani, F., Ryan, P.G., Reisser, J., 2014. Plastic Pollution in the World's Oceans: More than 5 Trillion Plastic Pieces Weighing over 250,000 Tons Afloat at Sea. PLoS One 9, 1–15. https://doi.org/10.1371/journal.pone.0111913

Erni-Cassola, G., Wright, R.J., Gibson, M.I., Christie-Oleza, J.A., 2020. Early Colonization of Weathered Polyethylene by Distinct Bacteria in Marine Coastal Seawater. Microb. Ecol. 79, 517–526. https://doi.org/10.1007/s00248-019-01424-5

Esmaeili, A., Pourbabaee, A.A., Alikhani, H.A., Shabani, F., Esmaeili, E., 2013. Biodegradation of Low-Density Polyethylene (LDPE) by Mixed Culture of Lysinibacillus xylanilyticus and Aspergillus

niger in Soil. PLoS One 8. https://doi.org/10.1371/journal.pone.0071720

Eyheraguibel, B., Traikia, M., Fontanella, S., Sancelme, M., Bonhomme, S., Fromageot, D., Lemaire, J., Lauranson, G., Lacoste, J., Delort, A.M., 2017. Characterization of oxidized oligomers from polyethylene films by mass spectrometry and NMR spectroscopy before and after biodegradation by a Rhodococcus rhodochrous strain. Chemosphere 184, 366–374. https://doi.org/10.1016/j.chemosphere.2017.05.137

Fazey, F.M.C., Ryan, P.G., 2016. Biofouling on buoyant marine plastics: An experimental study into the effect of size on surface longevity. Environ. Pollut. 210, 354–360. https://doi.org/10.1016/j.envpol.2016.01.026

Fouad, A.D., Teng, S., Mark, J.R., Liu, A., Alvarez-Illera, P., Ji, H., Du, A., Bhirgoo, P.D., Cornblath, E., Guan, S.A., Fang-Yen, C., 2018. Distributed rhythm generators underlie Caenorhabditis elegans forward locomotion. Elife 7, 1–34. https://doi.org/10.7554/eLife.29913

Francalanci, S., Paris, E., Solari, L., 2021. On the prediction of settling velocity for plastic particles of different shapes. Environ. Pollut. 290, 118068. https://doi.org/10.1016/j.envpol.2021.118068

Frère, L., Maignien, L., Chalopin, M., Huvet, A., Rinnert, E., Morrison, H., Kerninon, S., Cassone, A.L., Lambert, C., Reveillaud, J., Paul-Pont, I., 2018. Microplastic bacterial communities in the Bay of Brest: Influence of polymer type and size. Environ. Pollut. 242, 614–625. https://doi.org/10.1016/j.envpol.2018.07.023

Frias, J.P.G.L., Nash, R., 2019. Microplastics: Finding a consensus on the definition. Mar. Pollut. Bull. 138, 145–147. https://doi.org/10.1016/j.marpolbul.2018.11.022

Friot, D., Boucher, J., 2017. Primary microplastics in the oceans | IUCN Library System.

Gahleitner, M., Paulik, C., 2017. Polypropylene and Other Polyolefins, Brydson's Plastics Materials: Eighth Edition. Elsevier Ltd. https://doi.org/10.1016/B978-0-323-35824-8.00011-6

Gambarini, V., Pantos, O., Kingsbury, J.M., Weaver, L., Handley, K.M., Lear, G., 2022. PlasticDB: A database of microorganisms and proteins linked to plastic biodegradation. Database 2022, 1–12. https://doi.org/10.1093/database/baac008

García-Depraect, O., Bordel, S., Lebrero, R., Santos-Beneit, F., Börner, R.A., Börner, T., Muñoz, R., 2021a. Inspired by nature: Microbial production, degradation and valorization of biodegradable bioplastics for life-cycle-engineered products. Biotechnol. Adv. 53. https://doi.org/10.1016/j.biotechadv.2021.107772

García-Depraect, O., Lebrero, R., Rodriguez-Vega, S., Bordel, S., Santos-Beneit, F., Martínez-Mendoza, L.J., Aragão Börner, R., Börner, T., Muñoz, R., 2021b. Biodegradation of bioplastics under aerobic and anaerobic aqueous conditions: Kinetics, carbon fate and particle size effect.

Bioresour. Technol. 344, 126265. https://doi.org/10.1016/j.biortech.2021.126265

Gaylarde, C., Baptista-Neto, J.A., da Fonseca, E.M., 2021. Plastic microfibre pollution: how important is clothes' laundering? Heliyon 7, e07105. https://doi.org/10.1016/j.heliyon.2021.e07105

Gerritse, J., Leslie, H.A., de Tender, C.A., Devriese, L.I., Vethaak, A.D., 2020. Fragmentation of plastic objects in a laboratory seawater microcosm. Sci. Rep. 10, 1–16. https://doi.org/10.1038/s41598-020-67927-1

GESAMP, 2019. Guidelines for the monitoring and assessment of plastic litter in the ocean (Kershaw P.J., Turra A. and Galgani F. editors), (IMO/FAO/UNESCO-IOC/UNIDO/WMO/IAEA/UN/UNEP/UNDP/ISA Joint Group of Experts on the Scientific Aspects of Marine Environmental Prote. Rep. Stud. GESAMP no 99, 130p.

Gewert, B., Plassmann, M., Sandblom, O., Macleod, M., 2018. Identification of Chain Scission Products Released to Water by Plastic Exposed to Ultraviolet Light. Environ. Sci. Technol. Lett. 5, 272–276. https://doi.org/10.1021/acs.estlett.8b00119

Gewert, B., Plassmann, M.M., Macleod, M., 2015a. Pathways for degradation of plastic polymers floating in the marine environment. Environ. Sci. Process. Impacts 17, 1513–1521. https://doi.org/10.1039/c5em00207a

Gewert, B., Plassmann, M.M., MacLeod, M., 2015b. Pathways for degradation of plastic polymers floating in the marine environment. Environ. Sci. Process. Impacts 17, 1513–1521. https://doi.org/10.1039/C5EM00207A

Geyer, R., Jambeck, J.R., Law, K.L., 2017a. Production, use, and fate of all plastics ever made. Sci. Adv. 3, 25–29. https://doi.org/10.1126/sciadv.1700782

Geyer, R., Jambeck, J.R., Law, K.L., 2017b. Production , use , and fate of all plastics ever made 25–29.

Gigault, J., Halle, A. ter, Baudrimont, M., Pascal, P.Y., Gauffre, F., Phi, T.L., El Hadri, H., Grassl, B., Reynaud, S., 2018. Current opinion: What is a nanoplastic? Environ. Pollut. 235, 1030–1034. https://doi.org/10.1016/j.envpol.2018.01.024

Gigault, J., Pedrono, B., Maxit, B., Ter Halle, A., 2016. Marine plastic litter: The unanalyzed nano-fraction. Environ. Sci. Nano 3, 346–350. https://doi.org/10.1039/c6en00008h

Gilan, I. (Orr), Hadar, Y., Sivan, A., 2004. Colonization, biofilm formation and biodegradation of polyethylene by a strain of Rhodococcus ruber. Appl. Microbiol. Biotechnol. 65, 97–104. https://doi.org/10.1007/s00253-004-1584-8

Gilan, I., Sivan, A., 2013. Effect of proteases on biofilm formation of the plastic-degrading actinomycete Rhodococcus ruber C208 342, 18–23. https://doi.org/10.1111/1574-6968.12114

Gilbert, M., Patrick, S., 2017. Poly(Vinyl Chloride), Brydson's Plastics Materials: Eighth Edition. Elsevier Ltd. https://doi.org/10.1016/B978-0-323-35824-8.00013-X

Goldstein, M.C., Carson, H.S., Eriksen, M., 2014. Relationship of diversity and habitat area in North Pacific plastic-associated rafting communities. Mar. Biol. 161, 1441–1453. https://doi.org/10.1007/s00227-014-2432-8

Gong, H., Li, R., Li, F., Guo, X., Xu, L., Gan, L., Yan, M., Wang, J., 2023. Toxicity of nanoplastics to aquatic organisms: Genotoxicity, cytotoxicity, individual level and beyond individual level. J. Hazard. Mater. 443, 130266. https://doi.org/10.1016/j.jhazmat.2022.130266

Gong, J., Xie, P., 2020. Research progress in sources, analytical methods, eco-environmental effects, and control measures of microplastics. Chemosphere 254, 126790. https://doi.org/10.1016/j.chemosphere.2020.126790

Grady, E.N., MacDonald, J., Liu, L., Richman, A., Yuan, Z.C., 2016. Current knowledge and perspectives of Paenibacillus: A review. Microb. Cell Fact. 15, 1–18. https://doi.org/10.1186/s12934-016-0603-7

Gratton, S.E.A., Ropp, P.A., Pohlhaus, P.D., Luft, J.C., Madden, V.J., Napier, M.E., DeSimone, J.M., 2008. The effect of particle design on cellular internalization pathways. Proc. Natl. Acad. Sci. U. S. A. 105, 11613–11618. https://doi.org/10.1073/pnas.0801763105

Hansen, J., Melchiorsen, J., Ciacotich, N., Gram, L., Sonnenschein, E.C., 2021. Effect of polymer type on the colonization of plastic pellets by marine bacteria. FEMS Microbiol. Lett. 368, 1–9. https://doi.org/10.1093/femsle/fnab026

Harshvardhan, K., Jha, B., 2013. Biodegradation of low-density polyethylene by marine bacteria from pelagic waters, Arabian Sea, India. Mar. Pollut. Bull. 77, 100–106. https://doi.org/10.1016/j.marpolbul.2013.10.025

Hartmann, N., Hüffer, T., Thompson, R.C., Hassellöv, M., Verschoor, A., Daugaard, A.E., Rist, S., Karlsson, T.M., Brennholt, N., Cole, M., Herrling, M.P., Heß, M., Ivleva, N.P., Lusher, A.L., Wagner, M., 2019. Are we speaking the same language ? Recommendations for a definition and categorization framework for plastic debris. https://doi.org/10.1021/acs.est.8b05297

Hassan, P.A., Rana, S., Verma, G., 2015. Making sense of Brownian motion: Colloid characterization by dynamic light scattering. Langmuir 31, 3–12. https://doi.org/10.1021/la501789z

Hidalgo-Ruz, V., Gutow, L., Thompson, R.C., Thiel, M., 2012. Microplastics in the marine environment: A review of the methods used for identification and quantification. Environ. Sci. Technol. 46, 3060–3075. https://doi.org/10.1021/es2031505

Ho, B.T., Roberts, T.K., Lucas, S., 2018. An overview on biodegradation of polystyrene and modified

polystyrene: the microbial approach. Crit. Rev. Biotechnol. 38, 308–320. https://doi.org/10.1080/07388551.2017.1355293

Iñiguez, M.E., Conesa, J.A., Fullana, A., 2017. Microplastics in Spanish Table Salt 1–7. https://doi.org/10.1038/s41598-017-09128-x

Int-Veen, I., Nogueira, P., Isigkeit, J., Hanel, R., Kammann, U., 2021. Positively buoyant but sinking: Polymer identification and composition of marine litter at the seafloor of the North Sea and Baltic Sea. Mar. Pollut. Bull. 172, 112876. https://doi.org/10.1016/j.marpolbul.2021.112876

Ioakeimidis, C., Fotopoulou, K.N., Karapanagioti, H.K., Geraga, M., Zeri, C., Papathanassiou, E., Galgani, F., Papatheodorou, G., 2016. The degradation potential of PET bottles in the marine environment: An ATR-FTIR based approach. Sci. Rep. 6, 23501. https://doi.org/10.1038/srep23501

Jacquin, J., Cheng, J., Odobel, C., Pandin, C., Conan, P., Pujo-Pay, M., Barbe, V., Meistertzheim, A.L., Ghiglione, J.F., 2019. Microbial ecotoxicology of marine plastic debris: A review on colonization and biodegradation by the "plastisphere." Front. Microbiol. 10. https://doi.org/10.3389/fmicb.2019.00865

Jahnke, A., Arp, H.P.H., Escher, B.I., Gewert, B., Gorokhova, E., Ku, D., Ogonowski, M., Pottho, A., Rummel, C., Schmitt-jansen, M., Toorman, E., Macleod, M., 2017. Impacts of Weathering Plastic in the Marine Environment. https://doi.org/10.1021/acs.estlett.7b00008

Jambeck, J.R., Geyer, R., Wilcox, C., Siegler, T.R., Perryman, M., Andrady, A., Narayan, R., Law, K.L., 2015. Plastic waste inputs from land into the ocean. Ciencia 347, 768–771.

Jan Kole, P., Löhr, A.J., Van Belleghem, F.G.A.J., Ragas, A.M.J., 2017. Wear and tear of tyres: A stealthy source of microplastics in the environment. Int. J. Environ. Res. Public Health 14. https://doi.org/10.3390/ijerph14101265

Jenkins, S.H., 1982. Standard Methods for the Examination of Water and Wastewater. Water Res. 16, 1495–1496. https://doi.org/10.1016/0043-1354(82)90249-4

Jiang, B., Kauffman, A.E., Li, L., McFee, W., Cai, B., Weinstein, J., Lead, J.R., Chatterjee, S., Scott, G.I., Xiao, S., 2020. Health impacts of environmental contamination of micro- And nanoplastics: A review. Environ. Health Prev. Med. 25, 1–15. https://doi.org/10.1186/s12199-020-00870-9

Jin-Woo Lee, Ji-Hyun Nam, Yang-Hoon Kim, Kyu-Ho Lee, D.-H.L., 2008. Bacterial communities in the initial stage of marine biofilm formation on artificial surfaces. J. Microbiol. 46, 174–182. https://doi.org/10.1007/s12275-008-0032-3

Jinadasa, B.K.K.K., Uddin, S., Fowler, S.W., 2023. Microplastics (MPs) in marine food chains: Is it a food safety issue?, 1st ed, Advances in Food and Nutrition Research. Elsevier Inc.

https://doi.org/10.1016/bs.afnr.2022.07.005
Kaandorp, M.L.A., Dijkstra, H.A., van Sebille, E., 2021. Modelling size distributions of marine plastics under the influence of continuous cascading fragmentation. Environ. Res. Lett. 16. https://doi.org/10.1088/1748-9326/abe9ea
Kaiser, D., Estelmann, A., Kowalski, N., Glockzin, M., Waniek, J.J., 2019. Sinking velocity of sub-millimeter microplastic. Mar. Pollut. Bull. 139, 214–220. https://doi.org/10.1016/j.marpolbul.2018.12.035
Kaiser, D., Kowalski, N., Waniek, J.J., 2017. Effects of biofouling on the sinking behavior of microplastics. Environ. Res. Lett. 12. https://doi.org/10.1088/1748-9326/aa8e8b
Kalogerakis, N., Karkanorachaki, K., Kalogerakis, G.C., Triantafyllidi, E.I., Gotsis, A.D., Partsinevelos, P., Fava, F., 2017. Microplastics generation: Onset of fragmentation of polyethylene films in marine environment mesocosms. Front. Mar. Sci. 4, 3389. https://doi.org/10.3389/fmars.2017.00084
Kankanige, D., Babel, S., 2020. Smaller-sized micro-plastics (MPs) contamination in single-use PET-bottled water in Thailand. Sci. Total Environ. 717, 137232. https://doi.org/10.1016/j.scitotenv.2020.137232
Karami, A., Golieskardi, A., Choo, C.K., Larat, V., Galloway, T.S., 2017. The presence of microplastics in commercial salts from different countries. Nat. Publ. Gr. 1–11. https://doi.org/10.1038/srep46173
Karkanorachaki, K., Syranidou, E., Kalogerakis, N., 2021. Sinking characteristics of microplastics in the marine environment. Sci. Total Environ. 793, 148526. https://doi.org/10.1016/j.scitotenv.2021.148526
Karkanorachaki, K., Syranidou, E., Maravelaki, P., Kalogerakis, N., 2023. Intertwined synergistic abiotic and biotic degradation of polypropylene pellets in marine mesocosms. J. Hazard. Mater. 131710. https://doi.org/10.1016/j.jhazmat.2023.131710
Karlsson, T.M., Hassellöv, M., Jakubowicz, I., 2018. Influence of thermooxidative degradation on the in situ fate of polyethylene in temperate coastal waters. Mar. Pollut. Bull. 135, 187–194. https://doi.org/10.1016/j.marpolbul.2018.07.015
Kaur, K., Reddy, S., Barathe, P., Oak, U., Shriram, V., Kharat, S.S., Govarthanan, M., Kumar, V., 2022. Microplastic-associated pathogens and antimicrobial resistance in environment. Chemosphere 291, 133005. https://doi.org/10.1016/j.chemosphere.2021.133005
Kettner, M.T., Rojas-Jimenez, K., Oberbeckmann, S., Labrenz, M., Grossart, H.P., 2017. Microplastics alter composition of fungal communities in aquatic ecosystems. Environ. Microbiol. 19, 4447–

4459. https://doi.org/10.1111/1462-2920.13891

Khatmullina, L., Chubarenko, I., 2019. Transport of marine microplastic particles: why is it so difficult to predict? Anthr. Coasts 2, 293–305. https://doi.org/10.1139/anc-2018-0024

Khatmullina, L., Isachenko, I., 2017. Settling velocity of microplastic particles of regular shapes. Mar. Pollut. Bull. 114, 871–880. https://doi.org/10.1016/j.marpolbul.2016.11.024

Kibria, G., Imtiaz, N., Rafat, M., Huy, S., Nguyen, Q., Mourshed, M., 2023. Plastic Waste : Challenges and Opportunities to Mitigate Pollution and Effective Management, International Journal of Environmental Research. Springer International Publishing. https://doi.org/10.1007/s41742-023-00507-z

Kim, J.S., Lee, H.J., Kim, S.K., Kim, H.J., 2018. Global Pattern of Microplastics (MPs) in Commercial Food-Grade Salts: Sea Salt as an Indicator of Seawater MP Pollution. Environ. Sci. Technol. 52, 12819–12828. https://doi.org/10.1021/acs.est.8b04180

Kirstein, I.V., Wichels, A., Gullans, E., Krohne, G., Gerdts, G., 2019. The plastisphere – Uncovering tightly attached plastic "specific" microorganisms. PLoS One 14, 1–17. https://doi.org/10.1371/journal.pone.0215859

Kirstein, I. V, Wichels, A., Krohne, G., Gerdts, G., 2018. Mature biofilm communities on synthetic polymers in seawater - Specific or general ? Mar. Environ. Res. 142, 147–154. https://doi.org/10.1016/j.marenvres.2018.09.028

Klaeger, F., Tagg, A.S., Otto, S., Bienmüller, M., Sartorius, I., Labrenz, M., 2019. Residual Monomer Content Affects the Interpretation of Plastic Degradation. Sci. Rep. 9. https://doi.org/10.1038/s41598-019-38685-6

Koelmans, A.A., Gouin, T., Thompson, R., Wallace, N., Arthur, C., 2014. Plastics in the marine environment. Environ. Toxicol. Chem. 33, 5–10. https://doi.org/10.1002/etc.2426

Koelmans, A.A., Kooi, M., Law, K.L., van Sebille, E., 2017. All is not lost: deriving a top-down mass budget of plastic at sea. Environ. Res. Lett. 12, 114028. https://doi.org/10.1088/1748-9326/aa9500

Koh, J., Xiang, Z., Bairoliya, S., Thida, Z., Cao, B., 2023. Plastic-microbe interaction in the marine environment : Research methods and opportunities. Environ. Int. 171, 107716. https://doi.org/10.1016/j.envint.2022.107716

Kolandhasamy, P., Su, L., Li, J., Qu, X., Jabeen, K., Shi, H., 2018. Adherence of microplastics to soft tissue of mussels: A novel way to uptake microplastics beyond ingestion. Sci. Total Environ. 610–611, 635–640. https://doi.org/10.1016/j.scitotenv.2017.08.053

Kooi, M., Nes, E.H.V., Scheffer, M., Koelmans, A.A., 2017a. Ups and Downs in the Ocean: Effects of

Biofouling on Vertical Transport of Microplastics. Environ. Sci. Technol. 51, 7963–7971. https://doi.org/10.1021/acs.est.6b04702

Kooi, M., Van Nes, E.H., Scheffer, M., Koelmans, A.A., 2017b. Ups and Downs in the Ocean: Effects of Biofouling on Vertical Transport of Microplastics. Environ. Sci. Technol. 51, 7963–7971. https://doi.org/10.1021/acs.est.6b04702

Kosuth, M., Mason, S.A., Wattenberg, E. V., 2018. Anthropogenic contamination of tap water, beer, and sea salt. PLoS One 13, 1–18. https://doi.org/10.1371/journal.pone.0194970

Kowalski, N., Reichardt, A.M., Waniek, J.J., 2016a. Sinking rates of microplastics and potential implications of their alteration by physical, biological, and chemical factors. Mar. Pollut. Bull. 109, 310–319. https://doi.org/10.1016/j.marpolbul.2016.05.064

Kowalski, N., Reichardt, A.M., Waniek, J.J., 2016b. Sinking rates of microplastics and potential implications of their alteration by physical, biological, and chemical factors. Mar. Pollut. Bull. 109, 310–319. https://doi.org/10.1016/j.marpolbul.2016.05.064

Krom, M.D., Herut, B., Mantoura, R.F.C., 2004. Nutrient budget for the Eastern Mediterranean: Implications for phosphorus limitation. Limnol. Oceanogr. 49, 1582–1592. https://doi.org/10.4319/lo.2004.49.5.1582

Kukulka, T., Proskurowski, G., Morét-Ferguson, S., Meyer, D.W., Law, K.L., 2012. The effect of wind mixing on the vertical distribution of buoyant plastic debris. Geophys. Res. Lett. 39, 1–6. https://doi.org/10.1029/2012GL051116

Kulkarni, V., Butte, K., Rathod, S., 2012. Natural Polymers – A Comprehensive Review. Int. J. Res. Pharm. Biomed. Sci. 3, 1597–1613.

Kumar, R., Jin, Y., Marre, S., Poncelet, O., Brunet, T., Leng, J., Mondain-Monval, O., 2021. Drying kinetics and acoustic properties of soft porous polymer materials. J. Porous Mater. 28, 249–259. https://doi.org/10.1007/s10934-020-00987-w

Kumar, R., Manna, C., Padha, S., Verma, A., Sharma, P., Dhar, A., Ghosh, A., Bhattacharya, P., 2022. Micro(nano)plastics pollution and human health: How plastics can induce carcinogenesis to humans? Chemosphere 298, 134267. https://doi.org/10.1016/j.chemosphere.2022.134267

Kuroda, M., Uchida, K., Tokai, T., Miyamoto, Y., Mukai, T., Imai, K., Shimizu, K., Yagi, M., Yamanaka, Y., Mituhashi, T., 2020. The current state of marine debris on the seafloor in offshore area around Japan. Mar. Pollut. Bull. 161, 111670. https://doi.org/10.1016/j.marpolbul.2020.111670

Kutralam-Muniasamy, G., Pérez-Guevara, F., Elizalde-Martínez, I., Shruti, V.C., 2020. Branded milks – Are they immune from microplastics contamination? Sci. Total Environ. 714, 136823. https://doi.org/10.1016/j.scitotenv.2020.136823

Kvale, K., Prowe, A.E.F., Chien, C.T., Landolfi, A., Oschlies, A., 2020. The global biological microplastic particle sink. Sci. Rep. 10, 1–13. https://doi.org/10.1038/s41598-020-72898-4

Kvale, K.F., Friederike Prowe, A.E., Oschlies, A., 2020. A Critical Examination of the Role of Marine Snow and Zooplankton Fecal Pellets in Removing Ocean Surface Microplastic. Front. Mar. Sci. 6. https://doi.org/10.3389/fmars.2019.00808

Kwee, B., Lim, H., Thian, E.S., 2022. Science of the Total Environment Biodegradation of polymers in managing plastic waste — A review. Sci. Total Environ. 813, 151880. https://doi.org/10.1016/j.scitotenv.2021.151880

Lacerda, A.L. d. F., Rodrigues, L. dos S., van Sebille, E., Rodrigues, F.L., Ribeiro, L., Secchi, E.R., Kessler, F., Proietti, M.C., 2019. Plastics in sea surface waters around the Antarctic Peninsula. Sci. Rep. 9, 1–12. https://doi.org/10.1038/s41598-019-40311-4

Lacerda, A.L.F., Secchi, E.R., Taylor, J.D., 2020. Diverse groups of fungi are associated with plastics in the surface waters of the Western South Atlantic and the Antarctic Peninsula 1903–1918. https://doi.org/10.1111/mec.15444

Lambert, S., Scherer, C., Wagner, M., 2017. Ecotoxicity testing of microplastics: Considering the heterogeneity of physicochemical properties. Integr. Environ. Assess. Manag. 13, 470–475. https://doi.org/10.1002/ieam.1901

Lambert, S., Wagner, M., 2016. Formation of microscopic particles during the degradation of different polymers. Chemosphere 161, 510–517. https://doi.org/10.1016/j.chemosphere.2016.07.042

Lamichhane, G., Acharya, A., Marahatha, R., Modi, B., Paudel, R., Adhikari, A., Raut, B.K., Aryal, S., Parajuli, N., 2023. Microplastics in environment: global concern, challenges, and controlling measures. Int. J. Environ. Sci. Technol. 20, 4673–4694. https://doi.org/10.1007/s13762-022-04261-1

Latva, M., Dedman, C.J., Wright, R.J., Polin, M., Christie-oleza, J.A., 2022. Microbial pioneers of plastic colonisation in coastal seawaters. Mar. Pollut. Bull. 179, 113701. https://doi.org/10.1016/j.marpolbul.2022.113701

Law, K.L., 2017. Plastics in the marine environment. Ann. Rev. Mar. Sci. 9, 205–229. https://doi.org/doi.org/10.1146/annurev-marine-010816-060409

Lebreton, L., Andrady, A., 2019. Future scenarios of global plastic waste generation and disposal. Palgrave Commun. 5, 1–11. https://doi.org/10.1057/s41599-018-0212-7

Lebreton, L., Slat, B., Ferrari, F., Sainte-Rose, B., Aitken, J., Marthouse, R., Hajbane, S., Cunsolo, S., Schwarz, A., Levivier, A., Noble, K., Debeljak, P., Maral, H., Schoeneich-Argent, R., Brambini, R.,

Reisser, J., 2018. Evidence that the Great Pacific Garbage Patch is rapidly accumulating plastic. Sci. Rep. 8, 4666. https://doi.org/10.1038/s41598-018-22939-w

Li, P., Xu, T., Wu, S., Lei, L., He, D., 2017. Chronic exposure to graphene-based nanomaterials induces behavioral deficits and neural damage in Caenorhabditis elegans. J. Appl. Toxicol. 37, 1140–1150. https://doi.org/10.1002/jat.3468

Liao, Y. liang, Yang, J. yan, 2020. Microplastic serves as a potential vector for Cr in an in-vitro human digestive model. Sci. Total Environ. 703, 134805. https://doi.org/10.1016/j.scitotenv.2019.134805

Lin, Z., Jin, T., Zou, T., Xu, L., Xi, B., Xu, D., He, J., Xiong, L., Tang, C., Peng, J., Zhou, Y., Fei, J., 2022. Current progress on plastic/microplastic degradation: Fact influences and mechanism. Environ. Pollut. 304. https://doi.org/10.1016/j.envpol.2022.119159

Liu, C., Cui, Y., Li, X., Yao, M., 2021. Microeco: An R package for data mining in microbial community ecology. FEMS Microbiol. Ecol. 97, 1–9. https://doi.org/10.1093/femsec/fiaa255

Liu, L., Xu, M., Ye, Y., Zhang, B., 2021. On the degradation of (micro)plastics: Degradation methods, influencing factors, environmental impacts. Sci. Total Environ. 806, 151312. https://doi.org/10.1016/j.scitotenv.2021.151312

Liu, Y., Li, Y., Lin, Q., Zhang, Y., 2017. Assessment of the pathogenicity of marine Cladosporium spp. towards mangroves. For. Pathol. 47, 1–5. https://doi.org/10.1111/efp.12322

Lobelle, D., Cunliffe, M., 2011a. Early microbial biofilm formation on marine plastic debris. Mar. Pollut. Bull. 62, 197–200. https://doi.org/10.1016/j.marpolbul.2010.10.013

Lobelle, D., Cunliffe, M., 2011b. Early microbial biofilm formation on marine plastic debris. Mar. Pollut. Bull. 62, 197–200. https://doi.org/10.1016/j.marpolbul.2010.10.013

Long, M., Moriceau, B., Gallinari, M., Lambert, C., Huvet, A., Raffray, J., Soudant, P., 2015. Interactions between microplastics and phytoplankton aggregates: Impact on their respective fates. Mar. Chem. 175, 39–46. https://doi.org/10.1016/j.marchem.2015.04.003

LOWRY, O.H., ROSEBROUGH, N.J., FARR, A.L., RANDALL, R.J., 1951. Protein measurement with the Folin phenol reagent. J. Biol. Chem. 193, 265–275. https://doi.org/10.1016/s0021-9258(19)52451-6

M. A. Browne, T. Galloway, R.T., 2007. Microplastic—An Emerging Contaminant of Potential Concern? Integr. Environ. Assess. Manag. 3, 559–566. https://doi.org/https://doi.org/10.1002/ieam.5630030412

M. Wagner, C. Scherer, D. Alvarez-Muñoz, N. Brennholt, X. Bourrain, S. Buchinger, et al., 2014. Microplastics in freshwater ecosystems: what we know and what we need to know. Environ.

Sci. Eur. 26.

Mahler, G.J., Esch, M.B., Tako, E., Southard, T.L., Archer, S.D., Glahn, R.P., Shuler, M.L., 2012. Oral exposure to polystyrene nanoparticles affects iron absorption. Nat. Nanotechnol. 7, 264–271. https://doi.org/10.1038/nnano.2012.3

Malankowska, M., Echaide-Gorriz, C., Coronas, J., 2021. Microplastics in marine environment: A review on sources, classification, and potential remediation by membrane technology. Environ. Sci. Water Res. Technol. 7, 243–258. https://doi.org/10.1039/d0ew00802h

Manzur, A., Limón-González, M., Favela-Torres, E., 2004. Biodegradation of Physicochemically Treated LDPE by a Consortium of Filamentous Fungi. J. Appl. Polym. Sci. 92, 265–271. https://doi.org/10.1002/app.13644

Mao, R., Lang, M., Yu, X., Wu, R., Yang, X., Guo, X., 2020. Aging mechanism of microplastics with UV irradiation and its effects on the adsorption of heavy metals. J. Hazard. Mater. 393, 122515. https://doi.org/10.1016/j.jhazmat.2020.122515

Maroof, L., Khan, I., Yoo, H.S., Kim, S., Park, H.T., Ahmad, B., Azam, S., 2021. Identification and characterization of low density polyethylenedegrading bacteria isolated from soils of waste disposal sites. Environ. Eng. Res. 26, 0–2. https://doi.org/10.4491/eer.2020.167

Mart??nez-Romo, A., Gonz??lez-Mota, R., Soto-Bernal, J.J., Rosales-Candelas, I., 2015. Investigating the Degradability of HDPE, LDPE, PE-BIO, and PE-OXO Films under UV-B Radiation. J. Spectrosc. 2015. https://doi.org/10.1155/2015/586514

Martin, M., 2011. Cutadapt removes adapter sequences from high-throughput sequencing reads. EMBnet J. 17.

Matjašič, T., Simčič, T., Medvešček, N., Bajt, O., Dreo, T., Mori, N., 2021. Critical evaluation of biodegradation studies on synthetic plastics through a systematic literature review. Sci. Total Environ. 752. https://doi.org/10.1016/j.scitotenv.2020.141959

Mato, Y., Isobe, T., Takada, H., Kanehiro, H., Ohtake, C., Kaminuma, T., 2001. Plastic resin pellets as a transport medium for toxic chemicals in the marine environment. Environ. Sci. Technol. 35, 318–324. https://doi.org/10.1021/es0010498

Mattsson, K., Hansson, L.A., Cedervall, T., 2015. Nano-plastics in the aquatic environment. Environ. Sci. Process. Impacts 17, 1712–1721. https://doi.org/10.1039/c5em00227c

Mattsson, K., Jocic, S., Doverbratt, I., Hansson, L.A., 2018. Nanoplastics in the aquatic environment, Microplastic Contamination in Aquatic Environments: An Emerging Matter of Environmental Urgency. Elsevier Inc. https://doi.org/10.1016/B978-0-12-813747-5.00013-8

McGivney, E., Cederholm, L., Barth, A., Hakkarainen, M., Hamacher-Barth, E., Ogonowski, M.,

Gorokhova, E., 2020. Rapid Physicochemical Changes in Microplastic Induced by Biofilm Formation. Front. Bioeng. Biotechnol. 8, 1–14. https://doi.org/10.3389/fbioe.2020.00205

Meides, N., Mauel, A., Menzel, T., Altstädt, V., Ruckdäschel, H., Senker, J., Strohriegl, P., 2022. Quantifying the fragmentation of polypropylene upon exposure to accelerated weathering. Microplastics and Nanoplastics 2. https://doi.org/10.1186/s43591-022-00042-2

Mendrik, F., Fernández, R., Hackney, C.R., Waller, C., Parsons, D.R., 2023. Non-buoyant microplastic settling velocity varies with biofilm growth and ambient water salinity. Commun. Earth Environ. 4, 1–9. https://doi.org/10.1038/s43247-023-00690-z

Meng, J., Xu, B., Liu, F., Li, W., Sy, N., Zhou, X., Yan, B., 2021. Effects of chemical and natural ageing on the release of potentially toxic metal additives in commercial PVC microplastics. Chemosphere 283, 131274. https://doi.org/10.1016/j.chemosphere.2021.131274

Menges, F., 2022. F. Menges "Spectragryph - optical spectroscopy software", Version 1.2.16, 2022, http://www.effemm2.de/spectragryph/ 2022.

Michels, J., Stippkugel, A., Lenz, M., Wirtz, K., Engel, A., Michels, J., 2018. Rapid aggregation of biofilm-covered microplastics with marine biogenic particles.

Miller, M.E., Hamann, M., Kroon, F.J., 2020. Bioaccumulation and biomagnification of microplastics in marine organisms: A review and meta-analysis of current data. PLoS One 15, 1–25. https://doi.org/10.1371/journal.pone.0240792

Mincer, T.J., Zettler, E.R., 2016. Biofilms on Plastic Debris and Their Influence on Marine Nutrient Cycling , Productivity , and Hazardous Chemical Mobility Metadata of the chapter that will be visualized online. https://doi.org/10.1007/698

MohanKumar, S.M.J., Campbell, A., Block, M., Veronesi, B., 2008. Particulate matter, oxidative stress and neurotoxicity. Neurotoxicology 29, 479–488. https://doi.org/10.1016/j.neuro.2007.12.004

Montazer, Z., Habibi-Najafi, M.B., Mohebbi, M., Oromiehei, A., 2018. Microbial Degradation of UV-Pretreated Low-Density Polyethylene Films by Novel Polyethylene-Degrading Bacteria Isolated from Plastic-Dump Soil. J. Polym. Environ. 26, 3613–3625. https://doi.org/10.1007/s10924-018-1245-0

Moore, C.J., 2008. Synthetic polymers in the marine environment: A rapidly increasing, long-term threat. Environ. Res. 108, 131–139. https://doi.org/10.1016/j.envres.2008.07.025

Morét-Ferguson, S., Law, K.L., Proskurowski, G., Murphy, E.K., Peacock, E.E., Reddy, C.M., 2010. The size, mass, and composition of plastic debris in the western North Atlantic Ocean. Mar. Pollut. Bull. 60, 1873–1878. https://doi.org/10.1016/j.marpolbul.2010.07.020

Mothes, S., Hintzki, L., Moldaenke, L., Ruwe, M., Kalinowski, J., Kreikemeyer, B., 2021. Cross-Hemisphere Study Reveals Geographically Ubiquitous , Unexplored Biosphere.

Muhonja, C.N., Makonde, H., Magoma, G., Imbuga, M., 2018. Biodegradability of polyethylene by bacteria and fungi from Dandora dumpsite Nairobi-Kenya. PLoS One 13, 1–17. https://doi.org/10.1371/journal.pone.0198446

Myer Kutz, 2015. Mechanical Engineers' Handbook Fourth Edition Materials and Engineering Mechanics, John Wiley & Sons, Inc., Hoboken, New Jersey.

Näkki, P., Setälä, O., Lehtiniemi, M., 2017. Bioturbation transports secondary microplastics to deeper layers in soft marine sediments of the northern Baltic Sea. Mar. Pollut. Bull. 119, 255–261. https://doi.org/10.1016/j.marpolbul.2017.03.065

Napper, I.E., Davies, B.F.R., Clifford, H., Elvin, S., Koldewey, H.J., Mayewski, P.A., Miner, K.R., Potocki, M., Elmore, A.C., Gajurel, A.P., Thompson, R.C., 2020. Reaching New Heights in Plastic Pollution—Preliminary Findings of Microplastics on Mount Everest. One Earth 3, 621–630. https://doi.org/10.1016/j.oneear.2020.10.020

Nguyen, T.H., 2021. Settling behaviour of irregular-shaped polystyrene microplastics. Sci. Technol. Dev. Journal-Engineering Technol. 4, 1219–1228.

Nguyen, T.H., Tang, F.H.M., Maggi, F., 2020. Sinking of microbial-associated microplastics in natural waters. PLoS One 15, 1–20. https://doi.org/10.1371/journal.pone.0228209

Nilsson, R.H., Larsson, K.H., Taylor, A.F.S., Bengtsson-Palme, J., Jeppesen, T.S., Schigel, D., Kennedy, P., Picard, K., Glöckner, F.O., Tedersoo, L., Saar, I., Kõljalg, U., Abarenkov, K., 2019. The UNITE database for molecular identification of fungi: Handling dark taxa and parallel taxonomic classifications. Nucleic Acids Res. 47, D259–D264. https://doi.org/10.1093/nar/gky1022

Nisticò, R., 2020. Polyethylene terephthalate (PET) in the packaging industry. Polym. Test. 90. https://doi.org/10.1016/j.polymertesting.2020.106707

Nowak, J., Coenye, T., 2008. Diversity and occurrence of Burkholderia spp . in the natural environment. https://doi.org/10.1111/j.1574-6976.2008.00113.x

Oberbeckmann, S., Bartosik, D., Huang, S., Werner, J., Hirschfeld, C., Wibberg, D., Heiden, S.E., Bunk, B., Overmann, J., Becher, D., Kalinowski, J., Schweder, T., Labrenz, M., Markert, S., 2021. Genomic and proteomic pro fi les of biofilms on microplastics are decoupled from artificial surface properties 23, 3099–3115. https://doi.org/10.1111/1462-2920.15531

Oberbeckmann, S., Kreikemeyer, B., Labrenz, M., 2017. Environmental factors support the formation of specific bacterial assemblages on microplastics. Front. Microbiol. 8, 2709. https://doi.org/10.3389/FMICB.2017.02709

Oberbeckmann, S., Labrenz, M., 2020. Marine Microbial Assemblages on Microplastics: Diversity, Adaptation, and Role in Degradation. Ann. Rev. Mar. Sci. 12, 209–232. https://doi.org/10.1146/annurev-marine-010419-010633

Oberbeckmann, S., Loeder, M.G.J., Gerdts, G., Osborn, M.A., 2014. Spatial and seasonal variation in diversity and structure of microbial biofilms on marine plastics in Northern European waters. FEMS Microbiol. Ecol. 90, 478–492. https://doi.org/10.1111/1574-6941.12409

Oberbeckmann, S., Osborn, A.M., Duhaime, M.B., 2016. Microbes on a bottle: Substrate, season and geography influence community composition of microbes colonizing marine plastic debris. PLoS One 11, 1–24. https://doi.org/10.1371/journal.pone.0159289

OECD, 2022. Global Plastics Outlook: Policy Scenarios to 2060.

Ojha, N., Pradhan, N., Singh, S., Barla, A., Shrivastava, A., Khatua, P., Rai, V., Bose, S., 2017. Evaluation of HDPE and LDPE degradation by fungus, implemented by statistical optimization. Sci. Rep. 7, 1–13. https://doi.org/10.1038/srep39515

Oksanen, JariJari Oksanen, F. Guillaume Blanchet, Michael Friendly, Roeland Kindt, Pierre Legendre, Dan McGlinn, P., R. Minchin, R. B. O'Hara, Gavin L. Simpson, Peter Solymos, M. Henry H. Stevens, E.S. and H., Wagner, Legendre, P., O'Hara, B., Stevens, M.H.H., Oksanen, M.J., Suggests, M., 2020. The vegan package. Community Ecol. Packag.

Oliveira, M., Almeida, M., 2019. The why and how of micro(nano)plastic research. TrAC - Trends Anal. Chem. 114, 196–201. https://doi.org/10.1016/j.trac.2019.02.023

Oliveri Conti, G., Ferrante, M., Banni, M., Favara, C., Nicolosi, I., Cristaldi, A., Fiore, M., Zuccarello, P., 2020. Micro- and nano-plastics in edible fruit and vegetables. The first diet risks assessment for the general population. Environ. Res. 187, 109677. https://doi.org/10.1016/j.envres.2020.109677

Onink, V., Jongedijk, C.E., Hoffman, M.J., van Sebille, E., Laufkötter, C., 2021. Global simulations of marine plastic transport show plastic trapping in coastal zones. Environ. Res. Lett. 16. https://doi.org/10.1088/1748-9326/abecbd

Oriekhova, O., Stoll, S., 2018. Heteroaggregation of nanoplastic particles in the presence of inorganic colloids and natural organic matter. Environ. Sci. Nano 5, 792–799. https://doi.org/10.1039/c7en01119a

Pabortsava, K., Lampitt, R.S., 2020. High concentrations of plastic hidden beneath the surface of the Atlantic Ocean. Nat. Commun. 11, 1–11. https://doi.org/10.1038/s41467-020-17932-9

Palm, G.J., Reisky, L., Böttcher, D., Müller, H., Michels, E.A.P., Walczak, M.C., Berndt, L., Weiss, M.S., Bornscheuer, U.T., Weber, G., 2019. Structure of the plastic-degrading Ideonella sakaiensis

MHETase bound to a substrate. Nat. Commun. 10, 1–10. https://doi.org/10.1038/s41467-019-09326-3

Palmisano, A.C., Pettigrew, C.A., 1992. of Plastics Biodegradability Consistent methods for testing claims of biodegradability need to be developed. Am. Inst. Biol. Sci. 42, 680–685.

Pedà, C., Caccamo, L., Fossi, M.C., Gai, F., Andaloro, F., Genovese, L., Perdichizzi, A., Romeo, T., Maricchiolo, G., 2016. Intestinal alterations in European sea bass Dicentrarchus labrax (Linnaeus, 1758) exposed to microplastics: Preliminary results. Environ. Pollut. 212, 251–256. https://doi.org/10.1016/j.envpol.2016.01.083

Peng, G., Bellerby, R., Zhang, F., Sun, X., Li, D., 2020. The ocean's ultimate trashcan: Hadal trenches as major depositories for plastic pollution. Water Res. 168, 115121. https://doi.org/10.1016/j.watres.2019.115121

Pinnell, L.J., Turner, J.W., Turner, J.W., 2019. Shotgun Metagenomics Reveals the Benthic Microbial Community Response to Plastic and Bioplastic in a Coastal Marine Environment 10. https://doi.org/10.3389/fmicb.2019.01252

Pinto, M., Langer, T.M., Hüffer, T., Hofmann, T., Herndl, G.J., 2019. The composition of bacterial communities associated with plastic biofilms differs between different polymers and stages of biofilm succession. PLoS One 14, 1–20. https://doi.org/10.1371/journal.pone.0217165

Plastics Europe, G.M.R., Conversio Market & Strategy GmbH, 2019. Plastics - the Facts 2019.

PlasticsEurope, 2022. Plastics – the Facts 2022. PlasticEurope.

Pollet, T., Berdjeb, L., Garnier, C., Durrieu, G., Le Poupon, C., Misson, B., Jean-François, B., 2018. Prokaryotic community successions and interactions in marine biofilms: the key role of Flavobacteriia. FEMS Microbiol. Ecol. 94, 1–13. https://doi.org/10.1093/femsec/fiy083

Porter, A., Lyons, B.P., Galloway, T.S., Lewis, C., 2018. Role of Marine Snows in Microplastic Fate and Bioavailability. Environ. Sci. Technol. 52, 7111–7119. https://doi.org/10.1021/acs.est.8b01000

Powell, J.J., Thoree, V., Pele, L.C., 2007. Dietary microparticles and their impact on tolerance and immune responsiveness of the gastrointestinal tract. Br. J. Nutr. 98, 59–63. https://doi.org/10.1017/S0007114507832922

Pradel, A., Catrouillet, C., Gigault, J., 2023. The environmental fate of nanoplastics : What we know and what we need to know about aggregation To cite this version : HAL Id : insu-03962181. NANOIMPACT 100453. https://doi.org/10.1016/j.impact.2023.100453

Prata, J.C., da Costa, J.P., Lopes, I., Duarte, A.C., Rocha-Santos, T., 2020. Environmental exposure to microplastics: An overview on possible human health effects. Sci. Total Environ. 702, 134455.

https://doi.org/10.1016/j.scitotenv.2019.134455
Qi, X., Yan, W., Cao, Z., Ding, M., Yuan, Y., 2022. Current Advances in the Biodegradation and Bioconversion of Polyethylene Terephthalate 1–25.
Quast, C., Pruesse, E., Yilmaz, P., Gerken, J., Schweer, T., Yarza, P., Peplies, J., Glöckner, F.O., 2013. The SILVA ribosomal RNA gene database project: Improved data processing and web-based tools. Nucleic Acids Res. 41, 590–596. https://doi.org/10.1093/nar/gks1219
R Core Team, 2021. R: A Language and Environment for Statistical Computing.
Raddadi, N., Fava, F., 2019. Biodegradation of oil-based plastics in the environment: Existing knowledge and needs of research and innovation. Sci. Total Environ. 679, 148–158. https://doi.org/10.1016/j.scitotenv.2019.04.419
Raghul, S.S., Bhat, S.G., Chandrasekaran, M., Francis, V., Thachil, E.T., 2014. Biodegradation of polyvinyl alcohol-low linear density polyethylene-blended plastic film by consortium of marine benthic vibrios. Int. J. Environ. Sci. Technol. 11, 1827–1834. https://doi.org/10.1007/s13762-013-0335-8
Ragusa, A., Svelato, A., Santacroce, C., Catalano, P., Notarstefano, V., Carnevali, O., Papa, F., Rongioletti, M.C.A., Baiocco, F., Draghi, S., D'Amore, E., Rinaldo, D., Matta, M., Giorgini, E., 2021. Plasticenta: First evidence of microplastics in human placenta. Environ. Int. 146, 106274. https://doi.org/10.1016/j.envint.2020.106274
Rahman, A., Sarkar, A., Yadav, O.P., Achari, G., Slobodnik, J., 2021. Potential human health risks due to environmental exposure to nano- and microplastics and knowledge gaps: A scoping review. Sci. Total Environ. 757, 143872. https://doi.org/10.1016/j.scitotenv.2020.143872
Rajakumar, K., Sarasvathy, V., Thamarai Chelvan, A., Chitra, R., Vijayakumar, C.T., 2009. Natural weathering studies of polypropylene. J. Polym. Environ. 17, 191–202. https://doi.org/10.1007/s10924-009-0138-7
Reisser, J., Shaw, J., Hallegraeff, G., Proietti, M., Barnes, D.K.A., Thums, M., Wilcox, C., Hardesty, B.D., Pattiaratchi, C., 2014. Millimeter-sized marine plastics: A new pelagic habitat for microorganisms and invertebrates. PLoS One 9, 1–11. https://doi.org/10.1371/journal.pone.0100289
Reisser, J., Slat, B., Noble, K., Du Plessis, K., Epp, M., Proietti, M., De Sonneville, J., Becker, T., Pattiaratchi, C., 2015. The vertical distribution of buoyant plastics at sea: An observational study in the North Atlantic Gyre. Biogeosciences 12, 1249–1256. https://doi.org/10.5194/bg-12-1249-2015
Roager, L., Sonnenschein, E.C., 2019. Bacterial Candidates for Colonization and Degradation of

Marine Plastic Debris. Environ. Sci. Technol. 53, 11636–11643. https://doi.org/10.1021/acs.est.9b02212

Rochman, C.M., Hoh, E., Kurobe, T., Teh, S.J., 2013. Ingested plastic transfers hazardous chemicals to fish and induces hepatic stress. Sci. Rep. 3, 3263. https://doi.org/10.1038/srep03263

Rogers, K.L., Carreres-Calabuig, J.A., Gorokhova, E., Posth, N.R., 2020. Micro-by-micro interactions: How microorganisms influence the fate of marine microplastics. Limnol. Oceanogr. Lett. 5, 18–36. https://doi.org/10.1002/lol2.10136

Romera-Castillo, C., Pinto, M., Langer, T.M., Álvarez-Salgado, X.A., Herndl, G.J., 2018. Dissolved organic carbon leaching from plastics stimulates microbial activity in the ocean. Nat. Commun. 9. https://doi.org/10.1038/s41467-018-03798-5

Ronca, S., 2017. Polyethylene, Brydson's Plastics Materials: Eighth Edition. Elsevier Ltd. https://doi.org/10.1016/B978-0-323-35824-8.00010-4

Rousk, J., 2011. Growth of saprotrophic fungi and bacteria in soil ˚. https://doi.org/10.1111/j.1574-6941.2011.01106.x

Rubio, L., Marcos, R., Hernández, A., 2020. Potential adverse health effects of ingested micro- and nanoplastics on humans. Lessons learned from in vivo and in vitro mammalian models. J. Toxicol. Environ. Heal. - Part B Crit. Rev. 23, 51–68. https://doi.org/10.1080/10937404.2019.1700598

Rummel, C.D., Jahnke, A., Gorokhova, E., Kühnel, D., Schmitt-Jansen, M., 2017. Impacts of biofilm formation on the fate and potential effects of microplastic in the aquatic environment. Environ. Sci. Technol. Lett. 4, 258–267. https://doi.org/10.1021/acs.estlett.7b00164

Ryan, M.P., Adley, C.C., 2014. Ralstonia spp.: Emerging global opportunistic pathogens. Eur. J. Clin. Microbiol. Infect. Dis. 33, 291–304. https://doi.org/10.1007/s10096-013-1975-9

Ryan, P.G., 2015. Does size and buoyancy affect the long-distance transport of floating debris? Environ. Res. Lett. 10. https://doi.org/10.1088/1748-9326/10/8/084019

Sangeetha Devi, R., Rajesh Kannan, V., Nivas, D., Kannan, K., Chandru, S., Robert Antony, A., 2015. Biodegradation of HDPE by Aspergillus spp. from marine ecosystem of Gulf of Mannar, India. Mar. Pollut. Bull. 96, 32–40. https://doi.org/10.1016/j.marpolbul.2015.05.050

Sangkham, S., Faikhaw, O., Munkong, N., Sakunkoo, P., 2022. A review on microplastics and nanoplastics in the environment : Their occurrence , exposure routes , toxic studies , and potential effects on human health. Mar. Pollut. Bull. 181, 113832. https://doi.org/10.1016/j.marpolbul.2022.113832

Sarkhel, R., Sengupta, S., Das, P., Bhowal, A., 2020. Comparative biodegradation study of polymer

from plastic bottle waste using novel isolated bacteria and fungi from marine source. J. Polym. Res. 27. https://doi.org/10.1007/s10965-019-1973-4

Satterthwaite, K., 2017. Plastics Based on Styrene, Brydson's Plastics Materials: Eighth Edition. Elsevier Ltd. https://doi.org/10.1016/B978-0-323-35824-8.00012-8

Schliep, K.P., 2011. phangorn: Phylogenetic analysis in R. Bioinformatics 27, 592–593. https://doi.org/10.1093/bioinformatics/btq706

Schwabl, P., Koppel, S., Konigshofer, P., Bucsics, T., Trauner, M., Reiberger, T., Liebmann, B., 2019. Detection of various microplastics in human stool: A prospective case series. Ann. Intern. Med. 171, 453–457. https://doi.org/10.7326/M19-0618

Schymanski, D., Goldbeck, C., Humpf, H.U., Fürst, P., 2018. Analysis of microplastics in water by micro-Raman spectroscopy: Release of plastic particles from different packaging into mineral water. Water Res. 129, 154–162. https://doi.org/10.1016/j.watres.2017.11.011

Sebille, E. Van, Aliani, S., Law, K.L., Maximenko, N., n.d. The physical oceanography of the transport of floating marine debris 1–54.

Segata, N., Izard, J., Waldron, L., Gevers, D., Miropolsky, L., Garrett, W.S., Huttenhower, C., 2011. Metagenomic biomarker discovery and explanation. Genome Biol. 12, R60.

Shiu, R.F., Vazquez, C.I., Chiang, C.Y., Chiu, M.H., Chen, C.S., Ni, C.W., Gong, G.C., Quigg, A., Santschi, P.H., Chin, W.C., 2020. Nano- and microplastics trigger secretion of protein-rich extracellular polymeric substances from phytoplankton. Sci. Total Environ. 748, 141469. https://doi.org/10.1016/j.scitotenv.2020.141469

Shruti, V.C., Pérez-Guevara, F., Elizalde-Martínez, I., Kutralam-Muniasamy, G., 2020a. First study of its kind on the microplastic contamination of soft drinks, cold tea and energy drinks - Future research and environmental considerations. Sci. Total Environ. 726, 138580. https://doi.org/10.1016/j.scitotenv.2020.138580

Shruti, V.C., Pérez-Guevara, F., Kutralam-Muniasamy, G., 2020b. Metro station free drinking water fountain- A potential "microplastics hotspot" for human consumption. Environ. Pollut. 261. https://doi.org/10.1016/j.envpol.2020.114227

Silby, M.W., Winstanley, C., Godfrey, S.A.C., Levy, S.B., Jackson, R.W., 2011. Pseudomonas genomes : diverse and adaptable 35, 652–680. https://doi.org/10.1111/j.1574-6976.2011.00269.x

Singh, B., Sharma, N., 2008. Mechanistic implications of plastic degradation. Polym. Degrad. Stab. 93, 561–584. https://doi.org/10.1016/j.polymdegradstab.2007.11.008

Singh Jadaun, J., Bansal, S., Sonthalia, A., Rai, A.K., Singh, S.P., 2022. Biodegradation of plastics for sustainable environment. Bioresour. Technol. 347, 126697.

https://doi.org/10.1016/j.biortech.2022.126697
Song, X., Ding, J., Tian, W., Xu, H., Zou, H., Wang, Z., 2023. Effects of plastisphere on phosphorus availability in freshwater system: Critical roles of polymer type and colonizing habitat. Sci. Total Environ. 870, 161990. https://doi.org/10.1016/j.scitotenv.2023.161990
Song, Y.K., Hong, S.H., Jang, M., Han, G.M., Jung, S.W., Shim, W.J., 2017a. Combined Effects of UV Exposure Duration and Mechanical Abrasion on Microplastic Fragmentation by Polymer Type. Environ. Sci. Technol. 51, 4368–4376. https://doi.org/10.1021/acs.est.6b06155
Song, Y.K., Hong, S.H., Jang, M., Han, G.M., Jung, S.W., Shim, W.J., 2017b. Combined Effects of UV Exposure Duration and Mechanical Abrasion on Microplastic Fragmentation by Polymer Type. Environ. Sci. Technol. 51, 4368–4376. https://doi.org/10.1021/acs.est.6b06155
Sorasan, C., Edo, C., González-Pleiter, M., Fernández-Piñas, F., Leganés, F., Rodríguez, A., Rosal, R., 2021. Generation of nanoplastics during the photoageing of low-density polyethylene. Environ. Pollut. 289. https://doi.org/10.1016/j.envpol.2021.117919
Srikanth, M., Sandeep, T.S.R.S., Sucharitha, K., Godi, S., 2022. Biodegradation of plastic polymers by fungi : a brief review. Bioresour. Bioprocess. 4. https://doi.org/10.1186/s40643-022-00532-4
Stokes, G.G., 1850. On the Effect of the Internal Friction of Fluids on the Motion of Pendulums. Math. Phys. Pap. 1–10. https://doi.org/10.1017/cbo9780511702266.002
Stramski, D., Woźniak, S.B., 2005. On the role of colloidal particles in light scattering in the ocean. Limnol. Oceanogr. 50, 1581–1591. https://doi.org/10.4319/lo.2005.50.5.1581
Streit-bianchi, M., Cimadevila, M., Trettnak, W., Pollution, C.P., Science, T., 2020. Mare Plasticum - The Plastic Sea, Mare Plasticum - The Plastic Sea. https://doi.org/10.1007/978-3-030-38945-1
Suaria, G., Avio, C.G., Mineo, A., Lattin, G.L., Magaldi, M.G., Belmonte, G., Moore, C.J., Regoli, F., Aliani, S., 2016. The Mediterranean Plastic Soup: synthetic polymers in Mediterranean surface waters. Sci. Rep. 6. https://doi.org/10.1038/srep37551
Suaria, G., Avio, C.G., Regoli, F., Aliani, S., 2018. Sub-Basin Scale Heterogeneity in the Polymeric Composition of Floating Microplastics in the Mediterranean Sea. Springer Water 1–7. https://doi.org/10.1007/978-3-319-71279-6_1
Sudhakar, M., Doble, M., Murthy, P.S., Venkatesan, R., 2008. Marine microbe-mediated biodegradation of low- and high-density polyethylenes. Int. Biodeterior. Biodegradation 61, 203–213. https://doi.org/10.1016/j.ibiod.2007.07.011
Sudhakar, M., Priyadarshini, C., Doble, M., Sriyutha Murthy, P., Venkatesan, R., 2007. Marine bacteria mediated degradation of nylon 66 and 6. Int. Biodeterior. Biodegrad. 60, 144–151.

https://doi.org/10.1016/j.ibiod.2007.02.002

Sushmitha, T.J., Rajeev, M., Murthy, P.S., Ganesh, S., Rao, S., Id, T., Karutha, S., Id, P., 2021. Bacterial community structure of early-stage biofilms is dictated by temporal succession rather than substrate types in the southern coastal seawater of India 1–20. https://doi.org/10.1371/journal.pone.0257961

Syranidou, E., Kalogerakis, N., 2022. Interactions of microplastics , antibiotics and antibiotic resistant genes within WWTPs. Sci. Total Environ. 804, 150141. https://doi.org/10.1016/j.scitotenv.2021.150141

Syranidou, E., Karkanorachaki, K., Amorotti, F., Avgeropoulos, A., Kolvenbach, B., Zhou, N.Y., Fava, F., Corvini, P.F.X., Kalogerakis, N., 2019a. Biodegradation of mixture of plastic films by tailored marine consortia. J. Hazard. Mater. 375, 33–42. https://doi.org/10.1016/j.jhazmat.2019.04.078

Syranidou, E., Karkanorachaki, K., Amorotti, F., Avgeropoulos, A., Kolvenbach, B., Zhou, N.Y., Fava, F., Corvini, P.F.X., Kalogerakis, N., 2019b. Biodegradation of mixture of plastic films by tailored marine consortia. J. Hazard. Mater. 375, 33–42. https://doi.org/10.1016/j.jhazmat.2019.04.078

Syranidou, E., Karkanorachaki, K., Amorotti, F., Avgeropoulos, A., Kolvenbach, B., Zhou, N.Y., Fava, F., Corvini, P.F.X., Kalogerakis, N., 2019c. Biodegradation of mixture of plastic films by tailored marine consortia. J. Hazard. Mater. 375, 33–42. https://doi.org/10.1016/j.jhazmat.2019.04.078

Syranidou, E., Karkanorachaki, K., Amorotti, F., Franchini, M., Repouskou, E., Kaliva, M., Vamvakaki, M., Kolvenbach, B., Fava, F., Corvini, P.F.-X., Kalogerakis, N., 2017a. Biodegradation of weathered polystyrene films in seawater microcosms. Sci. Rep. 7, 17991. https://doi.org/10.1038/s41598-017-18366-y

Syranidou, E., Karkanorachaki, K., Amorotti, F., Repouskou, E., Kroll, K., Kolvenbach, B., Corvini, P., Fava, F., Kalogerakis, N., 2017b. Development of tailored indigenous marine consortia for the degradation of naturally weathered polyethylene films. PlosOne under revi, 1–21.

Syranidou, E., Karkanorachaki, K., Amorotti, F., Repouskou, E., Kroll, K., Kolvenbach, B., Corvini, P.F.X., Fava, F., Kalogerakis, N., 2017c. Development of tailored indigenous marine consortia for the degradation of naturally weathered polyethylene films. PLoS One 12, 1–21. https://doi.org/10.1371/journal.pone.0183984

Syranidou, E., Karkanorachaki, K., Barouta, D., Papadaki, E., Moschovas, D., Avgeropoulos, A., Kalogerakis, N., 2023. Relationship between the Carbonyl Index (CI) and Fragmentation of

Polyolefin Plastics during Aging. https://doi.org/10.1021/acs.est.3c01430

Taghavi, N., Zhuang, W.Q., Baroutian, S., 2021. Enhanced biodegradation of non-biodegradable plastics by UV radiation: Part 1. J. Environ. Chem. Eng. 9, 106464. https://doi.org/10.1016/j.jece.2021.106464

Takada, H., 2019. Hazardous Chemicals Associated with Plastics in the Marine Environment, The Handbook of Environmental Chemistry (Springer Nature).

Tender, C. De, Devriese, L.I., Haegeman, A., Maes, S., Vangeyte, J., Cattrijsse, A., Dawyndt, P., Ruttink, T., 2017. Temporal Dynamics of Bacterial and Fungal Colonization on Plastic Debris in the North Sea. https://doi.org/10.1021/acs.est.7b00697

Thakur, B., Singh, Jaswinder, Singh, Joginder, Angmo, D., Vig, A.P., 2023. Biodegradation of different types of microplastics: Molecular mechanism and degradation efficiency. Sci. Total Environ. 877, 162912. https://doi.org/10.1016/j.scitotenv.2023.162912

Thompson, R.C., 2004. Lost at Sea: Where Is All the Plastic? Science (80-.). 304, 838–838. https://doi.org/10.1126/science.1094559

Thompson, R.C., Moore, C.J., Saal, F.S., Swan, S.H., 2010. Plastics , the environment and human health : current consensus and future trends 2153–2166. https://doi.org/10.1098/rstb.2009.0053

Tong, H., Jiang, Q., Hu, X., Zhong, X., 2020. Occurrence and identification of microplastics in tap water from China. Chemosphere 252, 126493. https://doi.org/10.1016/j.chemosphere.2020.126493

Ullmann, U., 1998. Klebsiella spp . as Nosocomial Pathogens : Epidemiology , Taxonomy , Typing Methods , and Pathogenicity Factors 11, 589–603.

Van Cauwenberghe, L., Claessens, M., Vandegehuchte, M.B., Mees, J., Janssen, C.R., 2013. Assessment of marine debris on the Belgian Continental Shelf. Mar. Pollut. Bull. 73, 161–169. https://doi.org/10.1016/j.marpolbul.2013.05.026

Van Cauwenberghe, L., Devriese, L., Galgani, F., Robbens, J., Janssen, C.R., 2015. Microplastics in sediments: A review of techniques, occurrence and effects. Mar. Environ. Res. 111, 5–17. https://doi.org/10.1016/j.marenvres.2015.06.007

Van Melkebeke, M., Janssen, C., De Meester, S., 2020. Characteristics and Sinking Behavior of Typical Microplastics Including the Potential Effect of Biofouling: Implications for Remediation. Environ. Sci. Technol. 54, 8668–8680. https://doi.org/10.1021/acs.est.9b07378

van Rossum, G., 1995. Python tutorial, May 1995. CWI Rep. CS-R9526 1–65.

Van Sebille, E., Wilcox, C., Lebreton, L., Maximenko, N., Hardesty, B.D., Van Franeker, J.A., Eriksen, M.,

Siegel, D., Galgani, F., Law, K.L., 2015. A global inventory of small floating plastic debris. Environ. Res. Lett. 10, 124006. https://doi.org/10.1088/1748-9326/10/12/124006

Veerasingam, S., Ranjani, M., Venkatachalapathy, R., Bagaev, A., Mukhanov, V., Litvinyuk, D., Mugilarasan, M., Gurumoorthi, K., Guganathan, L., Aboobacker, V.M., Vethamony, P., 2020. Contributions of Fourier transform infrared spectroscopy in microplastic pollution research: A review. Crit. Rev. Environ. Sci. Technol. 51, 2681–2743. https://doi.org/10.1080/10643389.2020.1807450

Wagner, S., Reemtsma, T., 2019. Things we know and don't know about nanoplastic in the environment. Nat. Nanotechnol. 14, 300–301. https://doi.org/10.1038/s41565-019-0424-z

Waldschläger, K., Schüttrumpf, H., 2019. Effects of Particle Properties on the Settling and Rise Velocities of Microplastics in Freshwater under Laboratory Conditions. Environ. Sci. Technol. 53, 1958–1966. https://doi.org/10.1021/acs.est.8b06794

Wang, L., Wu, W.M., Bolan, N.S., Tsang, D.C.W., Li, Y., Qin, M., Hou, D., 2021. Environmental fate, toxicity and risk management strategies of nanoplastics in the environment: Current status and future perspectives. J. Hazard. Mater. 401, 123415. https://doi.org/10.1016/j.jhazmat.2020.123415

Wang, R., Liu, X., 2019. Environmental processes and ecological effects of microplastics in the ocean. IOP Conf. Ser. Earth Environ. Sci. 227. https://doi.org/10.1088/1755-1315/227/5/052047

Ward, C.P., Armstrong, C.J., Walsh, A.N., Jackson, J.H., Reddy, C.M., 2019. Sunlight Converts Polystyrene to Carbon Dioxide and Dissolved Organic Carbon. Environ. Sci. Technol. Lett. 6, 669–674. https://doi.org/10.1021/acs.estlett.9b00532

Wayman, C., Niemann, H., 2021. The fate of plastic in the ocean environment-a minireview. Environ. Sci. Process. Impacts 23, 198–212. https://doi.org/10.1039/d0em00446d

Werner, S., Budziak, A., Van Fanneker, J.A., Galgani, F., Hanke, G., Maes, T., Matiddi, M., Nilsson, P., Oosterbaan, L., Priestland, E., Thompson, R., Veiga, J.M., Vlachogianni, T., 2016. Harm caused by Marine Litter - European Commission, JRC Technical Report. https://doi.org/10.2788/690366

Wilkes, R. A., Aristilde, L., 2017. Degradation and metabolism of synthetic plastics and associated products by Pseudomonas sp.: capabilities and challenges. J. Appl. Microbiol. 123, 582–593. https://doi.org/10.1111/jam.13472

Wilkes, R A, Aristilde, L., 2017. Degradation and metabolism of synthetic plastics and associated products by Pseudomonas sp .: capabilities and challenges. https://doi.org/10.1111/jam.13472

Witt, V., Wild, C., Uthicke, S., 2011. Effect of substrate type on bacterial community composition in

biofilms from the Great Barrier Reef 323, 188–195. https://doi.org/10.1111/j.1574-6968.2011.02374.x

Woo, H., Seo, K., Choi, Y., Kim, J., Tanaka, M., Lee, K.H., Choi, J., 2021. Methods of analyzing microsized plastics in the environment. Appl. Sci. 11. https://doi.org/10.3390/app112210640

Woodall, L.C., Sanchez-Vidal, A., Canals, M., Paterson, G.L.J., Coppock, R., Sleight, V., Calafat, A., Rogers, A.D., Narayanaswamy, B.E., Thompson, R.C., 2014. The deep sea is a major sink for microplastic debris. R. Soc. Open Sci. 1. https://doi.org/10.1098/rsos.140317

Wright, E.S., 2016. Using DECIPHER v2.0 to analyze big biological sequence data in R. R J. 8, 352–359. https://doi.org/10.32614/rj-2016-025

Wright, Robyn Joanna, Erni-Cassola, G., Zadjelovic, V., Latva, M., Christie-Oleza, J., 2020. Marine plastic debris – a new surface for microbial colonization. Environ. Sci. Technol. acs.est.0c02305. https://doi.org/10.1021/acs.est.0c02305

Wright, Robyn J., Erni-Cassola, G., Zadjelovic, V., Latva, M., Christie-Oleza, J.A., 2020. Marine Plastic Debris: A New Surface for Microbial Colonization. Environ. Sci. Technol. 54, 11657–11672. https://doi.org/10.1021/acs.est.0c02305

Wright, R.J., Langille, M.G.I., Walker, T.R., Wright, R.J., 2021. Food or just a free ride ? A meta-analysis reveals the global diversity of the Plastisphere. ISME J. 789–806. https://doi.org/10.1038/s41396-020-00814-9

Wright, S.L., Thompson, R.C., Galloway, T.S., 2013. The physical impacts of microplastics on marine organisms: a review. Environ. Pollut. 178, 483–492. https://doi.org/10.1016/j.envpol.2013.02.031

Yang, J., Yang, Y., Wu, W.M., Zhao, J., Jiang, L., 2014. Evidence of polyethylene biodegradation by bacterial strains from the guts of plastic-eating waxworms. Environ. Sci. Technol. 48, 13776–13784. https://doi.org/10.1021/es504038a

Yans, D., Torre, Z. Dela, Santos, L.A.D., Reyes, M.L.C., Baculi, R.Q., 2018. Biodegradation of low-density polyethylene by bacteria isolated from serpentinization-driven alkaline spring 11, 1–12.

Ye, S., Andrady, A.L., 1991. Fouling of floating plastic debris under Biscayne Bay exposure conditions. Mar. Pollut. Bull. 22, 608–613. https://doi.org/10.1016/0025-326X(91)90249-R

Yilmaz, P., Parfrey, L.W., Yarza, P., Gerken, J., Pruesse, E., Quast, C., Schweer, T., Peplies, J., Ludwig, W., Glöckner, F.O., 2014. The SILVA and "all-species Living Tree Project (LTP)" taxonomic frameworks. Nucleic Acids Res. 42, 643–648. https://doi.org/10.1093/nar/gkt1209

Yoshida, S., Hiraga, K., Takehana, T., Taniguchi, I., Yamaji, H., Maeda, Y., Toyohara, K., Miyamoto, K.,

Kimura, Y., Oda, K., 2016. Una bacteria que degrada y asimila poli (tereftalato de etileno)Yoshida, S., Hiraga, K., Takehana, T., Taniguchi, I., Yamaji, H., Maeda, Y., Toyohara, K., Miyamoto, K., Kimura, Y., & Oda, K. (2016). Una bacteria que degrada y asimila poli (tereftalato de . Science (80-.). 353, 759.

Yu, Z., Yang, G., Zhang, W., 2022. A new model for the terminal settling velocity of microplastics. Mar. Pollut. Bull. 176, 113449. https://doi.org/10.1016/j.marpolbul.2022.113449

Yuan, J., Ma, J., Sun, Y., Zhou, T., Zhao, Y., Yu, F., 2020. Microbial degradation and other environmental aspects of microplastics/plastics. Sci. Total Environ. 715, 136968. https://doi.org/10.1016/j.scitotenv.2020.136968

Zadjelovic, V., Erni-Cassola, G., Lester, D., Eley, Y., Gibson, M., Dorador, C., Golyshin, P., Black, S., Wellington, E., Christie-Oleza, J., 2022. A Mechanistic Understanding of Polyethylene Biodegradation by the Marine Bacterium Alcanivorax, SSRN Electronic Journal. https://doi.org/10.2139/ssrn.3979990

Zalasiewicz, J., Waters, C.N., Ivar do Sul, J.A., Corcoran, P.L., Barnosky, A.D., Cearreta, A., Edgeworth, M., Gałuszka, A., Jeandel, C., Leinfelder, R., McNeill, J.R., Steffen, W., Summerhayes, C., Wagreich, M., Williams, M., Wolfe, A.P., Yonan, Y., 2016. The geological cycle of plastics and their use as a stratigraphic indicator of the Anthropocene. Anthropocene 13, 4–17. https://doi.org/10.1016/j.ancene.2016.01.002

Zeenat, Elahi, A., Bukhari, D.A., Shamim, S., Rehman, A., 2021. Plastics degradation by microbes: A sustainable approach. J. King Saud Univ. - Sci. 33, 101538. https://doi.org/10.1016/j.jksus.2021.101538

Zettler, E.R., Mincer, T.J., Amaral-Zettler, L.A., 2013. Life in the “plastisphere”: Microbial communities on plastic marine debris. Environ. Sci. Technol. 47. https://doi.org/10.1021/es401288x

Zhang, F., Yao, C., Xu, J., Zhu, L., Peng, G., Li, D., 2020. Composition, spatial distribution and sources of plastic litter on the East China Sea floor. Sci. Total Environ. 742, 140525. https://doi.org/10.1016/j.scitotenv.2020.140525

Zhang, J., Gao, D., Li, Q., Zhao, Yixuan, Li, L., Lin, H., Bi, Q., Zhao, Yucheng, 2020. Science of the Total Environment Biodegradation of polyethylene microplastic particles by the fungus Aspergillus fl avus from the guts of wax moth Galleria mellonella 704, 1–8. https://doi.org/10.1016/j.scitotenv.2019.135931

Zhang, K., Hamidian, A.H., Tubić, A., Zhang, Y., Fang, J.K.H., Wu, C., Lam, P.K.S., 2021. Understanding plastic degradation and microplastic formation in the environment: A review. Environ. Pollut.

274. https://doi.org/10.1016/j.envpol.2021.116554

Zhao, S., Zettler, E.R., Amaral-Zettler, L.A., Mincer, T.J., 2021. Microbial carrying capacity and carbon biomass of plastic marine debris. ISME J. 15, 67–77. https://doi.org/10.1038/s41396-020-00756-2

Zhu, L., Zhao, S., Bittar, T.B., Stubbins, A., Li, D., 2020. Photochemical dissolution of buoyant microplastics to dissolved organic carbon: Rates and microbial impacts. J. Hazard. Mater. 383, 121065. https://doi.org/10.1016/j.jhazmat.2019.121065

Δασενάκης, Μ., Λαδάκης, Μ., Τριανταφυλλάκη, Σ., Χαλκιαδάκη, Ό., Dassenakis, M., Ladakis, M., Triantafyllaki, S., Chalkiadaki, O., 2008. Περιβαλλον Του Κολπου Τησ Σουδασ the Influence of the Moronis River on the Marine Environment of the Bay of Souda.

APPENDIX I: Supplementary Figures

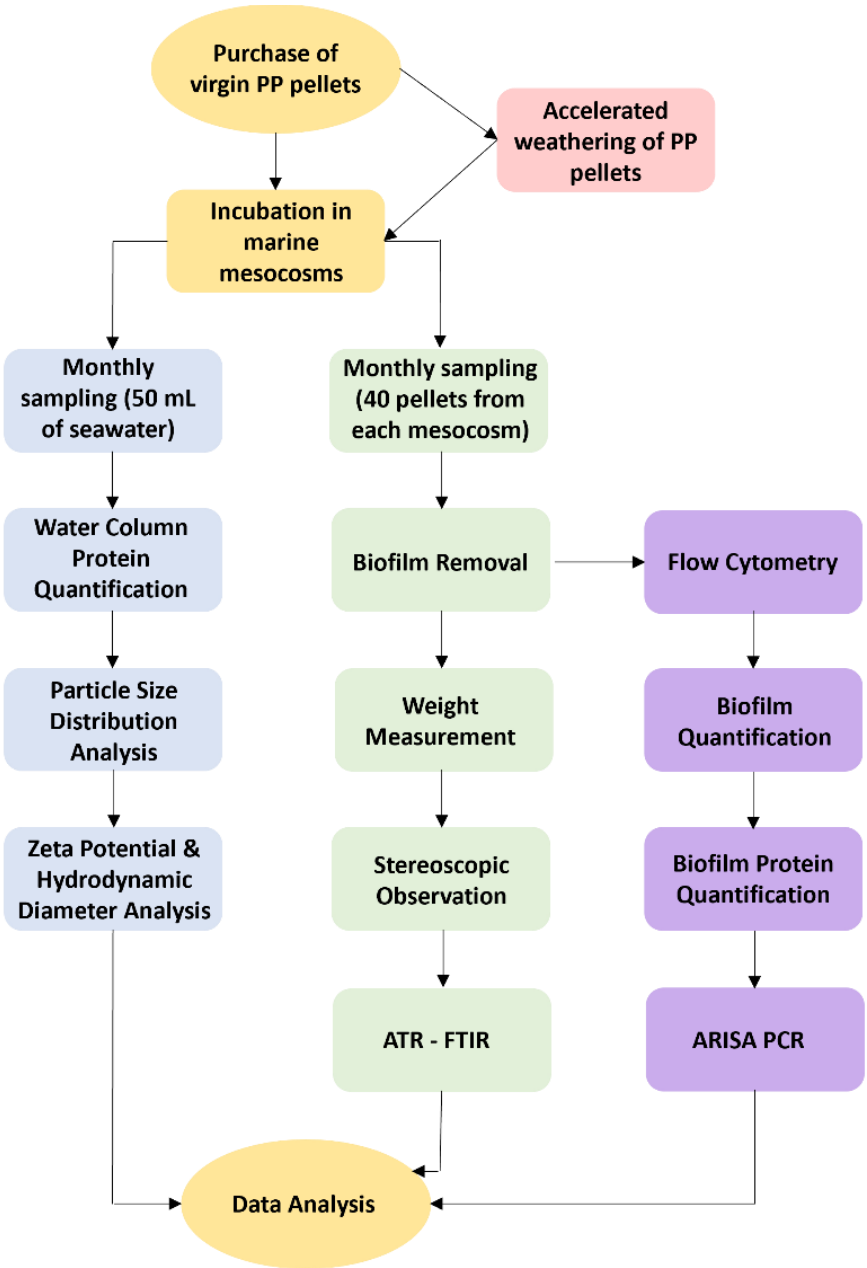

Figure S 1: Experimental procedure flowchart.

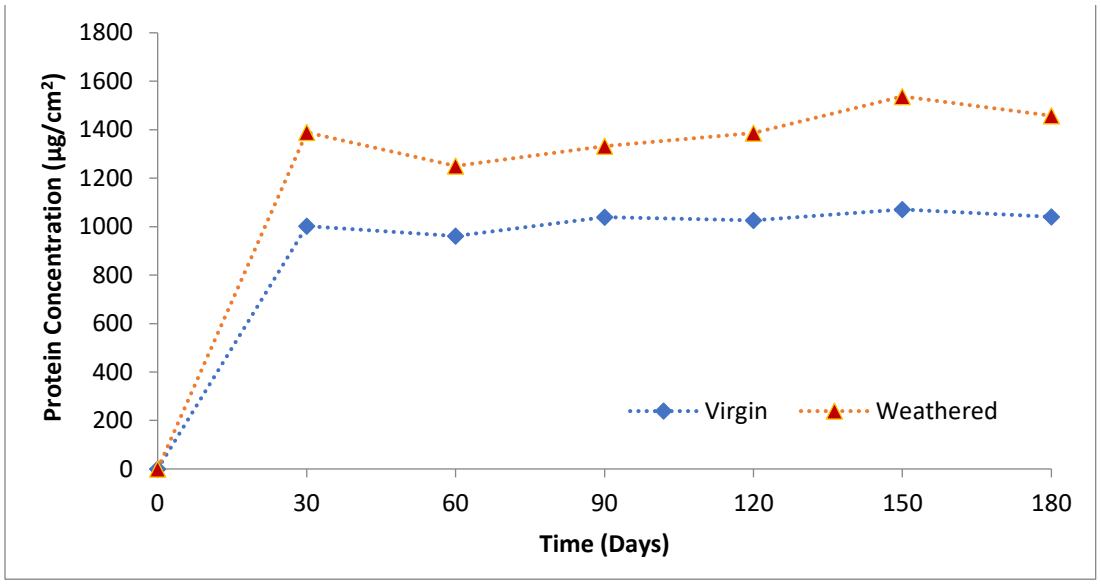

Figure S 2: Protein concentrations on the surface of virgin and weathered pellets from the mesocosms over time.

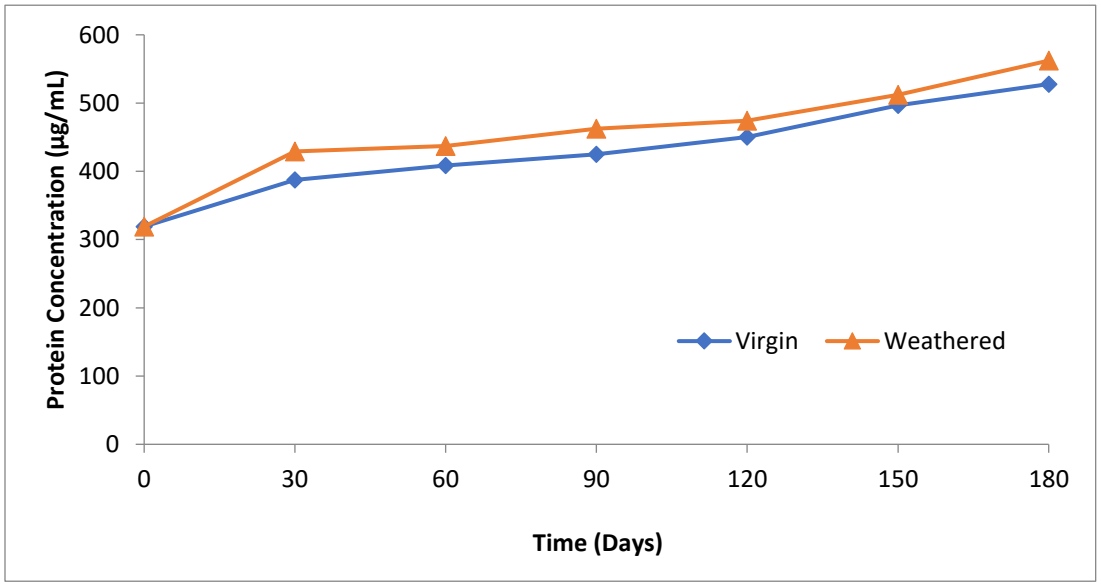

Figure S 3: Protein concentrations in the water column of the mesocosms over time.

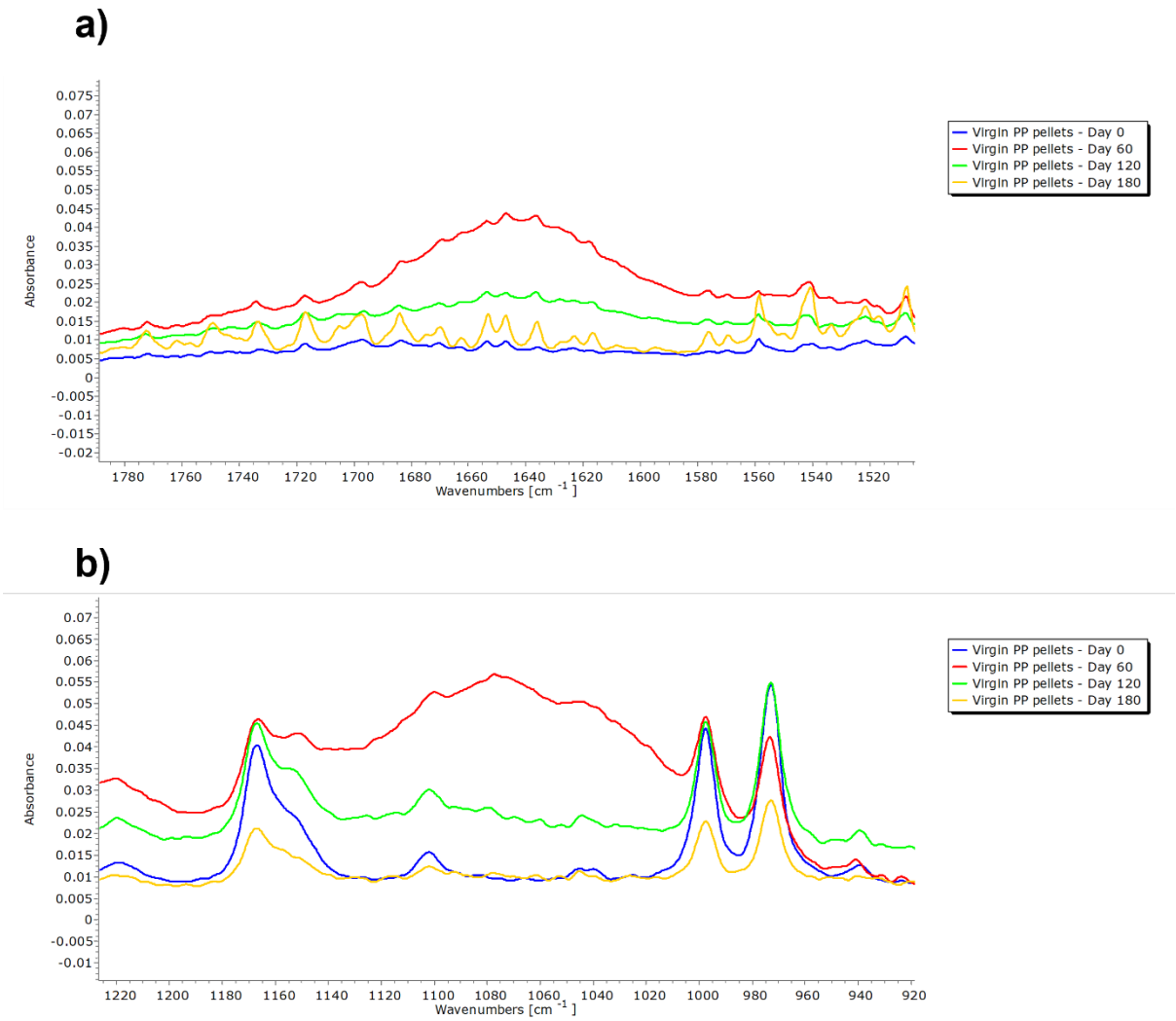

Figure S 4: Closer Inspection of virgin pellet spectra over time.

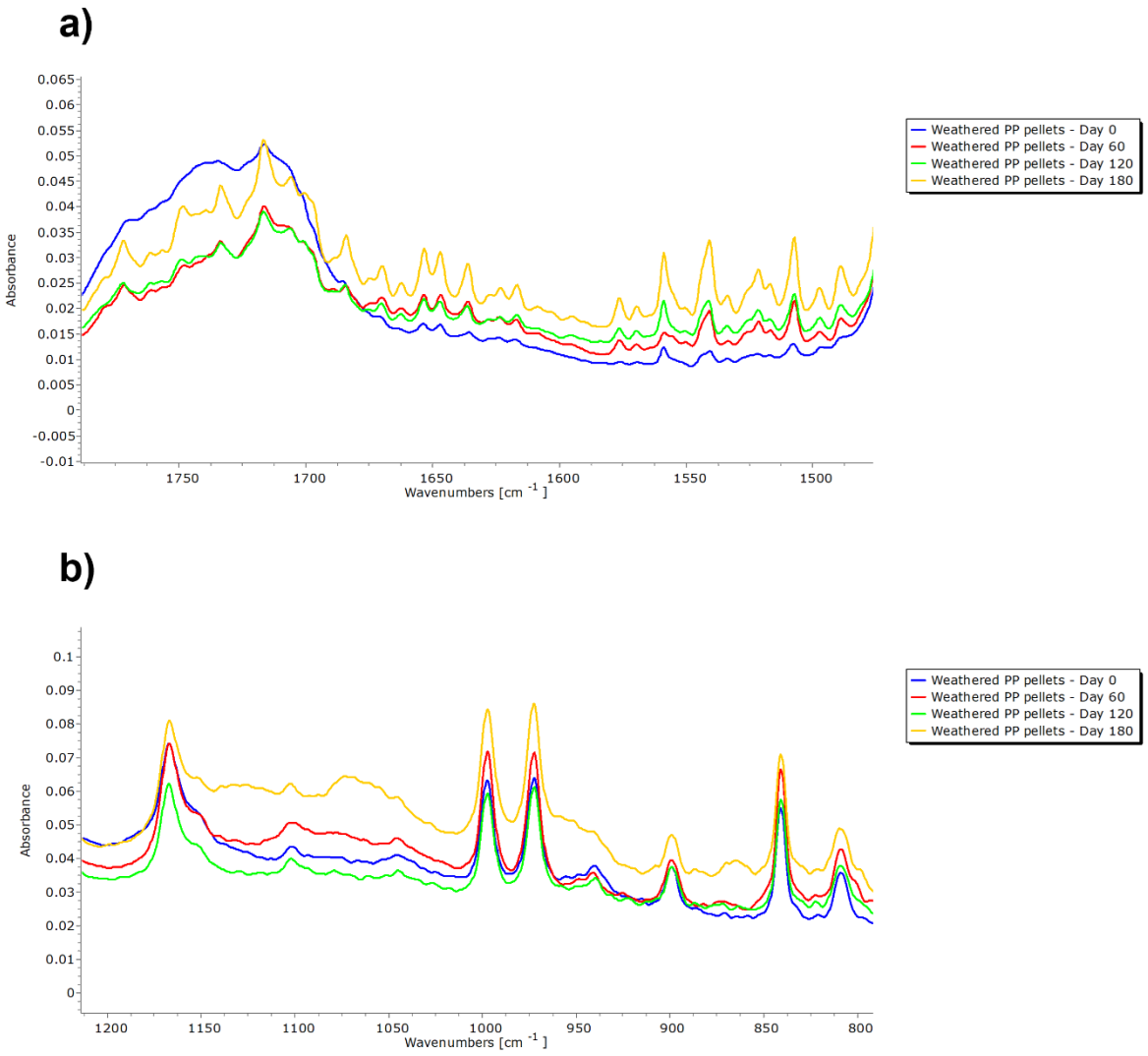

Figure S 5: Closer Inspection of weathered pellet spectra over time.

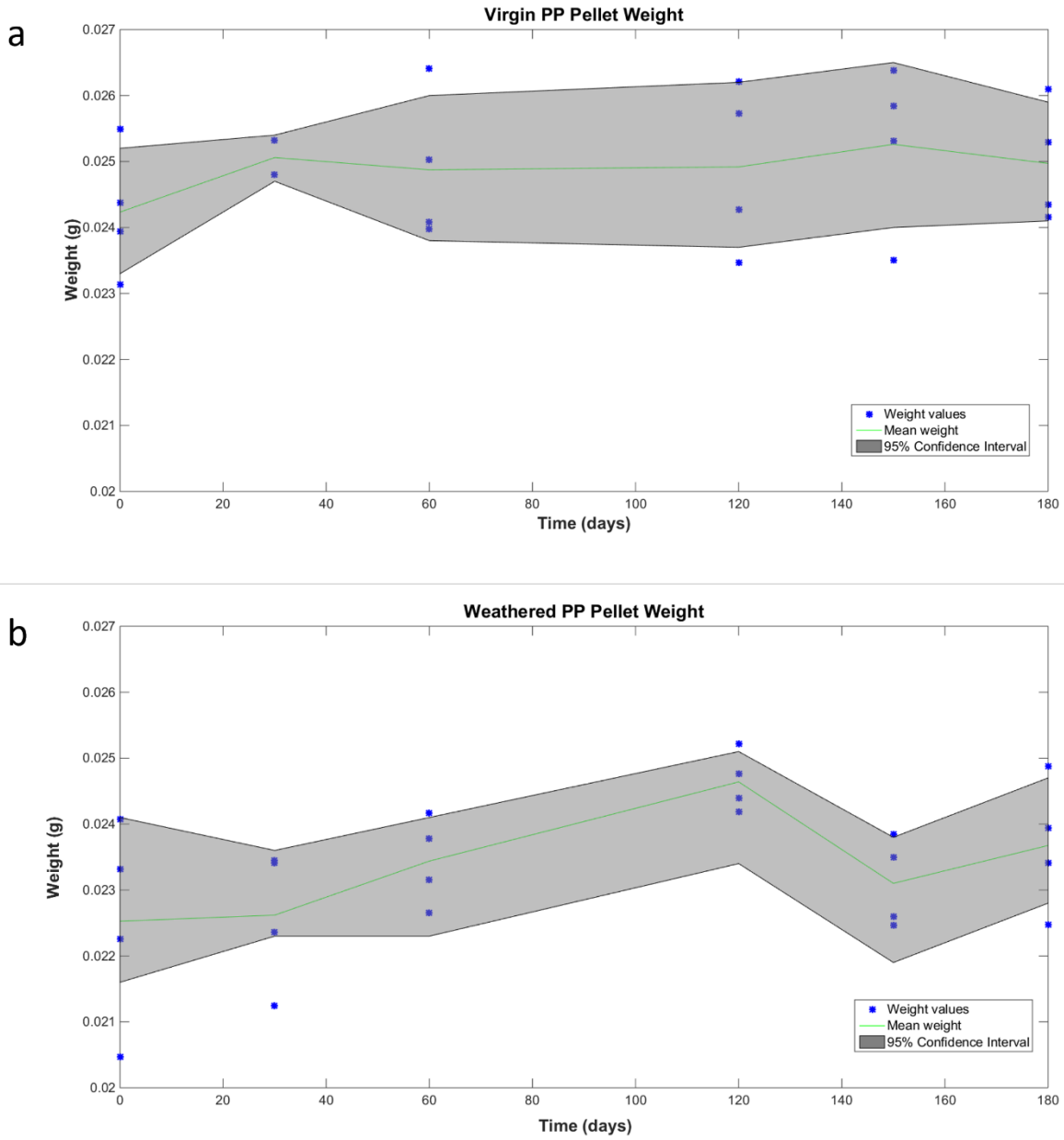

Figure S 6: Virgin (a) and weathered (b) pellet weight over time. The green line indicates the weight average, blue dots indicate individual weight measurements, and the grey area encloses the 95% confidence interval of the measurements.

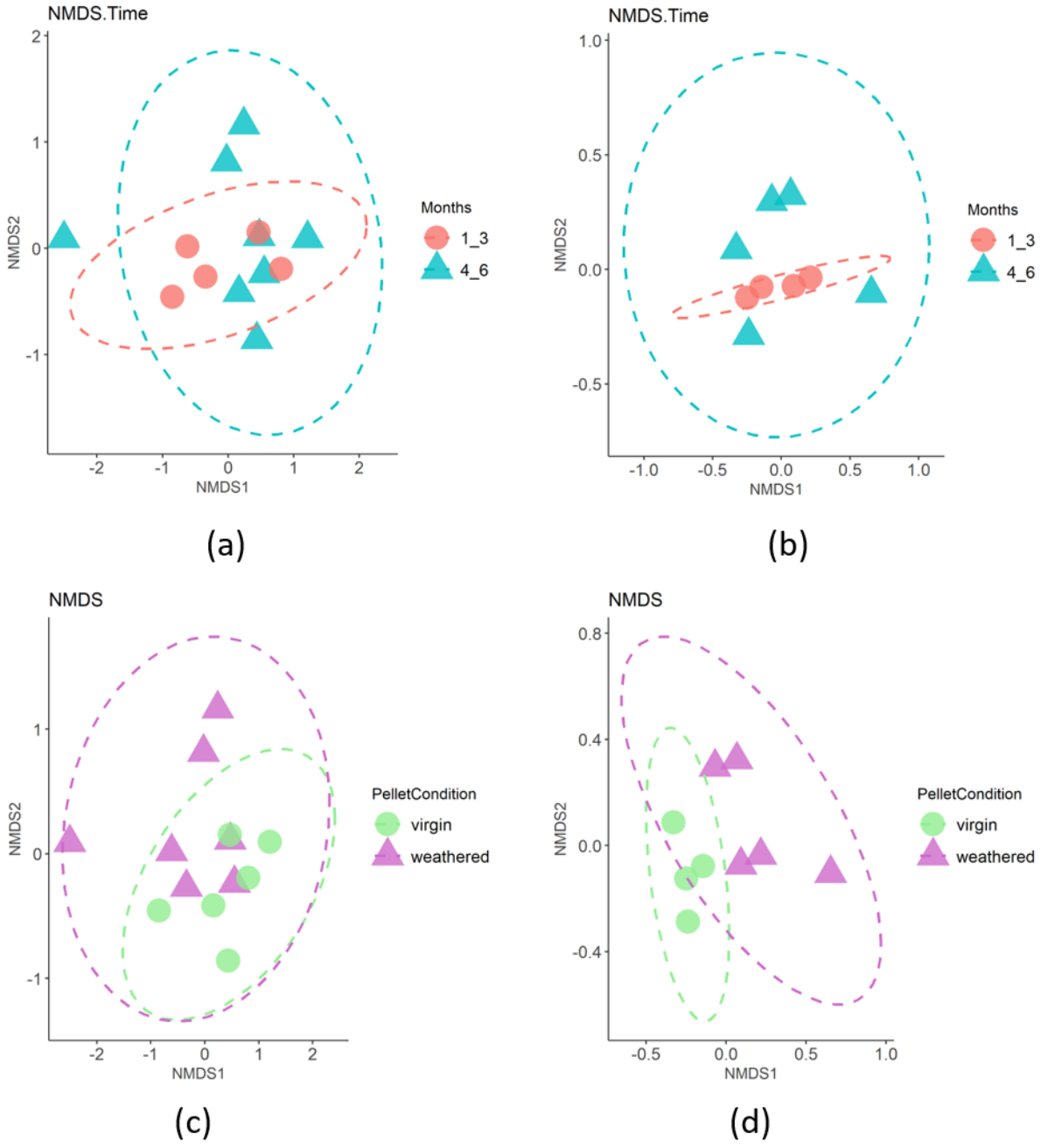

Figure S 7: Non-metric multidimensional scaling comparison of the: (a) and (c) the planktonic and biofilm bacterial communities; (b) and (d) the biofilm communities.

(a)

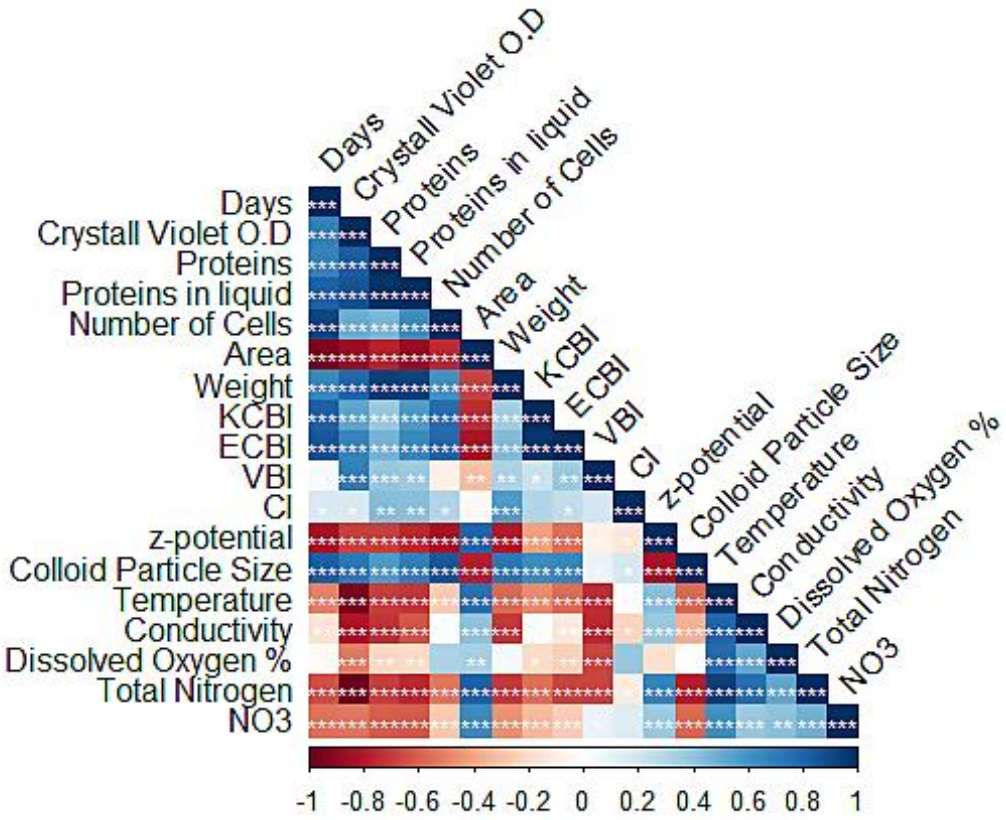
Days
Crystall Violet O.D
Proteins
Proteins in liquid
Number of Cells
Area
Weight
KCBI
ECBI
VBI
CI
z-potential
Colloid Particle Size
Temperature
Conductivity
Dissolved Oxygen %
Total Nitrogen
NO3
-1 -0.8 -0.6 -0.4 -0.2 0 0.2 0.4 0.6 0.8 1

(b)

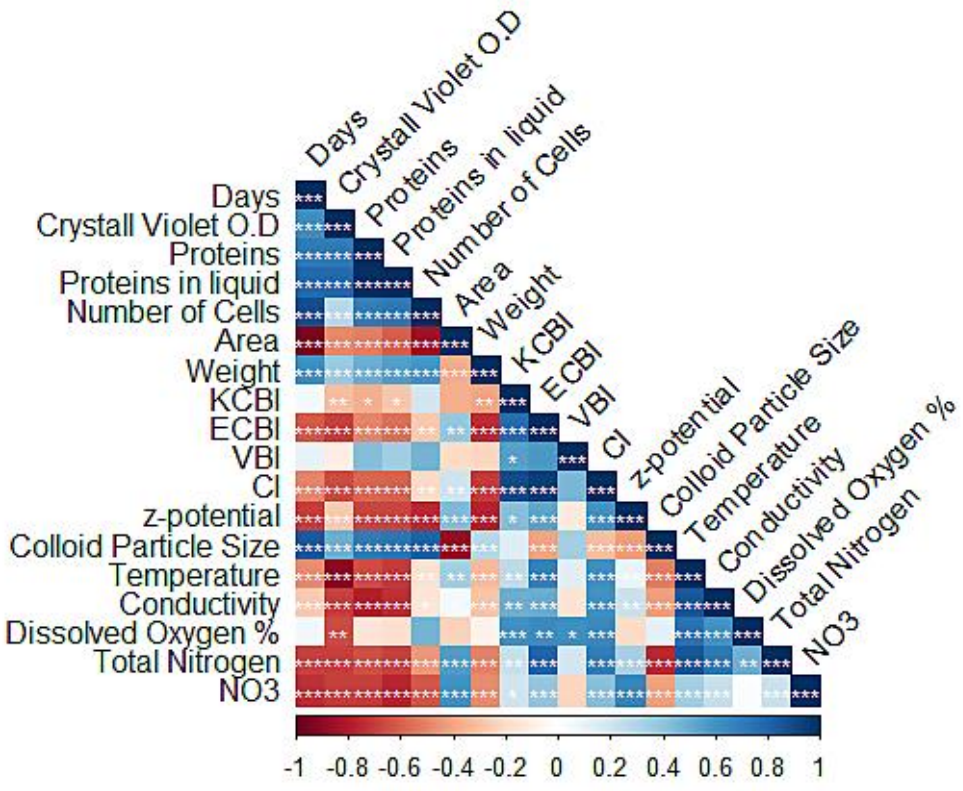

Figure S 8: Correlation plots of all parameters examined throughout the experiment: (a) virgin mesocosm; (b) weathered mesocosm. Stars indicate significance levels: one star for p-values <0.05, two stars for p-values <0.01, three stars for p-values <0.01.

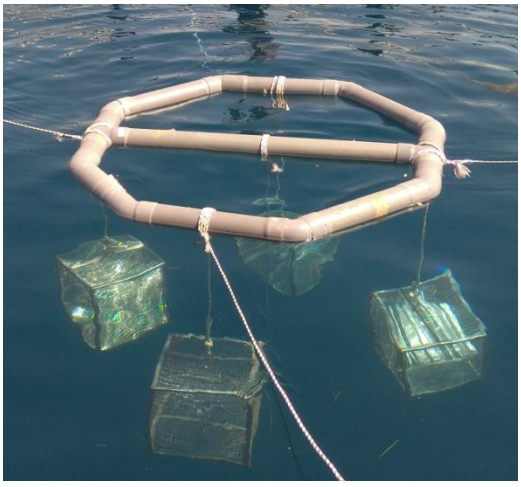

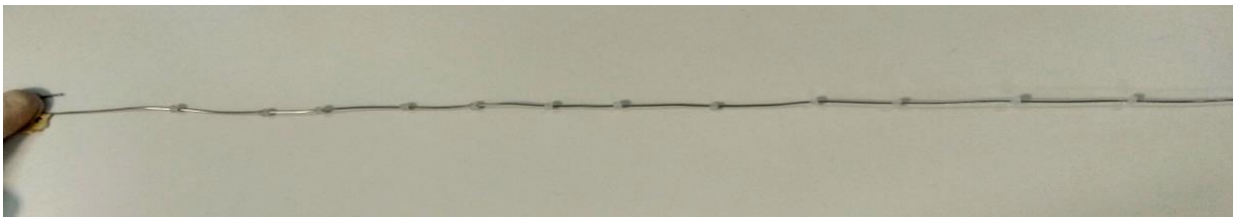

Figure S 9: Experimental setup (top left), plastic polymer samples (top right) and pellet samples (bottom).

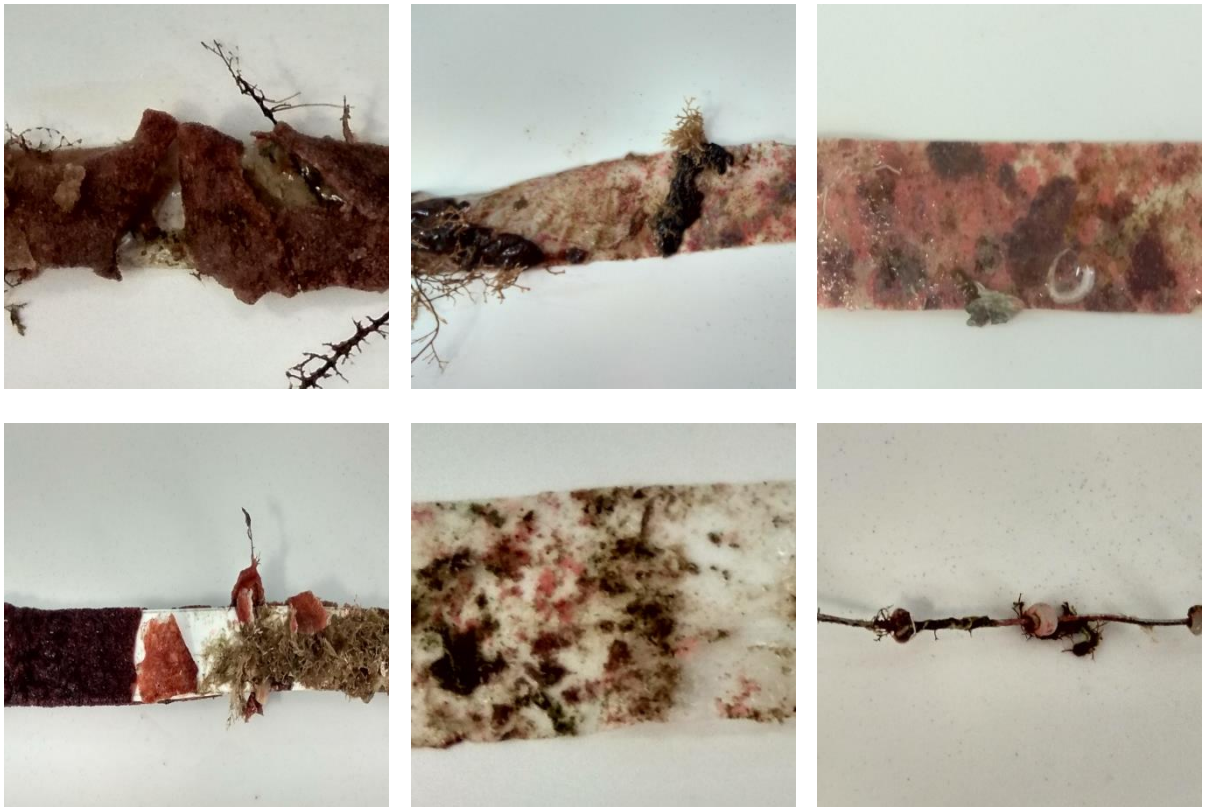

Figure S 10: LDPE strip after 300 days (top left), HDPE strip after 242 days (top middle), PP strip after 300 days (top right), PS strip after 300 days (bottom left), PET strip after 300 days (bottom middle), virgin LDPE pellets after 300 days (bottom right).

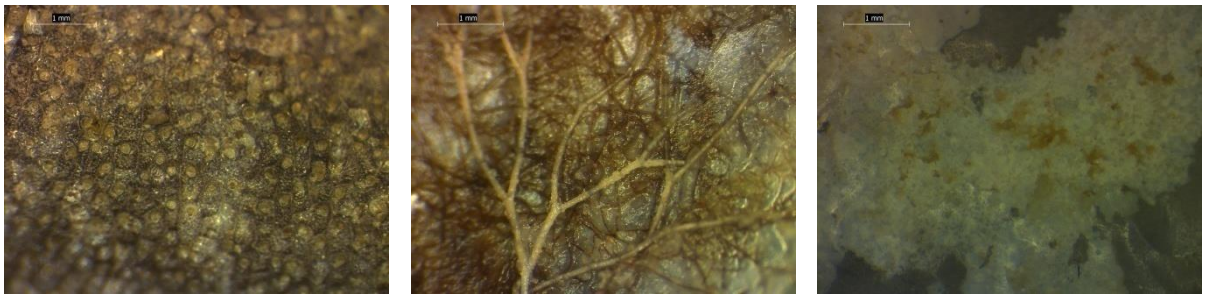

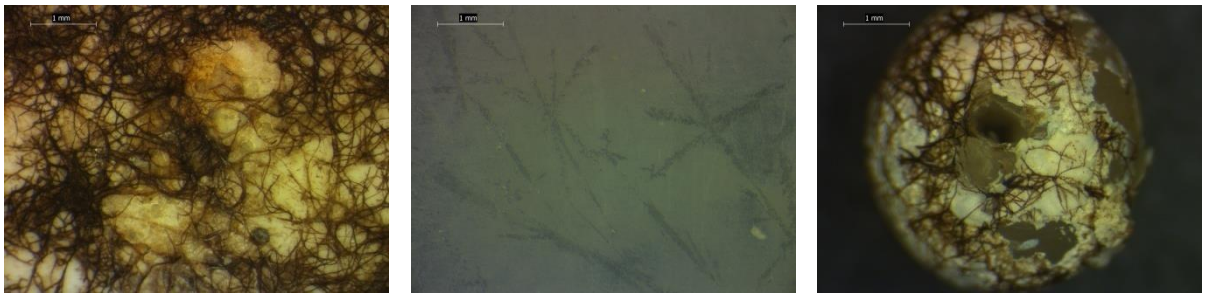

Figure S 11: Stereoscopic images of samples after 300 days in the marine environment (2x magnification): LDPE strip (top left), HDPE strip (top middle), PP strip scope (top right), PS strip (bottom left), PET strip (bottom middle), virgin LDPE pellet (bottom right)

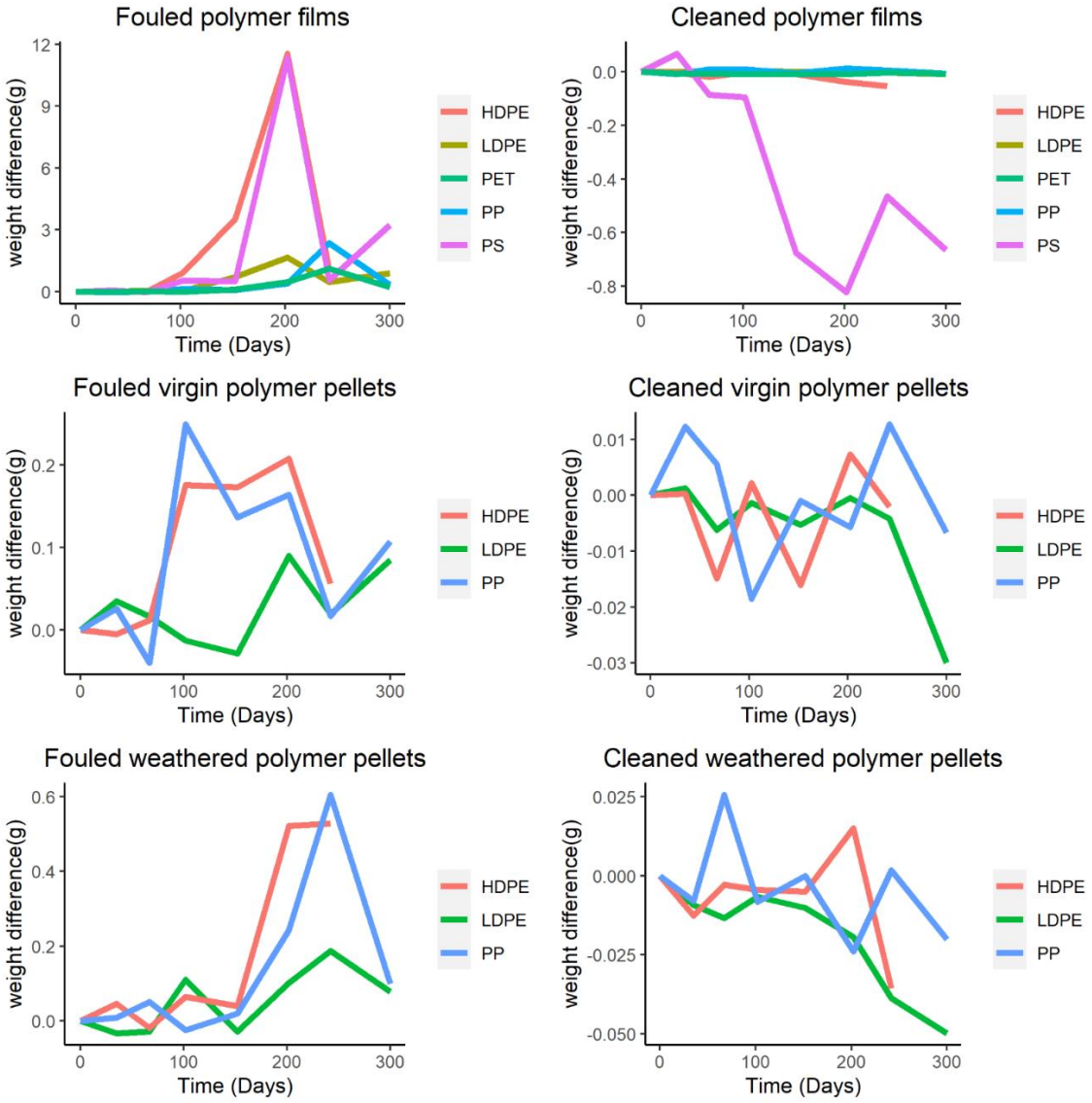

Figure S 12: Gravimetric weigh development over time.

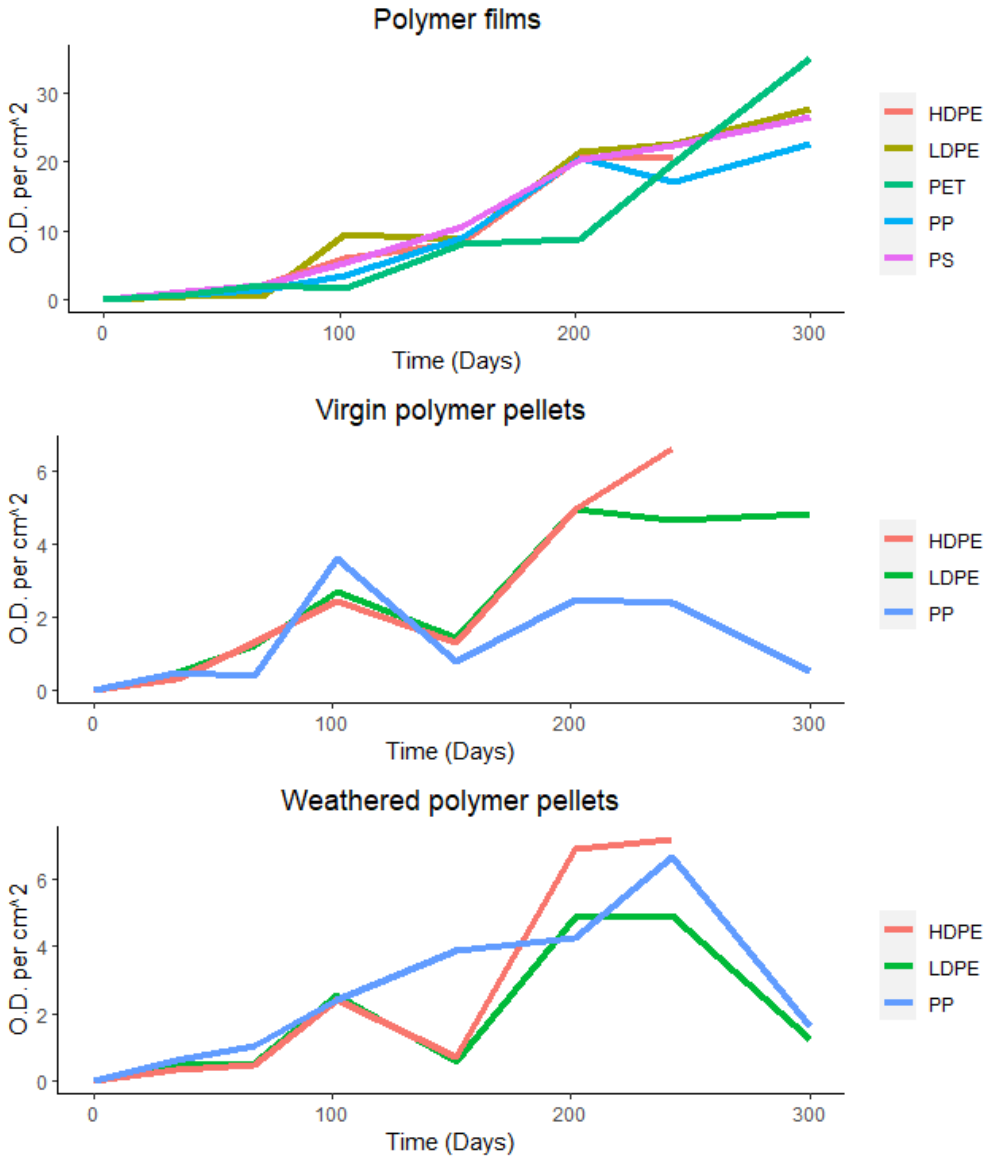

Figure S13: Biofilm attachment (expressed in Crystal Violet optical Density per cm²).

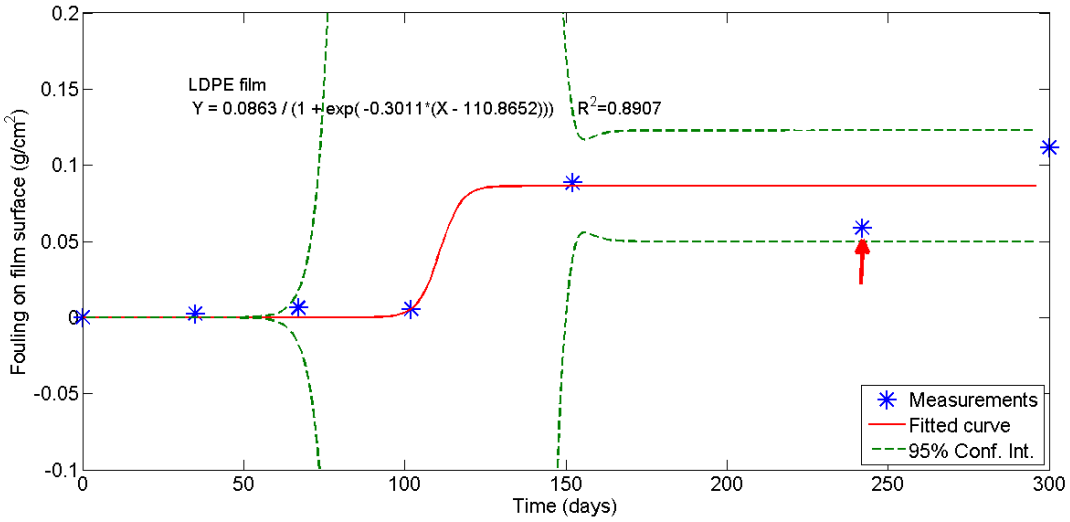

Figure S14: LDPE film fouling growth over time data curve fitting. The red arrow points to an outlier which was not included in the fitting process.

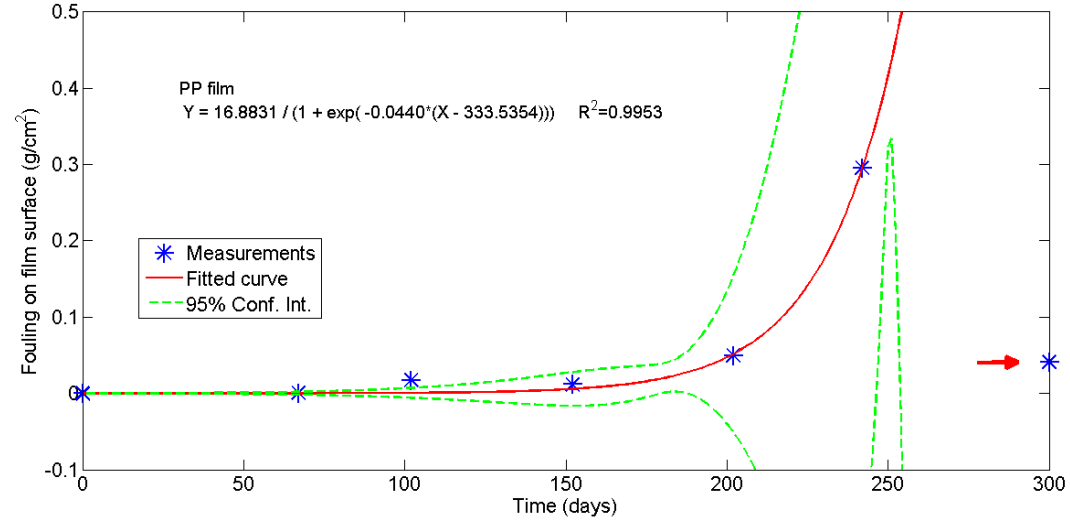

Figure S15: PP film fouling growth over time data curve fitting. The red arrow points to an outlier which was not included in the fitting process.

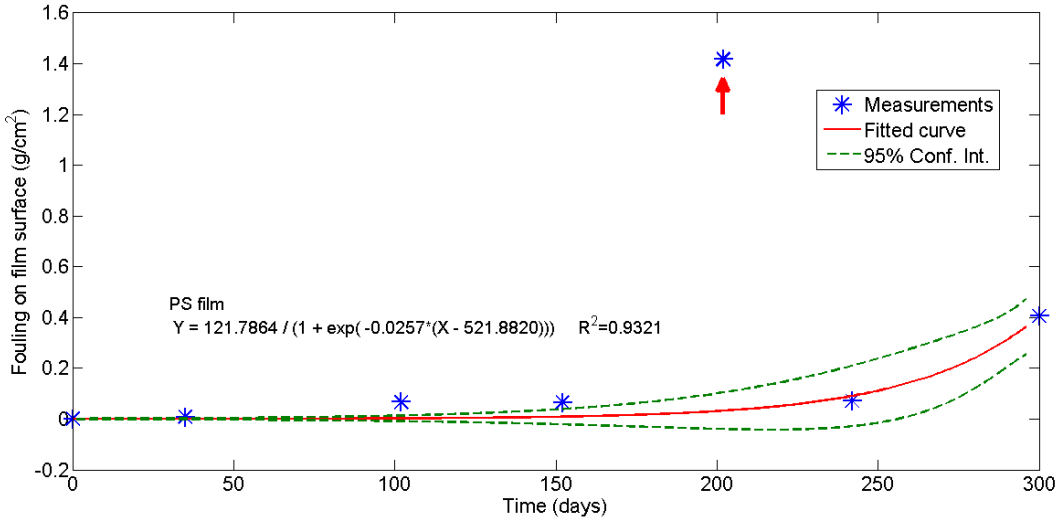

Figure S16: PS film fouling growth over time data curve fitting. The red arrow points to an outlier which was not included in the fitting process.

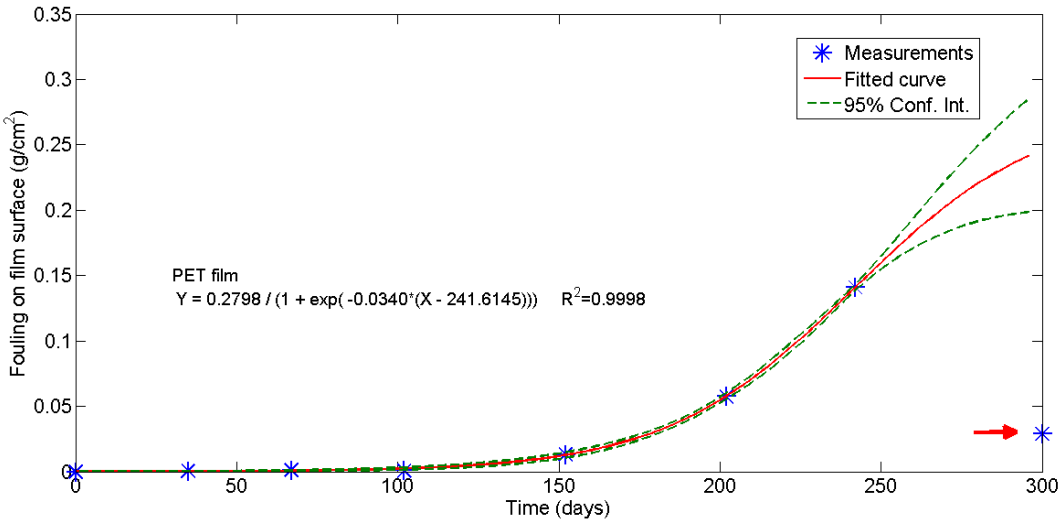

Figure S17: PET film fouling growth over time data curve fitting. The red arrow points to an outlier which was not included in the fitting process.

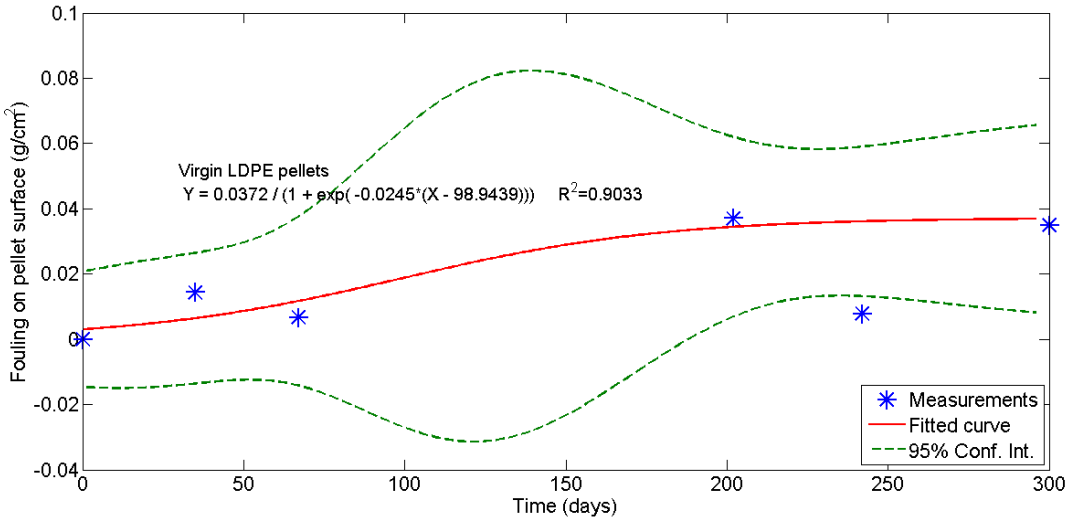

Figure S18: Virgin LDPE pellet fouling growth over time data curve fitting.

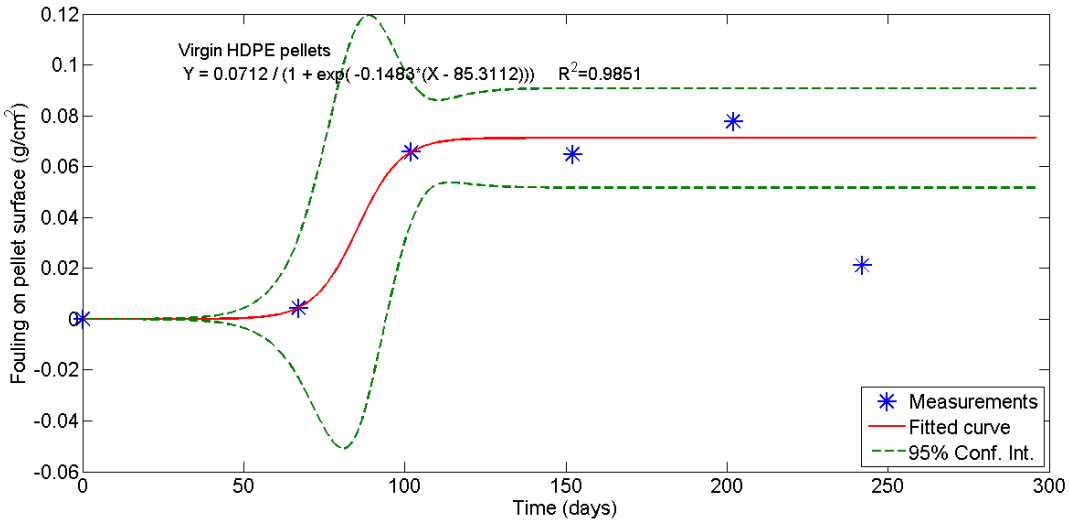

Figure S19: Virgin HDPE pellet fouling growth over time data curve fitting.

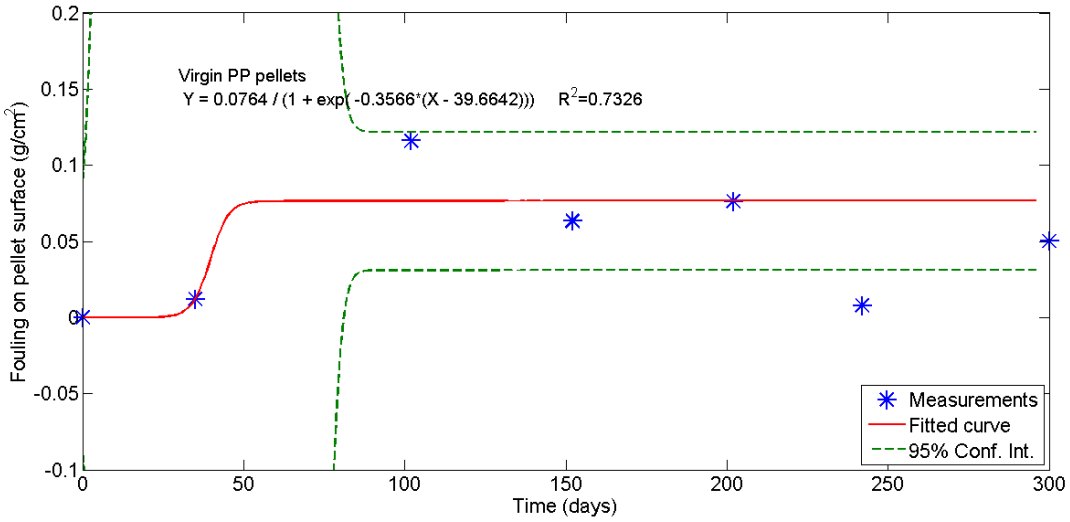

Figure S20: Virgin PP pellet fouling growth over time data curve fitting.

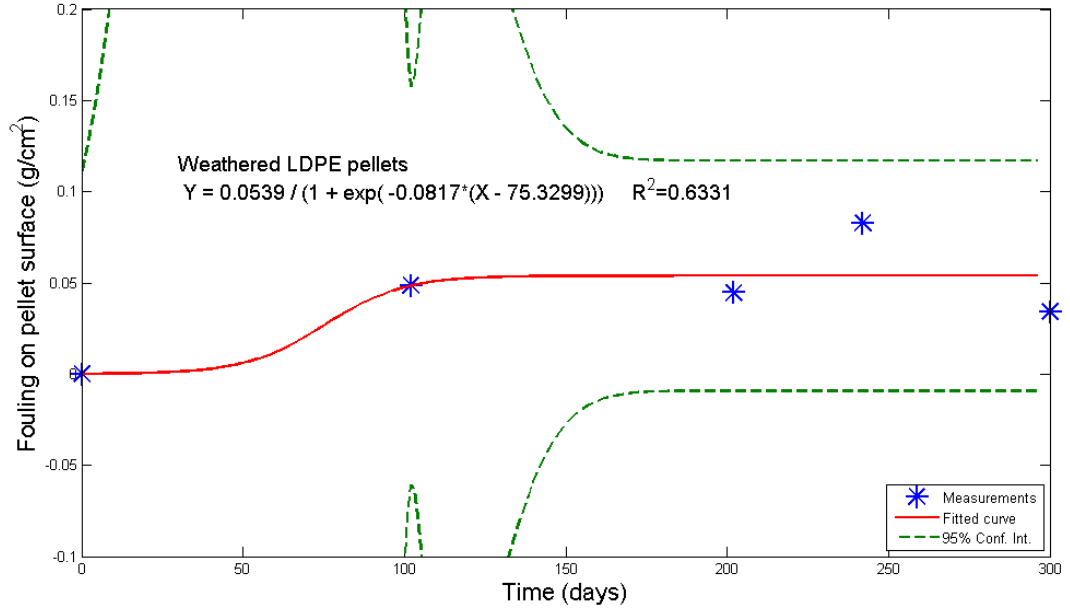

Figure S21: Weathered LDPE pellet fouling growth over time data curve fitting.

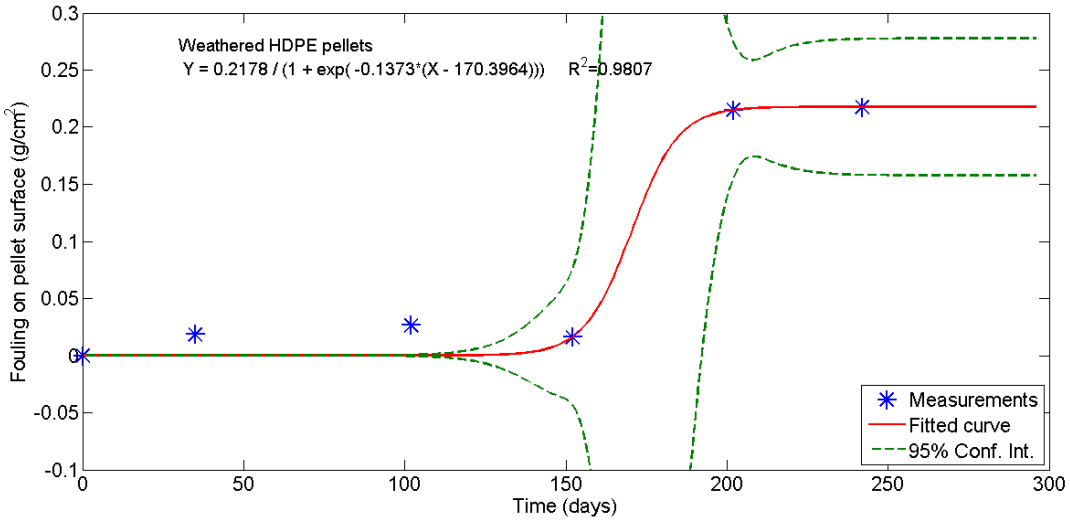

Figure S22: Weathered HDPE pellet fouling growth over time data curve fitting.

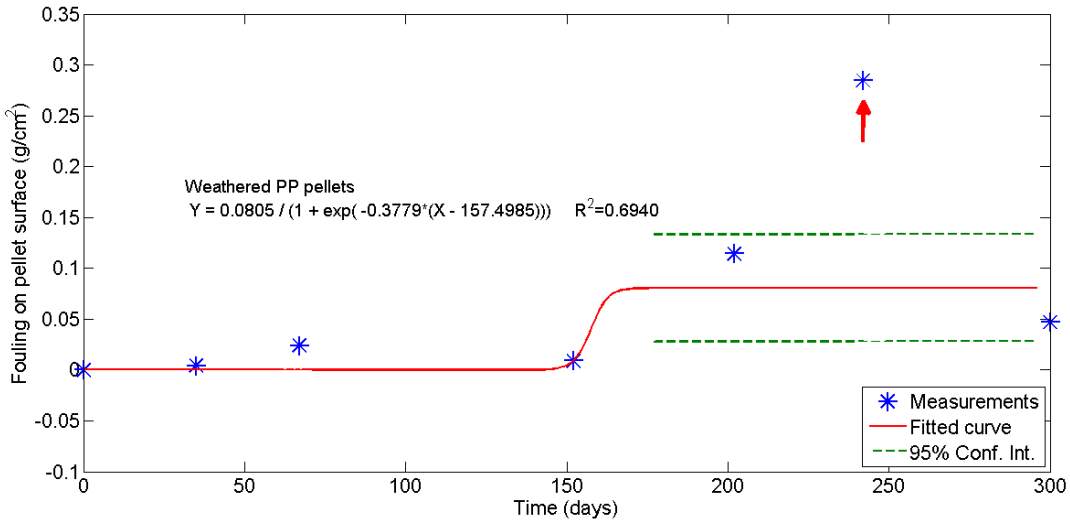

Figure S23: Weathered PP pellet fouling growth over time data curve fitting. The red arrow points to an outlier which was not included in the fitting process.

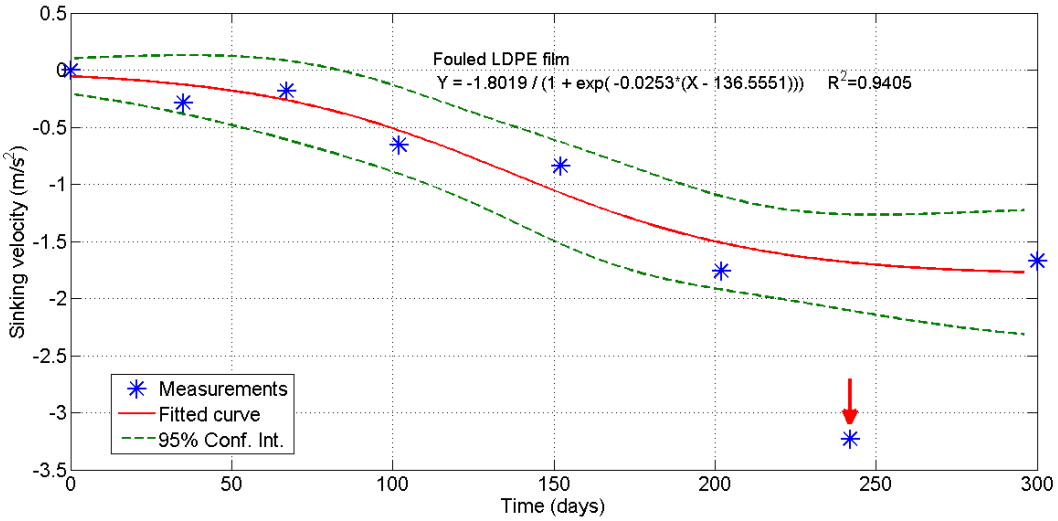

Figure S24: Fouled LDPE film sinking velocity over time data curve fitting. The red arrows point to outliers which were not included in the fitting process.

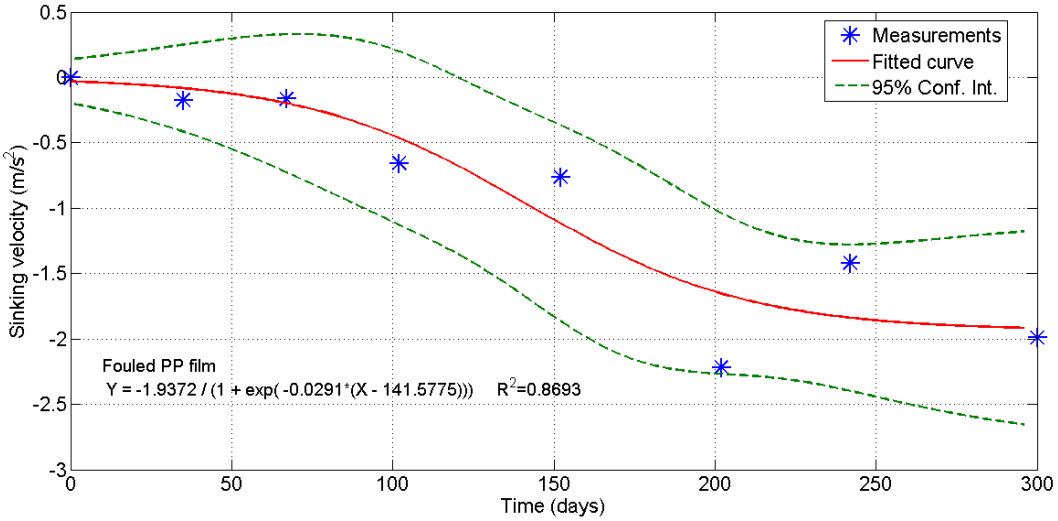

Figure S25: Fouled PP film sinking velocity over time data curve fitting.

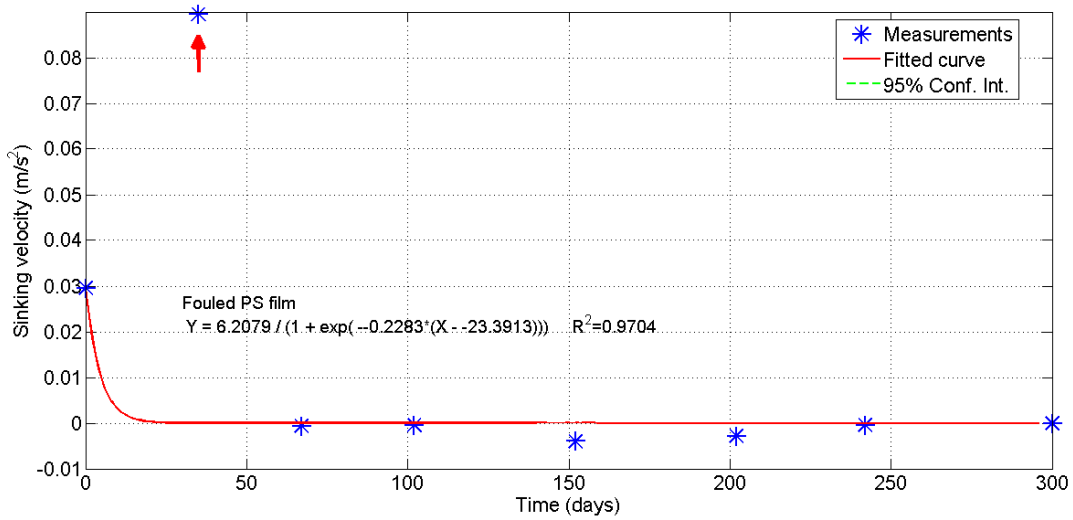

Figure S 26: Fouled PS film sinking velocity over time data curve fitting. The red arrow points to an outlier which was not included in the fitting process.

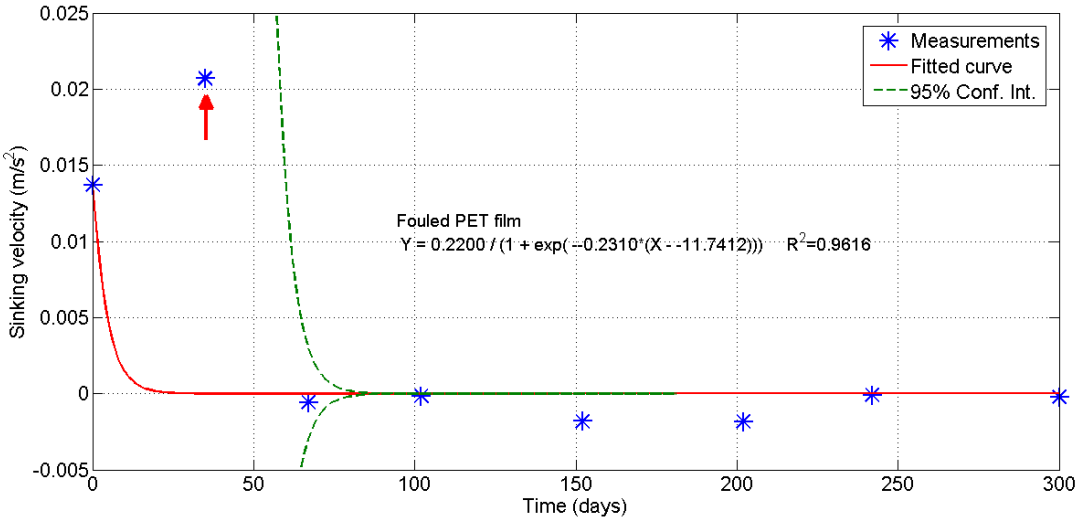

Figure S 27: Fouled PET film sinking velocity over time data curve fitting. The red arrow points to an outlier which was not included in the fitting process.

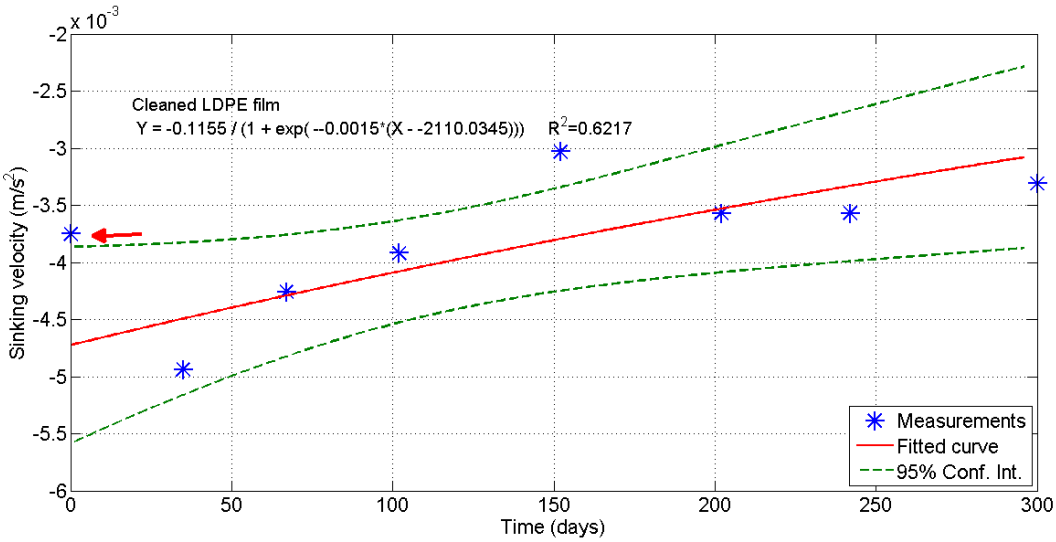

Figure S 28: Cleaned LDPE film sinking velocity over time data curve fitting. The red arrow points to an outlier which was not included in the fitting process.

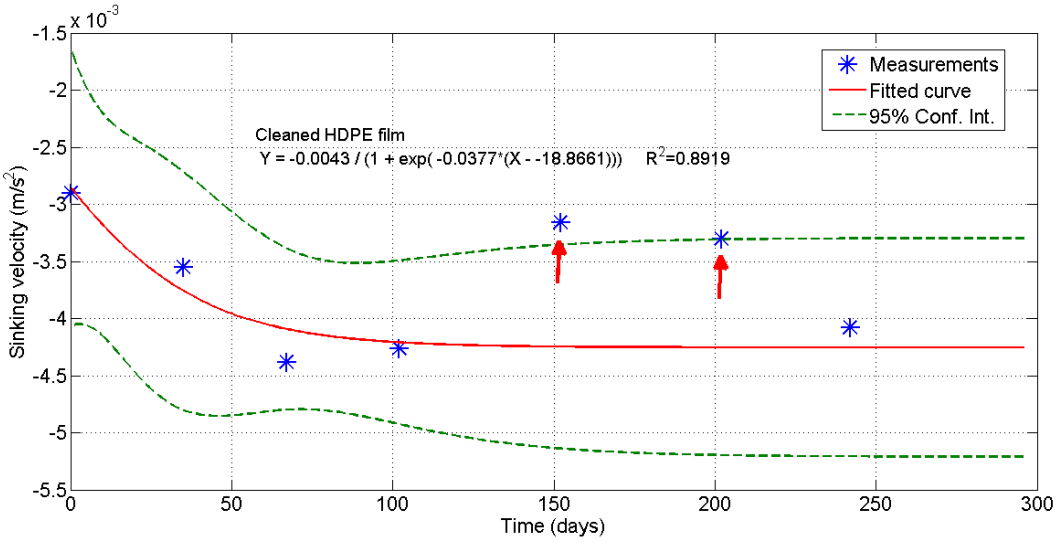

Figure S 29: Cleaned HDPE film sinking velocity over time data curve fitting. The red arrows point to outliers which were not included in the fitting process.

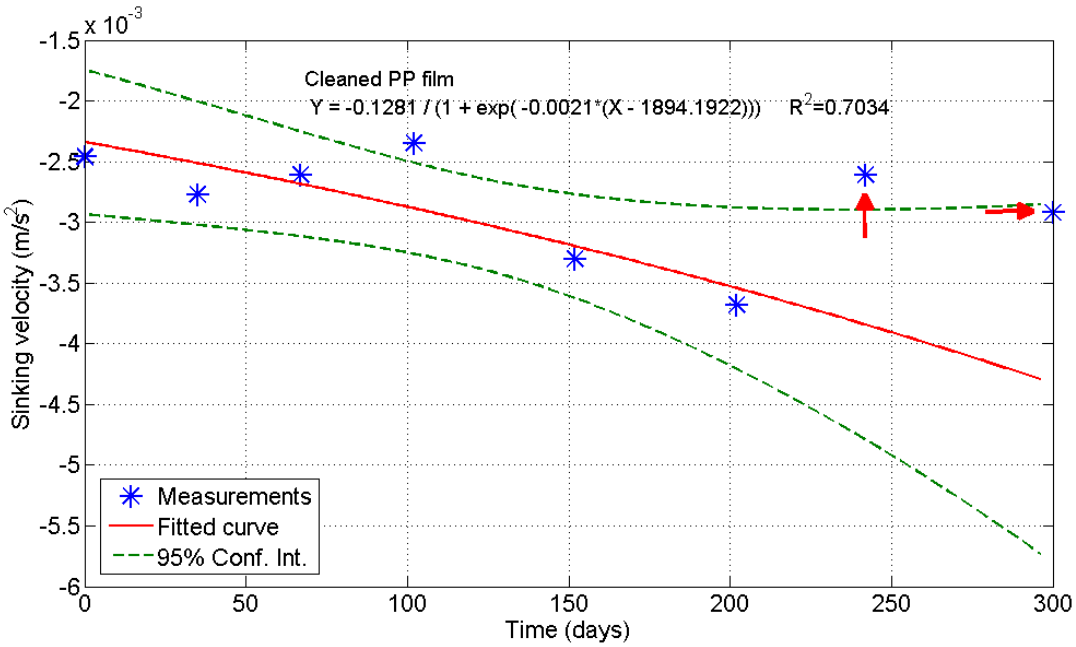

Figure S 30: Cleaned PP film sinking velocity over time data curve fitting. The red arrows point to outliers which were not included in the fitting process.

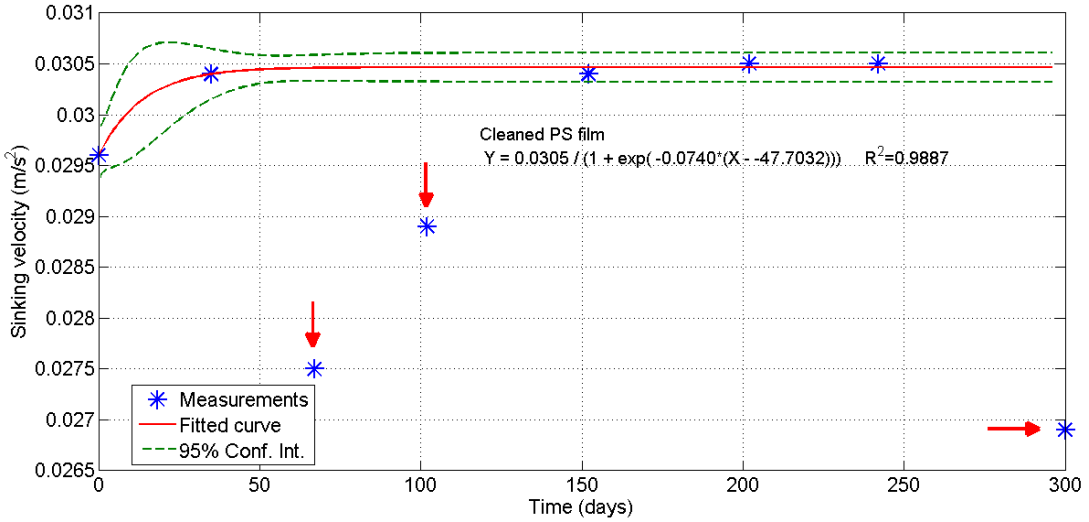

Figure S 31: Cleaned PS film sinking velocity over time data curve fitting. The red arrows point to outliers which were not included in the fitting process.

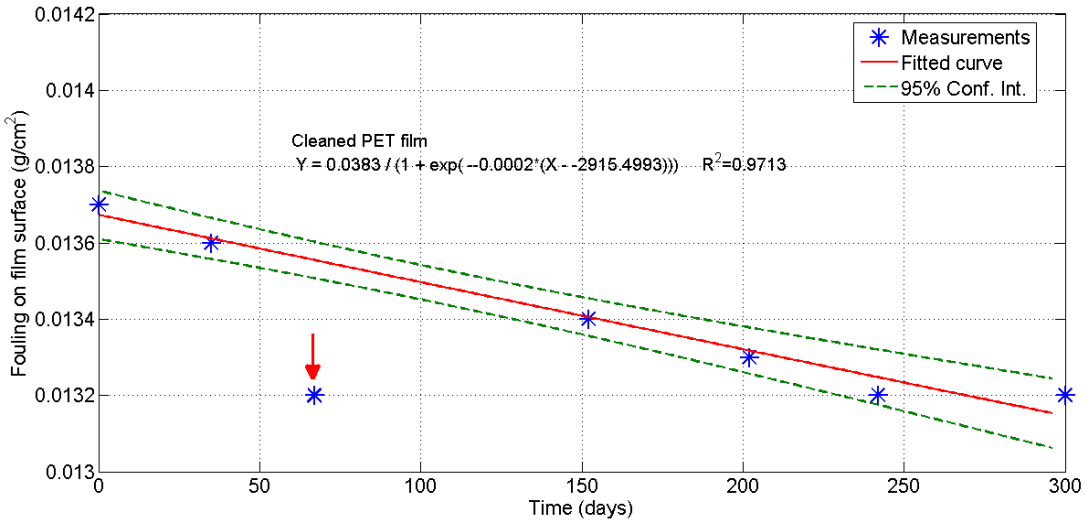

Figure S 32: Cleaned PET film sinking velocity over time data curve fitting. The red arrow points to an outlier which was not included in the fitting process.

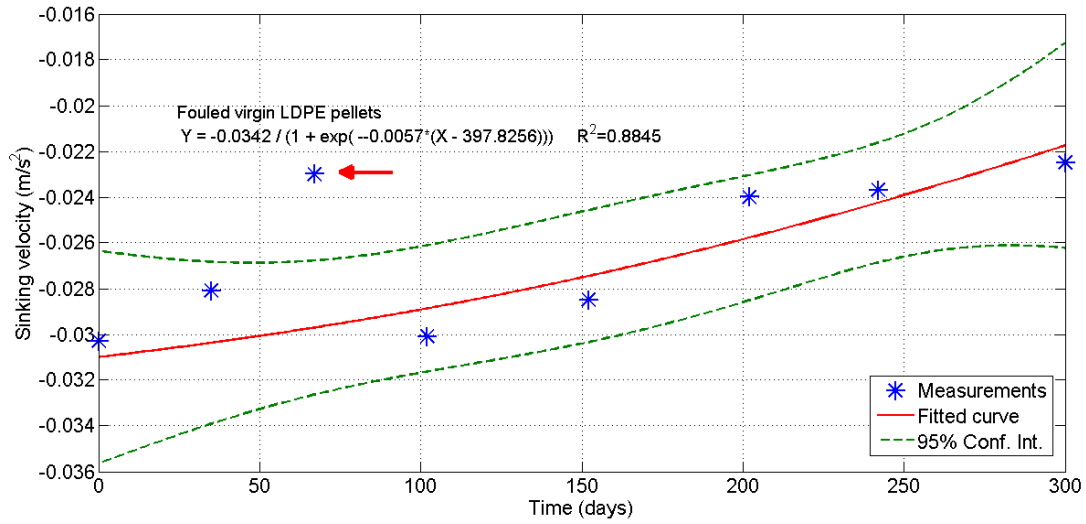

Figure S 33: Fouled virgin LDPE pellet sinking velocity over time data curve fitting. The red arrow points to an outlier which was not included in the fitting process.

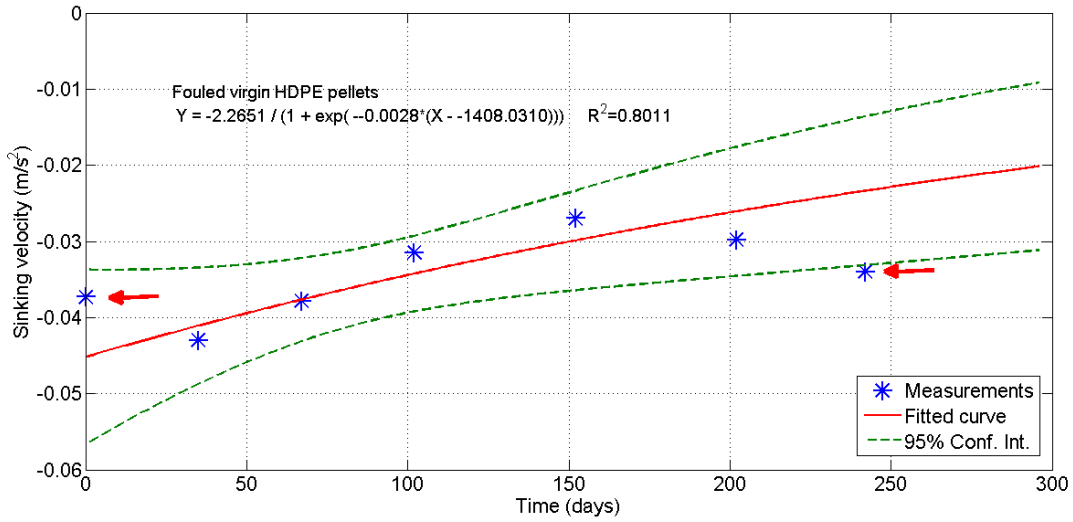

Figure S 34: Fouled virgin HDPE pellet sinking velocity over time data curve fitting. The red arrow points to an outlier which was not included in the fitting process.

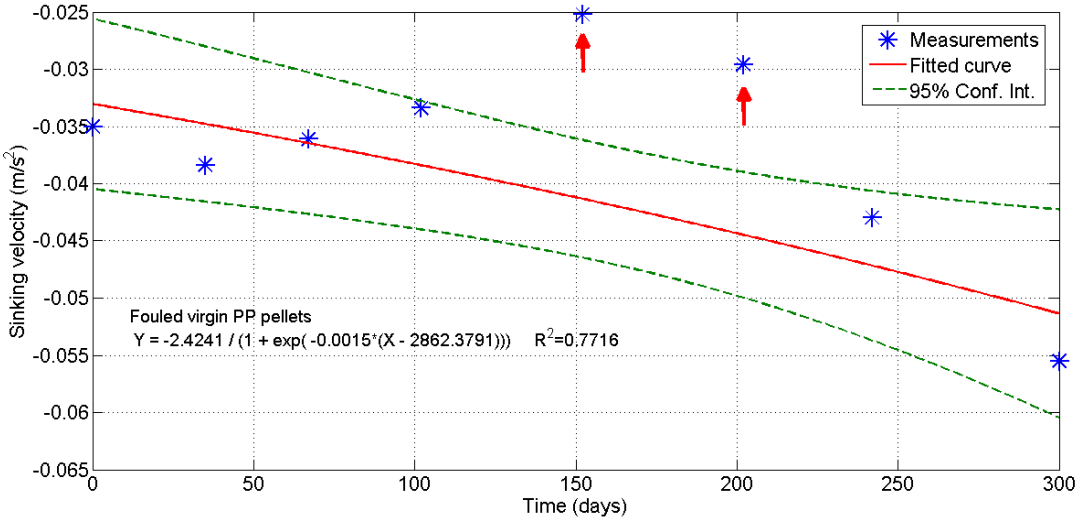

Figure S 35: Fouled virgin PP pellet sinking velocity over time data curve fitting. The red arrows point to outliers which were not included in the fitting process.

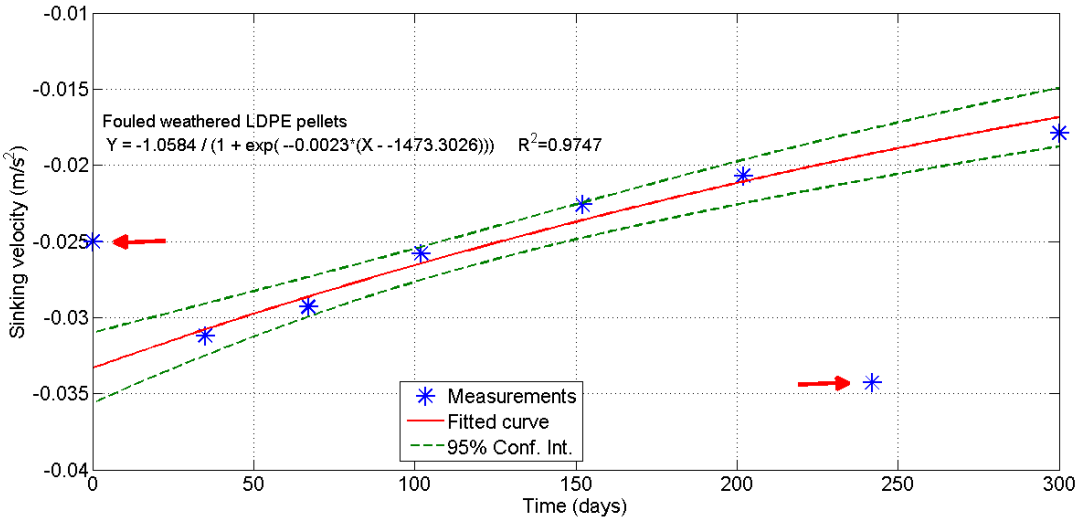

Figure S 36: Fouled weathered LDPE pellet sinking velocity over time data curve fitting. The red arrows point to outliers which were not included in the fitting process.

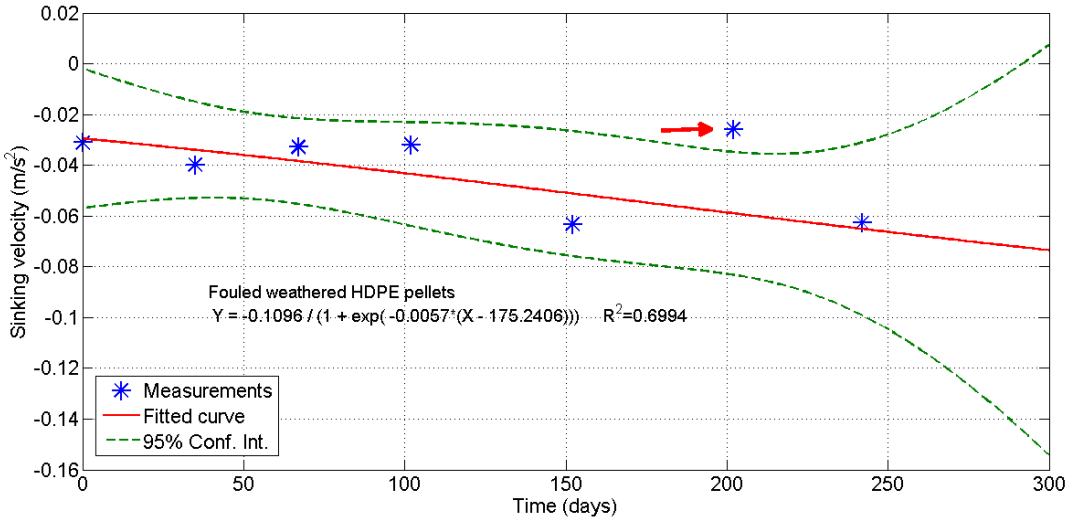

Figure S 37: Fouled weathered HDPE pellet sinking velocity over time data curve fitting. The red arrow points to an outlier which was not included in the fitting process.

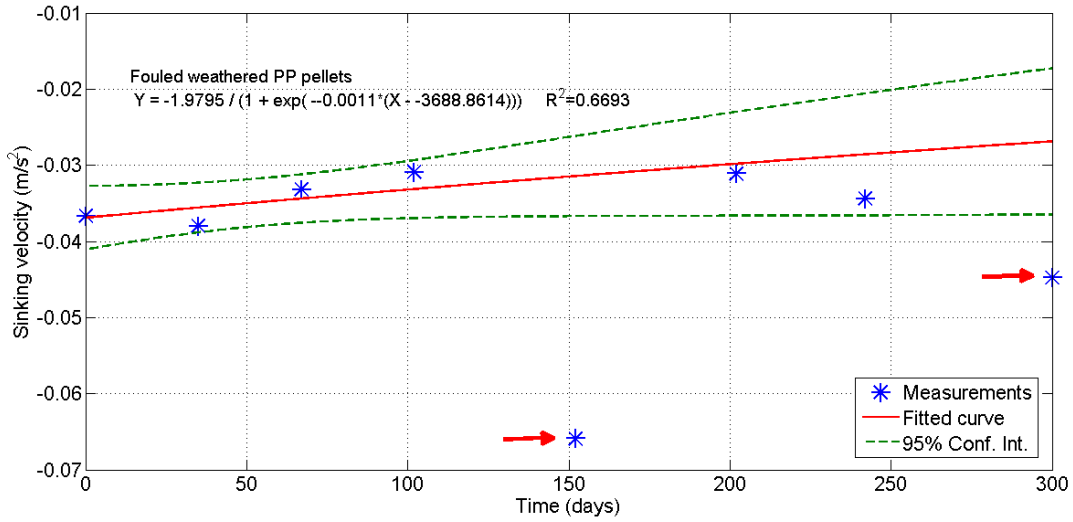

Figure S 38: Fouled weathered PP pellet sinking velocity over time data curve fitting. The red arrows point to outliers which were not included in the fitting process.

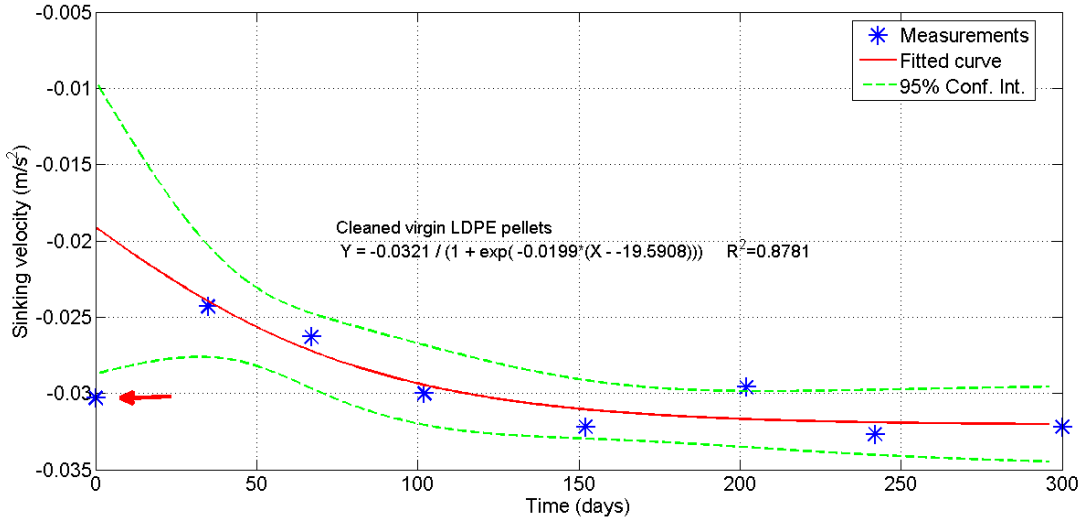

Figure S 39: Cleaned virgin LDPE pellet sinking velocity over time data curve fitting. The red arrow points to an outlier which was not included in the fitting process.

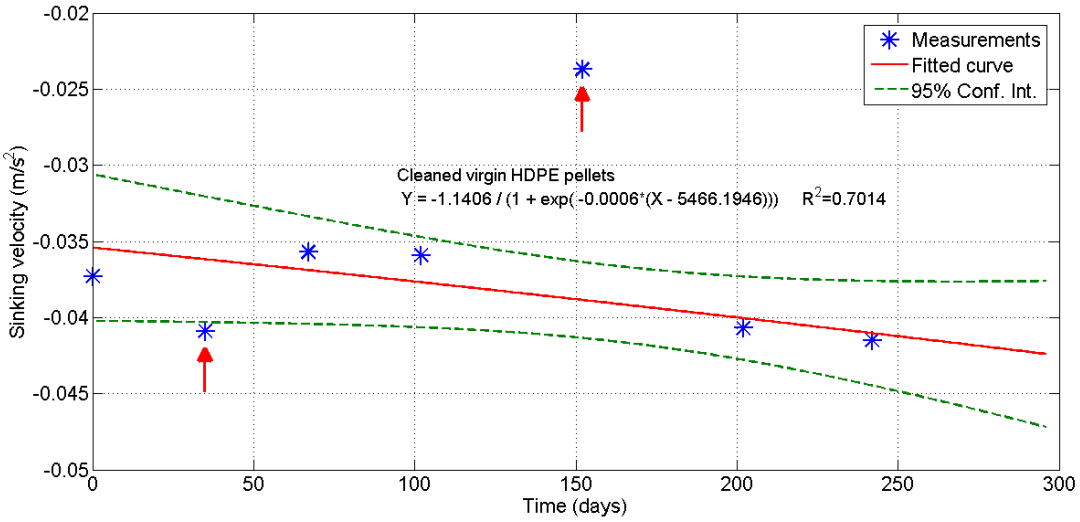

Figure S 40: Cleaned virgin HDPE pellet sinking velocity over time data curve fitting. The red arrows point to outliers which were not included in the fitting process.

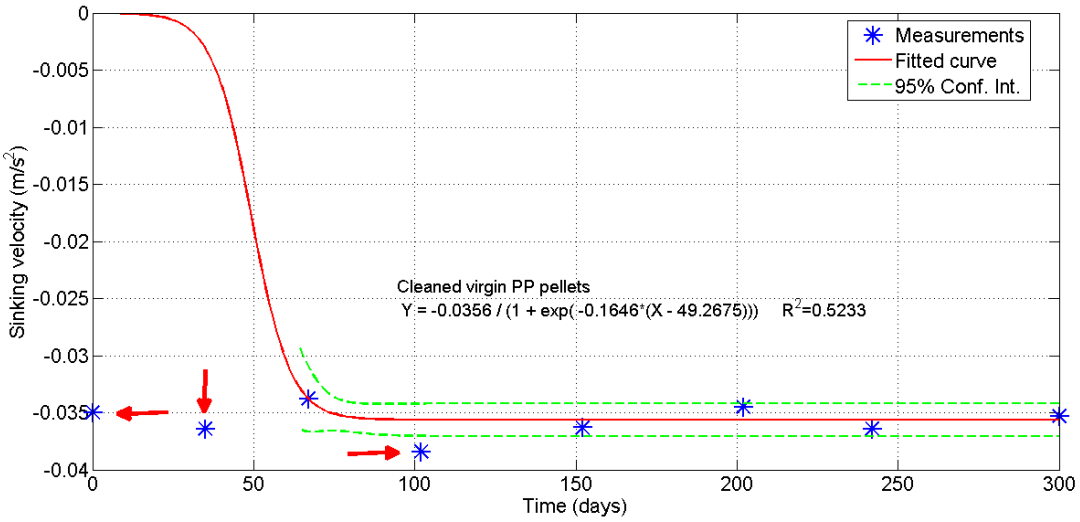

Figure S 41: Fouled virgin PP pellet sinking velocity over time data curve fitting. The red arrows point to outliers which were not included in the fitting process.

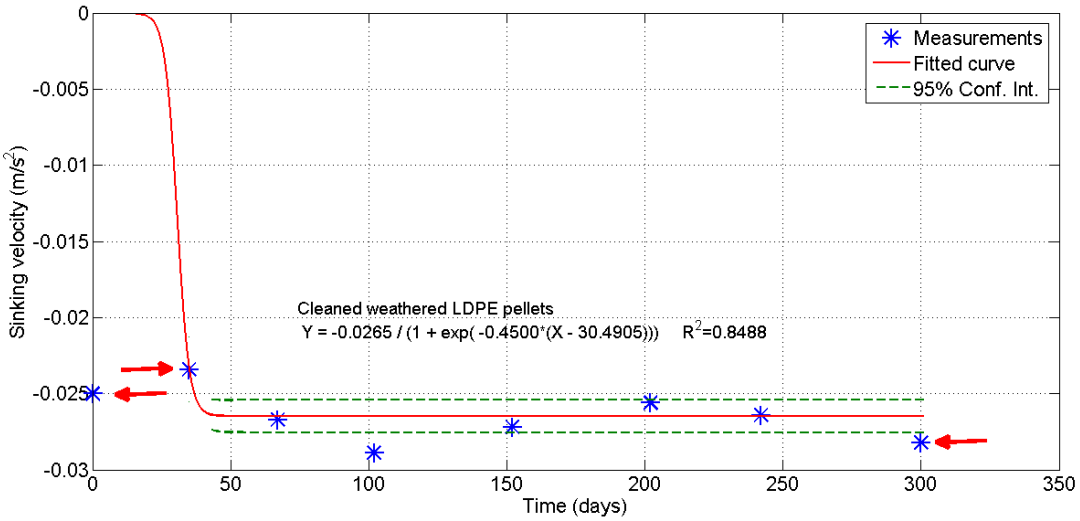

Figure S 42: Cleaned weathered LDPE pellet sinking velocity over time data curve fitting. The red arrows point to outliers which were not included in the fitting process.

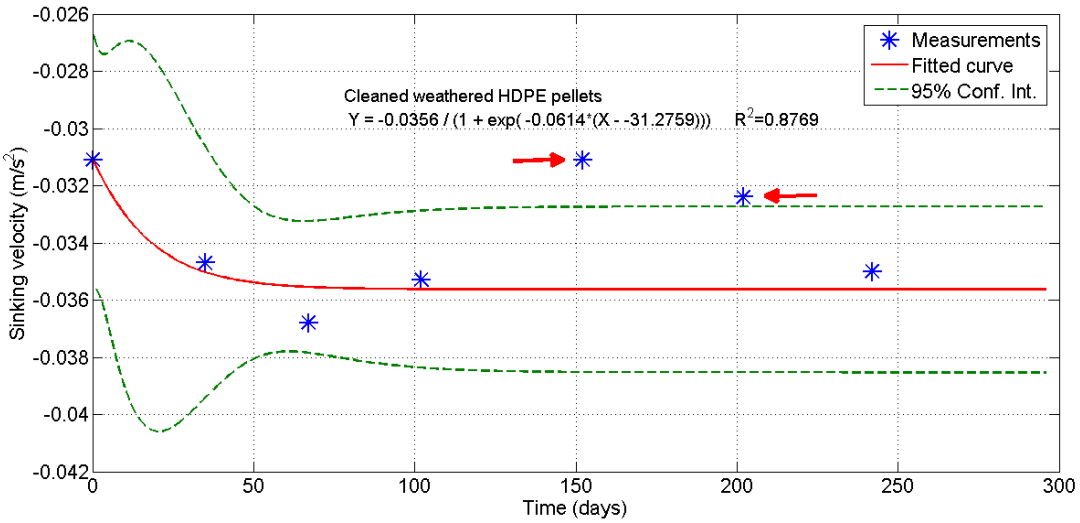

Figure S 43: Cleaned weathered HDPE pellet sinking velocity over time data curve fitting. The red arrows point to outliers which were not included in the fitting process.

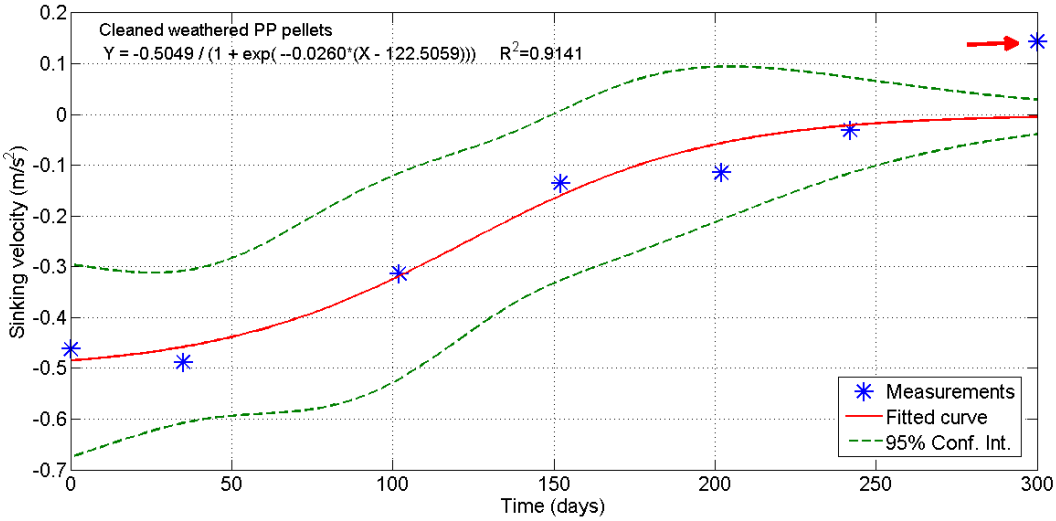

Figure S 44: Cleaned weathered PP pellet sinking velocity over time data curve fitting. The red arrow points to an outlier which was not included in the fitting process.

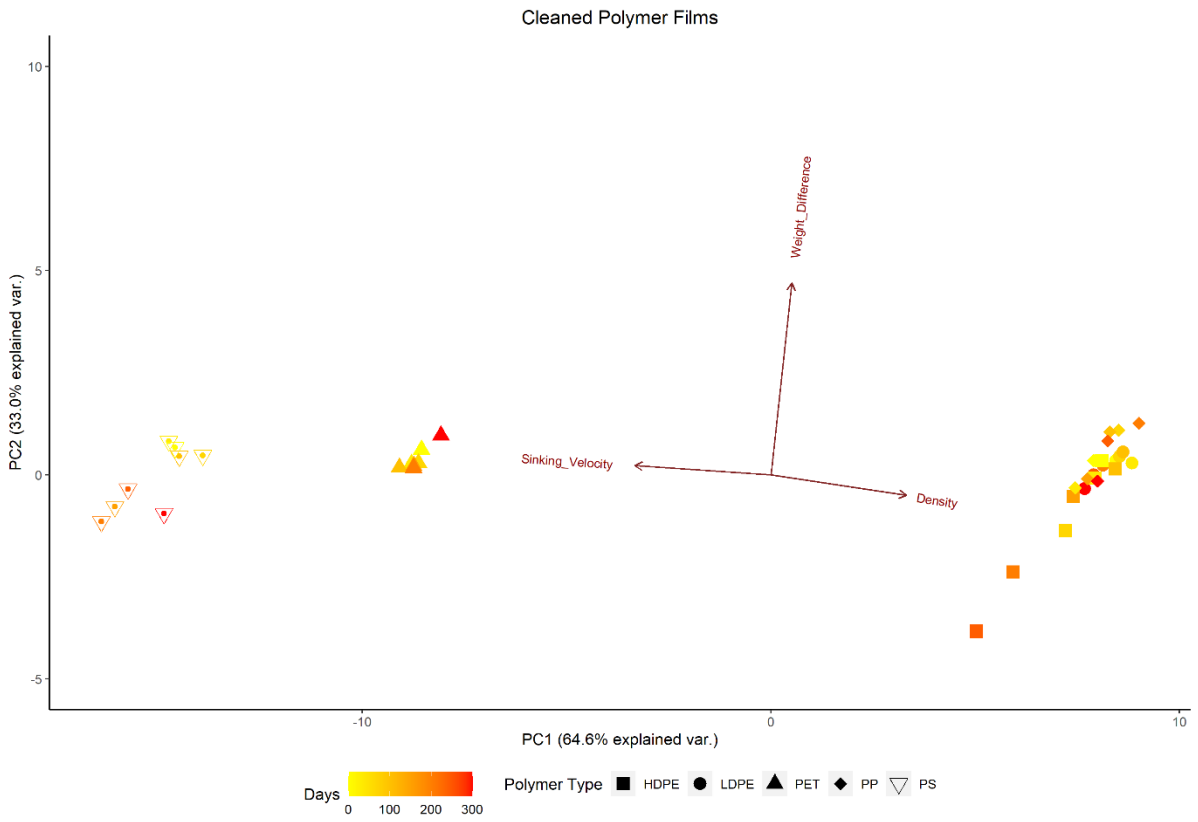

Figure S 45: PCA of cleaned polymer films

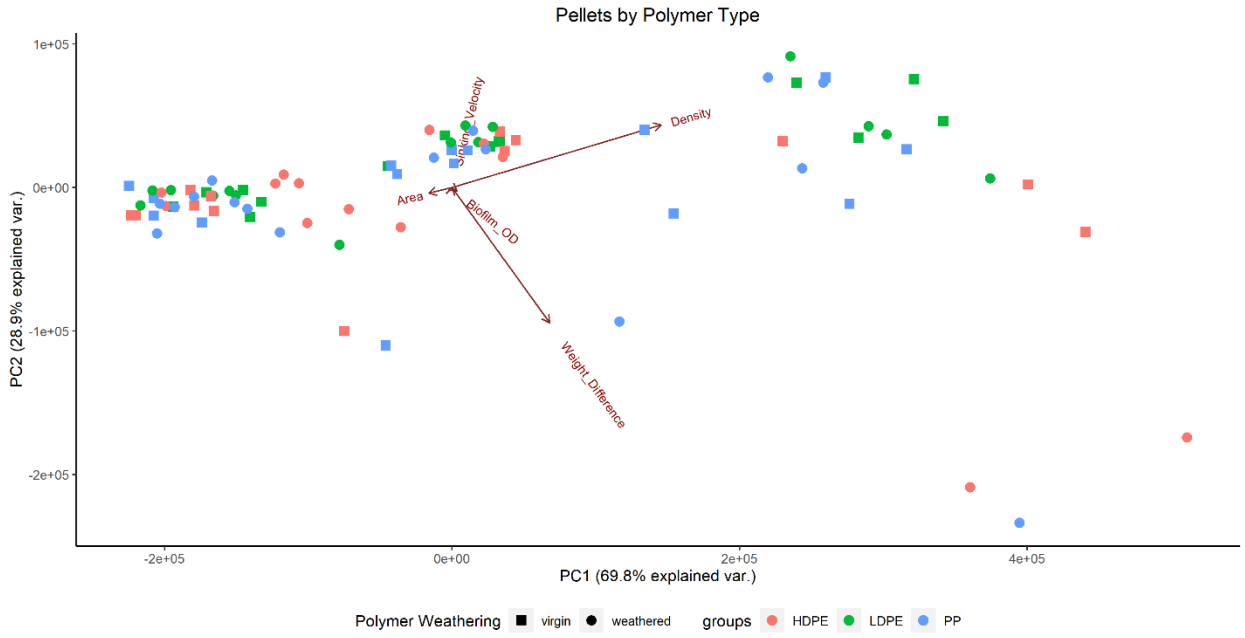

Figure S 46: PCA of pellets by polymer type

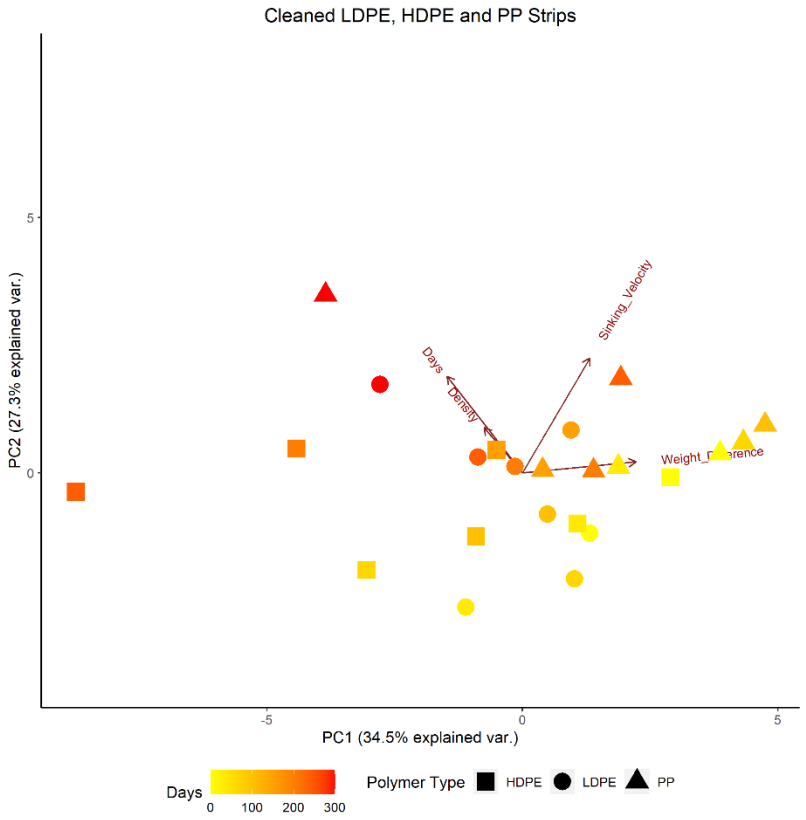

Figure S 47: PCA of cleaned LDPE, HDPE and PP films

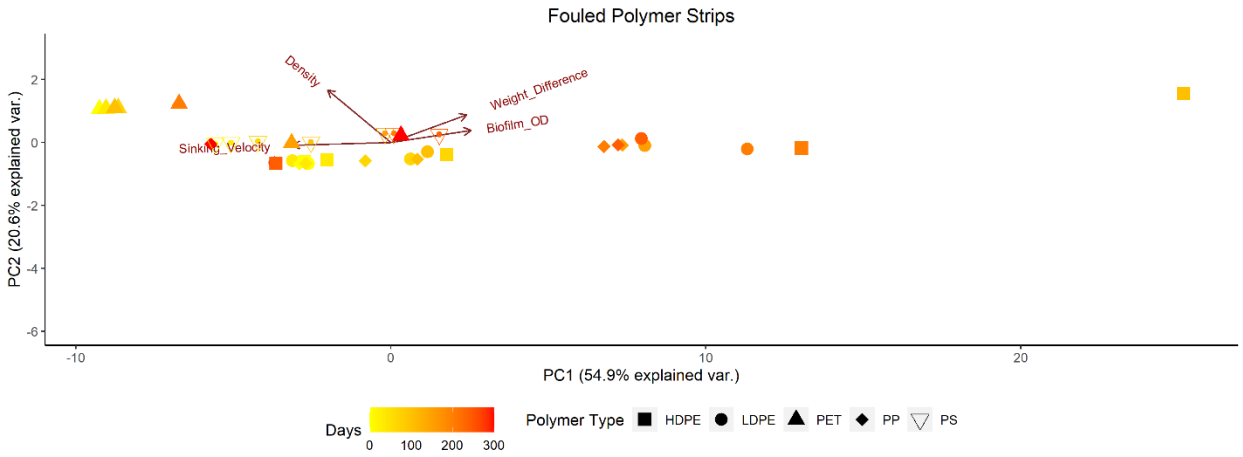

Figure S 48: PCA of fouled polymer films

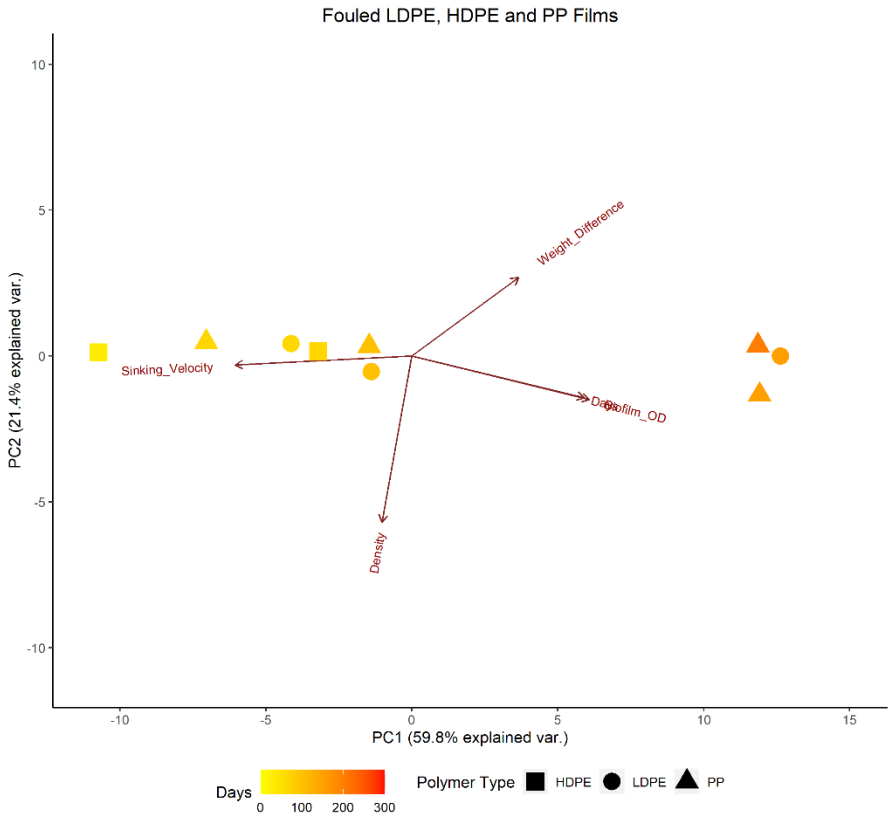

Figure S 49: PCA of fouled LDPE, HDPE and PP strips

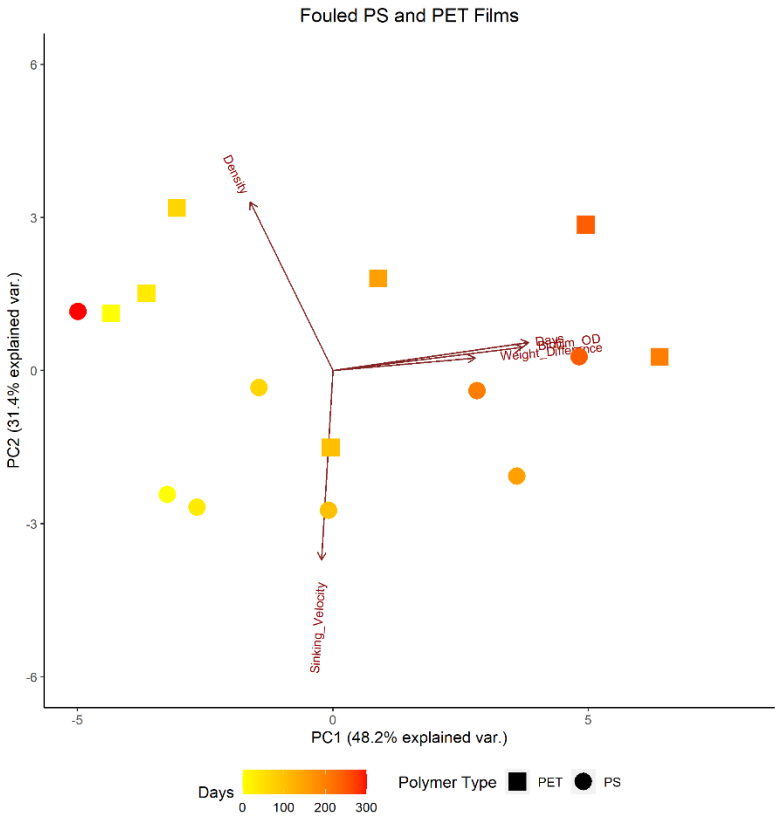

Figure S 50: PCA of fouled PS and PET strips

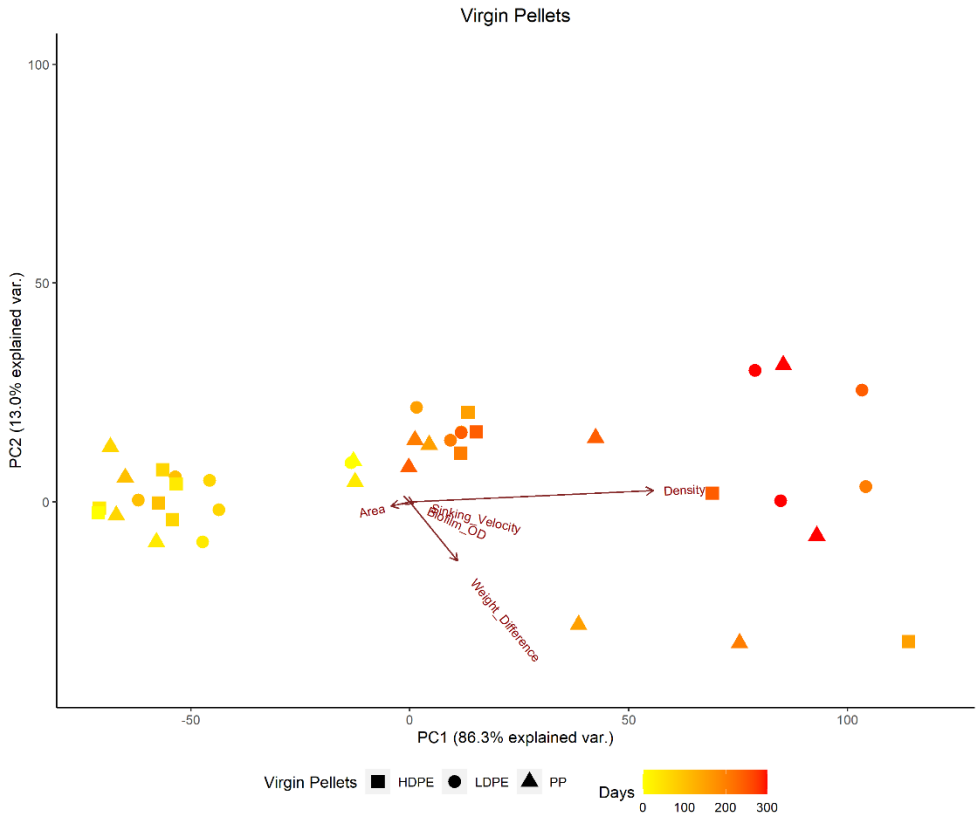

Figure S 51: PCA of virgin pellets

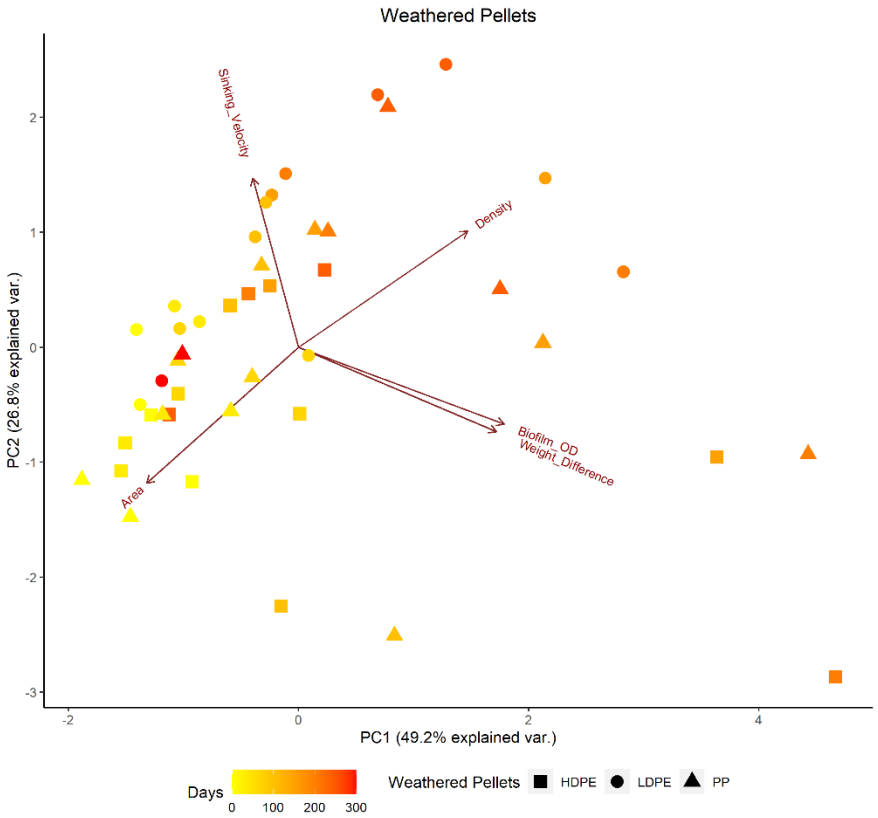

Figure S 52: PCA of weathered pellets.

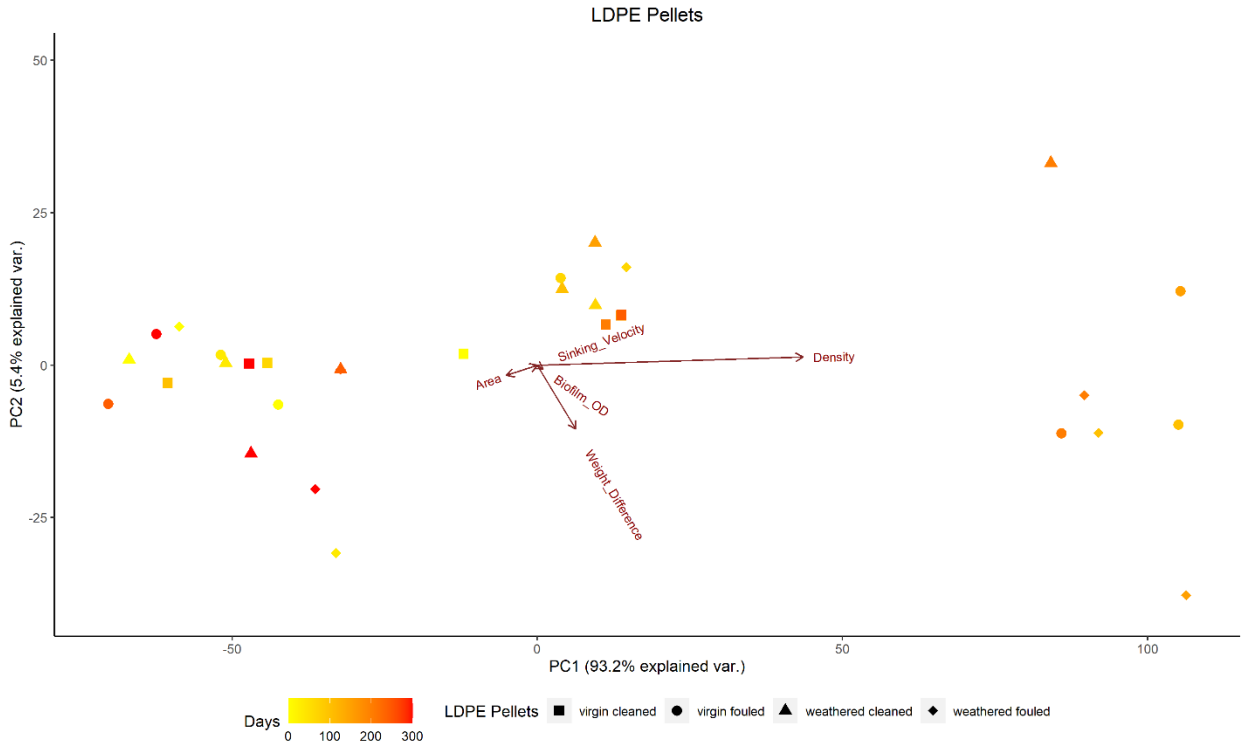

Figure S 53: PCA of LDPE pellets.

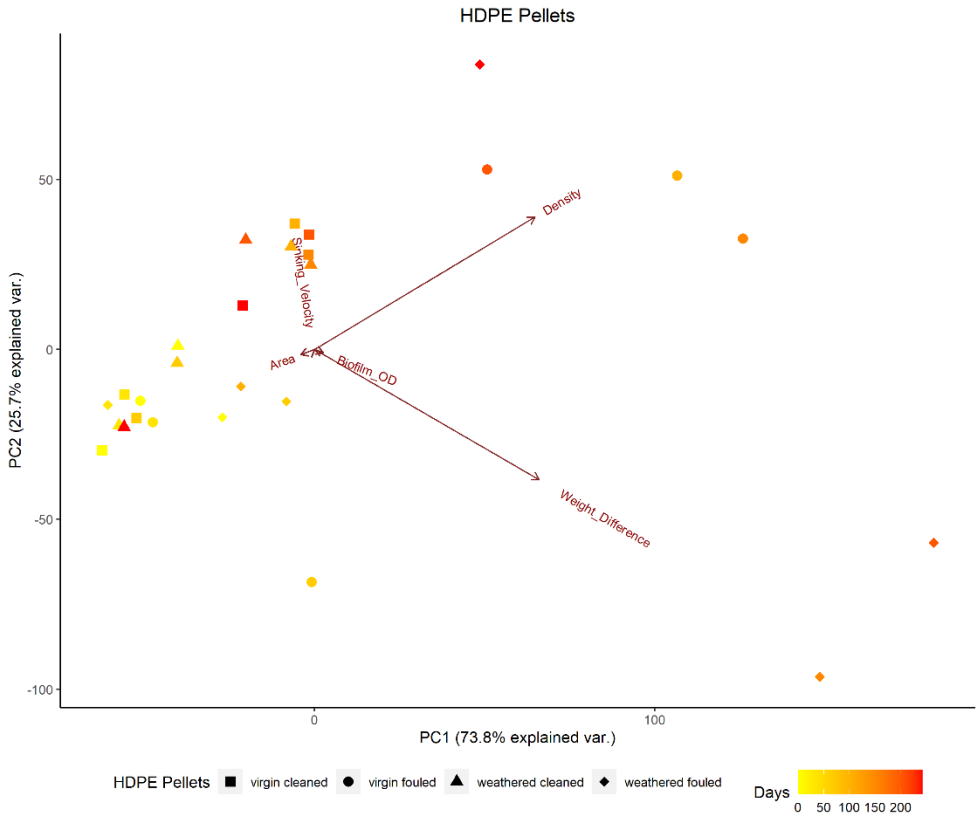

Figure S 54: PCA of HDPE pellets

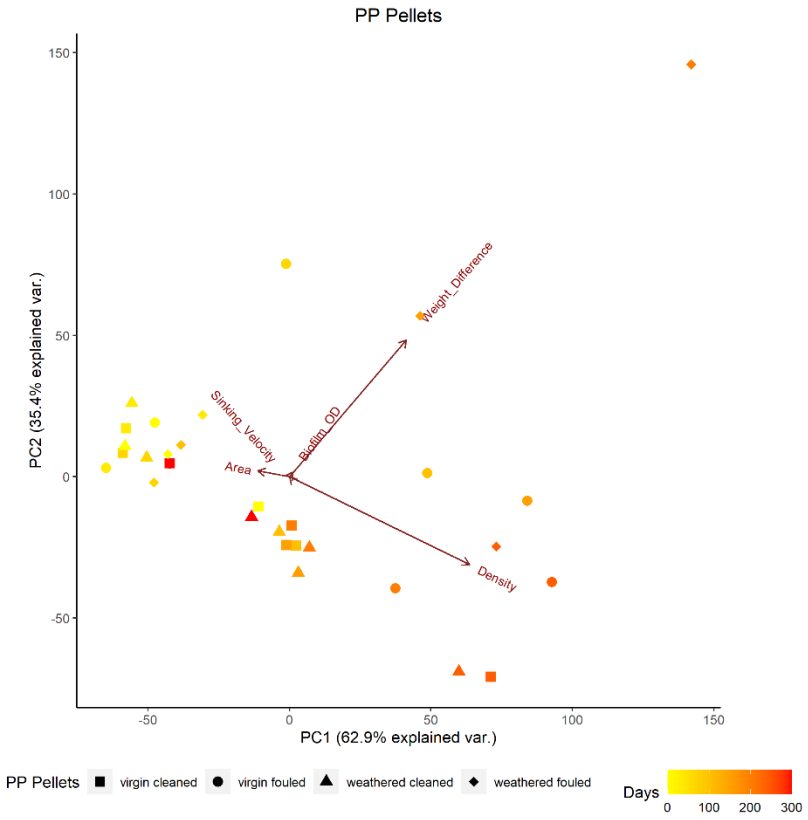

Figure S 55: PCA of PP pellets

a

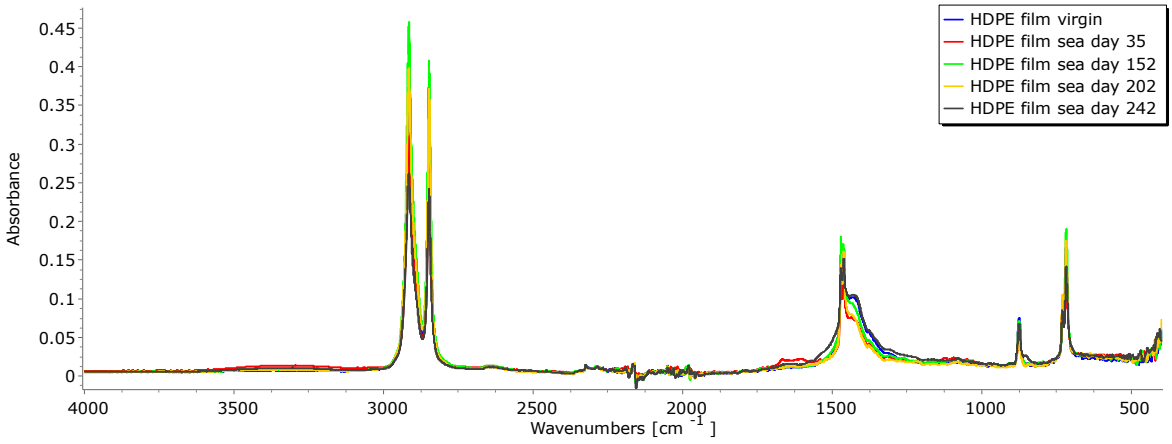

b

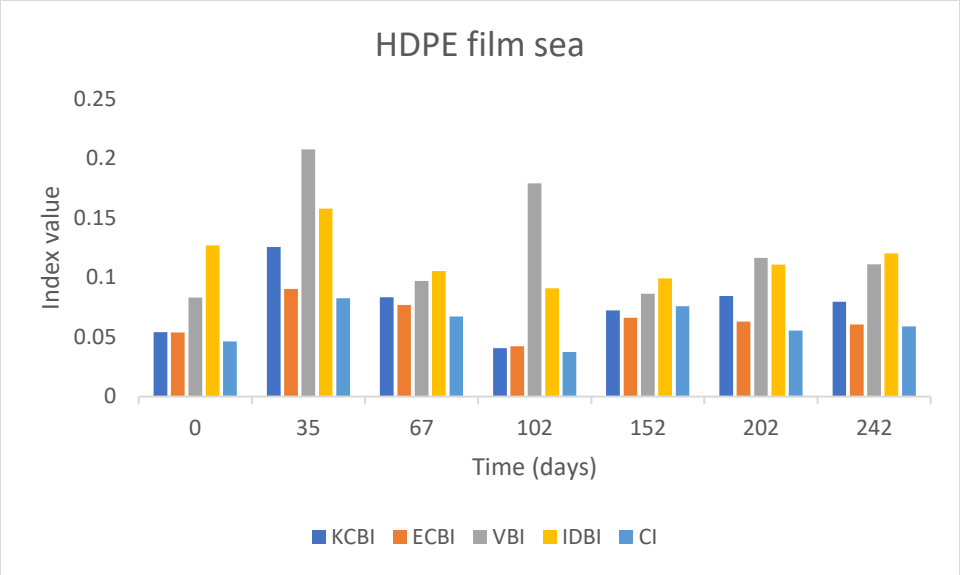

Figure S 56: (a) ATR-FTIR spectra of HDPE samples over time. (b) Index values for HDPE over time.

a

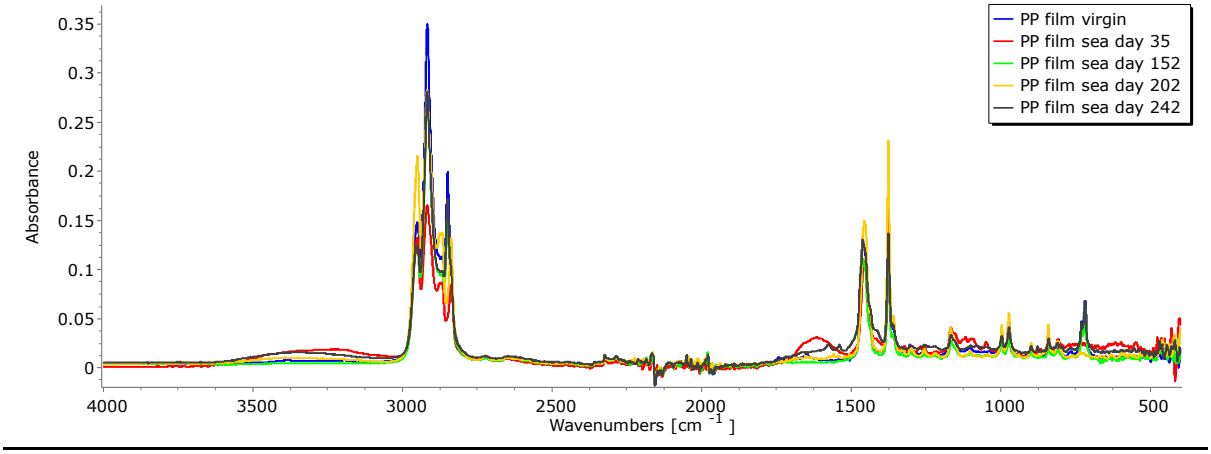

b

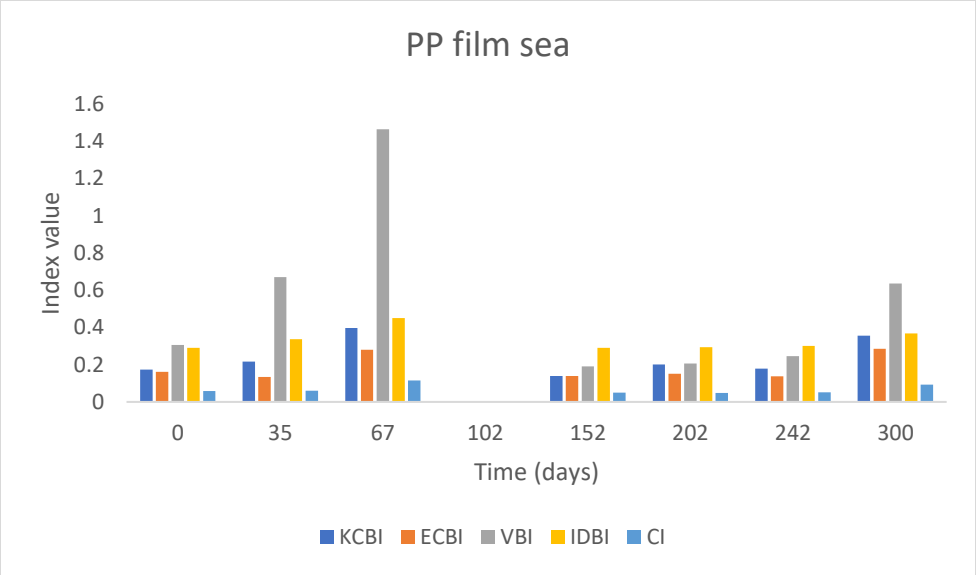

Figure S 57: (a) ATR-FTIR spectra of PP samples over time. (b) Index values for PP over time.

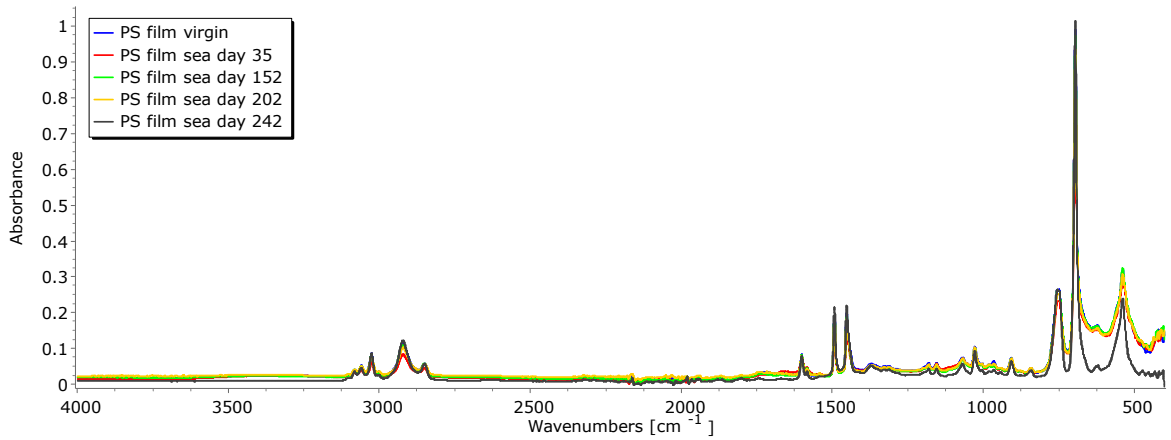

Figure S 58: ATR-FTIR spectrum of PS samples over time.

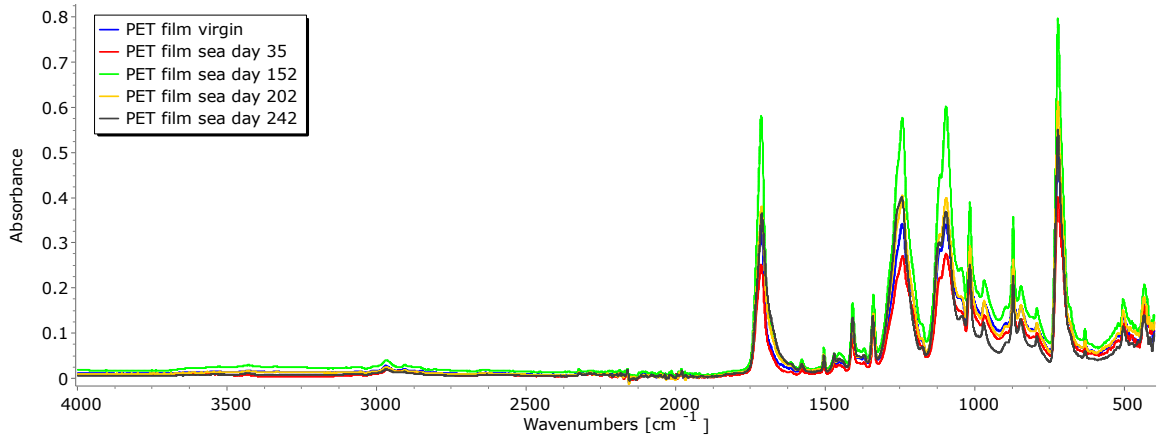

Figure S 59: ATR-FTIR spectra of PET samples over time.

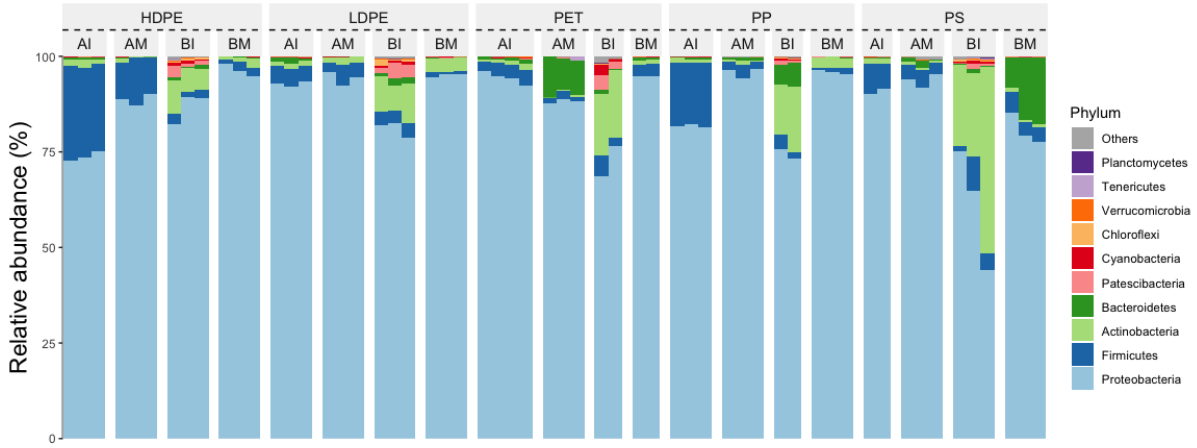

Figure S 60: Relative abundance of bacterial phyla present in bacterial biofilm collected from the surface of each polymer type, associated with fouling phase (AI, After removal Initial; AM, After removal Mature; BI, Before removal Initial; BM, Before removal Mature).

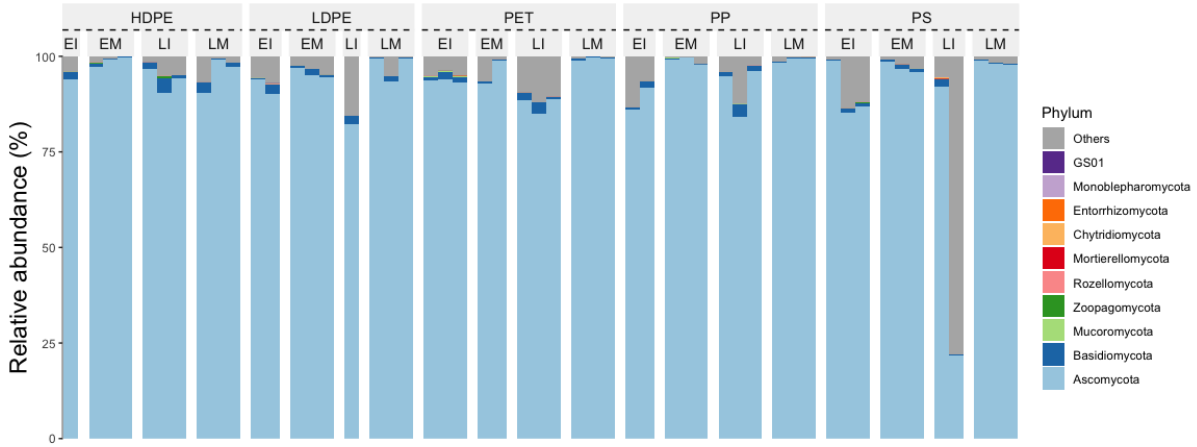

Figure S 61: Relative abundance of fungal phyla in fungal assemblages collected from the surface of each polymer type, associated with fouling phase (AI, After removal Initial; AM, After removal Mature; BI, Before removal Initial; BM, Before removal Mature).

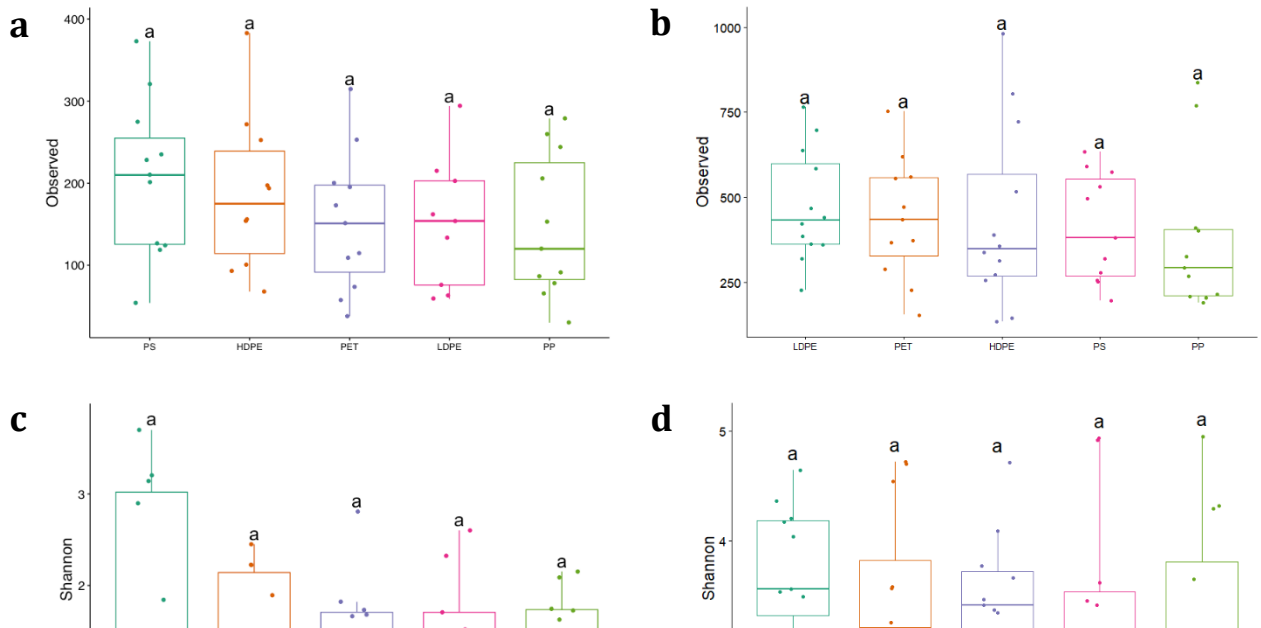

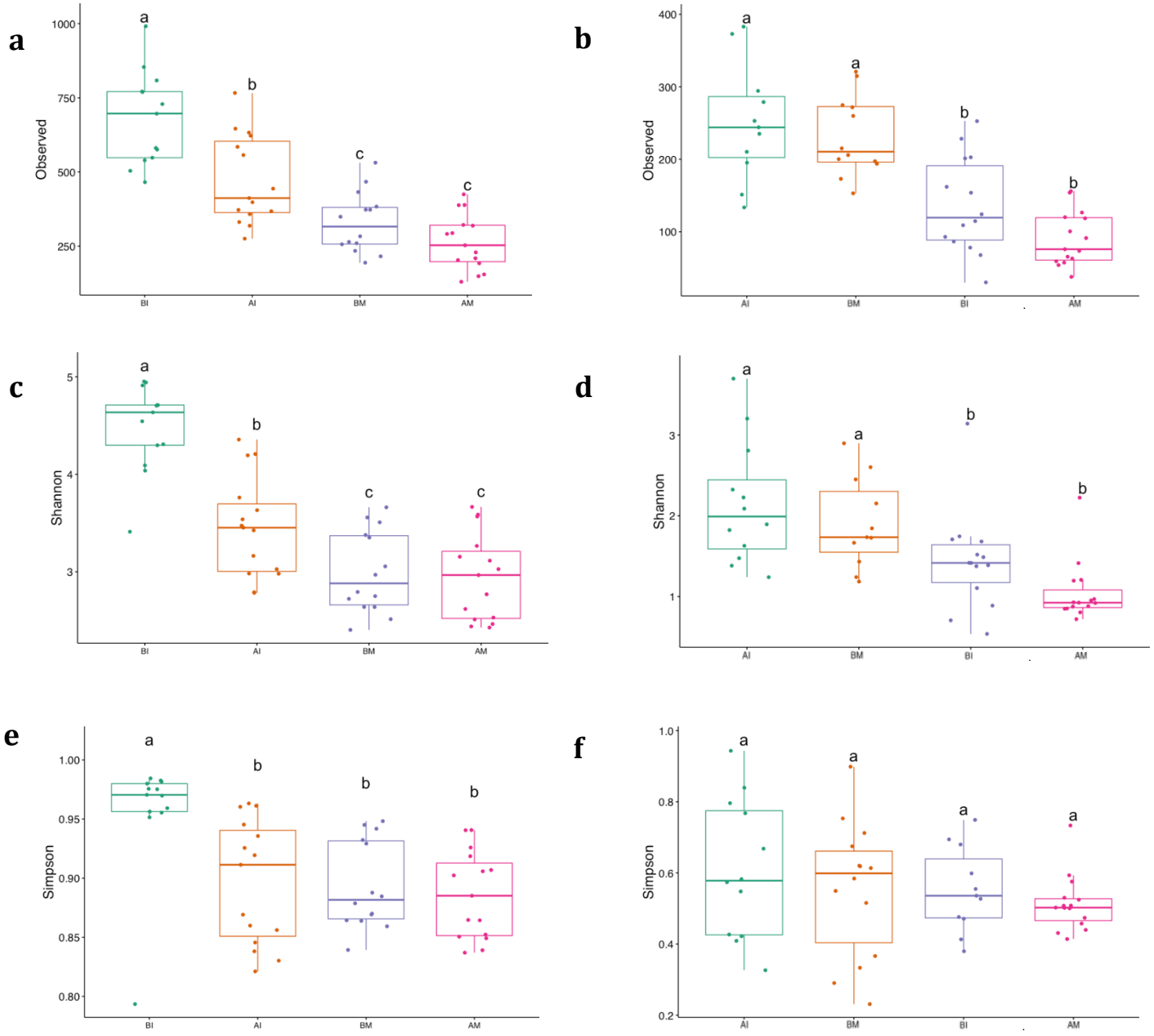

Figure S 63: Community alpha diversity – classified by biofouling phase: (a) Observed number of ASVs for bacterial community, (b) Observed number of ASVs for fungal community,(c) Shannon index for bacterial community, (d), Shannon index for fungal community (e) Shannon index for fungal community, (e) Simpson index for bacterial community, (f) Simpson index for fungal community. (a, b and ab signify significance

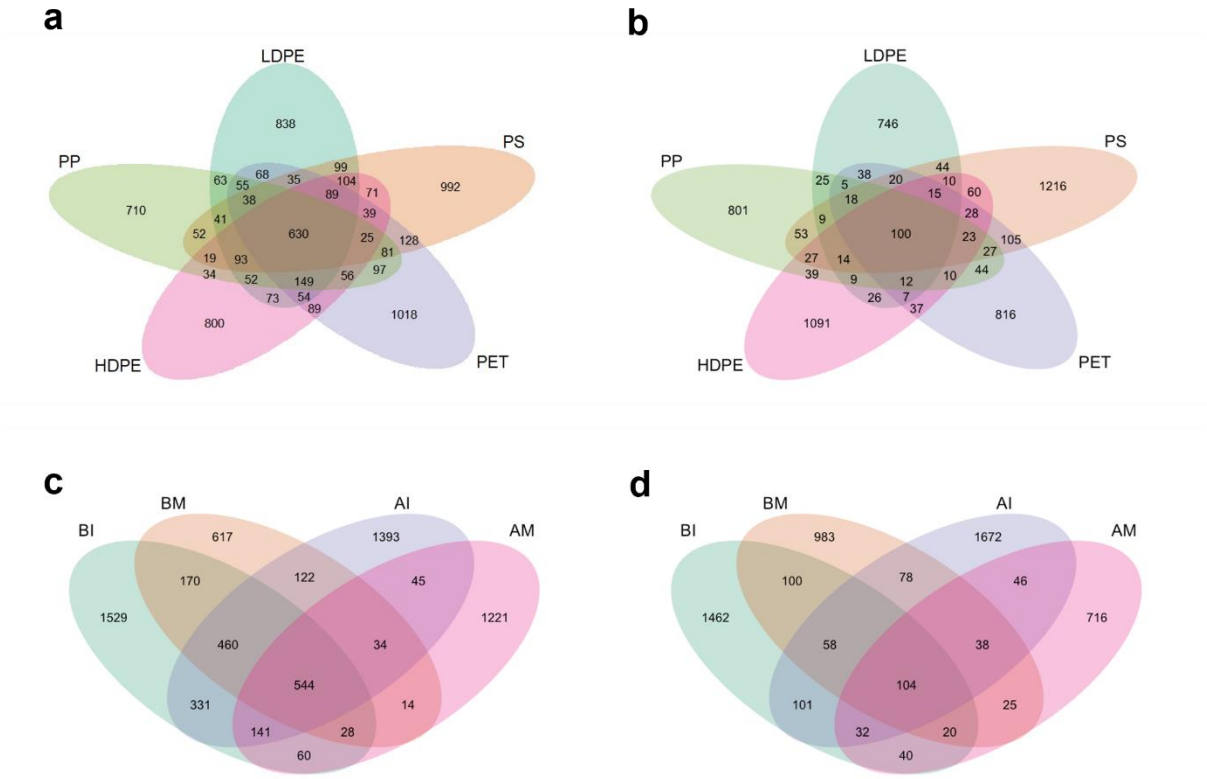

Figure S 64: The observed number of shared and unique ASVs: (a) bacterial on each substrate, (b) fungal on each substrate, (c) bacterial during each biofouling phase, (d) fungal during each biofouling stage.

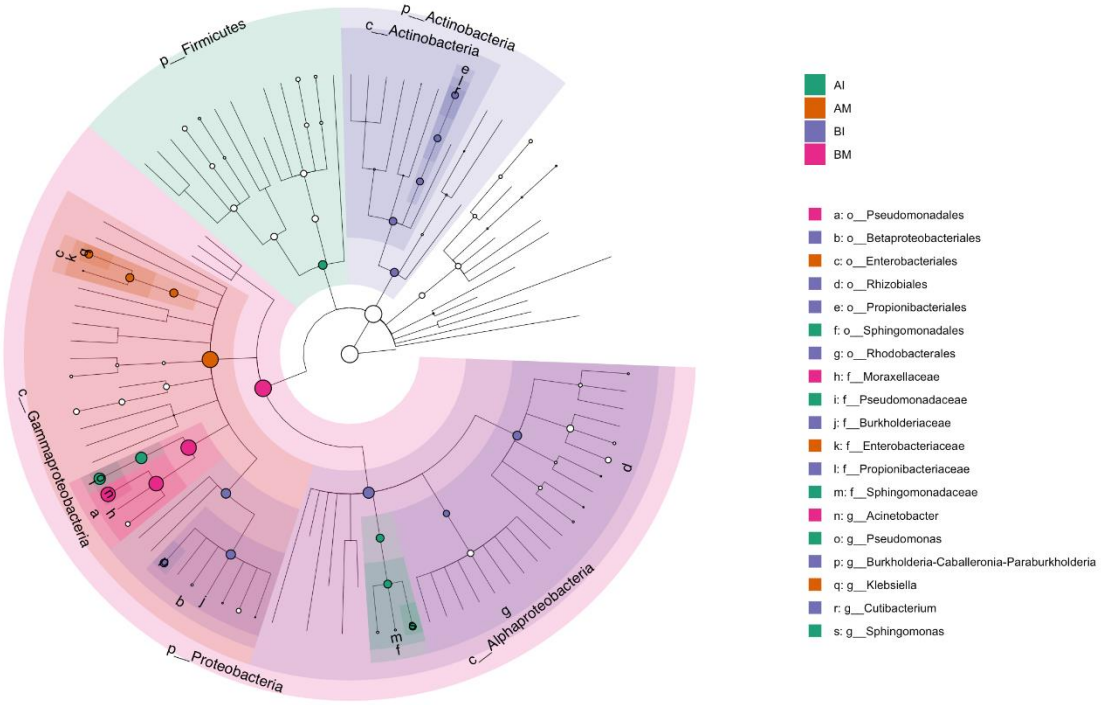

Figure S 65: LefSe analysis for bacterial biomarker identification.

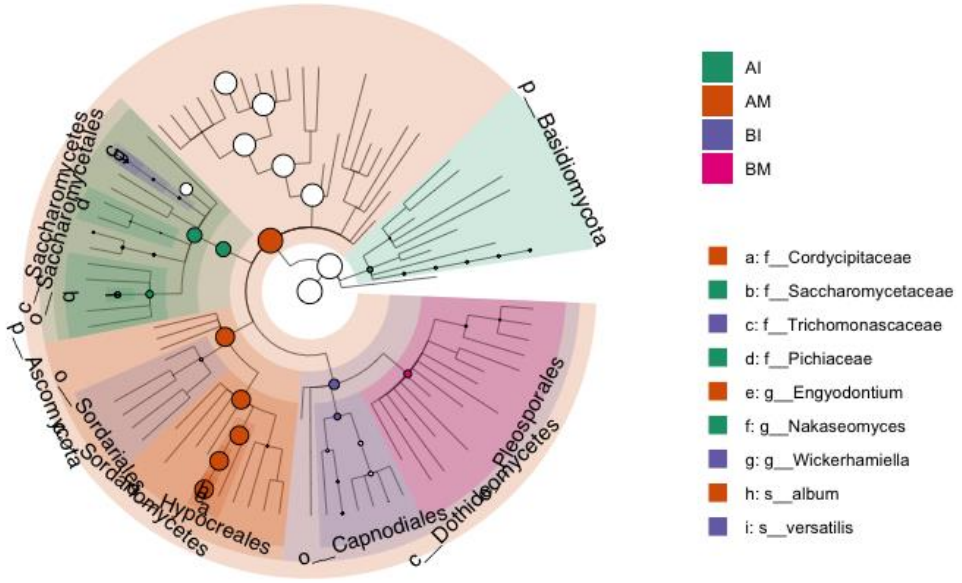

Figure S 66: LefSe analysis for fungal biomarker identification.

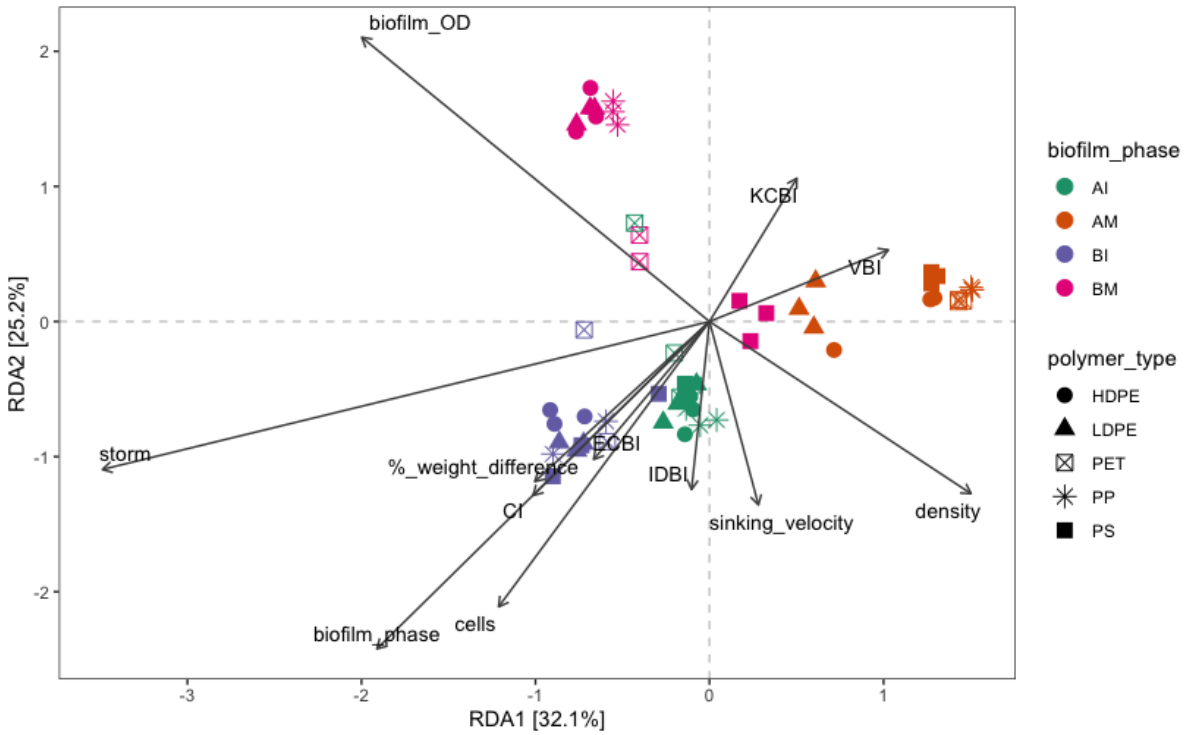

Figure S 67: Redundancy analysis (RDA) biplot for bacterial samples.

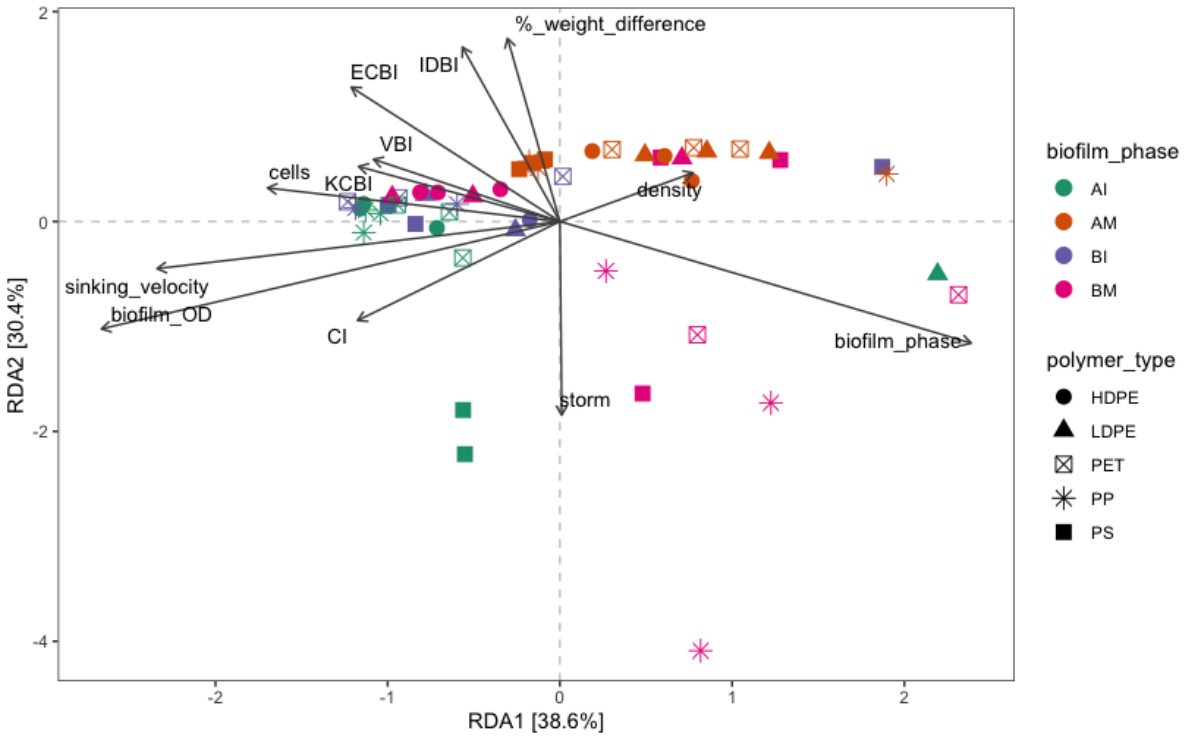

Figure S 68: Redundancy analysis (RDA) biplot for fungal samples.

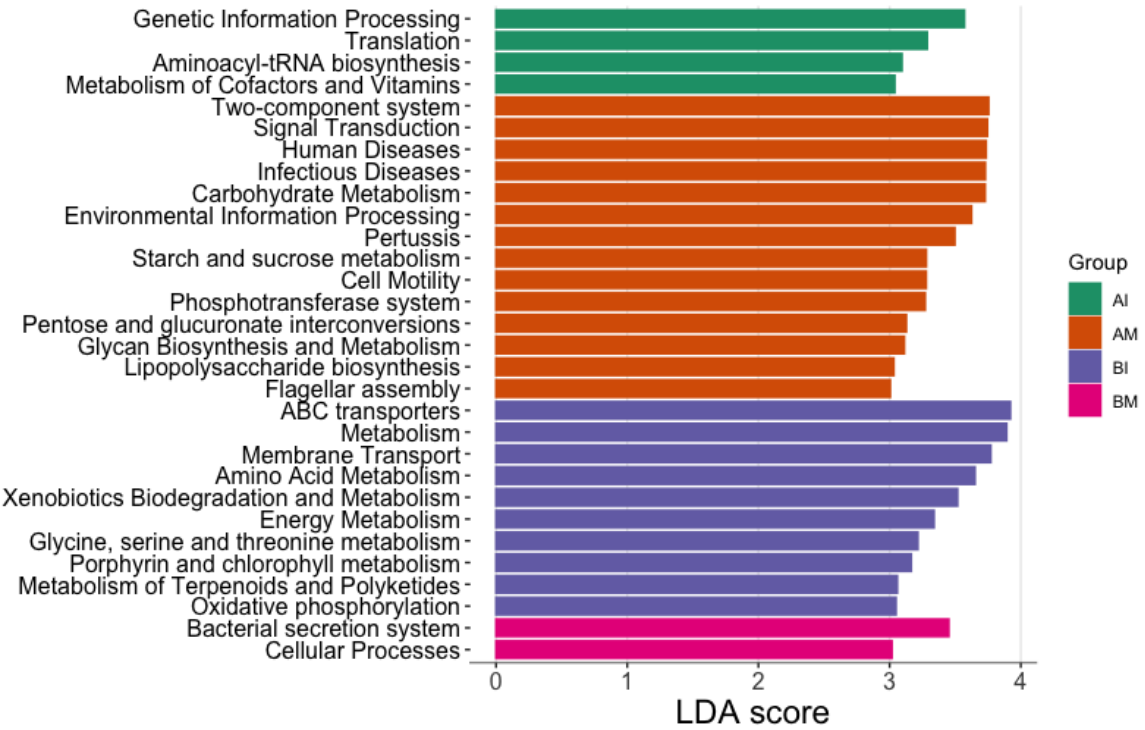

Figure S 69: Predicted enriched metabolic functions of bacterial communities using LefSe.

APPENDIX II: Supplementary Tables

Table S 1: Water quality parameters over time. BDL signifies values Below the Detection Limit of the measuring methods. TSS: Total suspended solids. V and W denote virgin and weathered polymer, respectively.

Time (Days)	Temperature		Conductivity (mS/cm)		Dissolved Oxygen (%)		Total Nitrogen (mg/L)		NO_3 (mg/L)		PO_4 (mg/L)		TSS (mg/L)		pH	
	V	W	V	W	V	W	V	W	V	W	V	W	V	W	V	W
0	27.0	27.0	73.5	73.5	97.6	97.6	17.2	17.2	0.276	0.276	BDL	BDL	35.0	35.0	8.13	8.13
30	22.5	22.3	53.3	53.5	98.7	98.6	12.8	15.7	0.192	0.158	BDL	BDL	35.9	36.2	8.13	8.22
60	12.3	12.0	43.8	43.6	89.7	88.1	2.7	3.07	0.182	0.223	BDL	BDL	36.1	36.7	7.92	8.09
90	16.9	17.7	53.2	53.5	93.0	89.3	8.8	9.37	BDL	0.087	BDL	BDL	38.3	39.0	8.01	8.14
120	21.9	21.7	61.0	56.8	97.3	98.1	11.3	8.17	0.226	0.151	0.079	0.050	39.5	40.1	8.21	8.33
150	17.2	17.8	51.1	52.5	98.1	96.2	2.42	2.6	0.145	0.177	BDL	BDL	39.6	40.7	8.37	8.49
180	16.9	17.2	63.0	59.7	95.1	97.0	6.3	7.8	0.076	0.044	BDL	BDL	41.2	41.7	8.19	8.23

Table S 2: Water quality parameters throughout the experimental period.

Time period → Parameter ↓	**18-06-19 (day 0)**	**24-07-19 (day 35)**	**23-08-19 (day 67)**	**28-09-19 (day 102)**	**30-11-19 (day 152)**	**25-01-20 (day 202)**	**29-02-20 (day 242)**	**18-04-20 (day 300)**
T (^oC)	25.1	28.3	29	27.8	22.7	19.1	16.1	16.6
pH (%)	8.03	8.1	8.16	8.13	8.1	7.98	7.98	8.4
DO (mg/L)	8.17	7.71	7.62	7.26	8.05	8.85	9.68	9.74
ORP (mV)	61.5	71.7	70.1	41.4	61.3	30.7	55	59
Conductivity (mS/cm)	59.5	60.7	61.3	63	65	44.5	50	60.3
BOD_5 (mg/L)	7	8	5	7	6	8	4	5
COD (mg/L)	24.7	36.8	23.7	20	92.5	20	8.62	10.2
TN (mg/L)	36.7	14.8	13.96	13.4	56.5	5	8.97	8.13
PO_4 (mg/L)	0	0	0	0	0	0	0	0
NO_3 (mg/L)	0.044	0.096	0.056	0.181	0.076	0.022	0.034	0.029
NH_4 (mg/L)	0.009	0	0	0	0	0	0	0

Table S 3: Changes of plastic pellet diameter over time.

	LDPE pellet diameter (mm)		HDPE pellet diameter (mm)		PP pellet diameter (mm)	
Time (days)	Virgin	Weathered	Virgin	Weathered	Virgin	Weathered
0	4.39 ± 0.07	4.25 ± 0.19	4.60 ± 0.28	4.39 ± 0.24	4.13 ± 0.17	4.11 ± 0.15
35	4.61 ± 0.25	4.34 ± 0.11	4.42 ± 0.32	4.47 ± 0.19	4.36 ± 0.33	4.80 ± 0.45
67	4.22 ± 0.08	3.78 ± 0.35	4.30 ± 0.23	4.53 ± 0.33	4.22 ± 0.28	4.16 ± 0.15
102	4.15 ± 0.13	3.96 ± 0.06	4.30 ± 0.01	4.22 ± 0.27	4.13 ± 0.36	3.98 ± 0.28
152	4.02 ± 0.14	3.79 ± 0.38	4.16 ± 0.14	4.14 ± 0.09	4.09 ± 0.06	3.70 ± 0.10
202	3.93 ± 0.24	3.49 ± 0.26	3.90 ± 0.20	3.85 ± 0.11	4.07 ± 0.11	3.19 ± 0.25
242	3.89 ± 0.17	3.32 ± 0.45	3.84 ± 0.25	3.80 ± 0.20	3.66 ± 0.48	3.14 ± 0.10
300	3.63 ± 0.33	3.16 ± 0.34	-	-	3.49 ± 0.40	3.05 ± 0.12

Table S 4: Index calculations from ATR-FTIR spectral absorbance values.

Index	Calculation Formula PE	Calculation Formula PP
KCBI	$KCBI = \frac{I_{1715}}{I_{1465}}$	$KCBI = \frac{I_{1715}}{I_{974}}$
ECBI	$ECBI = \frac{I_{1745}}{I_{1465}}$	$ECBI = \frac{I_{1740}}{I_{974}}$
VBI	$VBI = \frac{I_{1650}}{I_{1465}}$	$VBI = \frac{I_{1640}}{I_{974}}$
IDBI	$IDBI = \frac{I_{908}}{I_{1465}}$	$IDBI = \frac{I_{908}}{I_{974}}$
CI	$CI = \frac{I_{1740}}{I_{1460}}$	$CI = \frac{I_{1740}}{I_{1460}}$

Table S 5: Statistical comparison of alpha diversity on the examined polymer types (number of observed taxa, Shannon Index, Simpson Index, Fisher Index) using the Kruskal-Wallis one way analysis.

Measure	Group	Bacterial Communities		Fungal Communities	
		p-value	**Significance**	***p-value***	**Significance**
Number of Observed Taxa	LDPE vs PS	0.339	-	0.271	-
	LDPE vs PET	0.712	-	0.849	-
	LDPE vs HDPE	0.326	-	0.438	-
	LDPE vs PP	0.085	-	0.970	-
	PS vs PET	0.818	-	0.123	-
	PS vs HDPE	0.975	-	0.526	-
	PS vs PP	0.450	-	0.178	-
	PET vs HDPE	0.580	-	0.459	-
	PET vs PP	0.278	-	0.974	-
	HDPE vs PP	0.580	-	0.291	-
	LDPE vs PS vs PET vs HDPE vs PP	0.555	-	0.501	-
Shannon Index	LDPE vs PS	0.805	-	0.382	-
	LDPE vs PET	0.356	-	0.849	-
	LDPE vs HDPE	0.225	-	0.935	-
	LDPE vs PP	0.325	-	0.970	-
	PS vs PET	0.224	-	0.450	-
	PS vs HDPE	0.268	-	0.439	-
	PS vs PP	0.309	-	0.411	-
	PET vs HDPE	0.065	-	0.944	-
	PET vs PP	0.082	-	0.974	-
	HDPE vs PP	0.805	-	0.725	-
	LDPE vs PS vs PET vs HDPE vs	0.245	-	0.892	-

	PP				
Simpson Index	LDPE vs PS	0.853	-	0.518	-
	LDPE vs PET	0.124	-	0.849	-
	LDPE vs HDPE	0.453	-	0.462	-
	LDPE vs PP	0.712	-	0.425	-
	PS vs PET	0.053	-	0.490	-
	PS vs HDPE	0.498	-	0.324	-
	PS vs PP	0.718	-	0.082	-
	PET vs HDPE	0.014	*	0.622	-
	PET vs PP	0.045	*	0.309	-
	HDPE vs PP	0.712	-	0.888	-
	LDPE vs PS vs PET vs HDPE vs PP	0.134	-	0.551	-
Fisher Index	LDPE vs PS	0.340	-	0.271	-
	LDPE vs PET	0.712	-	0.849	-
	LDPE vs HDPE	0.326	-	0.438	-
	LDPE vs PP	0.085	-	0.970	-
	PS vs PET	0.818	-	0.123	-
	PS vs HDPE	0.975	-	0.526	-
	PS vs PP	0.450	-	0.178	-
	PET vs HDPE	0.580	-	0.459	-
	PET vs PP	0.279	-	0.974	-
	HDPE vs PP	0.580	-	0.291	-
	LDPE vs PS vs PET vs HDPE vs PP	0.555	-	0.501	-

Table S 6: Statistical comparison of alpha diversity among biofouling phase (number of observed taxa, Shannon Index, Simpson Index, Fisher Index) using the Kruskal-Wallis one way analysis.

Measure	**Group**	**Bacterial Communities**		**Fungal Communities**	
		p-value	**Significance**	***p-value***	**Significance**
Number of Observed Taxa	BI vs BM	$1.08 * 10^{-5}$	***	$1.93 * 10^{-3}$	**
	BI vs AI	$6.57 * 10^{-3}$	**	$6.22* 10^{-1}$	-
	BI vs AM	$7.06 * 10^{-6}$	***	$4.62 * 10^{-5}$	***
	BM vs AI	$1.13 * 10^{-2}$	*	$2.85 * 10^{-3}$	**
	BM vs AM	$1.01 * 10^{-1}$	-	$4.24 * 10^{-2}$	*
	AI vs AM	$3.45 * 10^{-4}$	***	$1.75 * 10^{-5}$	***
	BI vs BM vs AI vs AM	$2.09 * 10^{-4}$	***	$1.66 * 10^{-6}$	***
Shannon Index	BI vs BM	$1.65 * 10^{-5}$	***	$3.48 * 10^{-2}$	*
	BI vs AI	$2.73 * 10^{-4}$	***	$4.98 * 10^{-1}$	-

	BI vs AM	$1.34 * 10^{-5}$	***	$2.53 * 10^{-4}$	***
	BM vs AI	$4.47 * 10^{-2}$	*	$1.17 * 10^{-2}$	*
	BM vs AM	$6.33 * 10^{-1}$	-	$2.60 * 10^{-2}$	*
	AI vs AM	$1.84 * 10^{-2}$	*	$7.74 * 10^{-5}$	***
	BI vs BM vs AI vs AM	$1.63 * 10^{-6}$	***	$3.53 * 10^{-5}$	***
Simpson Index	BI vs BM	$1.44 * 10^{-4}$	***	$8.27 * 10^{-1}$	-
	BI vs AI	$1.61 * 10^{-3}$	**	$3.37 * 10^{-1}$	-
	BI vs AM	$1.44 * 10^{-4}$	***	$6.07 * 10^{-1}$	-
	BM vs AI	$5.41 * 10^{-1}$	-	$1.90 * 10^{-1}$	-
	BM vs AM	$2.54 * 10^{-1}$	-	$2.62 * 10^{-1}$	-
	AI vs AM	$6.94 * 10^{-1}$	-	$4.99 * 10^{-1}$	-
	BI vs BM vs AI vs AM	$1.80 * 10^{-4}$	***	$1.80 * 10^{-4}$	-
Fisher Index	BI vs BM	$1.08 * 10^{-5}$	***	$1.98 * 10^{-3}$	**
	BI vs AI	$6.58 * 10^{-3}$	**	$6.22 * 10^{-1}$	-
	BI vs AM	$7.05 * 10^{-6}$	***	$4.62 * 10^{-5}$	***
	BM vs AI	$1.13 * 10^{-2}$	*	$2.85 * 10^{-3}$	**
	BM vs AM	$1.01 * 10^{-1}$	-	$4.24 * 10^{-2}$	*
	AI vs AM	$3.45 * 10^{-4}$	***	$1.75 * 10^{-5}$	***
	BI vs BM vs AI vs AM	$2.09 * 10^{-7}$	***	$1.66 * 10^{-6}$	***